COMPUTATIONAL ANALYSIS OF MHD BLOOD FLOW THROUGH A STENOSED ARTERY IN THE PRESENCE OF BODY ACCELERATION AND CHEMICAL REACTION

Annord Mwapinga

A Dissertation Submitted in Partial Fulfillment of the Requirements for the Degree of Doctor of Philosophy in Mathematical and Computer Sciences and Engineering of the Nelson Mandela African Institution of Science and Technology

Arusha, Tanzania

October, 2021

ABSTRACT

The unsteady, laminar and two-dimensional pulsatile flow of both, Newtonian and non-Newtonian chemically reacting blood in an axisymmetric stenosed artery subject to body acceleration and magnetic fields were studied. In the case of non-Newtonian blood, heat transfer was taken into consideration. The combined effects of body acceleration, magnetic fields and chemical reaction on blood flow were considered. The non-Newtonian model was chosen to suit the Herschel-Bulkley fluid characteristics.

The non-dimensional governing equations were solved using the explicit finite difference method and executed using MATLAB package. The solutions showing the velocity, temperature and concentration profiles were illustrated. The effects of Reynolds number, Hartman number, Schmidt number, Eckert number and Peclet number were examined. Additionally, the effects of stenosis and body acceleration on blood flow were explored.

The study found that, body acceleration, magnetic fields and stenosis affect the normal flow of blood. Body acceleration was observed to have more effect on blood flow than the magnetic fields and stenosis. Furthermore, as the key findings of the study, it was noticed that the combined effect of stenosis, body acceleration, magnetic field and chemical reaction, reduce the concentration profile of the blood flow and the blood flow velocity. It was also observed that, the axial velocity, concentration and skin friction, decrease with increasing stenotic height. The velocity on the other hand increased as the body acceleration increased. Furthermore, as the Hartman number increased, both the radial and axial velocities diminished. The higher the chemical reaction parameter was, the lower were the concentration profiles.

For the non-Newtonian blood, the velocity profile diminished with increase in the Hartman number and increased with the body acceleration. The temperature profile was observed to rise by the increase of body acceleration and the Eckert number, while it diminished with the increase of the Peclet number. It was also found that, the concentration profile increased with the increase of the Soret number and decreased with the increase of the chemical reaction. It was further observed that the shear stress deviated more when the power law index, $n > 1$ than when $n < 1$.

DECLARATION

I, **Annord Mwapinga**, do hereby declare to the Senate of Nelson Mandela African Institution of Science and Technology that this dissertation is my own original work and that it has neither been submitted nor being concurrently submitted for degree award in any other institution.

Annord Mwapinga
(Candidate)

Date

The above declaration is confirmed

Prof. Verdiana Grace Masanja
(Supervisor 1)

Date

Prof. Eunice Mureithi
(Supervisor 2)

Date

Dr. James Makungu
(Supervisor 3)

Date

COPYRIGHT

CERTIFICATION

The undersigned certify that they have read and hereby recommend for acceptance by the Nelson Mandela African Institution of Science and Technology the dissertation entitled: ***Computational analysis of MHD blood flow through a stenosed artery in the presence of body acceleration and chemical reaction***, in fulfillment of the requirements for the degree of Doctor of Philosophy in Mathematical and Computer Sciences and Engineering of the Nelson Mandela African Institution of Science and Technology.

_____

Prof. Verdiana Grace Masanja
(Supervisor 1)

Date: .....

_____

Prof. Eunice Mureithi
(Supervisor 2)

Date: .....

_____

Dr. James Makungu
(Supervisor 3)

Date: .....

ACKNOWLEDGEMENTS

First and foremost, I thank the Almighty God for the gift of life and health to me, my family, and supervisors for the whole period of study.

My special appreciations go to my supervisors namely, Prof. Verdiana Grace Masanja of the Applied Mathematics and Computational Science Department (AMCS), School of Computational and Communication Science and Engineering (CoCSE) at the Nelson Mandela African Institution of Science and Technology (NM-AIST), Prof. Eunice Mureithi and Dr. James Makungu of the Mathematics Department, College of Natural and Applied Sciences (CONAS) at the University of Dar es salaam, for their tireless academic guidance and the moral support they provided to me. Their suggestions and positive criticisms made this work more valuable. May Almighty God pour them with more grace and blessings. Their good work done to me is highly appreciated. Parallel to this, I thank Prof. Dmitry Kuznetsov of the AMCS at the NM-AIST who was my first supervisor before the arrival of Prof. Verdiana Grace Masanja. His suggestions and constructive criticisms during research proposal preparation will always be remembered.

Special thanks also go to my employer, Mwenge Catholic University (MWECAU) under the leadership of the Vice-Chancellor Rev. Prof. Philibert Vumilia for allowing me to pursue PhD studies at the NM-AIST and financing the tuition fees required. I thank him very much for his encouragement and moral support.

Moreover, I thank my fellow PhD students at NM-AIST, without an order of importance or preference, the late Musa Antidius Mjankwi, Linus Kisoma, Furaha Chuma, Slaa Qanne, and Christian Kasumo. I also highly appreciate the mutual encouragement we shared with masters students Joel Efraim and Fred Kapange. In this regard therefore, I am using this opportunity to express my deepest appreciation to my dear colleagues at NM-AIST for their positive academic and moral contributions, efforts and encouragement. We have been working like a team and a family.

I also thank very much my brother Blasius Mwapinga and his wife Tirfonia Mgaya for following my progress from time to time. My father Donatus Mwapinga and my mother Mary Msemwa are strongly appreciated for their prayers.

A special mention of appreciation goes to my lovely and beautiful wife Ester Renatus Mligo

who constantly encouraged me and took care of our family. As I was away for studies, our children Peter, Mary, and Eusebius were well guided by her. It was during my absence for studies when our last born Eusebius was born. I thank very much my wife for patience and understanding. I am proud of you my wife.

DEDICATION

This work is dedicated to my lovely wife Ester Renatus Mligo and my children Peter, Mary and Eusebius.

TABLE OF CONTENTS

LIST OF TABLES

LIST OF FIGURES

LIST OF APPENDICES

LIST OF ABBREVIATIONS

AMCS	Applied Mathematics and Computational Sciences
CVDs	Cardiovascular diseases
CVS	Cardiovascular system
CONAS	College of Natural and Applied Sciences
MHD	Magnetohydrodynamics
FDM	Finite Difference Method
HB	Herschel-Bulkley
MRI	Magnetic resonance imaging
NM-AIST	The Nelson Mandela Institution of Science and Technology
CoCSE	Computational and Communication Science and Engineering
WHO	World Health Organization
MWECAU	Mwenge Catholic University
RTT	Reynolds Transport Theorem

CHAPTER ONE

INTRODUCTION

1.1 Background of the study

In day to day activities, the human body is subjected to different situations that disturb the normal flow of blood. There are several crucial roles played by blood in the human body. Hence when blood flow is not normal, it jeopardizes one's life. Blood transports (*inta alia*) oxygen to cells and tissues thus: (a) providing essential nutrients to cells (such as amino acids, fatty acids, and glucose) (b) removing waste materials such as carbon dioxide, urea, and lactic acid (c) protecting the body from infection and foreign bodies through the white blood cells, (d) transporting hormones from one part of the body to another and (e) regulating acidity (pH) levels of the body. Therefore, situations that disturb the normal flow of blood jeopardize human life. This brings one to the attention of studying the dynamics of blood flow theoretically (through mathematical modeling) and experimentally.

According to the World Health Organization (WHO)(2019), Cardiovascular Diseases (CVDs) are the number one cause of death globally. More people die annually from CVDs than any other cause. Cardiovascular disease usually refers to conditions that involve narrowing or blocking of blood vessels. This can lead to a heart attack or stroke (the sudden death of brain cells due to lack of oxygen which is caused by the blockage of the blood flow or the rupture of an artery that supplies the blood to the brain). Thus, CVDs often are caused by the condition that damage one's heart or blood vessels by atherosclerosis. The atherosclerosis is a build-up of fatty plaques in the blood vessels. Plaque build-up thickens and stiffens artery walls, and this can inhibit blood flow through arteries to tissues and organs.This narrowing of the artery is known as stenosis. Cardiovascular Diseases are sometimes referred to as the coronary artery disease because they involve the coronary arteries. Coronary heart disease refers to the narrowing of the coronary artery which is the major artery that supplies blood, oxygen, and other nutrients to the heart.

The presence of stenosis in arteries has attracted many mathematicians to model blood flow. The current study is motivated by the need to continue investigating the blood flow in stenosed arteries. In particular, the study focus is to model blood flow through a stenosed artery subject to different situations that disturb the normal flow of blood.

1.1.1 Circulatory system

Circulatory system (sometimes known as cardiovascular system, CVS) generally has three vital features: the fluid (in this case is the blood) which transports materials, the network of blood vessels and the heart that pumps the fluid through the vessels. The human circulatory system is closed in the manner that the blood is repeatedly cycled throughout the body inside a system of blood vessels. The blood flow in human arterial system can be considered as a fluid dynamics problem. Simulation of blood flow in the arterial network system will provide a better understanding of the physiology of human body. Hence, hemodynamics plays an important role in the development and progression of arterial stenosis (Thomas & Sumam, 2016).

The cardiovascular system circulates blood in two circuits: the Pulmonary circulation that transports oxygen-poor blood from the right ventricle to the lungs where blood picks up a new oxygen supply and the systemic circulation that returns oxygen rich blood and nutrients to the left atrium and is pumped out all over the body. Figure 1 shows the schematic diagram of the circulatory system. It shows the systemic and pulmonary circulations, the chambers of the heart, and the distribution of blood volume throughout the system.

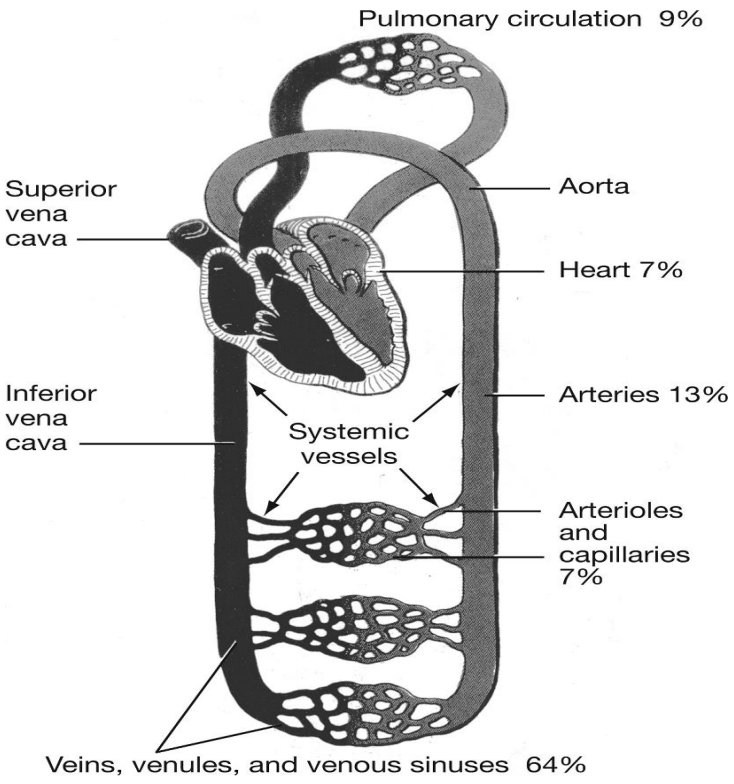

Figure 1: Schematic diagram of the circulatory system (Keener & Sneyd, 1998)

1.1.2 Blood vessels

Blood vessels involve the routes by which the blood travels to and through the tissues and back to the heart. There are three well known blood vessels; arteries, veins and capillaries. The blood vessels decrease in size as they move away from the heart to capillaries. Arteries are blood vessels that carry blood away from the heart to other parts of the body. They are much thicker than veins and capillaries because of the high pressure of blood coming from the heart. The veins transmit blood back to the heart. Veins have much thinner walls than arteries, making it susceptible of easy collapse. Capillaries carry blood from the arteries to the body's cells, and then back to the veins.

1.1.3 Blood flow in a stenosed artery

Mekheimer and El Kot (2015), Awaludin and Ahmad (2013) and Ismail *et al.* (2008) postulated that stenosis is a partial occlusion of the blood vessels due to the accumulation of cholesterol and fats and the abnormal growth of tissue. Stenosis is one of the main causes of anomaly in blood flow. The presence of stenosis in the arterial wall diminishes the diameter of the artery, and if stenosis continues to grow, it leads to cardiovascular diseases. Awojoyogbe *et al.* (2011) presented the normal and stenosed artery (Fig 2).

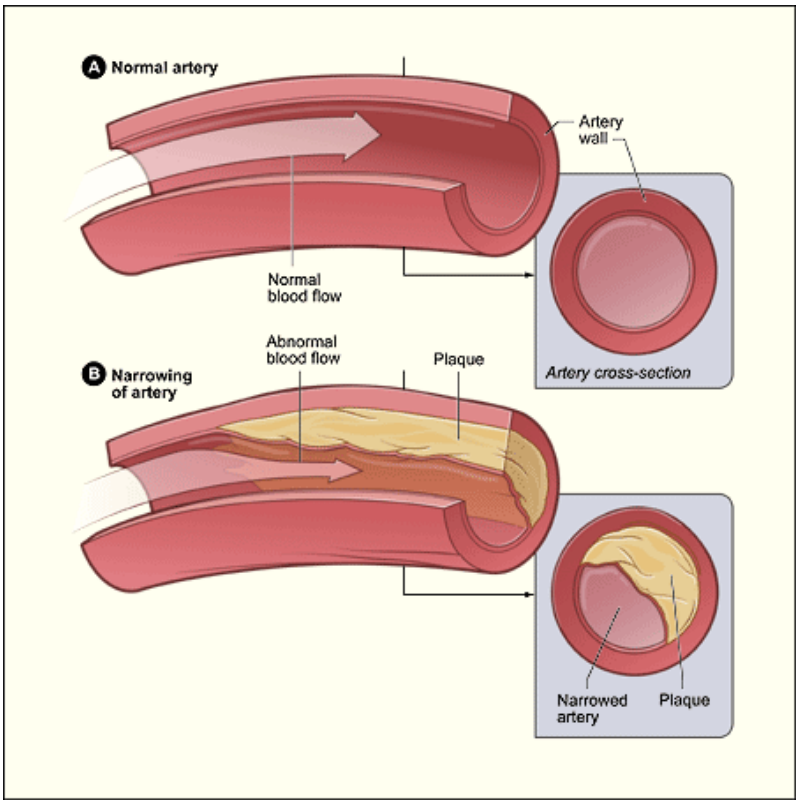

Figure 2: The normal and stenosed arteries (Awojoyogbe *et al*, 2011)

1.1.4 Basic equations governing the flow

The focus of the current study is computational modeling of chemically reacting blood flow, heat, and mass transfer through a stenosed artery in the presence of body acceleration and magnetic fields. Considering heat and mass transfer, the fluid flow is governed by the equations of continuity, motion (also known as Navier-Stokes Equations), energy and concentration transport. These equations, respectively, represent the conservation principles of mass, momentum, energy, and mass concentration transport via Ficks law.

1.1.5 Transport Phenomena

According to Hauke (2008), application of classical mechanics conservation principles of mass, momentum, energy, and concentration were initially developed for particle systems (Lagrangian) or pieces of matter (Eulerian). In transport phenomena, there are pieces of matter that deform in a complex way making it a difficult task to follow the motion and evolution of matter that are continuously changing their shape and size. Thus for convenience, the equations of mechanics and thermodynamics are best written in a way for solving transport problems by using transport theorems.

To solve a practical transport problem, it is convenient that the equations are applied to an arbitrarily chosen volume of fluid, part of which could be fixed or in motion. Matter could flow across boundaries of the arbitrary volume or its boundaries could follow the fluid. Such a volume is called a control volume and is defined as follows:

Definition: A control volume is an arbitrary volume selected to analyze a transport problem. It is denote by $V(t)$ and it moves with a velocity $\mathbf{v}$.

The control volumes contain only fluid, however a control volume can contain any parts of the analysed system. According to Hauke (2008), the transport integral equations are made of integrals of the form:

$$\frac{d}{dt}\iiint_{V(t)} f(\mathbf{x},t)dV \tag{1.1}$$

Upon differentiating the equation (1.1) with respect to time t, gives the transport integral equations. It is noticed that both the domain integral $V(t)$ and the integrand $f(\mathbf{x},t)$ depend on time t. Therefore to perform calculation on equation (1.1), the Leibnitz differentiation rule for integrals can be used.

1.1.6 Reynolds Transport Theorem

There are three Reynolds Transport Theorems (RTT). The 1st RTT is for a fluid volume, the 2nd RTT is for a control volume, and the 3rd RTT is for combined fluid volume and control volume. Considering the 2nd RTT is considered.

The 2nd RTT

Consider a closed control volume, $V(t)$, within a flow field. The control volume considered to be fixed in space and the fluid to be moving through it. The control volume is considered to occupy reasonably large finite region of the flow field.

The second RTT states that, *The rate of change of a thermodynamic entity, ϕ , of a system equals the sum of the rate of change of that entity inside the control volume and the rate of efflux of the entity across the control surface*.

Mathematically, the 2nd RTT is expressed as follows:

Theorem (2nd RTT): Let $V(t)$ be a region in Euclidean space with boundary $S(t)$. Let $\mathbf{x}(t)$ be the positions of points in the region and let $\mathbf{v}(\mathbf{x},t)$ be the velocity field in the region. Let $\mathbf{n}(\mathbf{x},t)$ be an outward unit normal to the boundary. Let $\phi(\mathbf{x},t)$ be a vector (or scalar) field in the region. Then:

$$\frac{D}{Dt}\iiint_{V(t)}\phi(\mathbf{x},t)dV = \iiint_{V(t)}\frac{\partial\phi(\mathbf{x},t)}{\partial t}dV + \iint_{S(t)}(\mathbf{v}.\mathbf{n})\phi(\mathbf{x},t)dS \tag{1.2}$$

Proof: Let $V(t)$ be the domain at time t, shown in Fig. 3 whose surface moves at velocity $\mathbf{v}$ At some time $t+\Delta t$ the domain will occupy space denoted by the volume $V(t,\Delta t)$. This volume at $t+\Delta t$ can be decomposed as:

$$V(t,\Delta t) = V(t) + V_2(\Delta t) - V_1(\Delta t) \tag{1.3}$$

The intersection of surfaces $V(t)$ and $V(t,\Delta t)$ decomposes $S(t)$ into two surfaces $S_1 t$ and $S_2 t$ as shown in Fig 3.

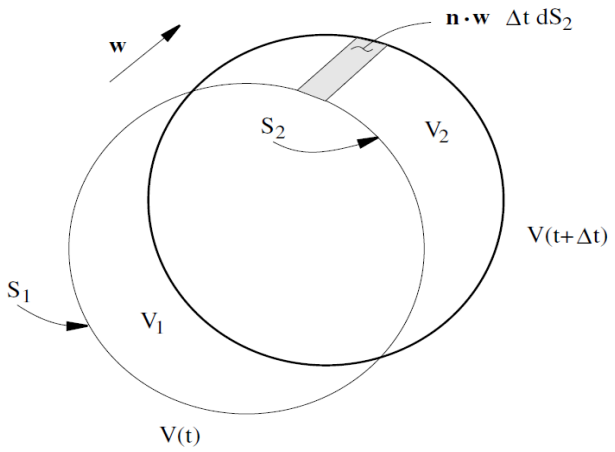

Figure 3: Moving domain of integration V(t) with surface S(t)

Applying the definition of derivative,

$$\frac{d}{dt}\iiint_{V(t)}\phi(\mathbf{x},t)dV=\lim_{\Delta t\to 0}\frac{1}{\Delta t}\left[\iiint_{V(t+\Delta t)}\phi(\mathbf{x},t+\Delta t)dV-\iiint_{V(t+\Delta t)}\phi(\mathbf{x},t)dV\right] \tag{1.4}$$

Next, the decomposition (1.3) is substituted in the integral on $V(t+\Delta t)$:

$$\begin{aligned}\frac{d}{dt}\iiint_{V(t)}\phi(\mathbf{x},t)dV=&\lim_{\Delta t\to 0}\frac{1}{\Delta t}\left[\iiint_{V(t)}\phi(\mathbf{x},t+\Delta t)dV+\iiint_{V_2(\Delta t)}\phi(\mathbf{x},t+\Delta t)dV\right]\\&-\lim_{\Delta t\to 0}\frac{1}{\Delta t}\left[\iiint_{V_1(\Delta t)}\phi(\mathbf{x},t+\Delta t)dV-\iiint_{V(t)}\phi(\mathbf{x},t)dV\right]\end{aligned} \tag{1.5}$$

By definition of derivative, the combination of the first and last integrals, gives

$$\iiint_{V(t)}\frac{\partial\phi(\mathbf{x},t)}{\partial t}dV=\lim_{\Delta t\to 0}\frac{1}{\Delta t}\left[\iiint_{V(t)}\phi(\mathbf{x},t+\Delta t)dV-\iiint_{V(t)}\phi(\mathbf{x},t)dV\right] \tag{1.6}$$

By the Stokes' theorem, the volume integrals over V_2 and V_1 are transformed into surface integrals, respectively as:

$$\iiint_{V_2(\Delta t)}\phi(\mathbf{x},t+\Delta t)dV=\iint_{S_2(t)}\phi(\mathbf{x},t)\mathbf{v}.\mathbf{n}dS \tag{1.7}$$

$$\iiint_{V_1(\Delta t)}\phi(\mathbf{x},t+\Delta t)dV=\iint_{S_1(t)}\phi(\mathbf{x},t)\mathbf{v}.\mathbf{n}dS \tag{1.8}$$

The efflux across the surface is given by the sum of the efflux over $S_1(t)$ and $S_2(t)$, i.e.

$$\iint_{S(t)}\phi(\mathbf{x},t)\mathbf{v}.\mathbf{n}dS=\iint_{S_1(t)}\phi(\mathbf{x},t)\mathbf{v}.\mathbf{n}dS+\iint_{S_2(t)}\phi(\mathbf{x},t)\mathbf{v}.\mathbf{n}dS \tag{1.9}$$

Gathering all the contributions, the desired result is attained.

1.1.7 Conservation Principles

(i) Principle of Mass Conservation

Principle of mass conservation states that mass of a fluid in a control volume, $\iiint_{V(t)} \rho dV$ is a constant, therefore its rate of change equals to zero. That is, *The rate of change of mass for a system equals the sum of the rate of change of mass inside the control volume and the rate of efflux of mass across the control surface*, thus:

$$\iiint_{V(t)} \frac{\partial \rho}{\partial t} dV + \iint_{S(t)} \rho(\mathbf{v}.\mathbf{n}) dS = 0 \tag{1.10}$$

By Stokes' Theorem and Leibnitz differentiation rule for integrals, Equation (1.10) becomes

$$\iiint_{V(t)} \left[\frac{\partial \rho}{\partial t} + \bigtriangledown.\rho\mathbf{v} \right] dV = 0 \tag{1.11}$$

Since all variables are continuous throughout $V(t)$, then equation (1.11) becomes

$$\frac{\partial \rho}{\partial t} + \bigtriangledown.\rho\mathbf{v} = 0 \tag{1.12}$$

Equation (1.12) is the conservation of mass, also known as continuity equation.

(ii) Principle of Momentum Conservation

Principle of linear momentum conversation states that the rate of change of linear momentum for a system is equal to the net external force acting on it. By RTT, "*The rate of change of momentum for a system equals the sum of the rate of change of momentum inside the control volume and the rate of efflux of momentum across the control surface*", hence

• Rate of change of momentum inside the control volume

$$\frac{\partial}{\partial t} \iiint_{V(t)} \rho\ \mathbf{v} dV = \iiint_{V(t)} \frac{\partial}{\partial t}(\rho\mathbf{v}) dV \tag{1.13}$$

The integral and derivative are interchanged since t is independent of space variable

• Rate of efflux of momentum through control surface

$$\iint_{S(t)} \rho\mathbf{v}(\mathbf{v}dS) = \iint_{S(t)} \rho\mathbf{v}\mathbf{v}.\mathbf{n}dS = \iiint_{V(t)} (\mathbf{v}(\bigtriangledown.\rho\mathbf{v}) + \rho\mathbf{v}.\bigtriangledown\mathbf{v}) dV \tag{1.14}$$

• Surface force acting on the control volume (with σ a symmetric stress tensor)

$$\iint_{S(t)} \sigma d\mathbf{A} = \iiint_{V(t)} (\bigtriangledown.\sigma) dV \tag{1.15}$$

• Body force acting on the control volume (with $f_{\mathbf{b}}$ the body force per unit mass)

$$\iiint_{V(t)} \rho f_{\mathbf{b}} dV \tag{1.16}$$

Now, equations (1.1) to (1.4) give,

$$\iiint_{V(t)} \left(\frac{\partial}{\partial t}(\rho \mathbf{v}) + (\mathbf{v}(\bigtriangledown.\rho \mathbf{v}) + \rho \mathbf{v}.\bigtriangledown \mathbf{v}) \right) dV = \iiint_{V(t)} (\bigtriangledown.\sigma + \rho f_{\mathbf{b}}) dV \tag{1.17}$$

Since the variables are continuous, thus:

$$\rho \frac{\partial \mathbf{v}}{\partial t} + \mathbf{v} \frac{\partial \rho}{\partial t} + \rho \mathbf{v}.\bigtriangledown \mathbf{v} + \mathbf{v}(\bigtriangledown.\rho \mathbf{v}) = \bigtriangledown.\sigma + \rho f_{\mathbf{b}} \tag{1.18}$$

or

$$\rho \left(\frac{\partial \mathbf{v}}{\partial t} + \mathbf{v}.\bigtriangledown \mathbf{v} \right) + \mathbf{v} \left(\frac{\partial \rho}{\partial t} + \bigtriangledown.\rho \mathbf{v} \right) = \bigtriangledown.\sigma + \rho f_{\mathbf{b}} \tag{1.19}$$

Since the mass conservation is $\frac{\partial \rho}{\partial t} + \bigtriangledown.\rho \mathbf{v} = 0$ (which is continuity equation), the equation (1.19) reduces to:

$$\rho \left(\frac{\partial \mathbf{v}}{\partial t} + \mathbf{v}.\bigtriangledown \mathbf{v} \right) = \bigtriangledown.\sigma + \rho f_{\mathbf{b}} \tag{1.20}$$

or

$$\rho \frac{D\mathbf{v}}{Dt} = \bigtriangledown.\sigma + \rho f_{\mathbf{b}} \tag{1.21}$$

Since $\frac{D}{Dt} \equiv \frac{\partial}{\partial t} + \mathbf{v}.\bigtriangledown$ is the material time (or constitutive) derivative.

(iii) Principle of Energy Conservation

From the first law of thermodynamics, the energy is conserved, which means, energy can neither be created nor destroyed, it can only be transferred or changed from one form to the other. The internal energy E of the system equals to the net heat transfer into the system Q plus the net work done on the system W. This is mathematically presented in equation (1.22).

$$E = Q + W \Longrightarrow \frac{dE}{dt} = \frac{dQ}{dt} + \frac{dW}{dt} \tag{1.22}$$

Following the similar procedure as done for mass and momentum conversations, the energy equation via RTT is obtained to be:

$$\rho \frac{De}{Dt} + e \left(\frac{Dp}{Dt} + \rho \bigtriangledown.\mathbf{v} \right) = - \bigtriangledown.\mathbf{q}'' + q''' - P \bigtriangledown.\mathbf{v} + \mu \Phi \tag{1.23}$$

where $\mathbf{q}''$ is the heat flux, e is specific internal energy, q''' is the rate of internal heat generation, P is the pressure, μ is the dynamic viscosity, Φ is the viscous dissipation function, and $\mathbf{v}$ is the flow velocity.

The advection-diffusion equation is now introduced. This equation is a result of Fick's second law. The concentration equation is sometimes referred to as the species equation. In this equation, the principle which states that 'the difference between the mass of material entering a control volume and that leaving the control volume must be equal to the rate of accumulation of concentration inside the control volume' is used. The known concentration equation is as expressed hereunder in equation (1.24);

$$\frac{\partial C}{\partial t} + \bigtriangledown.(\mathbf{v}C) = \bigtriangledown.(D \bigtriangledown C) - \beta C \tag{1.24}$$

where, D is the molecular diffusivity coefficient and β is the chemical reaction.

1.1.8 The Lorentz force (Electromagnetic forces)

The Lorentz force is defined as the force that is exerted on a charged particle moving with velocity $\mathbf{v}$ through an electric field $\mathbf{E}$ and magnetic field $\mathbf{B}$. Lorentz force is just the perpendicular force on a charged particle moving in magnetic fields. Now, consider the electromagnetic body force $\mathbf{F} = J \times \mathbf{B}$ where J is the current density presenting the generalized Ohm's law by ignoring the hall effect, as expressed in equation (1.25):

$$J = \sigma((\mathbf{E} + \mathbf{v} \times \mathbf{B})) \tag{1.25}$$

where, σ is the electrical conductivity of the fluid (blood), $\mathbf{E}$ the electric field and $\mathbf{B}$ is the magnetic field. The terms $\sigma\mathbf{E}$ and $\sigma\mathbf{v} \times \mathbf{B}$ respectively, represent the conduction and induction, Turkyilmazoglu (2010). The induced fields are assumed further to be negligibly small so that equation (1.25) reduces to equation (1.26).

$$J = \sigma(\mathbf{v} \times \mathbf{B}) \tag{1.26}$$

which eventually, leads to equation (1.27).

$$J = -\sigma B_0^2 w \tag{1.27}$$

where w is the velocity in the axis of the flow.

1.1.9 Blood as material

Keener and Sneyd (1998), reported that blood is composed of two major ingredients: the liquid blood plasma and several types of cells suspended within the plasma. The cells constitute approximately 40% of the total blood volume and are grouped into three major categories: erythrocytes (red blood cells), leukocytes (white blood cells), and thrombocytes (platelets). Red blood cells comprise water, hemoglobin and membrane components. Hemoglobin is biologically able to combine reversibly with oxygen and hence enables blood to carry substantial amounts of oxygen around the body. White blood cells include granulocytes, lymphocytes and monocytes, and have their primary role in the immune system, scavenging micro-organisms and forming antibodies. Platelets are cell fragments used in blood clotting and are useful to stop bleeding. The liquid component of blood is called plasma. This is the main component of blood and consists mostly of water, proteins, ions, nutrients, and wastes mixed in. Plasma carries different types of blood cells to all parts of the body. Besides the primary function of blood being to deliver oxygen and nutrients to body cells and to remove waste from the body cells, also specific functions of blood include defense, distribution of heat and maintenance of homeostasis (DeSaix *et al*, 2018).

1.1.10 Blood's viscosity

Blood has been treated to be a either a Newtonian fluid or a non-Newtonian fluid where various behaviours have been considered. Payne (2017) described that plasma is a pale yellow fluid that is a solution of proteins and electrolytes and that can be considered to be very close to a Newtonian fluid. The Newtonian fluid is the one that follows Newton's law of viscosity, that the shear stress τ is directly proportional to the velocity gradient. The constant of proportionality μ is referred to as the viscosity of the fluid.

$$\tau = \mu \frac{du}{dy} \tag{1.28}$$

Payne (2017) described further that though, plasma is a Newtonian fluid, the presence of other particles means that blood highly, shows non-Newtonian characteristics and the relationship between shear stress and strain rate is non-linear. At high shear rates, blood is thus close to a Newtonian fluid and an assumption of Newtonian behavior (with a suitable value for viscosity) is often made in large vessels.

Non-Newtonian fluids are the ones that do not obey the Newton's law of viscosity. In this

regard, the shear stress is not directly proportional to the velocity gradient.

$$\tau = \mu f(\dot{\gamma}) \tag{1.29}$$

where $\dot{\gamma}$ is the rate of strain. According to Sochi (2015), the most common descriptions of blood being a non-Newtonian fluid that have been given by various scholars, including the ones in equations $(1.30) - (1.36)$:

$$\tau = K\dot{\gamma}^n \qquad \text{Power law} \tag{1.30}$$

$$\tau = \tau_0 + \mu\dot{\gamma} \qquad \text{Bingham} \tag{1.31}$$

$$\sqrt{\tau} = \sqrt{\tau_0} + \sqrt{\mu\dot{\gamma}} \qquad \text{Casson} \tag{1.32}$$

$$\tau = \tau_0 + \mu\dot{\gamma}^n \qquad \text{Herschel-Bulkley} \tag{1.33}$$

$$\mu = \mu_\infty + \frac{\mu_0 - \mu_\infty}{1 + (\lambda\dot{\gamma})^n} \qquad \text{Cross} \tag{1.34}$$

$$\mu = \mu_\infty + (\mu_0 - \mu_\infty)\left[1 + (\lambda\dot{\gamma})^2\right]^{(n-1)/2} \qquad \text{Carreau} \tag{1.35}$$

$$\mu = \mu_\infty + (\mu_0 - \mu_\infty)\left[\frac{\sinh^{-1}(\dot{\gamma}\lambda)}{\dot{\gamma}\lambda}\right] \qquad \text{Powell-Eyring} \tag{1.36}$$

where, K is the consistency index, τ_0 is the yield stress, μ_0 the viscosity at zero shear rate, μ_∞ is the infinite-shear viscosity, and λ is the characteristic time constant. All models given by Equations (1.29) to (1.35) can be reduced to a Newtonian model with appropriate choices of model parameters. The current study considers both Newtonian and non-Newtonian models to describe the blood. For the non-Newtonian fluid, the Herschel-Bulkley model is considered because it is more advantageous as it gives more information than Casson, Bingham and power law.

The Herschel-Bulkley fluid is a non-Newtonian fluid that requires a certain amount of yield stress for it to flow. The stress tensor components are as given in equation(1.37):

$$\begin{aligned} \tau_{ij} &= \left(K\dot{\gamma}^{n-1} + \frac{\tau_0}{\dot{\gamma}}\right)\dot{\gamma}_{ij} \quad \text{for} \quad \tau \geq \tau_0 \\ \dot{\gamma} &= 0 \quad \text{for} \quad \tau < \tau_0 \end{aligned} \tag{1.37}$$

where, the subscripts $ij = r, z$. τ_0 is the yield stress at zero shear rate, K is the consistency coefficient, n is the flow behavior index and $\dot{\gamma}_{ij} = \left(\frac{\partial u_i}{\partial r_j} + \frac{\partial u_j}{\partial r_i}\right)$ are the components of the rate of strain tensor and $\dot{\gamma}$ is the second invariant of the rate of strain which is as given in equation (1.38):

$$\dot{\gamma} = \sqrt{2\left[\left(\frac{\partial u}{\partial r}\right)^2 + \left(\frac{u}{r}\right)^2 + \left(\frac{\partial w}{\partial z}\right)^2\right] + \left(\frac{\partial u}{\partial z} + \frac{\partial w}{\partial r}\right)^2} \tag{1.38}$$

From equation (1.37) there are special cases that can arise. Thus, one can be able to see different types of behaviors of fluids. This is as shown in table 1.

Table 1: Different types of behaviors of fluids

Type of fluid model	K	n	τ_0
Herschel-Bulkley	>0	$0<n<\infty$	>0
Newtonian	>0	1	$=0$
Power law for $n<1$ (shear-thinning)	>0	$0<n<1$	$=0$
Bingham	>0	1	>0
Power law for $n>1$ (shear-thickening)	>0	$1<n<\infty$	$=0$

1.1.11 Magnetohydrodynamics

According to Davidson (2002), Magnetohydrodynamics (MHD for short) is the study of the interaction between magnetic fields and moving, conducting fluids. Yuduvanshi and Parthasarathy (2010), described further that, the word magnetohydrodynamics is derived from magneto- meaning magnetic field, hydro- meaning liquid, and dynamics meaning movement. Magnetohydrodynamics therefore describes the dynamics of conducting fluids, which are grounded on the interaction of electromagnetic fields with the flow of particles in the fluid. The theory syndicates the Navier-Stokes equations of fluid dynamics with the electromagnetism defined by Maxwell's equations.

In Magnetohydrodynamics situation there is a mutual interaction of magnetic field $\mathbf{B}$ and the fluid velocity field $\mathbf{v}$ which arises partly as a result of laws of Faraday and Ampere, and partly due to the Lorentz force. This brings the relative movement of a conducting fluid (in this case is the blood) and a magnetic field causes an electromagnetic force $|\mathbf{v}\times\mathbf{B}|$ in accordance with the Faraday's law of induction. On the other hand, electrical currents will ensue, the current density being of order $\sigma(\mathbf{v}\times\mathbf{B})$, σ being the electrical conductivity. These induced currents must, according to Ampere's law, give rise to a second magnetic field. This complements to the original magnetic field and the change is such that the fluid looks to drag the magnetic field lines.

The combined magnetic field (imposed and induced) interacts with the induced currents density $\mathbf{J}$ to give rise to a Lorentz force $\mathbf{J}\times\mathbf{B}$. As indicated in subsection (1.1.5)

According to Nallapu (2015), in recent years, the study of magnetohydrodynamic (MHD) flow of blood through arteries has gained considerable interest because of its significant applications in physiology. It is known that blood is a suspension of several cells in plasma, the main bulk of the cells being erythrocytes. Since erythrocytes have negative charge (although small), an applied magnetic field can impact the motion of erythrocytes; thus, blood flow is affected due to the action of an external magnetic field Sinha *et al.* (2016). The use of magnetic fields in the field of medicine has been on the increase. This include, in hospitals, the use of magnetic resonance imaging (MRI). Magnetic resonance imaging for blood vessels such as arteries is used to check *inta alia*, the blocked blood arteries, cardiovascular diseases, problems caused by a heart attack, and problems with the structure of the heart. All these use strong magnetic fields.

Figure 4: Person being subjected into MRI (Stoppard, 2017)

The use of magnetic fields in health-related interventions is also manifested in various situations, including the treatment of ailments. In sports such as football and athletics, magnets are used to perform magnetic therapy to maintain health and treat illnesses. Magnetic therapy is an alternative medical practice that uses magnets to alleviate pain and other health concerns. It is, therefore, possible that magnetic therapy in sports can be applied to a person with stenosis

because all people are susceptible to have stenosis or plaques in the body.

1.1.12 Body acceleration

Body acceleration may be defined as the shaking or vibration of the human body. In day to day activities, the human body is subjected to accelerations such as when traveling in vehicles, boats, planes, or in doing physical exercises. These accelerations disturb the normal flow of blood that is why some people feel a headache or vomiting when traveling using vehicles or airplanes. Nagarani and Sarojamma (2008), Sankar and Ismail (2010), and Tanwar *et al.* (2016) highlighted that the prolonged exposure to high level unintended external body accelerations may cause disturbance to the blood flow and this leads to serious diseases which have symptoms like headache, abdominal pain, increase in pulse rate, venous pooling of blood in the extremities.

1.1.13 Chemical reaction

Chemical reaction involves the law of mass action. This law describes the rate at which chemicals, whether large macromolecules or simple ions, collide and interact to form different chemical combinations (Keener & Sneyd, 1998).

Biologically, blood reacts and is soluble at the arterial wall as arteries may be basically considered as a living tissues that need supply of metabolites including oxygen and removal of waste products. Every living cell in the body produces heat which needs to be spread around the body, and this is done by the blood, which heats some organs and cools others by conduction and other processes.

Misra and Adhikary (2016) pointed out that the rate at which blood flows through arteries can also be enhanced/slowed down by the application of drugs. They further explained that this is the observation of the clinicians, when they treat patients suffering from various types of degenerative/tissue-destroying diseases, including multiple atherosclerosis (narrowing of arterial lumen due to deposition of different fatty substances, cholesterol, etc.), arthritis, Alzheimer disease, Parkinson disease, heart failure.

According to Casiday and Frey (2007), when the human body is subjected to the external body acceleration such as physical exercise, the muscles consume a lot of oxygen as they convert chemical energy (in glucose) to mechanical energy. This oxygen gas comes from hemoglobin in the blood. Carbon dioxide gas (CO_2) and hydrogen irons (H^+) are produced during the

breakdown of glucose, and are removed from the muscle via the blood. The production and removal of CO_2 and H^+, together with the use and transport of oxygen gas, cause chemical changes in the blood (Fig. 5).

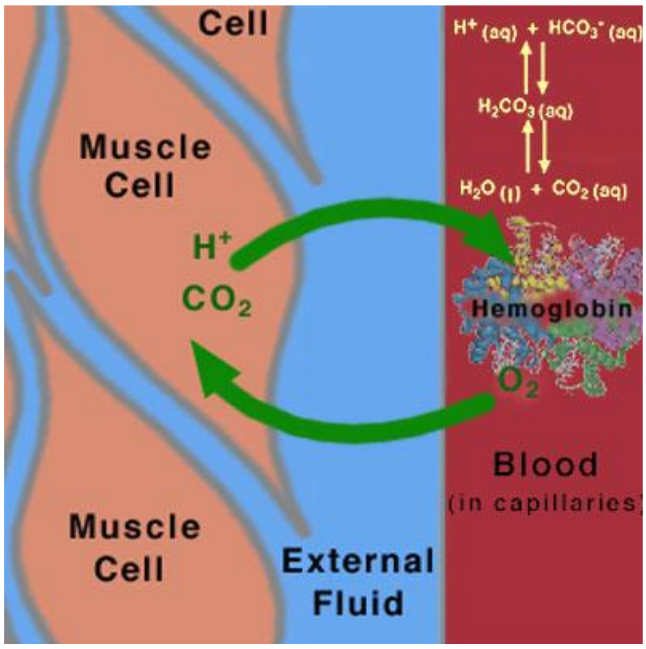

Figure 5: Reactions taking place during exercise (Casiday & Frey, 2007)

1.2 Statement of the problem

The arterial blood flow may be affected by several factors such as physical exercises. The normal flow of blood needs to be maintained so that human healthy is not jeopardized. It is therefore important to study and model different situations that endanger the arterial blood flow. Several scholars have studied arterial blood flow. This includes the study of Alsemiry *et al.* (2020) who investigated blood flow and mass transfer through a stenosed artery. The study assumed that the arterial wall had multiple stenoses. The magnetic fields and body acceleration were not taken into consideration. Liu and Liu (2020) investigated a non-Newtonian fluid model of blood flow through a tapered artery with stenosis. Heat transfer was also investigated. However Magnetic fields, body acceleration, and chemical reactions were not studied. Misra *et al.* (2018) modeled blood flow in arteries subject to vibrating environments. The presence of stenosis and magnetic fields were not considered. Sharma and Yadav (2019) analyzed a mathematical model of blood flow in arteries under the presence of magnetic fields. The aspect of body acceleration was not investigated. To the best of our knowledge, it is clearly seen that the computational modeling of unsteady arterial blood flow heat and mass transfer for chemically

reacting blood in the presence of body acceleration and magnetic fields is not studied despite its manifestation health-related interventions. The current study, therefore, intends to fill the gap by studying the combined effect of unsteady blood flow, heat, and mass transfer through a stenosed artery in the presence of body acceleration, magnetic fields, and chemical reaction.

1.3 The rationale of the study

Understanding the dynamics of heat, and mass transfer of blood flow when the body is subjected to body accelerations, magnetic fields, and chemical reaction is very important in the field of medicine and in the field of computation. Most authors model blood flow through a stenosed artery when the body is subjected to accelerations or to magnetic fields.For example Mwangi (2016), Saleem and Munawar (2016) and Sinha *et al.* (2016). The combined effect of body accelerations, magnetic fields, and chemical reactions has not been taken much attention in modeling despite its manifestation in different situations such as magnetic therapy in sports. The current study combines the effect of body acceleration, magnetic fields, and chemical reactions taking into consideration that the arterial wall has plaques or stenosis. This is beneficial in health-related matters, in the field of fluid dynamics, in the field of computational science and engineering in general as the findings of this study can be used in making or improving health devises such as MRI scanning machine.

1.4 Research objectives

1.4.1 General objective

The general objective of this study is to model and analyze heat and mass transfer of unsteady flow of blood in a stenosed artery in the presence of body acceleration, magnetic field, and chemical reaction.

1.4.2 Specific objectives

The specific objectives of this study are as follows:

(i) To formulate mathematical models for the unsteady MHD flow of a Newtonian and non-Newtonian blood through a stenosed artery in the presence of body acceleration, magnetic fields, and chemical reaction.

(ii) To solve and analyze the model for the Newtonian case and consider mass transfer.

(iii) To solve and analyze the model for the non-Newtonian case and consider heat and mass transfer.

(iv) To validate the model by comparing the current results with previous similar studies.

1.5 Research Questions

The study was guided by the following research questions:

(i) How can mathematical models for the unsteady MHD flow of a Newtonian and non-Newtonian blood through a stenosed artery in the presence of body acceleration, magnetic fields, and chemical reaction be formulated?

(ii) How can a mathematical model describing the unsteady MHD flow of a Newtonian blood and considering mass transfer be solved and analyzed?

(iii) How can a mathematical model describing the unsteady MHD flow of a non-Newtonian blood and considering heat and mass transfer be solved and analyzed?

(iv) How can mathematical models formulated be validated?

1.6 Significance of the study

This study is useful in the following ways:

(i) The study provides more knowledge on the dynamics of blood's velocity, temperature, and concentration subject to the combined effects of magnetic fields, vibration environment, and chemical reaction.

(ii) The study is useful for the clinical purpose which requires reducing the volumetric flow rate of the blood. For example during surgery.

(iii) The study is useful for scientists in medicine for further research, for example, to separate iron-oxide from the entire blood in case this is needed. This can be done by making use of magnetic fields.

(iv) The study is useful in quantifying the arterial wall shear stress and knowing their dynamics when subjected to vibrations and magnetic field.

1.7 Delimitation of the study

The current study focuses on both Newtonian and non-Newtonian blood. The arterial wall is taken to be rigid. The study therefore, does not consider the elasticity of the arterial wall. For non-Newtonian blood, the study only focuses on the Herschel-Bulkley constitutive model. Furthermore, the study is limited to theoretical model validation.

CHAPTER TWO

LITERATURE REVIEW

The purpose of this chapter is to review the relevant literature on blood flow through a stenosed artery. The study on unsteady blood flow through a stenosed artery in the presence of body acceleration, magnetic fields and chemical reaction draws much attention as their presence, may disturb the normal flow of blood, mass as well as the heat transfer. The chapter therefore puts in place the review of literature on studies involving body acceleration, magnetic fields, chemical reaction (mass transfer) and heat transfer.

Kumari *et al.* (2019) studied blood flow through a stenosed artery under the presence of magnetic fields. The arterial wall was assumed to be permeable. The blood was treated as the elastico-viscous, incompressible and electrically conducting. The study also investigated the effect of slip velocity. The expressions for axial velocity, volumetric flow rate and wall shear stress were presented and computed using appropriate transformation. The study concluded that the axial velocity and volumetric flow rate increases considerably with the increase of slip velocity parameters in the presence of magnetic field. Furthermore, the application of magnetic field was observed to be useful in controlling the axial velocity. The study assumed unidirectional flow where only one dimension was taken into consideration. The effect of body acceleration was not investigated.

An investigation of an oscillatory blood flow in an indented artery with heat source in the existence of magnetic field was carried out by Bunonyo *et al.* (2018). The models expressed for the study were solved using the Frobenius method. The computational results of velocity and temperature profiles were presented graphically. The study revealed that the blood flow is influenced by the presence of the magnetic field and the Grashof number. As it was expected, it was observed that the presence of magnetic field retards the velocity profile as well as the flow rate. It was concluded that the temperature profile increases with increasing values oscillatory frequency and radiative heat source parameter. The model on the energy equation did not include the viscous dissipation term, notwithstanding of its importance in exploring temperature profiles. Body acceleration and chemical reactions were also not examined.

Saleem and Munawar (2016) presented a study that dealt with the flow of blood through a stenotic artery in the presence of a uniform magnetic field. Different flow situations were taken

into account by considering the regular and irregular shapes of stenosis inside the walls of artery. The blood was assumed to suit the Eyring–Powell fluid. The solution for the axial velocity was obtained using the regular perturbation method. The study presented graphically the variations in pressure drop across the stenosis length, the impedance and the shear stress. The study concluded that the pressure variations and the pressure drop inside the channel for the case of asymmetric stenosis were large as compared to symmetric stenosis. Furthermore, The Eyring–Powell fluid was observed to be helpful in reducing the frictional effects inside the channel and hence helpful in reducing the resistance to flow. The resistance to the flow was observed to increase as the magnetic effects increases.

Mwangi (2016) investigated magnetohydrodynamic fluid flow in a collapsible tube. The study aimed at determining the velocity profiles, temperature profiles and the effects of fluctuating dimensionless numbers on the flow variables. The fixed magnetic field was perpendicular to the direction of flow of the conducting fluid. The equations governing the flow were non-linear and could not be solved analytically. Therefore, an approximate solution to the equations was determined numerically using the finite difference method. The study revealed that increase in Reynolds number leads to an increase in magnitude of the primary velocity of the flow. Increasing Hartmann number, results showed that the temperature profiles increases. Furthermore, increase in Eckert number was observed to increase the temperature profiles.

The study on the effect of heat transfer on unsteady MHD flow of blood in a permeable vessel in the presence of non-uniform heat source was also studied by Sinha *et al.* (2016). The non-uniform heat source or sink effect on blood flow and heat transfer was taken into consideration. The model equations were first treated mathematically by reducing to a system of coupled non-linear differential equations, which were then solved by employing the similarity transformation and boundary layer approximation. The resulting nonlinear coupled ordinary differential equations were then solved numerically by using an implicit finite difference scheme. The results of velocity, temperature, coefficient of skin friction, and heat transfer rate were obtained. The study revealed that heat transfer rate is boosted as the value of the unsteadiness parameter rises, but it diminishes as the space dependence parameter for heat source or sink rises. The effects of body acceleration and chemical reactions were not part of the study.

Sinha *et al.* (2016) presented a mathematical model which was established for studying the effect of body acceleration on pulsatile blood flow through a catheterized artery with an axially

non-symmetrical mild stenosis. The study considered blood to be a Newtonian fluid. The non-linear partial differential equations were solved using the perturbation method. The analytical expressions for velocity profile, volumetric flow rate, wall shear stress and effective viscosity were obtained. The study found that the axial velocity increases as the body acceleration increases and the axial velocity declines as the phase angle of body acceleration rises. The effect of magnetic field and chemical reactions were not investigated.

The study of arterial blood flow in vibrating environment was also done by Misra *et al.* (2018). In this case the blood was treated to be a couple stress fluid. The study also considered the oscillatory flow in a porous channel. Velocity of blood and the volumetric flow rate were both observed to diminish as the external pressure gradient is enhanced. Blood velocity, volumetric flow rate and also wall shear stress all were observed to reduce as the frequency of oscillation is raised. Furthermore, it was found that the presence of couple stress in the fluid boosts the velocity of the fluid in both axial and transverse directions, while a contrary phenomenon was observed for the wall shear stress.

Changidar and De (2015) developed a nonlinear mathematical model for blood flow in a multiple stenosed arterial segment under the impact of body acceleration. The finite difference scheme was employed to study the dynamics of blood flow through the cylindrical shape artery. To use that method, first they transformed the cylindrical domain into the rectangular domain by using the radial transformation. The study revealed that as the Reynolds number increases, the wall shear stress increases. The multiple stenosis was observed to have a significant effect on the wall shear stress in such a way that it developed more at the constricted locations than all other places of the artery.

Jamil *et al.* (2018) examined the unsteady blood flow with nanoparticles through a stenosed arteries in the existence of periodic body acceleration. The study modelled blood as a non-Newtonian Bingham plastic fluid subjected to periodic body acceleration and slip velocity. The flow governing equations were solved analytically by means of the perturbation method. By using the numerical approaches, the physiological parameters were scrutinized, and the blood flow velocity distributions were generated graphically and discussed. From the flow results, it was seen that the flow speed increases as slip velocity increases and decreases as the values of yield stress increases.

Mwapinga (2012) studied blood flow and heat transfer in a stenosed artery in the presence of body exercise. The study assumed the unidirectional flow in which one dimension was considered. The blood was assumed to be Newtonian in character. The study found that the increase of body acceleration rises the velocity of blood and temperature. It is also found that as stenotic height increases the velocity decreases. It was further shown that increasing the hematocrit ratio increases the velocity of the fluid. On the other hand, it was observed that increasing the radial distance, declines the temperature profile.

The study of the chemical reactions on blood flow has become quite interesting because of the quantitative prediction of blood flow rate. For the sake of examining the effects of the chemical reaction on blood flow through an artery, Chitra and Bhaskran (2019) studied the dynamical influence of heat and mass transfer on unsteady visco-elastic fluid on blood flow through an artery with the effects of chemical reaction. The model equations for the problem were solved analytically using the Bessel function. The main outcomes of the study were that concentration profile declines with increase in chemical reaction parameter. The increase in Schmidt number was also observed to increase the concentration profile. On the other hand, increase in Pecklet number revealed to enhance the temperature profile of blood. The study did not take into account the presence of stenosis on the arterial wall and the effect of body vibration.

Tripathi and Sharma (2018) presented the mathematical model of heat and mass transfer effects on an arterial blood flow under the effect of an applied magnetic field with chemical reaction. The corresponding non-linear differential equations were solved by using an analytical scheme, homotopy perturbation method was used to obtain the solution for the velocity, temperature and concentration profiles of the blood flow. The study showed that in an inclined artery, the size of the wall shear stress at stenosis throat increases as values of the applied magnetic field rise while it diminishes as the values of both the chemical reaction and porosity parameters increase. The study assumed that the flow is one dimensional and the effect of vibration was not in place.

The study on the influence of heat and chemical reactions on blood flow through an anisotropically tapered elastic arteries with overlapping stenosis was presented by Mekheimer *et al.* (2012). The blood was considered to be a micropolar fluid. The effect of varying the Soret number on concentration was done. The study showed that the concentration of the fluid decreases as the Soret number increases. The study did not involve the effect of body acceleration.

On the other hand, the effect of chemical reaction parameter received little attention.

Sarojamma *et al.* (2012) explained, that when blood flows in large vessels it shows the characteristics of Newtonian fluid, but when it flows in smaller diameter vessels, the apparent viscosity of blood increases markedly and hence shows a highly non-Newtonian character. The study of blood flow in the vascular system is complicated in many respects and thus simplifying assumptions are often made for the purpose of analysis. In large vessels of 1 to 3cm in diameter, where shear rates are high, blood is assumed to have constant viscosity and thus is assumed to be Newtonian (Khambhampati, 2013). Noutchie (2005) explained that blood flow in large arteries and clearly showed that in the larger vessels it is reasonable to assume blood has a constant viscosity, because the vessel diameters are large compared to the individual cell diameters and because shear rates are high enough for viscosity to be independent of them. Hence in these vessels the non-Newtonian behavior becomes insignificant and blood can be considered to be a Newtonian fluid.

Zaman *et al.* (2015) pointed out that, it is generally accepted that the rheological behavior of blood is assumed as Newtonian for values of shear rate greater than $100s^{-1}$ and a such situation occurs in larger arteries. But in smaller arteries the blood does not obey the Newtonian postulate and therefore cannot be modeled as a Newtonian fluid. Categorically, blood is classified as a non-Newtonian fluid. Tu and Deville (1996), Gijsen *et al.* (1999) and Rodkiewicz *et al.* (1990) concluded that it is very crucial that blood is modeled as a non – Newtonian fluid. The Herschel-Bulkley fluid is of general type and can be reduced to Newtonian, Bingham plastic and Power-law fluid models, by selecting appropriate flow parameters (Biswas & Laskar, 2011). According to Vajravelu *et al.* (2011), the Herschel-Bulkley constitutive equation contains one more parameter than the Casson equation does, and thus more information about the blood properties can be obtained when the Herschel-Bulkley equation is used than when the Casson one is used.

The current work studies blood flow in both cases, Newtonian and Non-Newtonian. In both cases the human body is assumed to be subjected to the magnetic fields, body acceleration and the chemical reactions. Blood is considered to flow in a tube (artery) with plaques/stenosis. The results obtained in both cases are compared.

CHAPTER THREE

MATERIALS AND METHODS

This chapter presents the model assumptions, formulation of the models and the solution of the models. The chapter is divided into two sub-chapters. The first section assumes that the blood is Newtonian in nature, in the second section blood is considered in its non-Newtonian character. In both sub-chapters, the assumptions considered are stipulated, then models formulated and the corresponding boundary conditions prescribed. Non-dimensionalisation is done and the method used to solve the formulated models explained.

3.1 Newtonian model for MHD arterial blood flow and mass transfer

In this section blood flow through a stenosed artery in the presence of magnetic fields, body acceleration and chemical reaction is considered. All these situations that may disturb the normal flow of blood, may be physically manifested through a case of magnetic therapy taken to a patient to reduce pain in sports.

3.1.1 Mathematical formulation of the theoretical model for the Newtonian case

The mathematical formulation, the following assumptions were considered:

(i) ***The flow is unsteady***: In this regard, the velocity varies with time and space. Throughout the study, it will therefore mathematically be considered partial derivative $\frac{\partial}{\partial t}(.) \neq 0$.

(ii) ***The flow is two dimensional***: The current study considers that two spatial variables describe the flow. In this case the two space variables are the radial direction and the axial direction, that is r and z.

(iii) ***The flow is laminar***: In this case, it is assumed that blood flows in infinitesimal parallel layers with no any disruption between them. That is, the layers slide in parallel, with no eddies or mixing. The study therefore is of streamline flow.

(iv) ***The flow is axisymmetric***: In this case, it is assumed that, the cylindrical velocity components are independent of the angular variable θ. This means that there is also no variation of the velocity with angle θ, therefore, $\frac{\partial}{\partial \theta}(.) = 0$ with $z-$ axis coinciding with the axis of symmetry of the flow.

(v) ***The flow is incompressible***: This takes into account that, the material density, ρ, of the blood is a constant, variations with pressure are considered negligible.

(vi) ***The flow is fully-developed***: In this case, it is assumed that the momentum of the fluid does not change in the flow direction. The momentum is considered to be changing only in the radial direction.

(vii) ***The fluid is Newtonian***: In this particular section, blood is assumed to follow Newton's law of viscosity where the shear stress τ is directly proportional to the velocity gradient.

(viii) Magnetic field B_0 is applied in the direction perpendicular to that of blood flow.

(ix) Electrical conductivity σ is constant.

(x) Diffusion coefficient D is constant.

(xi) The force due to electric field is very small compared with the Lorentz force due to magnetic field.

Figure 6, is the schematic blood flow diagram, where r and z are the radial and axial directions whose corresponding velocities are respectively u and v. B_0 is the applied magnetic field intensity, r_0 is the radius of the normal artery, δ is the protuberance of the stenosis, $2z_0$ is the length of stenosis, and $h(z)$ represents the radius of the stenosed artery.

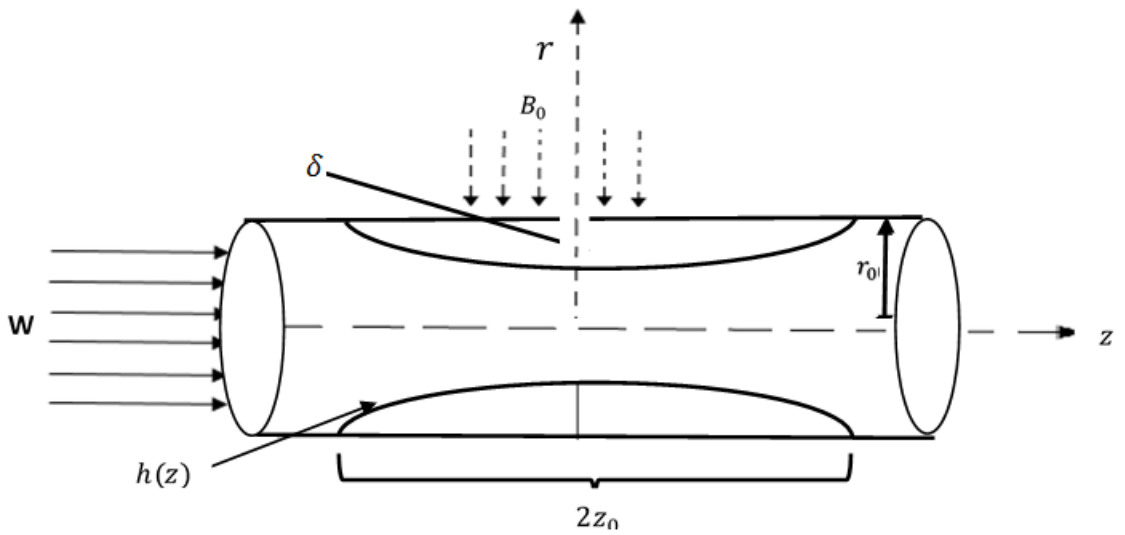

Figure 6: Schematic flow diagram

In cylindrical polar coordinate, under the mentioned assumptions, equations 1.12, 1,21, and 1,24 of respectively, continuity, motion and mass concentration reduce to:

$$\frac{\partial u}{\partial r}+\frac{u}{r}+\frac{\partial w}{\partial z}=0 \tag{3.1}$$

$$\rho\left(\frac{\partial u}{\partial t}+u\frac{\partial u}{\partial r}+w\frac{\partial u}{\partial z}\right)=-\frac{\partial P}{\partial r}+\mu\left(\frac{\partial^2 u}{\partial r^2}+\frac{1}{r}\frac{\partial u}{\partial r}-\frac{u}{r^2}+\frac{\partial^2 u}{\partial z^2}\right) \tag{3.2}$$

$$\rho\left(\frac{\partial w}{\partial t}+u\frac{\partial w}{\partial r}+w\frac{\partial w}{\partial z}\right)=-\frac{\partial P}{\partial z}+\mu\left(\frac{\partial^2 w}{\partial r^2}+\frac{1}{r}\frac{\partial w}{\partial r}+\frac{\partial^2 w}{\partial z^2}\right)+G(t)-\sigma B_0^2 w \tag{3.3}$$

$$\left(\frac{\partial C}{\partial t}+u\frac{\partial C}{\partial r}+w\frac{\partial C}{\partial z}\right)=D\left(\frac{\partial^2 C}{\partial r^2}+\frac{1}{r}\frac{\partial C}{\partial r}+\frac{\partial^2 C}{\partial z^2}\right)-\beta C \tag{3.4}$$

where ρ is the density of the blood, μ is its viscosity, P is the pressure, $G(t)$ is the body acceleration, C is the concentration, t is the time, D and β are the diffusion coeffient and chemical reaction parameters, respectively.

In the radial direction it is assumed that the pressure gradient is small due to the fact that the lumen radius of an artery is small in comparison to the pressure wave. Under such assumption therefore, the radial pressure gradient $\frac{\partial P}{\partial r}\approx 0$. Following Ismail *et al.* (2008), the pressure gradient in axial direction can be written as seen in equation 3.5:

$$-\frac{\partial P}{\partial z}=A_0+A_1\cos(n_1 t) \tag{3.5}$$

Where A_0 is the steady state part of pressure gradient, A_1 is the amplitude of pulsatile blood flow that gives rise to systolic and diastolic pressure, $n_1=2\pi f_1$, with f_1 being the pulse frequency. On other hand, according to Nagarani and Sarojamma (2007), body acceleration term $G(t)$ may be given as equation 3.6.

$$G(t)=\rho a_0\cos(n_2 t+\psi) \tag{3.6}$$

Where ρa_0 is the amplitude of body acceleration, $n_2=2\pi f_2$, with f_2 being body acceleration frequency, and ψ is the phase angle.

The equations can now be re-written as follows, see equations 3.1-3.4:

$$\frac{\partial u}{\partial r}+\frac{u}{r}+\frac{\partial w}{\partial z}=0 \tag{3.7}$$

$$\rho\left(\frac{\partial u}{\partial t}+u\frac{\partial u}{\partial r}+w\frac{\partial u}{\partial z}\right)=\mu\left(\frac{\partial^2 u}{\partial r^2}+\frac{1}{r}\frac{\partial u}{\partial r}-\frac{u}{r^2}+\frac{\partial^2 u}{\partial z^2}\right) \tag{3.8}$$

$$\begin{aligned}\rho\left(\frac{\partial w}{\partial t}+u\frac{\partial w}{\partial r}+w\frac{\partial w}{\partial z}\right)&=A_0+A_1\cos(n_1 t)+\mu\left(\frac{\partial^2 w}{\partial r^2}+\frac{1}{r}\frac{\partial w}{\partial r}+\frac{\partial^2 w}{\partial z^2}\right)\\&\quad+\rho a_0\cos(n_2 t+\psi)-\sigma B_0^2 w\end{aligned} \tag{3.9}$$

$$\left(\frac{\partial C}{\partial t}+u\frac{\partial C}{\partial r}+w\frac{\partial C}{\partial z}\right)=D\left(\frac{\partial^2 C}{\partial r^2}+\frac{1}{r}\frac{\partial C}{\partial r}+\frac{\partial^2 C}{\partial z^2}\right)-\beta C \tag{3.10}$$

Following Das and Saha (2009), the geometry of stenosis (Fig. 4) can mathematically be expressed as follows:

$$h(z) = \begin{cases} r_0 - \delta\left(1 + \cos\frac{\pi z}{z_0}\right) & -z_0 \leq z \leq z_0 \\ r_0 & \text{otherwise} \end{cases} \tag{3.11}$$

3.1.2 Boundary and initial conditions

In this part, the initial and boundary conditions are prescribed. In this work it is assumed there is no slip condition on the arterial wall. See equation 3.12:

$$u(r,z,t) = w(r,z,t) = 0 \quad \text{at} \quad r = h(z) \tag{3.12}$$

and at the center of the artery (at the line of symmetry) it is assumed that there is no shear rate and no radial flow. See equation 3.13 hereunder:

$$\frac{\partial w(r,z,t)}{\partial r} = u(r,z,t) = 0 \quad \text{at} \quad r = 0 \tag{3.13}$$

Similarly, for concentration, the boundary conditions are as shown in equation 3.14

$$\frac{\partial C(r,z,t)}{\partial r} = C(r,z,t) = 0 \quad \text{at} \quad r = h(z) \tag{3.14}$$

Since blood can flow even in the absence of magnetic field and body acceleration, it is therefore assumed that initially, there is non-zero velocity and concentration when $t = 0$. This is as shown in equation 3.15:

$$u(r,z,0) = u_0, \quad w(r,z,0) = w_0, \quad C(r,z,0) = C_0 \tag{3.15}$$

3.1.3 Skin friction

After determining the velocity, one can now easily determine the skin friction factor C_f. The skin friction in this regard, is the friction between the stenosed arterial wall and the fluid. Consider first the arterial wall shear stress τ_w as shown in equation 3.16.

$$\tau_w = \mu \frac{\partial w}{\partial r}\bigg|_{r=h(z)} \tag{3.16}$$

The skin friction is defined as:

$$C_f = \frac{\tau_w}{\rho w_c^2} \tag{3.17}$$

3.1.4 Non- dimensionalisation of variables

In this part the non-dimensional variables are introduced. The fluid's characteristic velocity and distance w_c and r_0 respectively are used. The w_c is assumed to be average blood's velocity flowing along the artery and r_0 is the radius of normal artery.

$$\eta = \frac{r}{r_0}, \quad z^* = \frac{z}{r_0}, \quad w^* = \frac{w}{w_c}, \quad u^* = \frac{u}{w_c}, \quad t^* = \frac{tw_c}{r_0}, \quad a_0^* = \frac{a_0 r_0}{w_c^2}, \quad A_0^* = \frac{A_0 r_0}{\rho w_c^2} \tag{3.18}$$

$$m_1 = \frac{r_0 n_1}{w_c}, \quad m_2 = \frac{r_0 n_2}{w_c}, \quad A_1^* = \frac{A_1 r_0}{\rho w_c^2}, \quad e = \frac{\delta}{r_0}, \quad C^* = \frac{C}{C_0}, \quad D^* = \frac{D}{\upsilon^2}, \quad \beta^* = \frac{\beta r_0^2}{\upsilon} \tag{3.19}$$

Now substitution of the non-dimensional variables into equations 3.7 to 3.17 is done. Upon substitution, the continuity equation 3.7 becomes:

$$\frac{w_c}{r_0}\left(\frac{\partial u^*}{\partial \eta} + \frac{u^*}{\eta} + \frac{\partial w^*}{\partial z^*}\right) = 0, \tag{3.20}$$

dividing throughout equation 3.20 by $\frac{w_c}{r_0}$ yields equation 3.21 below

$$\frac{\partial u^*}{\partial \eta} + \frac{u^*}{\eta} + \frac{\partial w^*}{\partial z^*} = 0, \tag{3.21}$$

Equation 3.21 above is our continuity equation in non-dimensional form. Again, substitution of the non dimensional variables into $u-$ momentum equation 3.8 is done.

$$\frac{\rho w_c^2}{r_0}\left(\frac{\partial u^*}{\partial t^*} + u^*\frac{\partial u^*}{\partial \eta} + w^*\frac{\partial u^*}{\partial z^*}\right) = \frac{\mu w_c}{r_0^2}\left(\frac{\partial^2 u^*}{\partial \eta^2} + \frac{1}{\eta}\frac{\partial u^*}{\partial \eta} - \frac{u^*}{\eta^2} + \frac{\partial^2 u^*}{\partial z^{*2}}\right) \tag{3.22}$$

dividing equation 3.22 by $\frac{\rho w_c^2}{r_0}$ leads to equation 3.23 hereunder:

$$\frac{\partial u^*}{\partial t^*} + u^*\frac{\partial u^*}{\partial \eta} + w^*\frac{\partial u^*}{\partial z^*} = \frac{\mu}{\rho r_0 w_c}\left(\frac{\partial^2 u^*}{\partial \eta^2} + \frac{1}{\eta}\frac{\partial u^*}{\partial \eta} - \frac{u^*}{\eta^2} + \frac{\partial^2 u^*}{\partial z^{*2}}\right) \tag{3.23}$$

which can be written as

$$\frac{\partial u^*}{\partial t^*} + u^*\frac{\partial u^*}{\partial \eta} + w^*\frac{\partial u^*}{\partial z^*} = \frac{1}{Re}\left(\frac{\partial^2 u^*}{\partial \eta^2} + \frac{1}{\eta}\frac{\partial u^*}{\partial \eta} - \frac{u^*}{\eta^2} + \frac{\partial^2 u^*}{\partial z^{*2}}\right) \tag{3.24}$$

where Re in equation 3.24 is the Reynolds's number defined as $Re = \frac{\rho w_c r_0}{\mu}$.

Similarly, the $v-$ momentum equation 3.9 becomes:

$$\frac{\rho w_c^2}{r_0}\left(\frac{\partial w^*}{\partial t^*} + u^*\frac{\partial w^*}{\partial \eta} + w^*\frac{\partial w^*}{\partial z^*}\right) = \frac{\rho w_c^2}{r_0}\left(A_0^* + A_1^*\cos m_1 t^*\right) + \frac{\mu w_c}{r_0^2}\left(\frac{\partial^2 w^*}{\partial \eta^2} + \frac{1}{\eta}\frac{\partial w^*}{\partial \eta} + \frac{\partial^2 w^*}{\partial z^{*2}}\right)$$
$$+ \frac{\rho w_c^2}{r_0}\cos(m_2 t^* + \psi) - w_c \sigma B_0^2 w^*, \tag{3.25}$$

dividing equation 3.25 by $\frac{\rho w_c^2}{r_0}$ leads to equation 3.26 hereunder:

$$\frac{\partial w^*}{\partial t^*} + u^* \frac{\partial w^*}{\partial \eta} + w^* \frac{\partial w^*}{\partial z^*} = A_0^* + A_1^* \cos m_1 t^* + \frac{\mu}{\rho r_0 w_c} \left(\frac{\partial^2 w^*}{\partial \eta^2} + \frac{1}{\eta} \frac{\partial w^*}{\partial \eta} + \frac{\partial^2 w^*}{\partial z^{*2}} \right) + \cos(m_2 t^* + \psi) - \frac{r_0 B_0^2 \sigma}{\rho w_c} w^* \tag{3.26}$$

which can be written as:

$$\frac{\partial w^*}{\partial t^*} + u^* \frac{\partial w^*}{\partial \eta} + w^* \frac{\partial w^*}{\partial z^*} = A_0^* + A_1^* \cos m_1 t^* + \frac{1}{Re} \left(\frac{\partial^2 w^*}{\partial \eta^2} + \frac{1}{\eta} \frac{\partial w^*}{\partial \eta} + \frac{\partial^2 w^*}{\partial z^{*2}} \right) + \cos(m_2 t^* + \psi) - \frac{H_a^2}{Re} w^* \tag{3.27}$$

where H_a is the Hartman number given as $H_a = r_0 B_0 \sqrt{\frac{\sigma}{\mu}}$.
One can then apply the non-dimensional variables to the concentration equation 3.10.

$$\frac{w_c C_0}{r_0} \left(\frac{\partial C^*}{\partial t^*} + u^* \frac{\partial C^*}{\partial \eta} + w^* \frac{\partial C^*}{\partial z^*} \right) = \frac{\upsilon C_0 D^*}{r_0^2} \left(\frac{\partial^2 C^*}{\partial \eta^2} + \frac{1}{\eta} \frac{\partial C^*}{\partial \eta} + \frac{\partial^2 C^*}{\partial z^{*2}} \right) - \frac{\upsilon C_0}{r_0^2} \beta C^* \tag{3.28}$$

dividing equation 3.28 by $\frac{w_c C_0}{r_0}$ gives the equation 3.29:

$$\frac{\partial C^*}{\partial t^*} + u^* \frac{\partial C^*}{\partial \eta} + w^* \frac{\partial C^*}{\partial z^*} = \frac{\upsilon D^*}{r_0 w_c} \left(\frac{\partial^2 C^*}{\partial \eta^2} + \frac{1}{\eta} \frac{\partial C^*}{\partial \eta} + \frac{\partial^2 C^*}{\partial z^{*2}} \right) - \frac{\upsilon}{r_0 w_c} \beta C^* \tag{3.29}$$

Equation 3.29 above can be written as shown in equation 3.30

$$\frac{\partial C^*}{\partial t^*} + u^* \frac{\partial C^*}{\partial \eta} + w^* \frac{\partial C^*}{\partial z^*} = \frac{1}{ScRe} \left(\frac{\partial^2 C^*}{\partial \eta^2} + \frac{1}{\eta} \frac{\partial C^*}{\partial \eta} + \frac{\partial^2 C^*}{\partial z^{*2}} \right) - \frac{1}{Re} \beta C^* \tag{3.30}$$

where Sc is the Schmidt number defined as $Sc = \frac{\upsilon}{D}$

The boundary and initial conditions in non-dimensional form becomes:

$$u^*(\eta, z^*, t^*) = w^*(\eta, z^*, t^*) = C^*(\eta, z^*, t^*) = 0 \qquad \text{at} \quad \eta = H(z^*) \tag{3.31}$$

$$\frac{\partial w(\eta, z^*, t^*)}{\partial \eta} = \frac{\partial C(\eta, z^*, t^*)}{\partial \eta} = u^*(\eta, z^*, t^*) = 0 \qquad \text{at} \quad \eta = 0 \tag{3.32}$$

$$u^*(\eta, z^*, 0) = U_0 \quad w^*(\eta, z^*, 0) = W_0 \quad C^*(\eta, z^*, 0) = c_0 \tag{3.33}$$

For convenience, the asterisks are dropped, yielding to the following model equations in non-dimensional form:

$$\frac{\partial u}{\partial \eta}+\frac{u}{\eta}+\frac{\partial w}{\partial z}=0 \tag{3.34}$$

$$\frac{\partial u}{\partial t}+u\frac{\partial u}{\partial \eta}+w\frac{\partial u}{\partial z}=\frac{1}{Re}\left(\frac{\partial^2 u}{\partial \eta^2}+\frac{1}{\eta}\frac{\partial u}{\partial \eta}-\frac{u}{\eta^2}+\frac{\partial^2 u}{\partial z^2}\right) \tag{3.35}$$

$$\begin{aligned}\frac{\partial w}{\partial t}+u\frac{\partial w}{\partial \eta}+w\frac{\partial w}{\partial z}=&A_0+A_1\cos m_1 t+\frac{1}{Re}\left(\frac{\partial^2 w}{\partial \eta^2}+\frac{1}{\eta}\frac{\partial w}{\partial \eta}+\frac{\partial^2 w}{\partial z^2}\right)\\&+\cos(m_2 t+\psi)-\frac{H_a^2}{Re}w\end{aligned} \tag{3.36}$$

$$\frac{\partial C}{\partial t}+u\frac{\partial C}{\partial \eta}+w\frac{\partial C}{\partial z}=\frac{1}{ScRe}\left(\frac{\partial^2 C}{\partial \eta^2}+\frac{1}{\eta}\frac{\partial C}{\partial \eta}+\frac{\partial^2 C}{\partial z^2}\right)-\frac{1}{Re}\beta C \tag{3.37}$$

subject to conditions:

$$u(\eta,z,t)=w(\eta,z,t)=C(\eta,z,t)=0 \qquad \text{at} \quad \eta=H(z) \tag{3.38}$$

$$\frac{\partial w(\eta,z,t)}{\partial \eta}=\frac{\partial C(\eta,z,t)}{\partial \eta}=u(\eta,z,t)=0 \qquad \text{at} \quad \eta=0 \tag{3.39}$$

$$u(\eta,z,0)=U_0 \quad w(\eta,z,0)=W_0 \quad C(\eta,z,0)=c_0 \tag{3.40}$$

On the other hand, skin friction (see equation 3.17) in non dimensionless form becomes:

$$C_f=\frac{1}{Re}\frac{\partial w}{\partial \eta} \tag{3.41}$$

3.1.5 Radial coordinate transformation

In this section the transformation of the equations from cylindrical to rectangular domain is done. The artery is taken to be cylindrical, with stenosis, Therefore transforming the constriction, another variable ξ is introduced, such that

$$\xi=\frac{\eta}{H(z)} \tag{3.42}$$

This suitable radial coordinate transformation helps to map the constricted domain into a rectangular one. Equation3.42 above has the effect of immobilizing the arterial wall in the transformed coordinate ξ. Using equation 3.42 and re-arranging, equations 3.34-3.41 become:

$$\frac{1}{H}\frac{\partial u}{\partial \xi}+\frac{u}{H\xi}+\frac{\partial w}{\partial z}-\frac{\xi}{H}\frac{dH}{dz}\frac{\partial w}{\partial \xi}=0 \tag{3.43}$$

$$\frac{\partial u}{\partial t}=-\frac{u\partial u}{H\partial \xi}-w\left(\frac{\partial u}{\partial z}-\frac{\xi}{H}\frac{dH}{dz}\frac{\partial u}{\partial \xi}\right)+\frac{1}{ReH^2}\left(\frac{\partial^2 u}{\partial \xi^2}+\frac{1}{\xi}\frac{\partial u}{\partial \xi}-\frac{u}{\xi^2}\right)+$$
$$\frac{1}{Re}\left[\frac{\partial^2 u}{\partial z^2}-\frac{2\xi}{H}\frac{dH}{dz}\frac{\partial^2 u}{\partial \xi \partial z}-\frac{\xi}{H}\frac{d^2H}{dz^2}\frac{\partial u}{\partial \xi}+\frac{\xi^2}{H^2}\left(\frac{dH}{dz}\right)^2\frac{\partial^2 u}{\partial \xi^2}+\frac{3\xi}{H^2}\left(\frac{dH}{dz}\right)^2\frac{\partial u}{\partial \xi}\right] \tag{3.44}$$

$$\frac{\partial w}{\partial t}=-\frac{u\partial w}{H\partial \xi}-w\left(\frac{\partial w}{\partial z}-\frac{\xi}{H}\frac{dH}{dz}\frac{\partial w}{\partial \xi}\right)+(A_0+A_1\cos(m_1 t))+a_0\cos(m_2 t+\psi)$$
$$+\frac{1}{ReH^2}\left(\frac{\partial^2 w}{\partial \xi^2}+\frac{1}{\xi}\frac{\partial w}{\partial \xi}\right)-\frac{1}{Re}H_a^2+$$
$$\frac{1}{Re}\left[\frac{\partial^2 w}{\partial z^2}-\frac{2\xi}{H}\frac{dH}{dz}\frac{\partial^2 w}{\partial \xi \partial z}-\frac{\xi}{H}\frac{d^2H}{dz^2}\frac{\partial w}{\partial \xi}+\frac{\xi^2}{H^2}\left(\frac{dH}{dz}\right)^2\frac{\partial^2 w}{\partial \xi^2}+\frac{3\xi}{H^2}\left(\frac{dH}{dz}\right)^2\frac{\partial w}{\partial \xi}\right] \tag{3.45}$$

$$\frac{\partial C}{\partial t}=-\frac{u\partial C}{H\partial \xi}-w\left(\frac{\partial C}{\partial z}-\frac{\xi}{H}\frac{dH}{dz}\frac{\partial C}{\partial \xi}\right)+\frac{1}{ScReH^2}\left(\frac{\partial^2 C}{\partial \xi^2}+\frac{1}{\xi}\frac{\partial C}{\partial \xi}\right)-\frac{1}{Re}\beta C+ \tag{3.46}$$
$$\frac{1}{ScRe}\left[\frac{\partial^2 C}{\partial z^2}-\frac{2\xi}{H}\frac{dH}{dz}\frac{\partial^2 C}{\partial \xi \partial z}-\frac{\xi}{H}\frac{d^2H}{dz^2}\frac{\partial C}{\partial \xi}+\frac{\xi^2}{H^2}\left(\frac{dH}{dz}\right)^2\frac{\partial^2 C}{\partial \xi^2}+\frac{3\xi}{H^2}\left(\frac{dH}{dz}\right)^2\frac{\partial C}{\partial \xi}\right]$$

subject to:

$$u(\xi,z,t)=w(\xi,z,t)=C(\xi,z,t)=0 \qquad \text{at} \quad \xi=1 \tag{3.47}$$

$$\frac{\partial w(\xi,z,t)}{\partial \xi}=\frac{\partial C(\xi,z,t)}{\partial \xi}=u(\xi,z,t)=0 \qquad \text{at} \quad \xi=0 \tag{3.48}$$

$$u(\xi,z,0)=U_0 \quad w(\xi,z,0)=W_0 \quad C(\xi,z,0)=c_0 \tag{3.49}$$

And, the skin friction (equation 3.41) becomes:

$$C_f=\frac{1}{ReH}\frac{\partial w}{\partial \xi}\bigg|_{\xi=1} \tag{3.50}$$

3.1.6 Radial velocity transformation

The radial velocity $u(\xi,z,t)$ is now obtained in terms of the axial velocity $w(\xi,z,t)$. The continuity equation 3.43 is then multiplied by ξH and then integrate it with respect to ξ. This leads to equation 3.51.

$$u(\xi,z,t)=\xi\frac{dH}{dz}w-\frac{2}{H}\frac{dH}{dz}\int_0^\xi w\xi d\xi-\frac{H}{\xi}\int_0^\xi \xi\frac{\partial w}{\partial z}d\xi \tag{3.51}$$

Applying our boundary conditions, yields equation 3.52:

$$\int_0^1 \frac{2}{H}\frac{dH}{dz}w\xi d\xi=-\frac{H}{\xi}\int_0^1 \xi\frac{\partial w}{\partial z}d\xi \tag{3.52}$$

Comparing the integrals and integrands of equation 3.52, results into equation 3.53:

$$\frac{\partial w}{\partial z}=-\frac{2}{H}\frac{dH}{dz}w \tag{3.53}$$

Substituting equation 3.53 into 3.51 yields

$$u(\xi,z,t) = \xi \frac{dH}{dz} w \tag{3.54}$$

Equation 3.54 is the radial velocity component expressed in terms of axial velocity.
Now, substitution of the radial velocity obtained into $v-$ momentum equation (see equation 3.45) and into the concentration equation (see equation 3.46) is done. Also, using the product rule one ca easily find the derivatives $\frac{\partial u}{\partial \xi}$ and $\frac{\partial u}{\partial z}$ as shown in equations 3.55 and 3.56

$$\frac{\partial u}{\partial \xi} = \frac{dH}{dz}\left(\xi \frac{\partial w}{\partial \xi} + w\right) \tag{3.55}$$

$$\frac{\partial u}{\partial z} = \xi\left(\frac{dH}{dz}\frac{\partial w}{\partial z} + w\frac{d^2H}{dz^2}\right) \tag{3.56}$$

This process therefore, eliminates u, and write radial velocity u in terms of axial velocity w. In this regard, the equations 3.57 and 3.58 are easily obtained. These are the model equations that need to be numerically solved.

$$\begin{aligned}\frac{\partial w}{\partial t} = &-\left(\frac{\xi}{H}\frac{dH}{dz}w\right)\frac{\partial w}{\partial \xi} - w\left(\frac{\partial w}{\partial z} - \frac{\xi}{H}\frac{dH}{dz}\frac{\partial w}{\partial \xi}\right) + (A_0 + A_1\cos(m_1 t)) + a_0\cos(m_2 t + \psi) \\ &+ \frac{1}{ReH^2}\left(\frac{\partial^2 w}{\partial \xi^2} + \frac{1}{\xi}\frac{\partial w}{\partial \xi}\right) - \frac{1}{Re}H_a^2 w + \\ &\frac{1}{Re}\left[\frac{\partial^2 w}{\partial z^2} - \frac{2\xi}{H}\frac{dH}{dz}\frac{\partial^2 w}{\partial \xi \partial z} - \frac{\xi}{H}\frac{d^2H}{dz^2}\frac{\partial w}{\partial \xi} + \frac{\xi^2}{H^2}\left(\frac{dH}{dz}\right)^2\frac{\partial^2 w}{\partial \xi^2} + \frac{3\xi}{H^2}\left(\frac{dH}{dz}\right)^2\frac{\partial w}{\partial \xi}\right]\end{aligned} \tag{3.57}$$

$$\begin{aligned}\frac{\partial C}{\partial t} = &-\left(\frac{\xi}{H}\frac{dH}{dz}w\right)\frac{\partial C}{\partial \xi} - w\left(\frac{\partial C}{\partial z} - \frac{\xi}{H}\frac{dH}{dz}\frac{\partial C}{\partial \xi}\right) + \frac{1}{ScReH^2}\left(\frac{\partial^2 C}{\partial \xi^2} + \frac{1}{\xi}\frac{\partial C}{\partial \xi}\right) - \frac{1}{Re}\beta C + \\ &\frac{1}{ScRe}\left[\frac{\partial^2 C}{\partial z^2} - \frac{2\xi}{H}\frac{dH}{dz}\frac{\partial^2 C}{\partial \xi \partial z} - \frac{\xi}{H}\frac{d^2H}{dz^2}\frac{\partial C}{\partial \xi} + \frac{\xi^2}{H^2}\left(\frac{dH}{dz}\right)^2\frac{\partial^2 C}{\partial \xi^2} + \frac{3\xi}{H^2}\left(\frac{dH}{dz}\right)^2\frac{\partial C}{\partial \xi}\right]\end{aligned} \tag{3.58}$$

The model equations above, are solved subject to the boundary and initial conditions expressed in equations 3.47-3.49.

3.1.7 Numerical Discretization by Finite Difference Method

In this section, the solution of the problem is obtained. Equations 3.57 and 3.58 are non-linear, therefore, it is very difficult to find its analytical solution subject to the boundary described by equations 3.47-3.49. Therefore, a numerical procedure has been employed to obtain the solution of problem (see sub-section 3.1.8 below).

3.1.8 Finite difference schemes

The finite difference method (FDM) substitutes derivatives in the governing field equations by difference quotients, which comprise values of the solution at discrete mesh points in the area under study. That is for all numerical solutions, the continuous partial differential equations are written in finite difference form. The numerical solution is identified only at a finite number of points in the physical domain. There are several finite difference techniques that can be applied to solve the model equations. In this study, the explicit finite difference method was employed, where quantities at time $k+1$ depend explicitly on quantities at time k.

The finite difference scheme is based on the use of the central difference approximations to discretize all the spatial derivatives and the explicit forward finite difference approximation to discretize the time derivatives. This is done in the following manner:

$$\frac{\partial w}{\partial \xi} = \frac{w^k_{i,j+1} - w^k_{i,j-1}}{2\Delta\xi}, \frac{\partial^2 w}{\partial \xi^2} = \frac{w^k_{i,j+1} - 2w^k_{i,j} + w^k_{i,j-1}}{(\Delta\xi)^2}, \frac{\partial w}{\partial t} = \frac{w^{k+1}_{i,j} - w^k_{i,j}}{\Delta t} \tag{3.59}$$

$$\frac{\partial w}{\partial z} = \frac{w^k_{i+1,j} - w^k_{i-1,j}}{2\Delta z}, \frac{\partial^2 w}{\partial z^2} = \frac{w^k_{i+1,j} - 2w^k_{i,j} + w^k_{i-1,j}}{(\Delta z)^2} \tag{3.60}$$

Similar expressions are also obtained for other spatial derivatives of $C(i,j,k)$. See equation 3.61 and 3.62 here under:

$$\frac{\partial C}{\partial \xi} = \frac{C^k_{i,j+1} - C^k_{i,j-1}}{2\Delta\xi}, \frac{\partial^2 C}{\partial \xi^2} = \frac{C^k_{i,j+1} - 2C^k_{i,j} + C^k_{i,j-1}}{(\Delta\xi)^2}, \frac{\partial C}{\partial t} = \frac{C^{k+1}_{i,j} - C^k_{i,j}}{\Delta t} \tag{3.61}$$

$$\frac{\partial C}{\partial z} = \frac{C^k_{i+1,j} - C^k_{i-1,j}}{2\Delta z}, \frac{\partial^2 C}{\partial z^2} = \frac{C^k_{i+1,j} - 2C^k_{i,j} + C^k_{i-1,j}}{(\Delta z)^2} \tag{3.62}$$

where $\Delta\xi$ is the increment in radial direction, Δz is the increment in axial direction and Δt is the increment in time.

Also the discretization of $w(i,j,k)$ and $C(i,j,k)$ is done by writing it as $w^k_{i,j}$ and $C^k_{i,j}$ respectively.

It is further defined:

$$\xi_j = (j-1)\Delta\xi; \quad j = 1,2,3,...,N+1 \quad \text{where,} \quad \xi_{N+1} = 1 \tag{3.63}$$

$$z_i = (j-1)\Delta z; \quad i = 1,2,3,...,M+1 \tag{3.64}$$

$$t_k = (k-1)\Delta t; \quad k = 1,2,3... \tag{3.65}$$

The boundary conditions (see equation 3.47-3.49) are also discretized. The Neumann boundary

condition at $\xi = 0$ is given as:

$$\frac{\partial w}{\partial \xi} = \frac{w^k_{i,j+1} - w^k_{i,j-1}}{2\Delta\xi} = 0 \tag{3.66}$$

This gives, $w^k_{i,j+1} - w^k_{i,j-1} = 0$ which implies that $w^k_{i,j+1} = w^k_{i,j-1}$. Now at $\xi = 0$ implies that $j = 1$ which eventually gives $w^k_{i,2} = w^k_{i,0}$. Since $w^k_{i,0}$ is a ghost point, the derivative $\left.\frac{\partial w}{\partial \xi}\right|_{j=1}$ is now approximated using the denominator $\Delta\xi$ as shown in equation 3.67.

$$\left.\frac{\partial w}{\partial \xi}\right|_{j=1} = \frac{w^k_{i,j+1} - w^k_{i,j}}{\Delta\xi} = 0 \tag{3.67}$$

which gives $w^k_{i,2} = w^k_{i,1}$. In the same way, the Neumann boundary condition is obtained at $\xi = 0$. Thus, the discretized conditions are as given in equation 3.68.

$$w^k_{i,2} = w^k_{i,1}, \quad C^k_{i,2} = C^k_{i,1}, \quad w^1_{i,j} = W_0, \quad C^1_{i,j} = c_0 \tag{3.68}$$

the initial axial velocity $W_0 = W(\xi)$ is given as

$$W_0 = \left(\frac{A_0 + A_1}{4}\right)\left(1 - (H\xi_i)^2\right) \tag{3.69}$$

The equations (3.59)-(3.62) are then substituted into equations 3.57 and 3.58. This gives (in discretized form) the equations 3.70 and 3.71. In this regard, $w^k_{i,j+1}$ and $C^k_{i,j+1}$ are made the subject of the formula.

$$\begin{aligned}
w^k_{i,j+1} =& w^k_{i,j} - \Delta t\left[\frac{\xi_j}{H_i}\left(\frac{dH}{dz}\right)_i\left(\frac{w^k_{i,j+1} - w^k_{i,j-1}}{2\Delta\xi}\right)\right] + (A_0 + A_1\cos(m_1 t)) + a_0\cos(m_2 t + \psi) \\
&-\Delta t w^k_{i,j}\left[\frac{w^k_{i+1,j} - w^k_{i-1,j}}{2\Delta z} - \frac{\xi_j}{H_i}\left(\frac{dH}{dz}\right)_i\frac{w^k_{i,j+1} - w^k_{i,j-1}}{2\Delta\xi}\right] \\
&+\frac{\Delta t}{ReH^2}\left[\frac{w^k_{i,j+1} - 2w^k_{i,j} + w^k_{i,j-1}}{(\Delta\xi)^2} + \frac{1}{\xi_j}\left(\frac{w^k_{i,j+1} - w^k_{i,j-1}}{2\Delta\xi}\right)\right] \\
&+\frac{\Delta t}{Re}\left[\frac{w^k_{i+1,j} - 2w^k_{i,j} + w^k_{i-1,j}}{(\Delta z)^2} - \frac{2\xi_j}{H_i}\left(\frac{dH}{dz}\right)_i\left(\frac{w^k_{i+1,j+1} - w^k_{i-1,j+1} - w^k_{i+1,j-1} + w^k_{i-1,j-1}}{4\Delta\xi\Delta z}\right)\right] \\
&-\frac{\Delta t\xi_j}{ReH_i}\left(\frac{d^2H}{dz^2}\right)_i\left(\frac{w^k_{i,j+1} - w^k_{i,j-1}}{2\Delta\xi}\right) + \frac{\Delta t\xi_j^2}{ReH_i^2}\left(\frac{dH}{dz}\right)^2_i\left(\frac{w^k_{i,j+1} - 2w^k_{i,j} + w^k_{i,j-1}}{(\Delta\xi)^2}\right) \\
&+\frac{3\Delta t\xi_j}{ReH_i^2}\left(\frac{dH}{dz}\right)^2_i\left(\frac{w^k_{i,j+1} - w^k_{i,j-1}}{2\Delta\xi}\right) - \frac{\Delta t}{Re}Ha^2 w^k_{i,j}
\end{aligned} \tag{3.70}$$

$$
\begin{aligned}
C_{i,j+1}^{k} =& C_{i,j}^{k} - \Delta t \left[\frac{\xi_j}{H_i} \left(\frac{dH}{dz} \right)_i \left(\frac{C_{i,j+1}^{k} - C_{i,j-1}^{k}}{2\Delta\xi} \right) \right] \\
& - \Delta t w_{i,j}^{k} \left[\frac{C_{i+1,j}^{k} - C_{i-1,j}^{k}}{2\Delta z} - \frac{\xi_j}{H_i} \left(\frac{dH}{dz} \right)_i \frac{C_{i,j+1}^{k} - C_{i,j-1}^{k}}{2\Delta\xi} \right] \\
& + \frac{\Delta t}{ReScH^2} \left[\frac{C_{i,j+1}^{k} - 2C_{i,j}^{k} + C_{i,j-1}^{k}}{(\Delta\xi)^2} + \frac{1}{\xi_j} \left(\frac{C_{i,j+1}^{k} - C_{i,j-1}^{k}}{2\Delta\xi} \right) \right] \\
& + \frac{\Delta t}{ReSc} \left[\frac{C_{i+1,j}^{k} - 2C_{i,j}^{k} + C_{i-1,j}^{k}}{(\Delta z)^2} - \frac{2\xi_j}{H_i} \left(\frac{dH}{dz} \right)_i \left(\frac{C_{i+1,j+1}^{k} - C_{i-1,j+1}^{k} - C_{i+1,j-1}^{k} + C_{i-1,j-1}^{k}}{4\Delta\xi\Delta z} \right) \right] \\
& - \frac{\Delta t \xi_j}{ReScH_i} \left(\frac{d^2H}{dz^2} \right)_i \left(\frac{C_{i,j+1}^{k} - C_{i,j-1}^{k}}{2\Delta\xi} \right) + \frac{\Delta t \xi_j^2}{ReScH_i^2} \left(\frac{dH}{dz} \right)_i^2 \left(\frac{C_{i,j+1}^{k} - 2C_{i,j}^{k} + C_{i,j-1}^{k}}{(\Delta\xi)^2} \right) \\
& + \frac{3\Delta t \xi_j}{ReScH_i^2} \left(\frac{dH}{dz} \right)_i^2 \left(\frac{C_{i,j+1}^{k} - C_{i,j-1}^{k}}{2\Delta\xi} \right) - \frac{\Delta t \beta}{Re} C_{i,j}^{k}
\end{aligned} \tag{3.71}
$$

The skin friction in discretized form is as shown in equation 3.72

$$
C_{f_i} = \frac{1}{ReH_i} \frac{w_{i,j+1}^{k} - w_{i,j}^{k}}{\Delta\xi} \tag{3.72}
$$

3.2 Magnetohydrodynamics blood flow through a stenosed artery, a case of non-Newtonian model

In this sub-section, a mathematical model of MHD flow of blood through a stenosed artery is studied. Blood is considered to be non-Newtonian of Herschel-Bulkley type. Effects of mass and heat transfer on the flow are investigated in the presence of body acceleration, magnetic fields and chemical reaction.

3.2.1 Theoretical model formulation of the problem

In this work, it is considered that the flow is unsteady, laminar, two-dimensional, pulsatile, incompressible, and axisymmetric in the sense that there is no variation of the velocity with the angle θ in the cylindrical polar coordinate system (r, θ, z), with the z-axis coinciding with the axis of symmetry of the flow. The blood is considered to behave as a non - Newtonian fluid satisfying the Herschel-Bulkley model. Furthermore, body acceleration $(G(t))$, and the strength of magnetic field (B_0) act in the axial direction of the artery. Biologically, every cell in the body can produce heat which needs to be spread around the body, and this is done by the blood, which heats some organs and cools others by conduction and other processes. Thus,

the study takes into account the presence of the chemical reaction such as exothermic reaction. Figure 7 shows the schematic diagram of the stenosed artery.

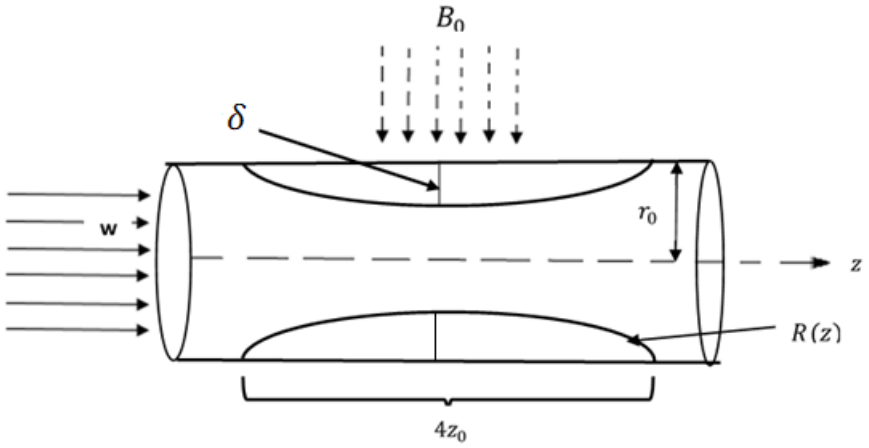

Figure 7: Schematic diagram of the stenosed artery

where δ is the height of stenosis and $4z_0$ is the total length of stenosis.

The geometry of stenosis using cosine function is defined as shown in equation 3.73

$$R(z) = \begin{cases} r_0 - \delta\left(1+\cos\frac{\pi z}{2z_0}\right) & -2z_0 \le z \le 2z_0 \\ r_0 & \text{otherwise} \end{cases} \tag{3.73}$$

Under mentioned assumptions, the equations for the z and r components of momentum together with the equation of continuity, energy and concentration in the cylindrical coordinate system are as shown in equations 3.74-3.78:

$$\frac{\partial u}{\partial r} + \frac{u}{r} + \frac{\partial w}{\partial z} = 0 \tag{3.74}$$

$$\rho\left(\frac{\partial u}{\partial t} + u\frac{\partial u}{\partial r} + w\frac{\partial u}{\partial z}\right) = -\frac{\partial P}{\partial r} + \frac{1}{r}\frac{\partial(r\tau_{rr})}{\partial r} + \frac{\partial(\tau_{rz})}{\partial z} \tag{3.75}$$

$$\rho\left(\frac{\partial w}{\partial t} + u\frac{\partial w}{\partial r} + w\frac{\partial w}{\partial z}\right) = -\frac{\partial P}{\partial z} + \frac{1}{r}\frac{\partial(r\tau_{rz})}{\partial r} + \frac{\partial(\tau_{zz})}{\partial z} + F(t) - \sigma B_0^2 w \tag{3.76}$$

$$\rho c_p\left(\frac{\partial T}{\partial t} + u\frac{\partial T}{\partial r} + w\frac{\partial T}{\partial z}\right) = k\left(\frac{\partial^2 T}{\partial r^2} + \frac{1}{r}\frac{\partial T}{\partial r} + \frac{\partial^2 T}{\partial z^2}\right) + \tau_{rr}\frac{\partial u}{\partial r} + \tau_{rz}\frac{\partial w}{\partial r} + \tau_{rz}\frac{\partial u}{\partial z} + \tau_{zz}\frac{\partial w}{\partial z} \tag{3.77}$$

$$\left(\frac{\partial C}{\partial t} + u\frac{\partial C}{\partial r} + w\frac{\partial C}{\partial z}\right) = D_f\left(\frac{\partial^2 C}{\partial r^2} + \frac{1}{r}\frac{\partial C}{\partial r} + \frac{\partial^2 C}{\partial z^2}\right) + \frac{D_f K_T}{T_0}\left(\frac{\partial^2 T}{\partial r^2} + \frac{1}{r}\frac{\partial T}{\partial r} + \frac{\partial^2 T}{\partial z^2}\right) - \beta(C - C_0) \tag{3.78}$$

In the above equations, u, w, T and C are respectively radial velocity, axial velocity, temperature and concentration of the fluid. $c_p, k, K_T, D_f,$ and β are, respectively the specific heat capacity, thermal conductivity, the thermal-diffusion ratio, diffusion coefficient, and chemical reaction parameter. Furthermore, τ_{rr}, and τ_{zz} represent the normal stress components. τ_{rz} is the shear stress component. The current study considers that blood obeys the Herschel-Bulkley constitutive model. The stress tensor components are as given in equation 3.79.

$$\begin{aligned} \tau_{ij} &= \left(K\dot{\gamma}^{n-1} + \frac{\tau_0}{\dot{\gamma}} \right) \dot{\gamma}_{ij} \quad \text{for} \quad \tau \geq \tau_0 \\ \dot{\gamma} &= 0 \quad \text{for} \quad \tau < \tau_0 \end{aligned} \tag{3.79}$$

where, K is the consistency index, n is the flow behavior index and τ_0 is the yield stress at zero shear rate.

Now,from equation 3.79 the shear stresses are written as shown in equations 3.80-3.82.

$$\tau_{rr} = 2\left(K\dot{\gamma}^{n-1} + \tau_0\dot{\gamma}^{-1}\right)\left(\frac{\partial u}{\partial r}\right) \tag{3.80}$$

$$\tau_{zz} = 2\left(K\dot{\gamma}^{n-1} + \tau_0\dot{\gamma}^{-1}\right)\left(\frac{\partial w}{\partial z}\right) \tag{3.81}$$

$$\tau_{rz} = 2\left(K\dot{\gamma}^{n-1} + \tau_0\dot{\gamma}^{-1}\right)\left(\frac{\partial u}{\partial z} + \frac{\partial w}{\partial r}\right) \tag{3.82}$$

The pulsatile pressure gradient which is responsible for driving the blood's flow in the axial direction and the body acceleration term are as given in equation 3.5 and 3.6 respectively.

3.2.2 Boundary and initial conditions

The boundary and initial conditions for the developed model are as shown in equations 3.83-3.87

$$w(r,z,t) = 0, \quad u(r,z,t) = 0 \quad \text{on} \quad r = R(z) \tag{3.83}$$

$$\frac{\partial w(r,z,t)}{\partial r} = 0, \quad u(r,z,t) = 0 \quad \text{on} \quad r = 0 \tag{3.84}$$

$$\frac{\partial T(r,z,t)}{\partial r} = 0, \quad \text{on} \quad r = 0 \quad \text{and} \quad T(r,z,t) = T_w \quad \text{on} \quad r = R(z) \tag{3.85}$$

$$\frac{\partial C(r,z,t)}{\partial r} = 0, \quad \text{on} \quad r = 0 \quad \text{and} \quad C(r,z,t) = C_w \quad \text{on} \quad r = R(z) \tag{3.86}$$

$$u(r,z,0) = u_0, \quad w(r,z,0) = w_0, \quad C(r,z,0) = C_0 \tag{3.87}$$

where, T_w, C_w stands for arterial wall temperature and concentration on the arterial wall, respectively.

3.2.3 Non - dimensionalisation of the model variables

In this section, the non-dimensional variables are introduced. It is considered that, w_c as the average fluid's velocity which is therefore the characteristic velocity. It is also defined that, r_0 as the radius of normal artery. The dimensionless variables are now as shown in equations 3.88 to 3.90.

$$\eta = \frac{r}{r_0}, \quad w^* = \frac{w}{w_c}, \quad u^* = \frac{u}{w_c}, \quad t^* = \frac{tw_c}{r_0}, \quad z^* = \frac{z}{r_0}, \quad P^* = \frac{P}{\rho w_c^2}, \tag{3.88}$$

$$A_0^* = \frac{A_0 r_0}{\rho w_c^2}, \quad A_1^* = \frac{A_1 r_0}{\rho w_c^2}, \quad m_1 = \frac{r_0 m_1}{w_c}, \quad m_2 = \frac{r_0 m_2}{w_c}, \quad a_0^* = \frac{r_0 a_0}{w_c^2}, \quad \tau_{ij}^* = \frac{\tau_{ij}}{\rho w_c^2} \tag{3.89}$$

$$T^* = \frac{T - T_0}{T_w - T_0}, \quad C^* = \frac{C - C_0}{C_w - C_0}, \quad \beta^* = \frac{\beta r_0^2}{\nu}, \quad e = \frac{\delta}{r_0} \quad R^*(z^*) = \frac{R(z)}{r_0}. \tag{3.90}$$

Now, substitution of equations 3.88 to 3.90 into equations 3.74-3.87 is done. However, for convenience, the asterisk/stars are dropped.

$$\frac{\partial u}{\partial \eta} + \frac{u}{\eta} + \frac{\partial w}{\partial z} = 0 \tag{3.91}$$

$$\frac{\partial u}{\partial t} + u\frac{\partial u}{\partial \eta} + w\frac{\partial u}{\partial z} = \frac{\partial P}{\partial \eta} + \left(\frac{\partial \tau_{rr}}{\partial \eta} + \frac{1}{\eta}\tau_{rr} + \frac{\partial \tau_{rz}}{\partial z}\right) \tag{3.92}$$

$$\begin{aligned}\frac{\partial w}{\partial t} + u\frac{\partial w}{\partial \eta} + w\frac{\partial w}{\partial z} &= (A_0 + A_1\cos(m_1 t)) + \left(\frac{\partial \tau_{rz}}{\partial \eta} + \frac{1}{\eta}\tau_{rz} + \frac{\partial \tau_{zz}}{\partial z}\right) \\ &\quad + a_0\cos(m_2 t + \psi) - \frac{H_a^2}{R_{eG}}w\end{aligned} \tag{3.93}$$

$$\begin{aligned}\frac{\partial T}{\partial t} + u\frac{\partial T}{\partial \eta} + w\frac{\partial T}{\partial z} &= \frac{1}{P_e}\left(\frac{\partial^2 T}{\partial \eta^2} + \frac{\partial T}{\eta \partial \eta} + \frac{\partial^2 T}{\partial z^2}\right) \\ &\quad + E_c\left[\tau_{rr}\frac{\partial u}{\partial \eta} + \tau_{rz}\frac{\partial w}{\partial \eta} + \tau_{rz}\frac{\partial u}{\partial z} + \tau_{zz}\frac{\partial w}{\partial z}\right]\end{aligned} \tag{3.94}$$

$$\begin{aligned}\frac{\partial C}{\partial t} + u\frac{\partial C}{\partial \eta} + w\frac{\partial C}{\partial z} &= \frac{1}{P_e}\left(\frac{\partial^2 C}{\partial \eta^2} + \frac{1}{\eta}\frac{\partial C}{\partial \eta} + \frac{\partial^2 C}{\partial z^2}\right) \\ &\quad + S_r\left(\frac{\partial^2 T}{\partial \eta^2} + \frac{1}{\eta}\frac{\partial T}{\partial \eta} + \frac{\partial^2 T}{\partial z^2}\right) - \frac{\beta C}{Re}\end{aligned} \tag{3.95}$$

Where, $R_{eG} = \dfrac{r_0^n \rho}{K w_c^{n-2}}$, $Ha = B_0\sqrt{\dfrac{\sigma r_0^{n+1}}{K w_c^{n-1}}}$, $P_e = \dfrac{\rho w_c r_0 c_p}{k}$, $E_c = \dfrac{w_c^2}{c_p(T_w - T_0)}$ and $S_r = \dfrac{D_f K_T (T_w - T_0)}{\nu T_m (C_w - C_0)}$ are the, generalized Reynold, Hartman, Peclet, Eckert, and Soret numbers respectively (see appendix 1 for more elaboration on the generalized Reynolds and Hartman numbers). The stress component in non-dimensional form is as shown in equation 3.96.

$$\begin{aligned}\tau_{ij} &= \left(\frac{1}{R_{eG}}\dot{\gamma}^{n-1} + \tau_0\dot{\gamma}^{-1}\right)\dot{\gamma}_{ij} \\ \dot{\gamma} &= 0 \quad \text{for} \quad \tau < \tau_0\end{aligned} \tag{3.96}$$

with second invariant of the rate of strain given in equation 3.97

$$\dot{\gamma} = \sqrt{2\left[\left(\frac{\partial u}{\partial \eta}\right)^2 + \left(\frac{u}{\eta}\right)^2 + \left(\frac{\partial w}{\partial z}\right)^2\right] + \left(\frac{\partial u}{\partial z} + \frac{\partial w}{\partial \eta}\right)^2} \tag{3.97}$$

and

$$\tau_{rr} = 2\left(R_{eG}\dot{\gamma}^{n-1} + \tau_0\dot{\gamma}^{-1}\right)\left(\frac{\partial u}{\partial \eta}\right) \tag{3.98}$$

$$\tau_{zz} = 2\left(R_{eG}\dot{\gamma}^{n-1} + \tau_0\dot{\gamma}^{-1}\right)\left(\frac{\partial w}{\partial z}\right) \tag{3.99}$$

$$\tau_{rz} = 2\left(R_{eG}\dot{\gamma}^{n-1} + \tau_0\dot{\gamma}^{-1}\right)\left(\frac{\partial u}{\partial z} + \frac{\partial w}{\partial \eta}\right) \tag{3.100}$$

subject to the dimensionless initial and boundary conditions

$$w(\eta,z,0) = w_0, \quad T(\eta,z,0) = T_0, \quad C(\eta,z,0) = C_0 \tag{3.101}$$

$$w(\eta,z,t) = u(\eta,z,t) = 0, T(\eta,z,t) = T_w, C(\eta,z,t) = C_w \quad \text{on} \quad \eta = R(z) \tag{3.102}$$

$$\frac{\partial w(\eta,z,t)}{\partial \eta} = \quad \frac{\partial T(\eta,z,t)}{\partial \eta} = \frac{\partial C(\eta,z,t)}{\partial \eta} = u(\eta,z,t) = 0, \text{on}\eta = 0 \tag{3.103}$$

3.2.4 Transformation of domain

To obtain the numerical solution, the cylindrical domain is transformed into the rectangular domain by using the following radial transformation, then the new variable ξ is introduced such that $\xi = \frac{\eta}{R(z)}$. This transformation, leads to equations 3.104-3.115. This method of transforming the constricted part into rectangular domain was also adapted by Nezamidoost *et al.* (2013), Mustapha and Amin (2008), Changidar and De (2015), Mandal (2005), Majee and Shit (2017) and Joshua *et al.* (2020).

$$\frac{1}{R}\frac{\partial u}{\partial \xi}+\frac{u}{R\xi}+\frac{\partial w}{\partial z}-\frac{\xi}{R}\frac{dR}{dz}\frac{\partial w}{\partial \xi}=0 \tag{3.104}$$

$$\frac{\partial u}{\partial t}=-\frac{\partial P}{R\partial \xi}-\frac{u\partial u}{R\partial \xi}-w\left(\frac{\partial u}{\partial z}-\frac{\xi}{R}\frac{dR}{dz}\frac{\partial u}{\partial \xi}\right)+\frac{1}{R}\frac{\partial \tau_{\xi\xi}}{\partial \xi}+\frac{\tau_{\xi\xi}}{R\xi}+\frac{\partial \tau_{\xi z}}{\partial z}-\frac{\xi}{R}\frac{dR}{dz}\frac{\partial \tau_{\xi z}}{\partial \xi} \tag{3.105}$$

$$\begin{aligned}\frac{\partial w}{\partial t}=&(A_0+A_1\cos(m_1 t))-\frac{u\partial w}{R\partial \xi}-w\left(\frac{\partial w}{\partial z}-\frac{\xi}{R}\frac{dR}{dz}\frac{\partial w}{\partial \xi}\right)+\frac{1}{R}\frac{\partial \tau_{\xi z}}{\partial \xi}+\frac{\tau_{\xi z}}{H\xi}+\frac{\partial \tau_{zz}}{\partial z}\\&-\frac{\xi}{R}\frac{dR}{dz}\frac{\partial \tau_{zz}}{\partial \xi}+a_0\cos(m_2 t+\psi)-\frac{H_a^2}{R_{eG}}w\end{aligned} \tag{3.106}$$

$$\begin{aligned}\frac{\partial T}{\partial t}=&-\frac{u\partial T}{R\partial \xi}-w\left(\frac{\partial T}{\partial z}-\frac{\xi}{R}\frac{dR}{dz}\frac{\partial T}{\partial \xi}\right)+\frac{1}{P_e}\left(\frac{\partial^2 T}{R^2\partial \xi^2}+\frac{1}{R^2\xi}\frac{\partial T}{\partial \xi}+\frac{\partial^2 T}{\partial z^2}\right)\\&+\frac{1}{P_e}\left[\frac{3\xi}{R^2}\left(\frac{dR}{dz}\right)^2\frac{\partial T}{\partial \xi}-\frac{2\xi}{R}\frac{dR}{dz}\frac{\partial^2 T}{\partial \xi\partial z}-\frac{\xi}{R}\frac{d^2R}{dz^2}\frac{\partial T}{\partial \xi}+2\left(\frac{\xi}{R}\frac{dR}{dz}\right)^2\frac{\partial^2 T}{\partial \xi^2}\right]\\&+E_c\left(\frac{\tau_{\xi\xi}}{R}\frac{\partial u}{\partial \xi}+\frac{\tau_{\xi z}}{R}\frac{\partial w}{\partial \xi}\right)+E_c\tau_{\xi z}\left(\frac{\partial u}{\partial z}-\frac{\xi}{R}\frac{dR}{dz}\frac{\partial u}{\partial \xi}\right)+E_c\tau_{zz}\left(\frac{\partial w}{\partial z}-\frac{\xi}{R}\frac{dR}{dz}\frac{\partial w}{\partial \xi}\right)\end{aligned} \tag{3.107}$$

$$\begin{aligned}\frac{\partial C}{\partial t}=&-\frac{u\partial C}{R\partial \xi}-w\left(\frac{\partial C}{\partial z}-\frac{\xi}{R}\frac{dR}{dz}\frac{\partial C}{\partial \xi}\right)+\frac{1}{P_e}\left(\frac{\partial^2 C}{R^2\partial \xi^2}+\frac{1}{R^2\xi}\frac{\partial C}{\partial \xi}+\frac{\partial^2 C}{\partial z^2}\right)\\&+\frac{1}{P_e}\left[\frac{3\xi}{R^2}\left(\frac{dR}{dz}\right)^2\frac{\partial C}{\partial \xi}-\frac{2\xi}{R}\frac{dR}{dz}\frac{\partial^2 C}{\partial \xi\partial z}-\frac{\xi}{R}\frac{d^2R}{dz^2}\frac{\partial C}{\partial \xi}+2\left(\frac{\xi}{R}\frac{dR}{dz}\right)^2\frac{\partial^2 C}{\partial \xi^2}\right]-\frac{\beta C}{Re}\\&+S_r\left[\frac{3\xi}{R^2}\left(\frac{dR}{dz}\right)^2\frac{\partial T}{\partial \xi}-\frac{2\xi}{R}\frac{dR}{dz}\frac{\partial^2 T}{\partial \xi\partial z}-\frac{\xi}{R}\frac{d^2R}{dz^2}\frac{\partial T}{\partial \xi}+2\left(\frac{\xi}{R}\frac{dR}{dz}\right)^2\frac{\partial^2 T}{\partial \xi^2}\right]\end{aligned} \tag{3.108}$$

With,

$$\dot{\gamma}=\sqrt{2\left[\left(\frac{\partial u}{R\partial \xi}\right)^2+\left(\frac{u}{R\xi}\right)^2+\left(\frac{\partial w}{\partial z}-\frac{\xi}{R}\frac{dR}{dz}\frac{\partial w}{\partial \xi}\right)^2\right]+\left(\frac{\partial u}{\partial z}-\frac{\xi}{R}\frac{dR}{dz}\frac{\partial u}{\partial \xi}+\frac{\partial w}{R\partial \xi}\right)^2} \tag{3.109}$$

$$\tau_{\xi\xi}=2\left(R_{eG}\dot{\gamma}^{n-1}+\tau_0\dot{\gamma}^{-1}\right)\left(\frac{\partial u}{R\partial \xi}\right) \tag{3.110}$$

$$\tau_{zz}=2\left(R_{eG}\dot{\gamma}^{n-1}+\tau_0\dot{\gamma}^{-1}\right)\left(\frac{\partial w}{\partial z}-\frac{\xi}{R}\frac{dR}{dz}\frac{\partial w}{\partial \xi}\right) \tag{3.111}$$

$$\tau_{\xi z}=2\left(R_{eG}\dot{\gamma}^{n-1}+\tau_0\dot{\gamma}^{-1}\right)\left(\frac{\partial u}{\partial z}-\frac{\xi}{R}\frac{dR}{dz}\frac{\partial u}{\partial \xi}+\frac{\partial w}{\partial \eta}\right) \tag{3.112}$$

Radial transformation leads to the following boundary and initial conditions:

$$w(\xi,z,0)=w_0,\quad T(\xi,z,0)=T_0,\quad C(\xi,z,0)=C_0 \tag{3.113}$$

$$w(\xi,z,t)=u(\xi,z,t)=0,\quad T(\xi,z,t)=T_w, C(\xi,z,t)=C_w\quad\text{on}\quad \xi=1 \tag{3.114}$$

$$\frac{\partial w(\xi,z,t)}{\partial \xi}=\quad\frac{\partial T(\xi,z,t)}{\partial \xi}=\quad\frac{\partial C(\xi,z,t)}{\partial \xi}=\quad u(\xi,z,t)=0,\quad\text{on}\quad \xi=0 \tag{3.115}$$

3.2.5 Transformation of the Radial velocity

In this part, the radial velocity is obtained, this will be substituted into $v-$ momentum, energy and concentration equations. The equation 3.104 is multiplied by $\xi R(z)$ and then integrated with respect to ξ to obtain equation 3.116:

$$\int \xi \frac{\partial u}{\partial \xi} d\xi + \int u d\xi + \int \xi R \frac{\partial w}{\partial z} d\xi + \int \xi^2 \frac{dR}{dz} \frac{\partial w}{\partial \xi} d\xi \tag{3.116}$$

Re-arranging equation 3.116 yields equation 3.117:

$$\int \xi \frac{\partial u}{\partial \xi} d\xi + \int u d\xi = \int \xi^2 \frac{dR}{dz} \frac{\partial w}{\partial \xi} d\xi - \int \xi R \frac{\partial w}{\partial z} d\xi \tag{3.117}$$

Applying integration by parts and simplifying the equation 3.117 results into equation 3.118:

$$u = \frac{dR}{dz} \xi w - \frac{2}{\xi} \frac{dR}{dz} \int w \xi d\xi - \frac{R}{\xi} \int \xi \frac{\partial w}{\partial z} d\xi \tag{3.118}$$

Making use of the boundary conditions in equations 3.114 and 3.115 and making re-arrangement, the equation 3.119 is obtained:

$$\frac{2}{\xi} \frac{dR}{dz} \int_0^1 w \xi d\xi = -\frac{R}{\xi} \int_0^1 \xi \frac{\partial w}{\partial z} d\xi \tag{3.119}$$

Multiplying by ξ and dividing by R yields 3.120

$$\frac{2}{R} \frac{dR}{dz} \int_0^1 w \xi d\xi = -\int_0^1 \xi \frac{\partial w}{\partial z} d\xi \tag{3.120}$$

Now, making comparison of the integrals and the integrands of equation 3.120, the equation 3.121 is obtained.

$$\frac{\partial w}{\partial z} = -\frac{2}{R} \frac{dR}{dz} w \tag{3.121}$$

Now substitution of equation 3.121 into equation 3.119 is done. Such substitution gives equation 3.122:

$$u = \frac{dR}{dz} \xi w - \frac{2}{\xi} \frac{dR}{dz} \int w \xi d\xi - \frac{R}{\xi} \int \xi \left(-\frac{2}{R} \frac{dR}{dz} w \right) d\xi \tag{3.122}$$

which simplifies to equation 3.123:

$$u = \left(\xi \frac{dR}{dz} w \right) \tag{3.123}$$

Equation 3.123 above, is the radial velocity component which needs to be calculated. Now, the substitution of this radial velocity into axial momentum, energy and concentration equations is done. Also, using the product rule the derivatives, $\frac{\partial u}{\partial \xi} = \frac{dR}{dz} \left(\xi \frac{\partial w}{\partial \xi} + w \right)$ and

$\frac{\partial u}{\partial z} = \xi\left(\frac{dR}{dz}\frac{\partial w}{\partial z} + w\frac{d^2R}{dz^2}\right)$ are obtained. This process therefore eliminates u, as the radial velocity u is now written in terms of axial velocity w. This gives equations 3.124-3.130. These equations are later written in the discretized form.

$$\frac{\partial w}{\partial t} = (A_0 + A_1\cos(m_1 t)) - \left(\xi\frac{dR}{dz}w\right)\frac{\partial w}{R\partial\xi} - w\left(\frac{\partial w}{\partial z} - \frac{\xi}{H}\frac{dR}{dz}\frac{\partial w}{\partial\xi}\right) + \frac{1}{R}\frac{\partial\tau_{\xi z}}{\partial\xi} + \frac{\tau_{\xi z}}{R\xi} + \frac{\partial\tau_{zz}}{\partial z} - \frac{\xi}{R}\frac{dR}{dz}\frac{\partial\tau_{zz}}{\partial\xi} + a_0\cos(m_2 t + \psi) - \frac{H_a^2}{R_{eG}}w \tag{3.124}$$

$$\begin{aligned}\frac{\partial T}{\partial t} =& -\left(\frac{\xi}{R}\frac{dR}{dz}w\right)\frac{\partial T}{\partial\xi} - w\left(\frac{\partial T}{\partial z} - \frac{\xi}{R}\frac{dR}{dz}\frac{\partial T}{\partial\xi}\right) + \frac{1}{P_e}\left(\frac{\partial^2 T}{R^2\partial\xi^2} + \frac{1}{R^2\xi}\frac{\partial T}{\partial\xi} + \frac{\partial^2 T}{\partial z^2}\right)\\ &+ \frac{1}{P_e}\left[\frac{3\xi}{R^2}\left(\frac{dR}{dz}\right)^2\frac{\partial T}{\partial\xi} - \frac{2\xi}{R}\frac{dR}{dz}\frac{\partial^2 T}{\partial\xi\partial z} - \frac{\xi}{R}\frac{d^2R}{dz^2}\frac{\partial T}{\partial\xi} + 2\left(\frac{\xi}{R}\frac{dR}{dz}\right)^2\frac{\partial^2 T}{\partial\xi^2}\right]\\ &+ E_c\left[\frac{\tau_{\xi\xi}}{R}\frac{dR}{dz}\left(\xi\frac{\partial w}{\partial\xi} + w\right) + \frac{\tau_{\xi z}}{R}\frac{\partial w}{\partial\xi}\right] + E_c\tau_{\xi z}\left[\xi\left(\frac{dR}{dz}\frac{\partial w}{\partial z} + w\frac{d^2R}{dz^2}\right)\right]\\ &- E_c\tau_{\xi z}\left[\frac{\xi}{R}\left(\frac{dR}{dz}\right)^2\left(\xi\frac{\partial w}{\partial\xi} + w\right)\right] + E_c\tau_{\xi z}\left(\frac{\partial w}{\partial z} - \frac{\xi}{R}\frac{dR}{dz}\frac{\partial w}{\partial\xi}\right)\end{aligned} \tag{3.125}$$

$$\begin{aligned}\frac{\partial C}{\partial t} =& -\left(\frac{\xi}{R}\frac{dR}{dz}w\right)\frac{\partial C}{\partial\xi} - w\left(\frac{\partial C}{\partial z} - \frac{\xi}{R}\frac{dR}{dz}\frac{\partial C}{\partial\xi}\right) + \frac{1}{P_e}\left(\frac{\partial^2 C}{R^2\partial\xi^2} + \frac{1}{R^2\xi}\frac{\partial C}{\partial\xi} + \frac{\partial^2 C}{\partial z^2}\right)\\ &+ \frac{1}{P_e}\left[\frac{3\xi}{R^2}\left(\frac{dR}{dz}\right)^2\frac{\partial C}{\partial\xi} - \frac{2\xi}{R}\frac{dR}{dz}\frac{\partial^2 C}{\partial\xi\partial z} - \frac{\xi}{R}\frac{d^2R}{dz^2}\frac{\partial C}{\partial\xi} + 2\left(\frac{\xi}{R}\frac{dR}{dz}\right)^2\frac{\partial^2 C}{\partial\xi^2}\right]\\ &+ S_r\left[\frac{3\xi}{R^2}\left(\frac{dR}{dz}\right)^2\frac{\partial T}{\partial\xi} - \frac{2\xi}{R}\frac{dR}{dz}\frac{\partial^2 T}{\partial\xi\partial z} - \frac{\xi}{R}\frac{d^2R}{dz^2}\frac{\partial T}{\partial\xi} + 2\left(\frac{\xi}{R}\frac{dR}{dz}\right)^2\frac{\partial^2 T}{\partial\xi^2}\right]\\ &+ S_r\left(\frac{\partial^2 T}{R^2\partial\xi^2} + \frac{1}{R^2\xi}\frac{\partial T}{\partial\xi} + \frac{\partial^2 T}{\partial z^2}\right) - \frac{\beta C}{Re}\end{aligned} \tag{3.126}$$

With,

$$\dot{\gamma} = \sqrt{\begin{aligned}&(2\left[\left(\frac{dR}{Rdz}\left(\xi\frac{\partial w}{\partial\xi} + w\right)\right)^2 + \left(\frac{dR}{Rdz}w\right)^2 + \left(\frac{\partial w}{dz} - \frac{\xi}{R}\frac{dR}{dz}\frac{\partial w}{\partial\xi}\right)^2\right] +\\ &\left(\xi\left(\frac{dR}{dz}\frac{\partial w}{\partial z} + w\frac{d^2R}{dz^2}\right) - \frac{\xi}{R}\frac{dR}{dz}\frac{dR}{dz}\left(\xi\frac{\partial w}{\partial\xi} + w\right) + \frac{\partial w}{R\partial\xi}\right)^2\end{aligned}} \tag{3.127}$$

and

$$\tau_{\xi\xi} = 2\left(R_{eG}\dot{\gamma}^{n-1} + \tau_0\dot{\gamma}^{-1}\right)\left(\frac{dR}{dz}\left(\xi\frac{\partial w}{\partial\xi} + w\right)\right) \tag{3.128}$$

$$\tau_{zz} = 2\left(R_{eG}\dot{\gamma}^{n-1} + \tau_0\dot{\gamma}^{-1}\right)\left(\frac{\partial w}{\partial z} - \frac{\xi}{R}\frac{dR}{dz}\frac{\partial w}{\partial\xi}\right) \tag{3.129}$$

$$\tau_{\xi z} = 2\left(R_{eG}\dot{\gamma}^{n-1} + \tau_0\dot{\gamma}^{-1}\right)\left[\xi\left(\frac{dR}{dz}\frac{\partial w}{\partial z} + w\frac{d^2R}{dz^2}\right) - \frac{\xi}{R}\left(\frac{dR}{dz}\right)^2\left(\xi\frac{\partial w}{\partial\xi} + w\right) + \frac{\partial w}{R\partial\xi}\right] \tag{3.130}$$

3.2.6 Numerical discretization by Finite difference method

In this part, the application of the finite difference discretization scheme to solve nonlinear model equations 3.124-3.126 is done. The finite difference schemes are based on the central difference approximations for all the spatial derivatives and the explicit forward finite difference approximation to discretize the time derivative. The approximate derivatives are as given here under equations 3.131-3.133. Similar method was adapted by Liu and Liu (2020), Zaman and Khan (2020), Haghighi and Aliashrafi (2018), Priyadharshini and Ponalagusamy (2019), Reddy *et al.* (2017), Sankar *et al.* (2010) and Hossain and Haque (2017).

$$\frac{\partial w}{\partial \xi} = \frac{w^k_{i,j+1} - w^k_{i,j-1}}{2\Delta\xi}, \frac{\partial^2 w}{\partial \xi^2} = \frac{w^k_{i,j+1} - 2w^k_{i,j} + w^k_{i,j-1}}{(\Delta\xi)^2}, \frac{\partial w}{\partial t} = \frac{w^{k+1}_{i,j} - w^k_{i,j}}{\Delta t} \tag{3.131}$$

$$\frac{\partial T}{\partial \xi} = \frac{T^k_{i,j+1} - T^k_{i,j-1}}{2\Delta\xi}, \frac{\partial^2 T}{\partial \xi^2} = \frac{T^k_{i,j+1} - 2T^k_{i,j} + T^k_{i,j-1}}{(\Delta\xi)^2}, \frac{\partial T}{\partial t} = \frac{T^{k+1}_{i,j} - T^k_{i,j}}{\Delta t} \tag{3.132}$$

$$\frac{\partial C}{\partial \xi} = \frac{C^k_{i,j+1} - C^k_{i,j-1}}{2\Delta\xi}, \frac{\partial^2 C}{\partial \xi^2} = \frac{C^k_{i,j+1} - 2T^k_{i,j} + T^k_{i,j-1}}{(\Delta\xi)^2}, \frac{\partial C}{\partial t} = \frac{C^{k+1}_{i,j} - C^k_{i,j}}{\Delta t} \tag{3.133}$$

Partial derivatives with respect to z are obtained in a similar manner, furthermore, the approximations of derivatives of $\tau_{\xi z}$, and τ_{zz} are as given in equation 3.134

$$\frac{\partial \tau_{\xi z}}{\partial \xi} = \frac{\left(\tau_{\xi z}\right)^k_{i,j+1} - \left(\tau_{\xi z}\right)^k_{i,j-1}}{2\Delta\xi}, \frac{\partial \tau_{zz}}{\partial \xi} = \frac{(\tau_{zz})^k_{i,j+1} - (\tau_{zz})^k_{i,j-1}}{2\Delta\xi}, \frac{\partial \tau_{zz}}{\partial z} = \frac{(\tau_{zz})^k_{i+1,j} - (\tau_{zz})^k_{i-1,j}}{2\Delta z} \tag{3.134}$$

where ξ_j, t_k and z_i are as defined in equations 3.63-3.65. Now, substitution of equations 3.131-3.134 into equations 3.124-3.130 and make subject $w, T,$ and C is done. The discretization of radial velocity from equation 3.123 is also included. This yields the equations 3.135-3.144 in discretized form.

$$u^{k+1}_{i,j} = \xi_j \left(\frac{dR}{dz}\right)_i w^k_{i,j} \tag{3.135}$$

$$\begin{aligned} w^{k+1}_{i,j} = {} & w^k_{i,j} + \Delta t \left(A_0 + A_1 \cos(m_1 t_k) + a_0 \cos(m_2 t_k + \psi) - \frac{H_a^2}{R_{eG}} w^k_{i,j}\right) \\ & - \Delta t \left(\frac{\xi_j}{R_i}\left(\frac{dR}{dz}\right)_i w^k_{i,j}\right)\left(\frac{w^k_{i,j+1} - w^k_{i,j-1}}{2\Delta\xi}\right) - \Delta t w^k_{i,j}\left(\frac{w^k_{i+1,j} - w^k_{i-1,j}}{2\Delta z}\right) \\ & + \Delta t w^k_{i,j} \frac{\xi_j}{R_i}\left(\frac{dR}{dz}\right)_i \left(\frac{w^k_{i,j+1} - w^k_{i,j-1}}{2\Delta\xi}\right) - \frac{\xi_j}{R_i}\left(\frac{dR}{dz}\right)_i \left(\frac{(\tau_{zz})^k_{i,j+1} - (\tau_{zz})^k_{i,j-1}}{2\Delta\xi}\right) \\ & + \Delta t \left[\frac{1}{R_i}\left(\frac{\left(\tau_{\xi z}\right)^k_{i,j+1} - \left(\tau_{\xi z}\right)^k_{i,j-1}}{2\Delta\xi}\right) + \frac{\left(\tau_{\xi z}\right)^k_{i,j}}{R_i \xi_j} + \left(\frac{(\tau_{zz})^k_{i+1,j} - (\tau_{zz})^k_{i-1,j}}{2\Delta z}\right)\right] \end{aligned} \tag{3.136}$$

$$
\begin{aligned}
T_{i,j}^{k+1} &= T_{i,j}^{k} - \Delta t \left[\frac{\xi_j}{R_i} \left(\frac{dR}{dz} \right)_i (w_{i,j}^k) \left(\frac{T_{i,j+1}^k - T_{i,j-1}^k}{2\Delta\xi} \right) \right] - \Delta t w_{i,j}^k \left(\frac{T_{i+1,j}^k - T_{i-1,j}^k}{2\Delta z} \right) \\
&+ \Delta t \left[w_{i,j}^k \frac{\xi_j}{R_i} \left(\frac{dR}{dz} \right)_i \left(\frac{T_{i,j+1}^k - T_{i,j-1}^k}{2\Delta\xi} \right) \right] + \frac{\Delta t}{P_e} \left(\frac{T_{i,j+1}^k - 2T_{i,j}^k + T_{i,j-1}^k}{H_i^2 (\Delta\xi)^2} \right) \\
&+ \frac{\Delta t}{P_e} \left[\frac{T_{i,j+1}^k - T_{i,j-1}^k}{2\xi_j R_i^2 \Delta\xi} + \frac{T_{i+1,j}^k - 2T_{i,j}^k + T_{i-1,j}^k}{(\Delta z)^2} \right] + \frac{\Delta t}{P_e} \left[\frac{3\xi_j}{R_i^2} \left(\frac{dR}{dz} \right)_i^2 \left(\frac{T_{i,j+1}^k - T_{i,j-1}^k}{2\Delta\xi} \right) \right] \\
&- \frac{2\xi_j(\Delta t)}{P_e R_i} \left(\frac{dR}{dz} \right)_i \left(\frac{T_{i+1,j+1}^k - T_{i-1,j+1}^k - T_{i+1,j-1}^k + T_{i-1,j-1}^k}{4\Delta\xi\Delta z} \right) \\
&- \frac{\Delta t}{P_e} \left[\frac{\xi_j}{R_i} \left(\frac{d^2R}{dz^2} \right)_i \left(\frac{T_{i,j+1}^k - T_{i,j-1}^k}{2\Delta\xi} \right) \right] + \frac{2\Delta t}{P_e} \left(\frac{\xi_j}{R_i} \frac{dR}{dz} \right)_i^2 \left(\frac{T_{i,j+1}^k - 2T_{i,j}^k + T_{i,j-1}^k}{(\Delta\xi)^2} \right) \\
&+ \Delta t E_c \left[\frac{(\tau_{\xi\xi})_{i,j}^k}{H_i} \left(\frac{dR}{dz} \right)_i \left(\xi_j \left(\frac{w_{i,j+1}^k - w_{i,j-1}^k}{2\Delta\xi} \right) + w_{i,j}^k \right) + \frac{(\tau_{\xi z})_{i,j}^k}{R_i} \left(\frac{w_{i,j+1}^k - w_{i,j-1}^k}{2\Delta\xi} \right) \right] \\
&+ \Delta t E_c (\tau_{\xi z})_{i,j}^k \left[\xi_j \left(\left(\frac{dR}{dz} \right)_i \left(\frac{w_{i+1,j}^k - w_{i-1,j}^k}{2\Delta z} \right) + w_{i,j}^k \left(\frac{d^2R}{dz^2} \right)_i \right) \right] \\
&- \Delta t E_c (\tau_{\xi z})_{i,j}^k \left[\frac{\xi_j}{R_i} \left(\frac{dR}{dz} \right)_i^2 \left(\xi_j \left(\frac{w_{i,j+1}^k - w_{i,j-1}^k}{2\Delta\xi} \right) + w_{i,j}^k \right) \right] \\
&- \Delta t E_c (\tau_{\xi z})_{i,j}^k \frac{\xi_j}{R_i} \left(\frac{dR}{dz} \right)_i \left(\frac{w_{i,j+1}^k - w_{i,j-1}^k}{2\Delta\xi} \right) + \Delta t E_c (\tau_{\xi z})_{i,j}^k \left(\frac{w_{i+1,j}^k - w_{i-1,j}^k}{2\Delta z} \right)
\end{aligned}
\tag{3.137}
$$

$$
\begin{aligned}
C_{i,j}^{k+1} &= C_{i,j}^{k} - \Delta t \left[\frac{\xi_j}{R_i} \left(\frac{dR}{dz} \right)_i \left(w_{i,j}^k \right) \left(\frac{C_{i,j+1}^k - C_{i,j-1}^k}{2\Delta\xi} \right) \right] \\
&- \Delta t \left[w_{i,j}^k \left(\frac{C_{i+1,j}^k - C_{i-1,j}^k}{2\Delta z} - \frac{\xi_j}{H_i} \left(\frac{dR}{dz} \right)_i \left(\frac{C_{i,j+1}^k - C_{i,j-1}^k}{2\Delta\xi} \right) \right) \right] \\
&+ \frac{\Delta t}{P_e} \left[\frac{C_{i,j+1}^k - 2C_{i,j}^k + C_{i,j-1}^k}{R_i^2 (\Delta\xi)^2} + \frac{C_{i,j+1}^k - C_{i,j-1}^k}{2\xi_j R_i^2 \Delta\xi} + \frac{C_{i+1,j}^k - 2C_{i,j}^k + C_{i-1,j}^k}{(\Delta z)^2} \right] \\
&+ \frac{\Delta t}{S_c R_e} \left[\frac{3\xi_j}{R_i^2} \left(\frac{dR}{dz} \right)_i^2 \left(\frac{C_{i,j+1}^k - C_{i,j-1}^k}{2\Delta\xi} \right) \right] + S_r \Delta t \frac{3\xi_j}{R_i^2} \left(\frac{dR}{dz} \right)_i^2 \left(\frac{T_{i,j+1}^k - T_{i,j-1}^k}{2\Delta\xi} \right) \\
&- \frac{2\xi_j(\Delta t)}{P_e R_i} \left(\frac{dR}{dz} \right)_i \left(\frac{C_{i+1,j+1}^k - C_{i-1,j+1}^k - C_{i+1,j-1}^k + C_{i-1,j-1}^k}{4\Delta\xi\Delta z} \right) \\
&- \frac{\Delta t}{P_e} \left[\frac{\xi_j}{R_i} \left(\frac{d^2R}{dz^2} \right)_i \left(\frac{C_{i,j+1}^k - C_{i,j-1}^k}{2\Delta\xi} \right) \right] + \frac{2\Delta t}{P_e} \left(\frac{\xi_j}{R_i} \frac{dR}{dz} \right)_i^2 \left(\frac{C_{i,j+1}^k - 2C_{i,j}^k + C_{i,j-1}^k}{(\Delta\xi)^2} \right) \\
&- \frac{2\xi_j \Delta t}{R_i} \left(\frac{dR}{dz} \right)_i \left(\frac{T_{i+1,j+1}^k - T_{i-1,j+1}^k - T_{i+1,j-1}^k + T_{i-1,j-1}^k}{4\Delta\xi\Delta z} \right) \\
&- S_r \Delta t \left[\frac{\xi_j}{R_i} \left(\frac{d^2R}{dz^2} \right)_i \left(\frac{T_{i,j+1}^k - T_{i,j-1}^k}{2\Delta\xi} \right) \right] + 2\Delta t S_r \left(\frac{\xi_j}{R_i} \right)^2 \left(\frac{dR}{dz} \right)_i^2 \left(\frac{T_{i,j+1}^k - 2T_{i,j}^k + T_{i,j-1}^k}{(\Delta\xi)^2} \right)
\end{aligned}
\tag{3.138}
$$

With,

$$\dot{\gamma} = \sqrt{\begin{aligned} &2\left[\left(\frac{1}{R_i}\left(\frac{dR}{dz}\right)_i\left(\xi_j\left(\frac{w^k_{i,j+1}-w^k_{i,j-1}}{2\Delta\xi}+w^k_{i,j}\right)\right)\right)^2+\left(\frac{1}{R_i}\left(\frac{dR}{dz}\right)_i w^k_{i,j}\right)^2\right] \\ &+2\left(\frac{w^k_{i+1,j}-w^k_{i-1,j}}{2\Delta z}-\frac{\xi_j}{R_i}\left(\frac{dR}{dz}\right)_i\left(\frac{w^k_{i,j+1}-w^k_{i,j-1}}{2\Delta\xi}\right)\right)+(D^k_{i,j})^2\end{aligned}}$$

where

$$\begin{aligned}(D^k_{i,j}) = &\left[\xi_j\left(\frac{dR}{dz}\right)_i\left(\frac{w^k_{i+1,j}-w^k_{i-1,j}}{2\Delta z}\right)+w^k_{i,j}\left(\frac{d^2R}{dz^2}\right)_i\right] \\ &-\left[\frac{\xi_j}{R_i}\left(\frac{dR}{dz}\right)^2_i\left(\xi_j\frac{w^k_{i,j+1}-w^k_{i,j-1}}{2\Delta\xi}+w^k_{i,j}\right)+\frac{1}{R_i}\frac{w^k_{i,j+1}-w^k_{i,j-1}}{2\Delta\xi}\right]\end{aligned} \tag{3.139}$$

and

$$\left(\tau_{\xi\xi}\right)^k_{i,j} = 2\left(R_{eG}\dot{\gamma}^{n-1}+\tau_0\dot{\gamma}^{-1}\right)\left(\left(\frac{dR}{dz}\right)_i\left(\xi_j\frac{w^k_{i,j+1}-w^k_{i,j-1}}{2\Delta\xi}+w^k_{i,j}\right)\right) \tag{3.140}$$

$$\begin{aligned}\left(\tau_{\xi z}\right)^k_{i,j} = &\,2\left(R_{eG}\dot{\gamma}^{n-1}+\tau_0\dot{\gamma}^{-1}\right)\left[\xi_j\left(\left(\frac{dR}{dz}\right)_i\left(\frac{w^k_{i+1,j}-w^k_{i-1,j}}{2\Delta z}\right)\right)+w^k_{i,j}\left(\frac{d^2R}{dz^2}\right)_i\right]- \\ &2\left(R_{eG}\dot{\gamma}^{n-1}+\tau_0\dot{\gamma}^{-1}\right)\left[\frac{\xi_j}{R_i}\left(\frac{dR}{dz}\right)^2_i\left(\xi_j\frac{w^k_{i,j+1}-w^k_{i,j-1}}{2\Delta\xi}+w^k_{i,j}\right)+\frac{w^k_{i,j+1}-w^k_{i,j-1}}{2R_i\Delta\xi}\right]\end{aligned} \tag{3.141}$$

$$\left(\tau_{zz}\right)^k_{i,j} = 2\left(R_{eG}\dot{\gamma}^{n-1}+\tau_0\dot{\gamma}^{-1}\right)\left[\frac{w^k_{i+1,j}-w^k_{i-1,j}}{2\Delta z}-\frac{\xi_j}{R_i}\left(\frac{dR}{dz}\right)_i\left(\frac{w^k_{i,j+1}-w^k_{i,j-1}}{2\Delta\xi}\right)\right] \tag{3.142}$$

The boundary and initial conditions are also discretized as follows:

$$w^1_{i,j} = w_0, \quad T^1_{i,j} = T_0, \quad C^1_{i,j} = C_0; \quad w^k_{i,2} = w^k_{i,1}, \quad T^k_{i,2} = T^k_{i,1}, \quad C^k_{i,2} = C^k_{i,1} \tag{3.143}$$

$$w^k_{i,N+1} = 0, \quad u^k_{i,N+1} = 0, \quad T^k_{i,N+1} = T_w, \quad C^k_{i,N+1} = C_w, \quad \left(\tau_{\xi z}\right)^k_{i,1} = 0. \tag{3.144}$$

Condition for Stability

The explicit finite difference method is conditionally stable. The condition of stability as per Von Neumann analysis was taken into consideration. In that regard therefore, $0 < \dfrac{\Delta t}{(\Delta\xi)^2} \leq 0.5$.

CHAPTER FOUR

RESULTS AND DISCUSSION

In this chapter, the numerical results and discussion of the study are presented. The chapter includes both, the numerical results of the Newtonian model and that of non-Newtonian model. The chapter first presents the numerical results of the Newtonian model. Later, the results for non-Newtonian will be presented. The MATLAB codes for the discretized equations (3.70)-(3.71) were written and implemented to produce graphs. To maintain stability using the explicit finite difference method, it was ensured that $0 < \frac{\Delta t}{(\Delta \xi)^2} \leq 0.5$. The constants and parameters were chosen by following other scholars and some were assumed by ensuring that they are realistic situations.For example, the Reynolds number was changed to suit the laminar flow. For convenience, constants were wisely chosen as follows:

Table 2: Values of the parameters

Parameters	Range of values	Source
Hartman number Ha	$1-3$	Sharma *et al* (2019)
Stenotic height e	$0.1-0.3$	Sankar and Ismail, (2010)
Body acceleration a_0	$1-3$	Tanwar *et al.* (2016)
Reynolds number Re	$3-100$	Assumed
Schmidt number Sc	$3-4$	Liu and Liu, (2020)
Chemical reaction β	$0.1-0.8$	Kumar *et al.* (2021)

The following constants were also used:

Table 3: Values of the constants used

Constants	Value	Source
Steady state part of pressure gradient A_0	1	Mathur and Jain (2011)
Amplitude of the pulsatile A_1	0.5	Mathur and Jain (2011)
Pulse frequency m_1	1	Agarwal and Varshney (2016)
Body acceleration frequency m_2	1	Agarwal and Varshney (2016)
Phase angle Φ	0.6	Agarwal and Varshney (2016)

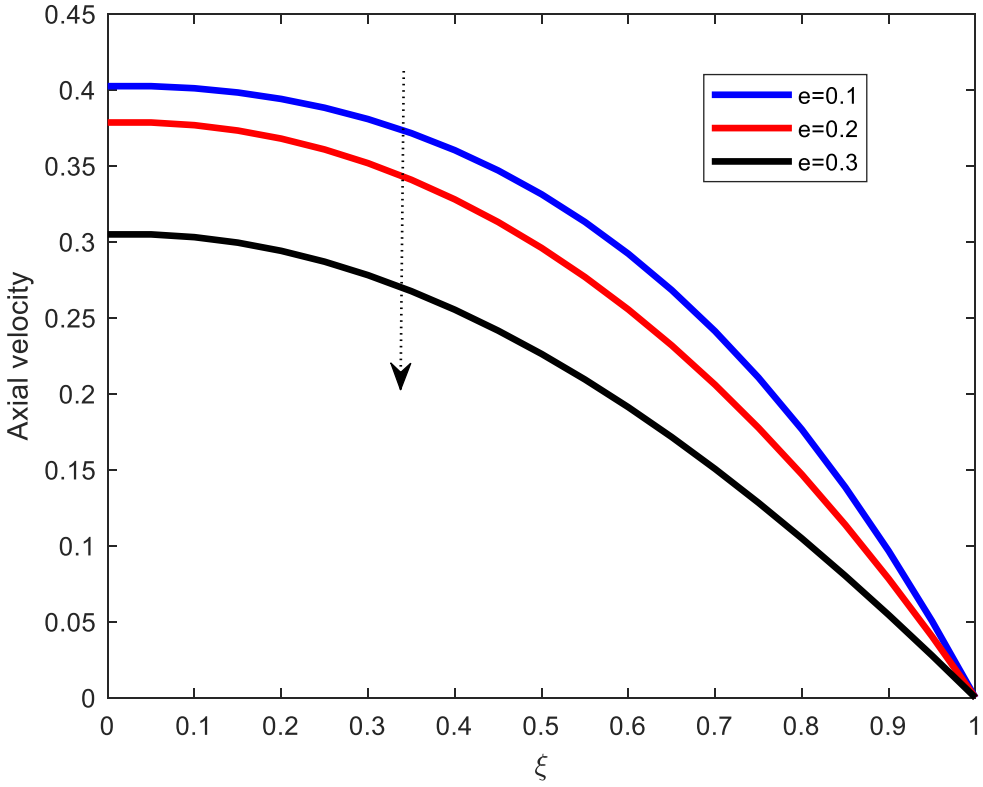

Figure 8: Effect of increasing stenotic height on axial velocity

The effect of increasing stenotic height on axial velocity is shown in Fig. 8. It is shown (as expected) that as stenosis increases, the axial velocity diminishes. The decline of axial velocity is due to the reason that increase in stenosis makes more blood (which is viscous) be on contact with arterial wall. This can further be explained physically that as stenotic height increases, the size of the artery in terms of radius is reduced, that is the vasoconstriction or narrowing the size of the artery. Now as the resistance is inversely proportional to the radius, decrease in radius therefore, increases the resistance of blood to flow and hence, the velocity decreases. Medically, if the stenosis keeps on growing therefore, velocity will keep on decreasing affecting supply of oxygen in different parts of the body, including brain. This can result into heart attack or stroke. Figure 9 displays the variation of the axial velocity profile due to Hartman number. From the Fig. 9 it is observed that, increase in Hartman number reduces the axial velocity. This can be explained physically that the velocity decreases due to the fact that as the magnetic fields is applied to the body, the Lorentz force tend to oppose the blood flow and as a results the velocity get decreased. The Lorentz force is able to oppose the motion of the blood because blood consists of red blood cells which contains ions. Similar result was obtained by Uddin *et al.* (2020), Sharma and Yadav (2019) and Maiti *et al.* (2020).

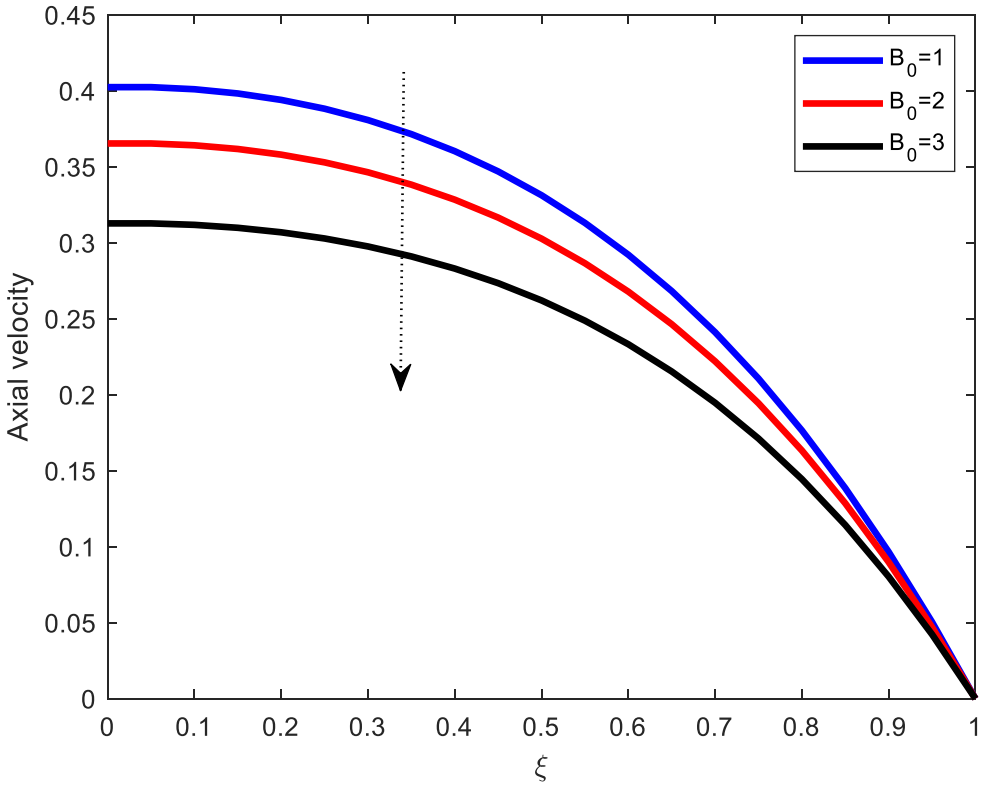

Figure 9: Effect of increasing Hartman number on axial velocity

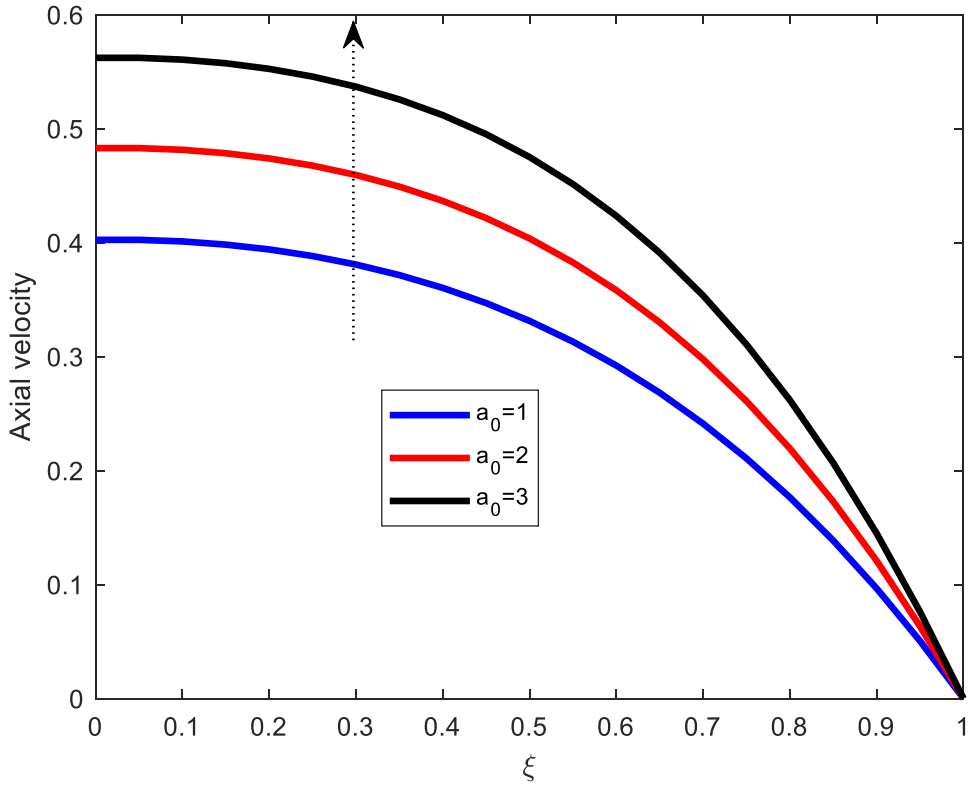

Figure 10: Effect of increasing body acceleration on axial velocity

Figure 10 shows the effect of increasing body acceleration on axial velocity. From the graph it is observed that for the fixed values of Hartman number and height of stenosis, axial velocity

increases as body acceleration increases. The increase in velocity is due to the reason that body acceleration increases the heart beats and the pulse rate. When the body is subjected to body acceleration, the heart speeds up to pump blood so that more blood can reach the muscles. This helps to supply more oxygen and other nutrients in different parts of the body.

The effect of increasing Reynolds number R_e on axial velocity is illustrated on Fig. 11. The Reynolds number is the ratio of a fluid's inertial force to its viscous force. This dimensionless number plays a prominent role in foreseeing the patterns in a fluid's behavior. Increasing Reynolds number implies that inertial force is dominant than the viscous force. This in turn enhances the fluid's velocity.

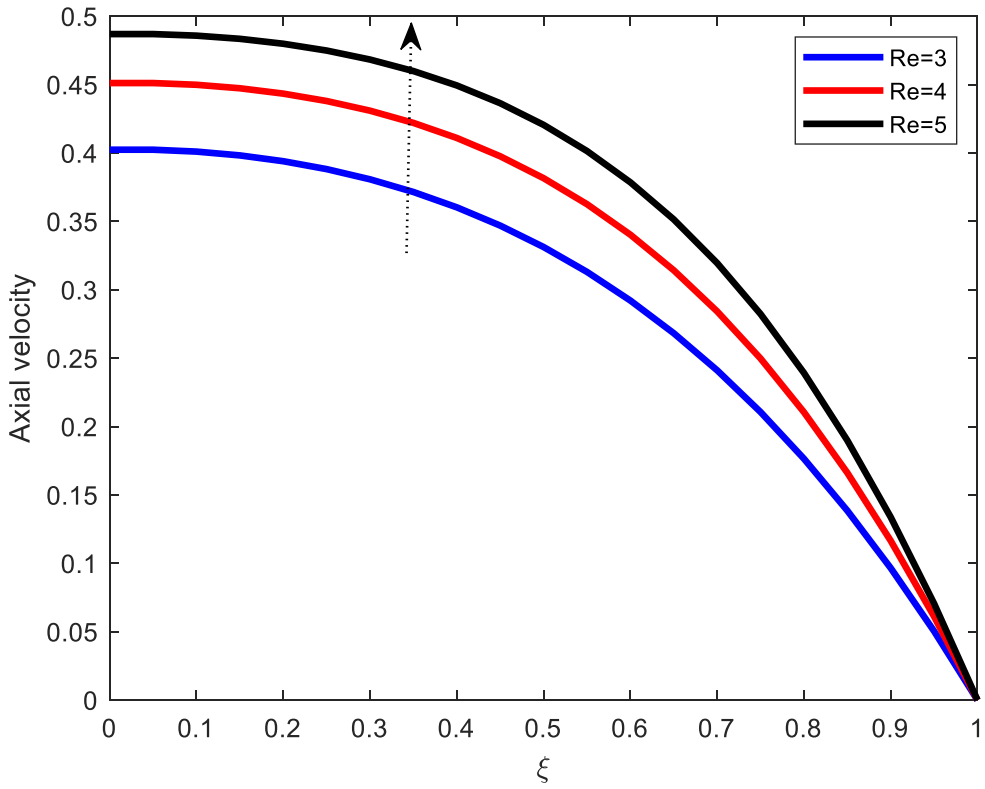

Figure 11: Effect of increasing body the Reynolds number on axial velocity

It is also observed that, both steady state part of pressure gradient and the amplitude of its oscillatory part influences the axial velocity. Their increase leads to the increase in axial velocity. This is exhibited in Fig. 12 and 13. This is also due to the reason that their increase enhances pressure gradient of blood and consequently increasing the blood flow rate.

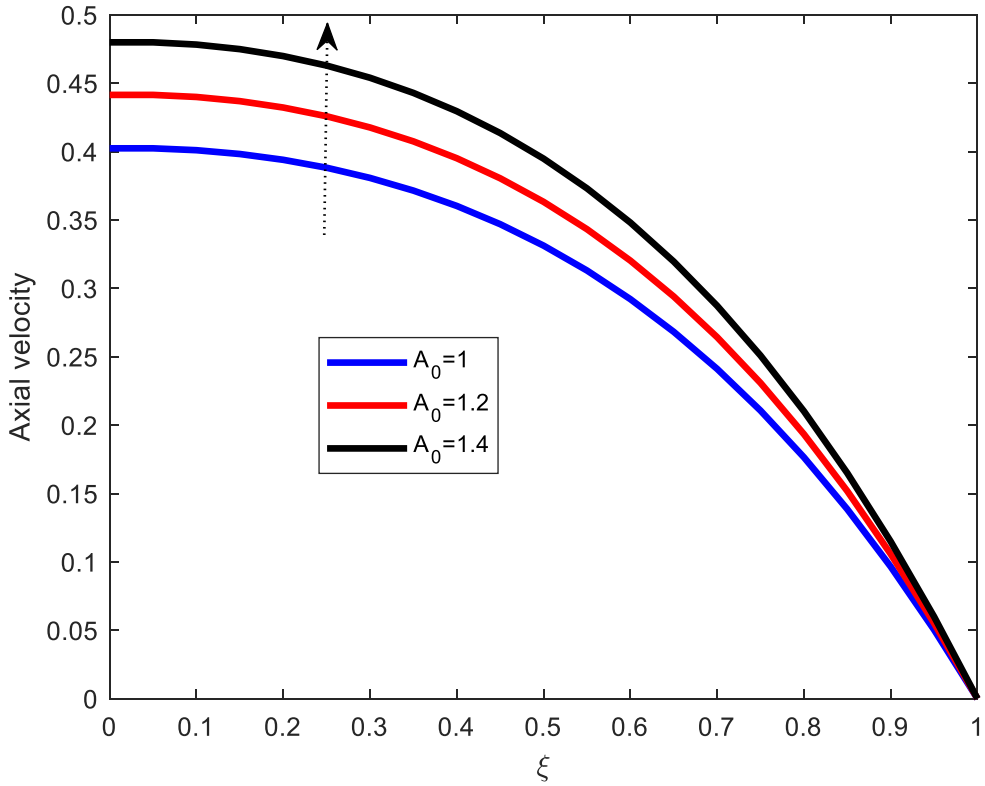

Figure 12: Effect of increasing steady state part of pressure gradient

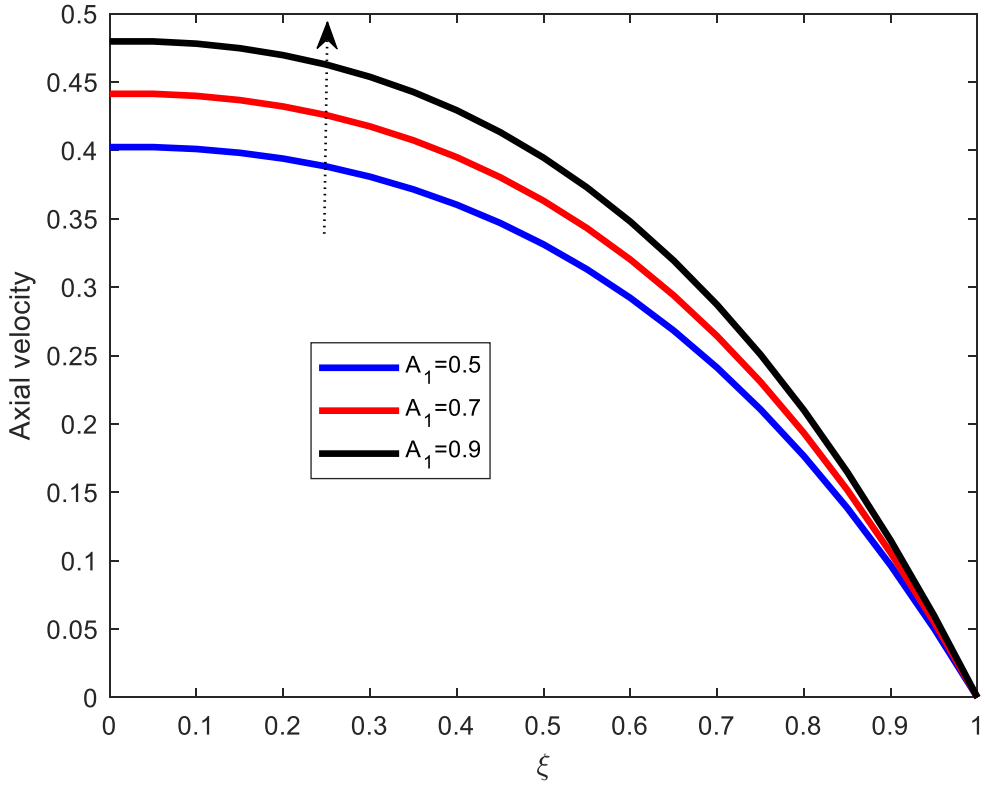

Figure 13: Effect of increasing amplitude of oscillatory

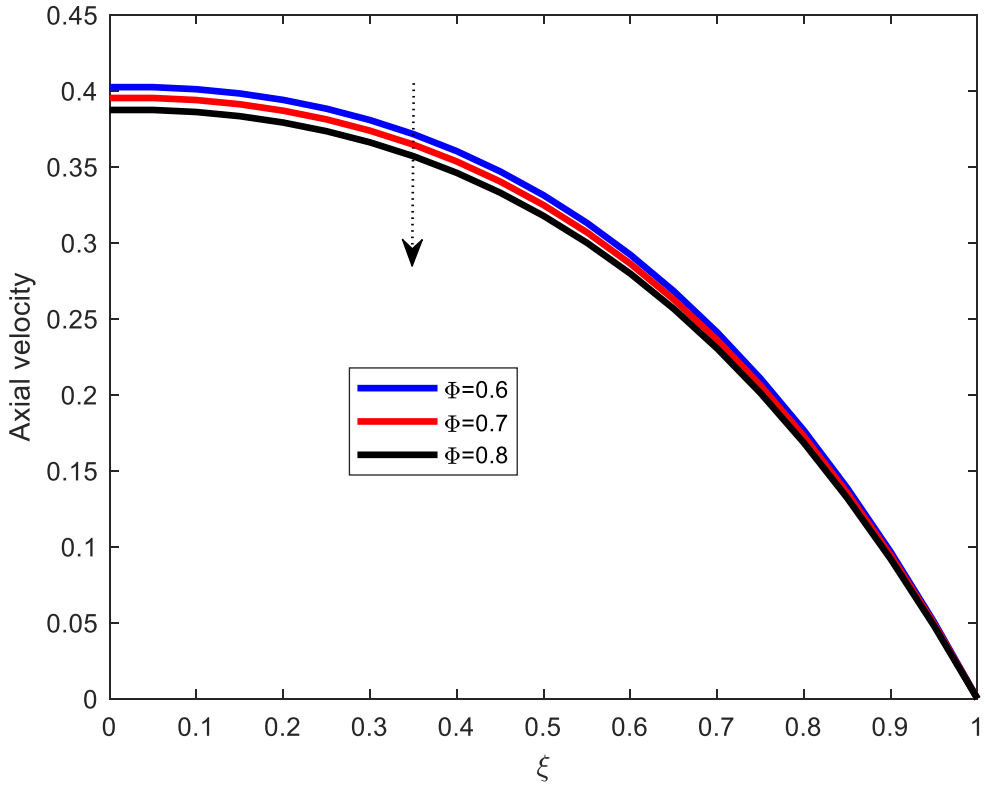

Figure 14: Effect of increasing Phase angle on axial velocity

The variation of blood's axial velocity with phase angle is displayed in Fig. 14. The computational results show that axial velocity declines as the phase angle increases. The variation of radial velocity due to flow parameters and constants are illustrated in Fig. 15 to Fig. 20.

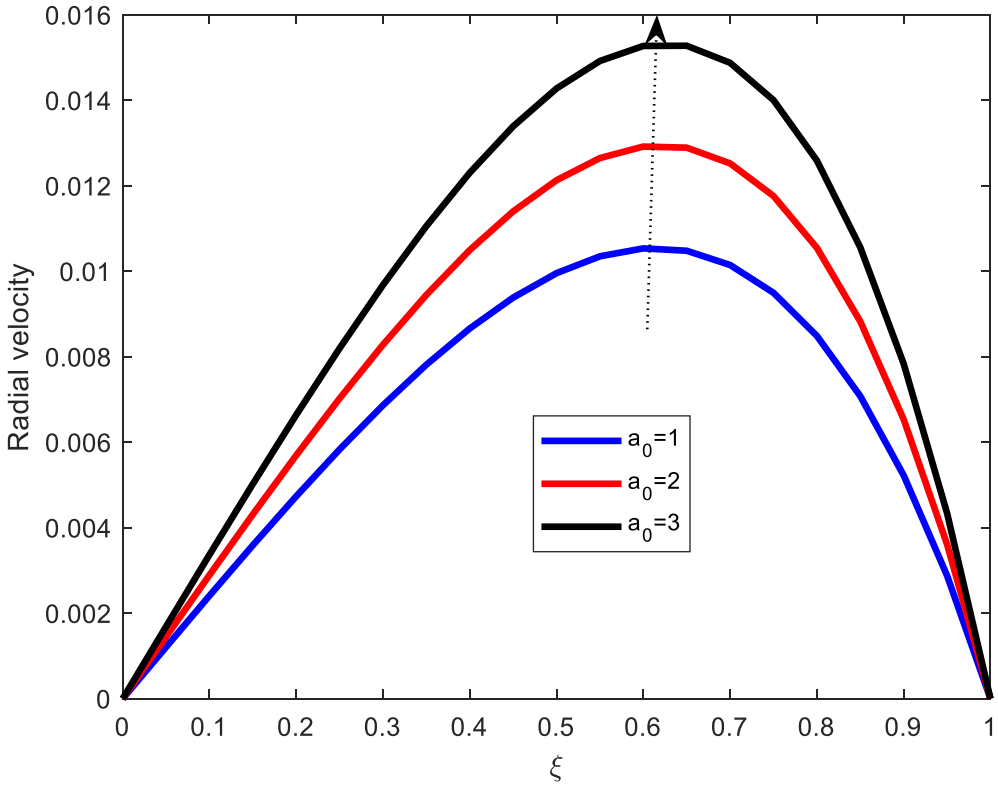

Figure 15: Effect of increasing body acceleration on radial velocity

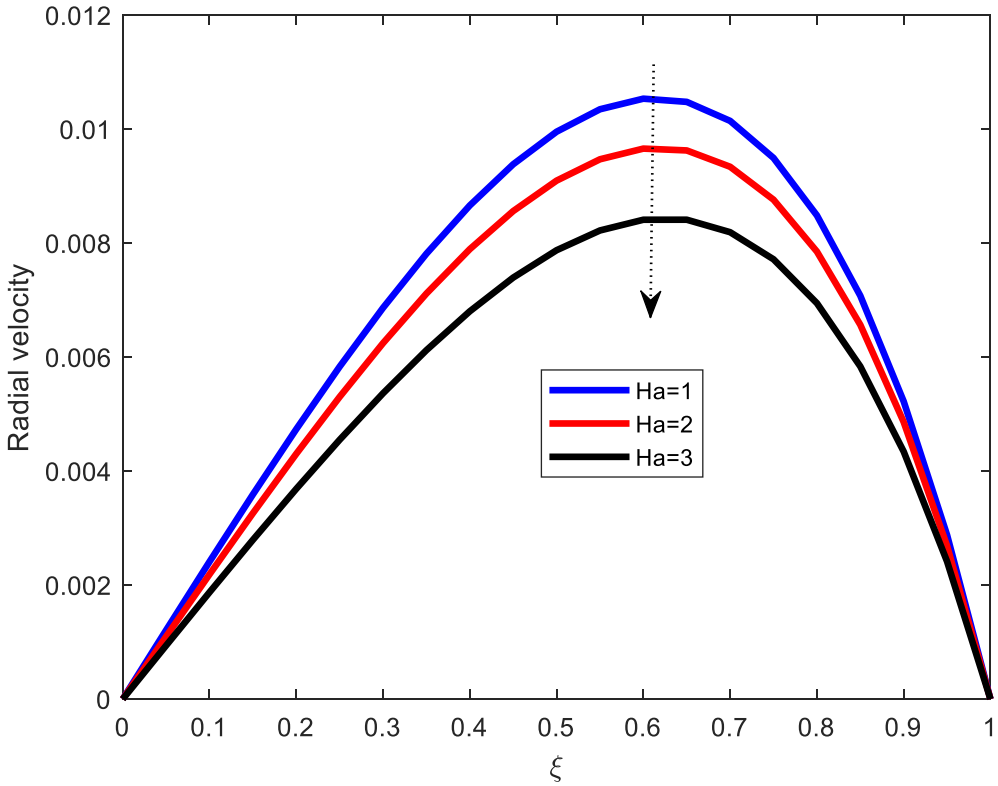

Figure 16: Effect of increasing Hartman number radial velocity

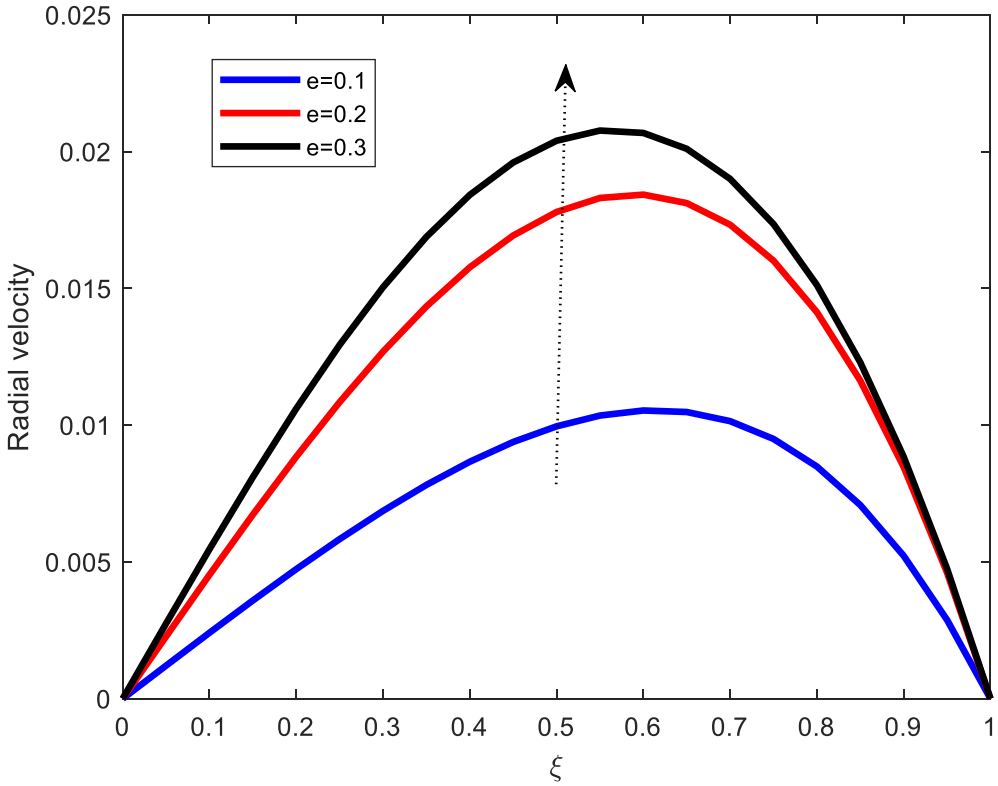

Figure 17: Effect of increasing stenosis radial velocity

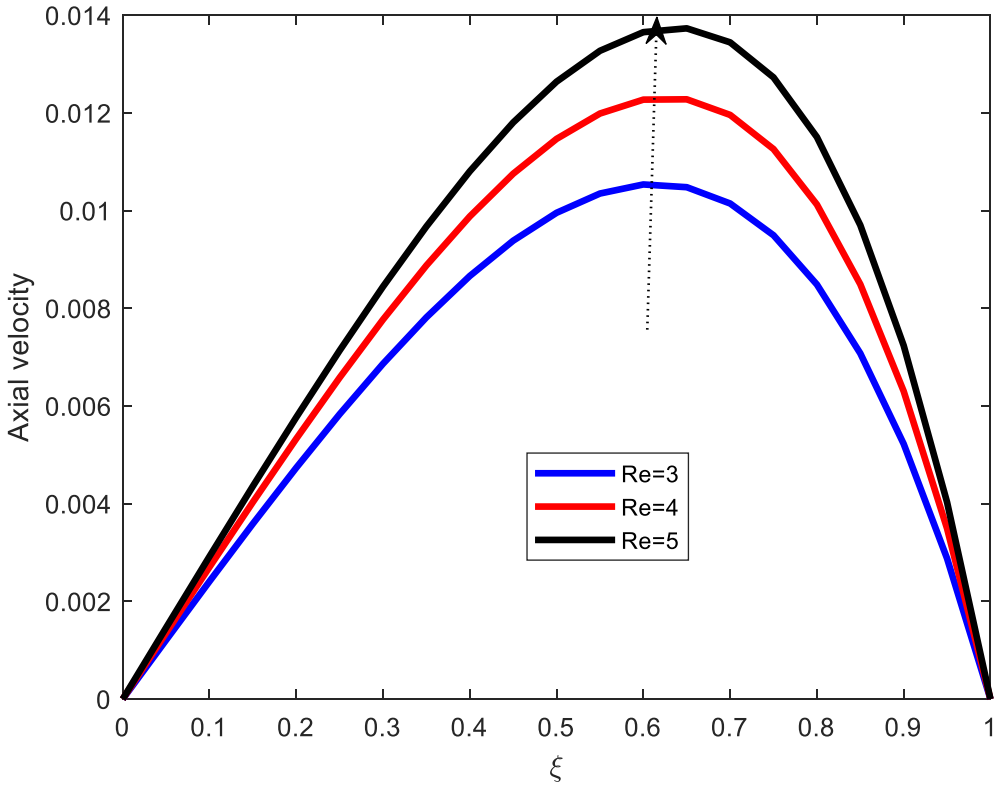

Figure 18: Effect of increasing Reynolds number radial velocity

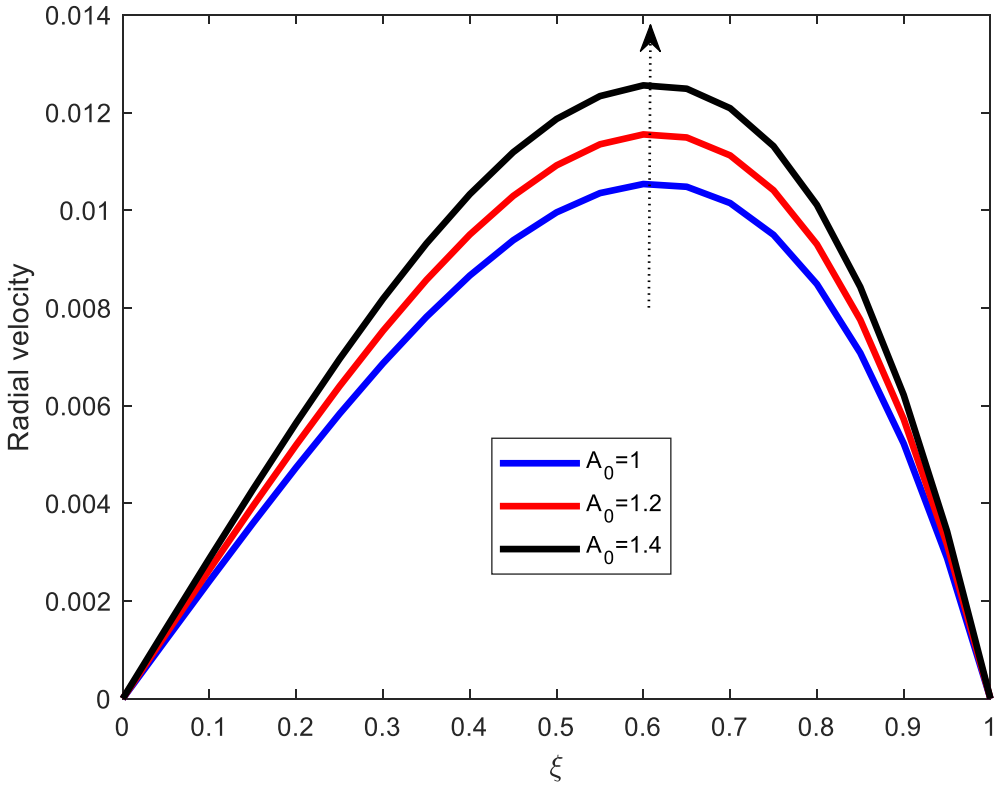

Figure 19: Effect of increasing A_0 on radial velocity

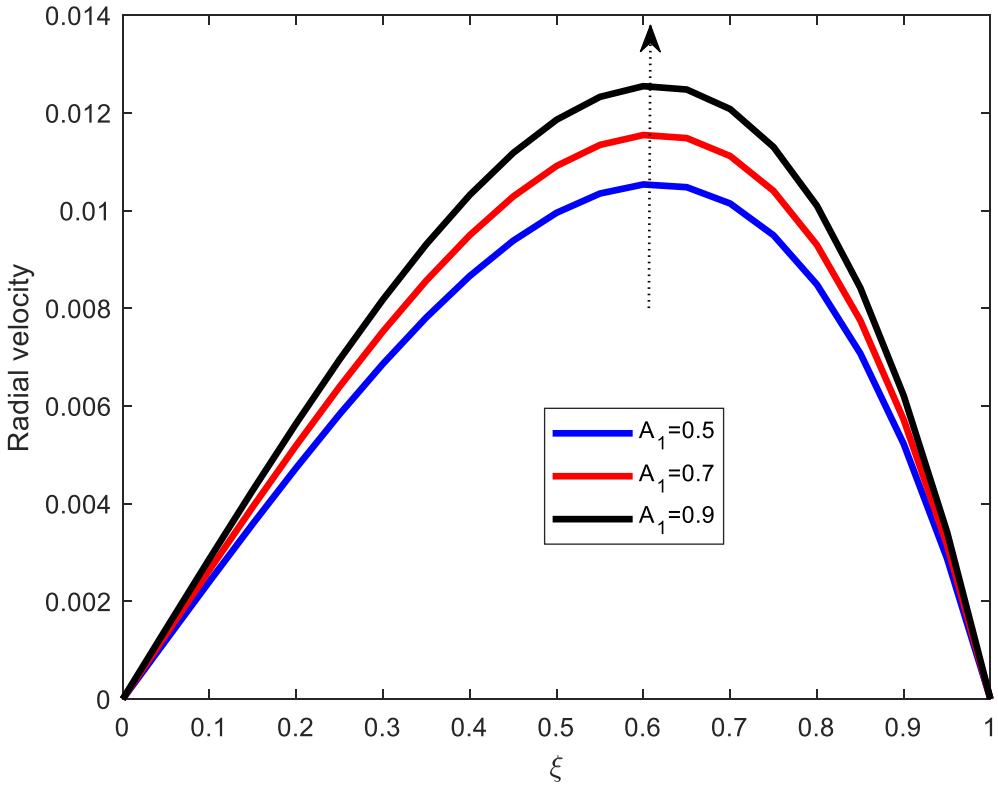

Figure 20: Effect of increasing A_1 on radial velocity

From Fig. 15, it is observed that increasing body acceleration on radial velocity brings the same effect as in axial velocity. That is, the velocity get increased. Figure 16 also reveals that radial velocity declines as Hartman number increases. The same was observed in axial velocity (Fig. 9). The difference and interesting pattern is observed in Fig. 17. From the Fig. 17, it is seen that increase in stenosis, the radial velocity increases too. It is therefore, very interesting to note that it has been revealed that increase in stenosis, decreases the axial velocity but increases the radial velocity. The radial velocity increases as compensation to the axial velocity which decreases. However, this may medically endanger a person by harming the arterial wall for prolonged situation. It is also shown that Fig. 19 and 20, the steady state part of pressure gradient and the amplitude of oscillation, play the same role as in axial velocity. Their increase lead to the increase in velocity, both axial and radial velocities. Figure 21 illustrates both, the axial velocity

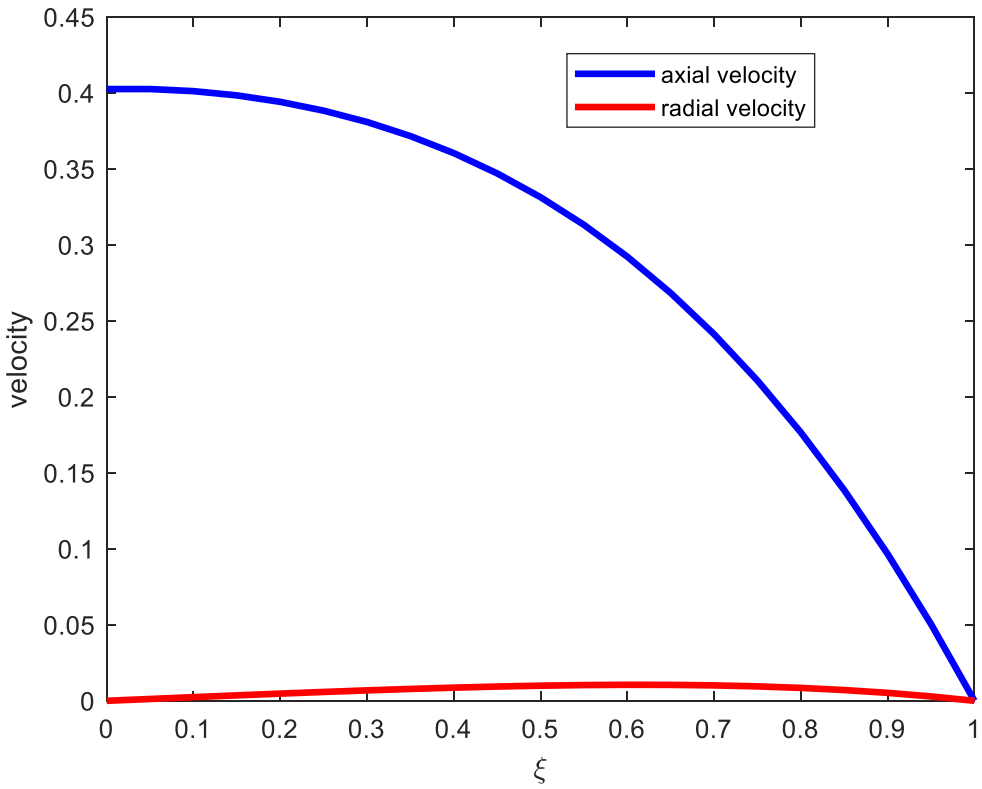

Figure 21: Axial and radial velocities

and the radial velocity. From the graph it is shown that the axial velocity is higher than the radial velocity. This is due to the fact that the pressure gradient is more dominant in the axial direction than in radial direction. On the other hand, it is also observe that, the axial velocity is maximum along the axis of symmetry and it is zero on the boundary. The axial velocity is decreasing as one moves towards the boundary because of the no slip condition at the boundary. The radial velocity is zero along the line of symmetry because there is no radial flow along that axis. Also,

it is zero at the boundary, to satisfy the no slip condition. The Transient effects of axial velocity profiles and radial velocity profiles are illustrated in Fig. 22 and Fig. 23:

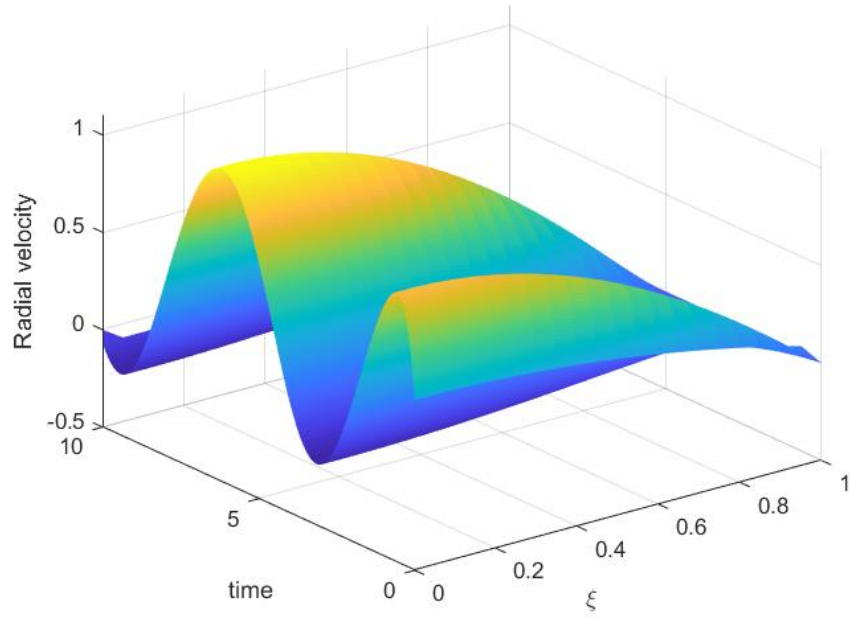

Figure 22: Transient effects of radial velocity profiles

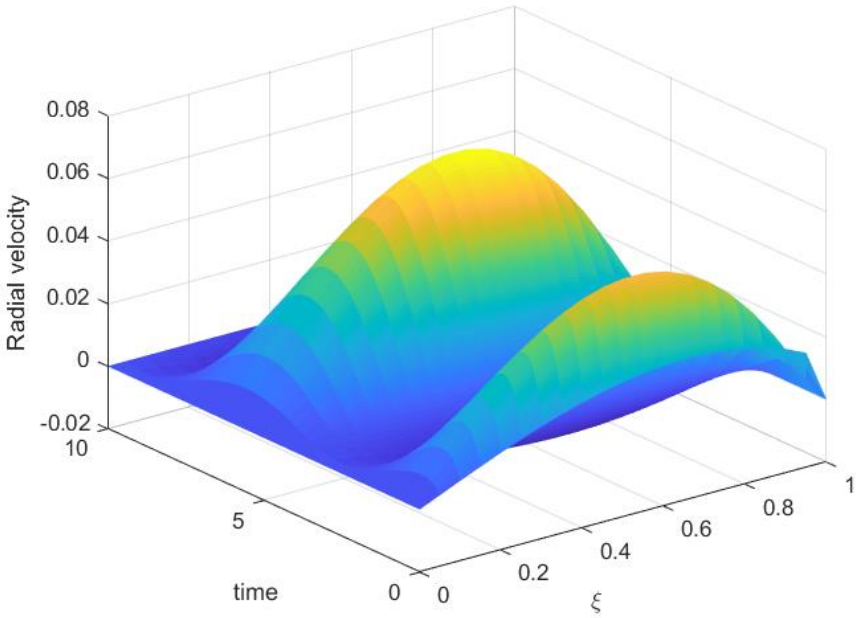

Figure 23: Transient effects of axial velocity profiles

The combined effect of stenosis, body acceleration and magnetic fields is shown in Fig. 24. From the graph it is clearly observed that, the combination of stenosis, body acceleration and magnetic fields highly reduces the velocity of the blood. On the other hand, body exercise seems to have more effect than magnetic fields and stenosis. In this regard therefore, since body exercise highly raises the blood's speed, magnetic therapy for a stenosed person applied in sports is more advantageous, not only for reducing pain but also regulating blood theology by reducing blood's velocity. It is further shown that magnetic fields and stenosis have very small difference in lowering the blood's velocity. Stenosis being slightly more hazardous in reducing axial velocity than magnetic fields.

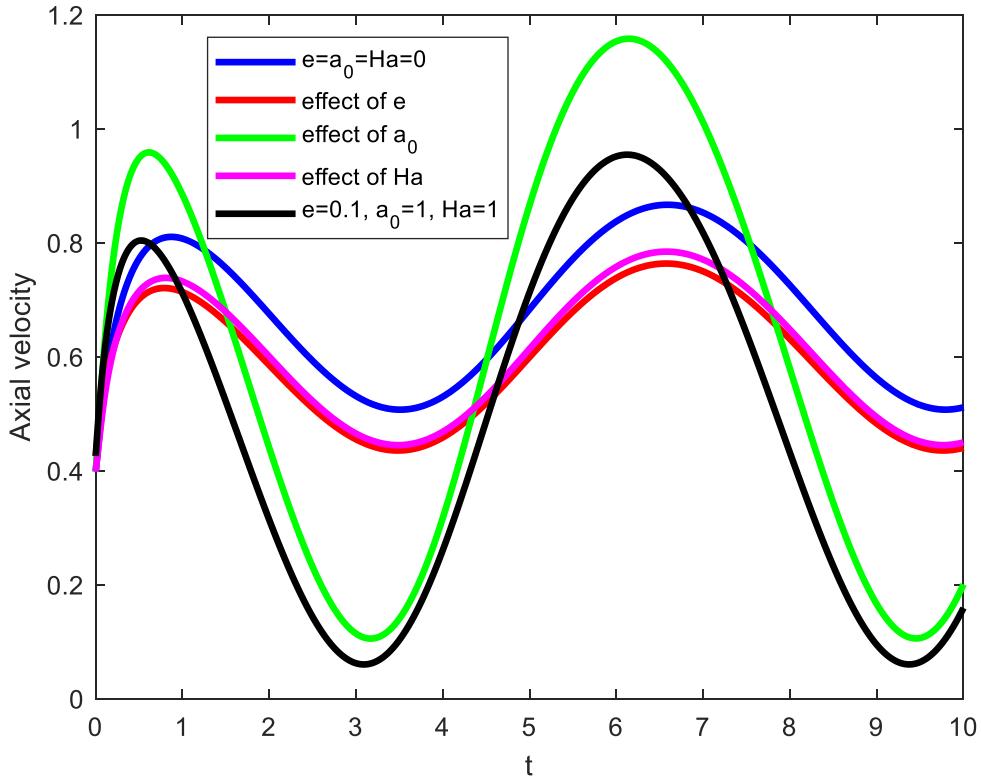

Figure 24: General effects of some parameters

Here below, the simulations of concentration profiles are presented.The effects of stenosis, body acceleration, magnetic fields and chemical reaction are illustrated and discussed. The effects of varying the Schmidt number *Sc* and the Reynolds number *Re* is also illustrated.

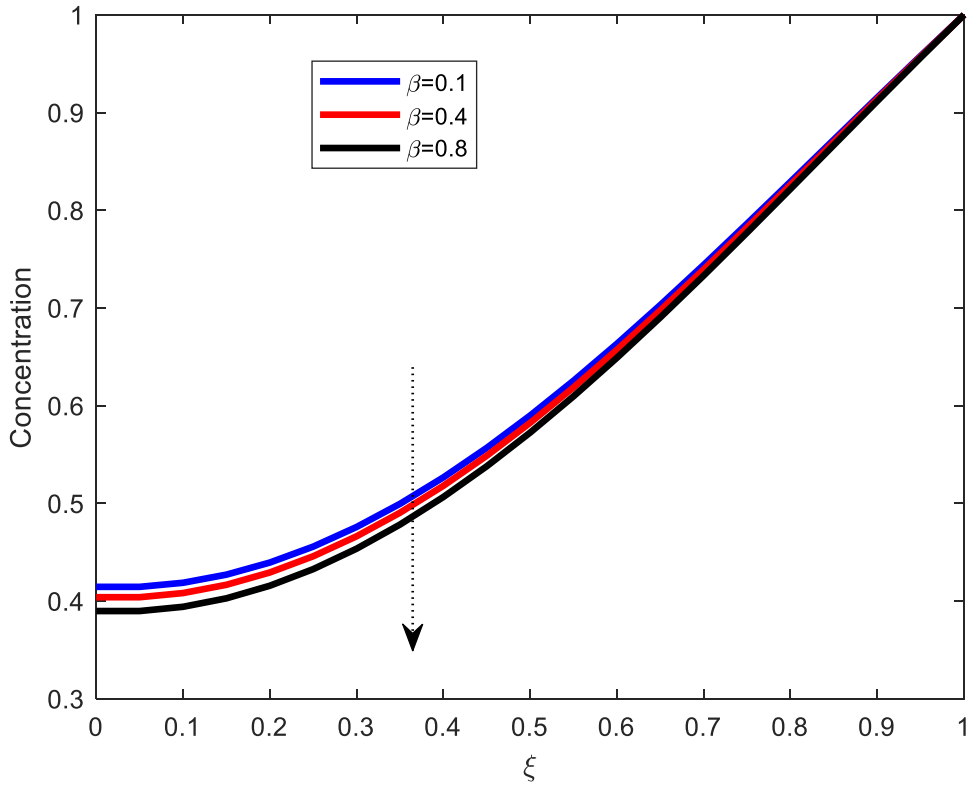

Figure 25: Effect of Chemical reaction on concentration

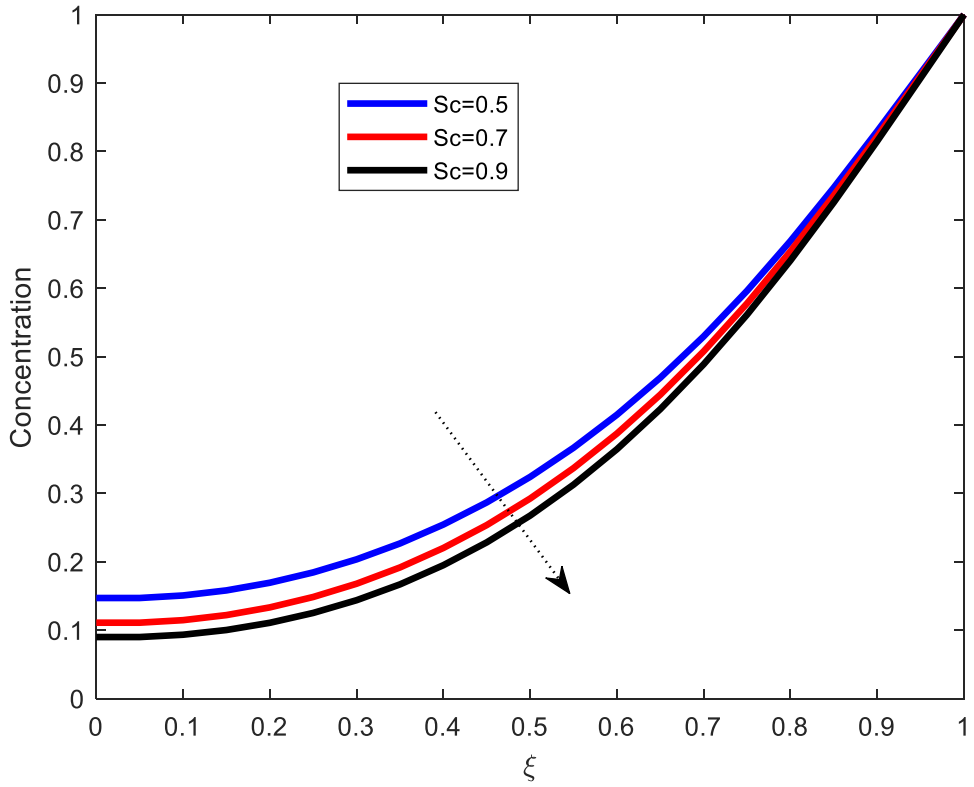

Figure 26: Effect of Schmidt number on concentration

The effect of chemical reaction parameter on the concentration profile is displayed in Fig. 25. From the Fig. 25, it is clearly observed that, as the chemical reaction parameter increases, the concentration decreases. The decrease of concentration is due to the fact that the presence of chemical reaction acts as the consumption or destructive agent of chemical species. This leads to the reduction of the concentration. Figure 26 shows typical concentration profile for various values of Schmidt number *Sc*. From the Fig. 26, it is shown that the increase in Schmidt number diminishes the concentration profiles. The Schmidt number is a dimensionless number which is the ratio of momentum diffusivity to mass diffusivity. The increase of Schmidt number implies decrease of molecular diffusion. Hence the decrease in concentration profile with the increase of Schmidt number is revealed. The effect of Hartman number on the concentration profile is illustrated in Fig. 27. In the figure, it is observe that, increase in Hartman number increases the concentration of the fluid. The increase of concentration is due to the reason that, the presence of magnetic fields induces Lorentz force which effectively impedes the flow of the fluid and thus more concentration occurs. The reverse situation is observed in case of increasing body acceleration, it is revealed that as body acceleration increases, the concentration profile diminishes. The body acceleration increases the fluid's velocity and therefore making the concentration profile decline.

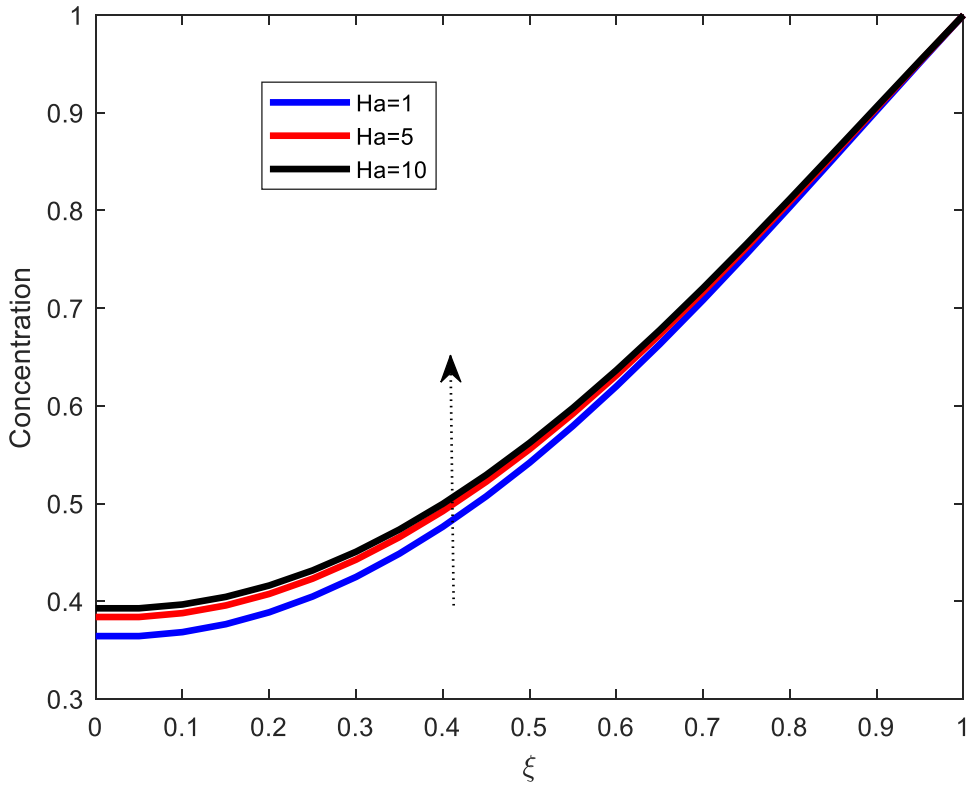

Figure 27: Effect of Hartman number on concentration

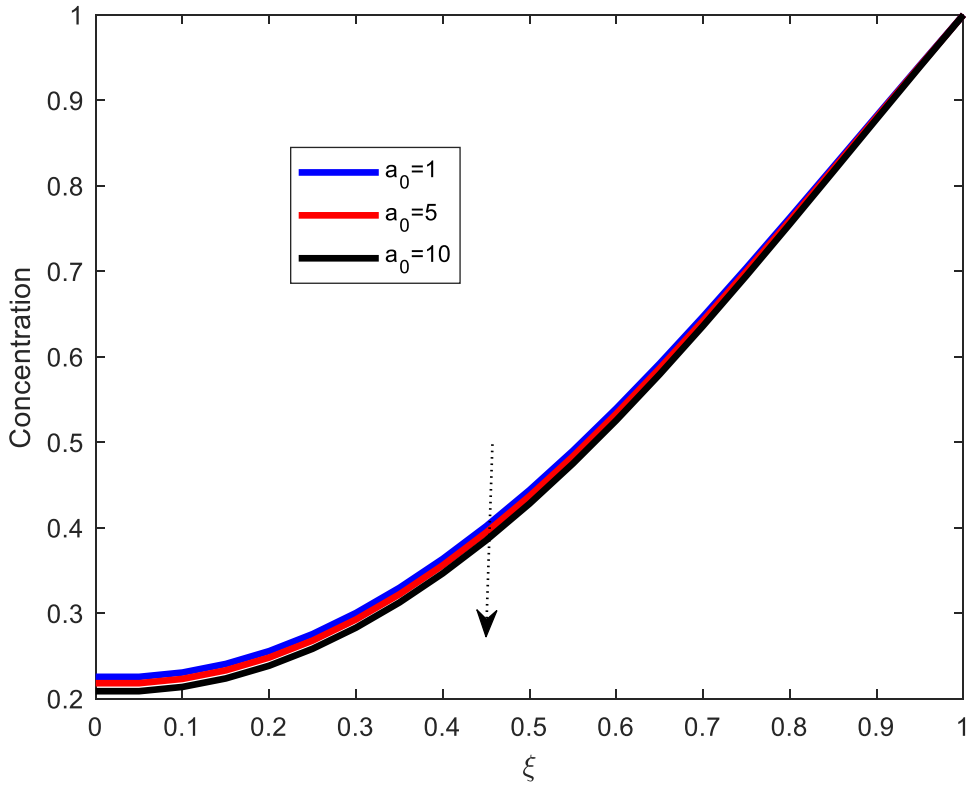

Figure 28: Effect of body acceleration on concentration

In a similar manner, it is observed that the Reynolds number reduces the concentration of blood. As it is noticed that Reynolds number enhances velocity (both axial and radial velocities), this therefore diminishes concentration (Fig. 29). The opposite situation is observed when stenotic height increases. As shown in Fig. 30, as stenosis increases, the concentration profile increases too. This is due to the reason that stenosis diminishes the velocity which in turn influences the concentration profile. Figure 31 exhibits a mesh plot for transient effects of concentration profile.

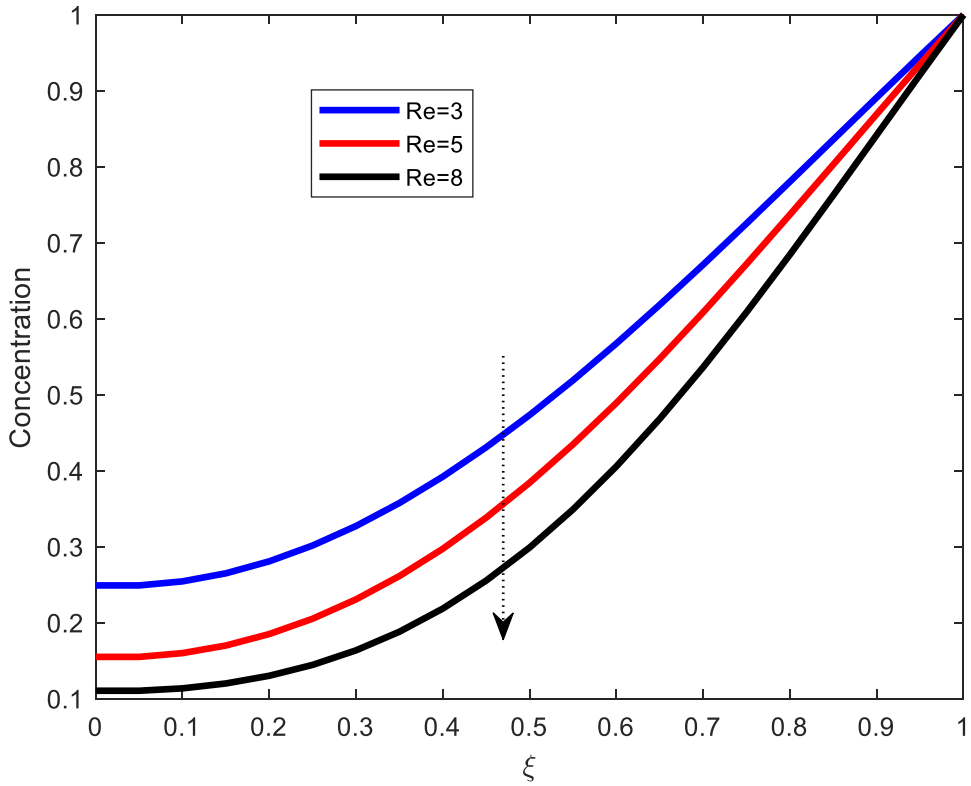

Figure 29: Effect of Reynolds number on concentration

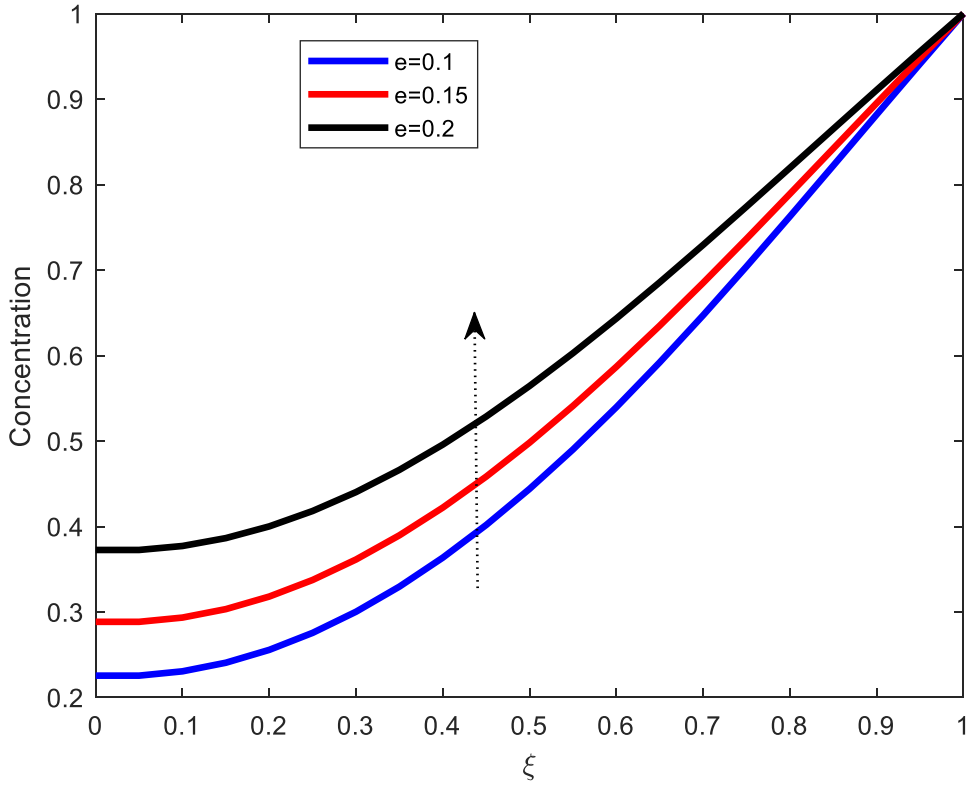

Figure 30: Effect of stenosis on concentration

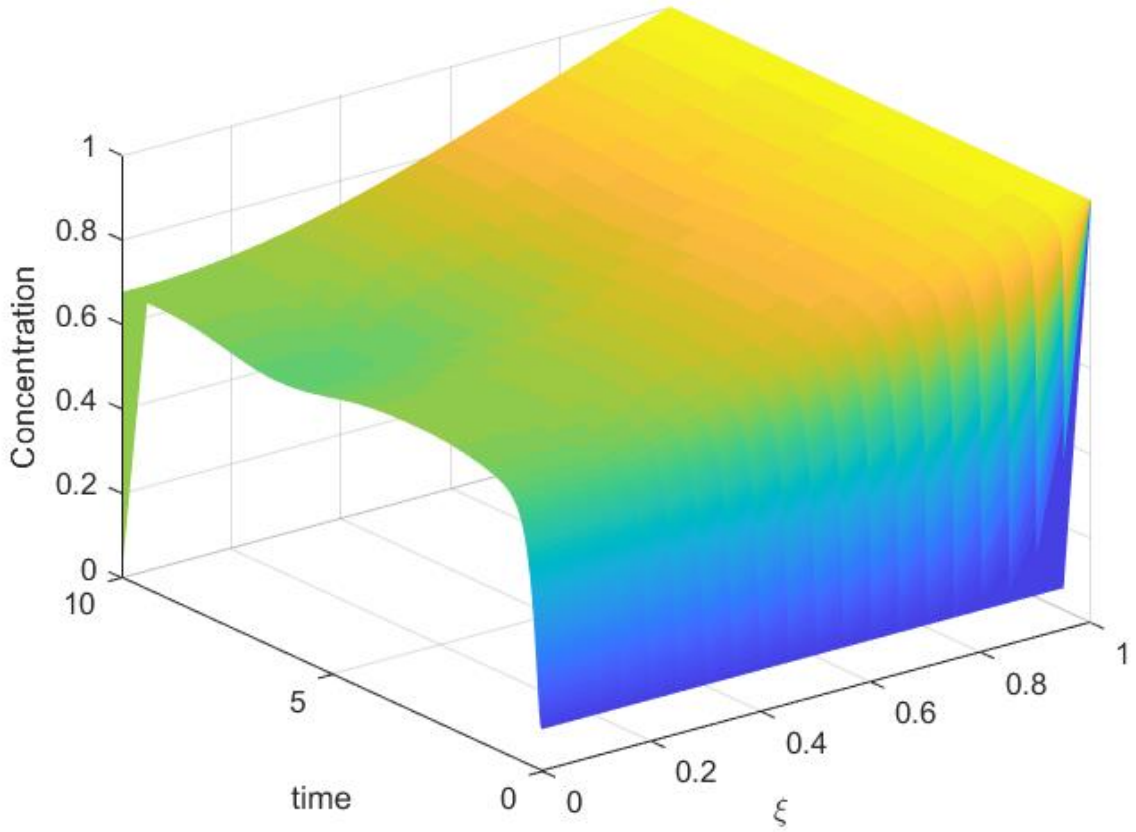

Figure 31: Transient effects of concentration

Variation of skin friction due to Reynolds number, Hartman number, body acceleration and phase angle is shown in Fig. 32-35. Its is observed that, increasing Reynolds number generally decreases the skin friction. Raising Reynolds number implies increasing the inertial forces than the viscous force. Now, as viscous forces become small, the skin skin friction declines accordingly (Fig. 32). The same behavior has been shown when Hartman number increases. This is displayed in Fig. 33. It is interesting to note that the magnitude of skin friction has shown to increase with body acceleration.

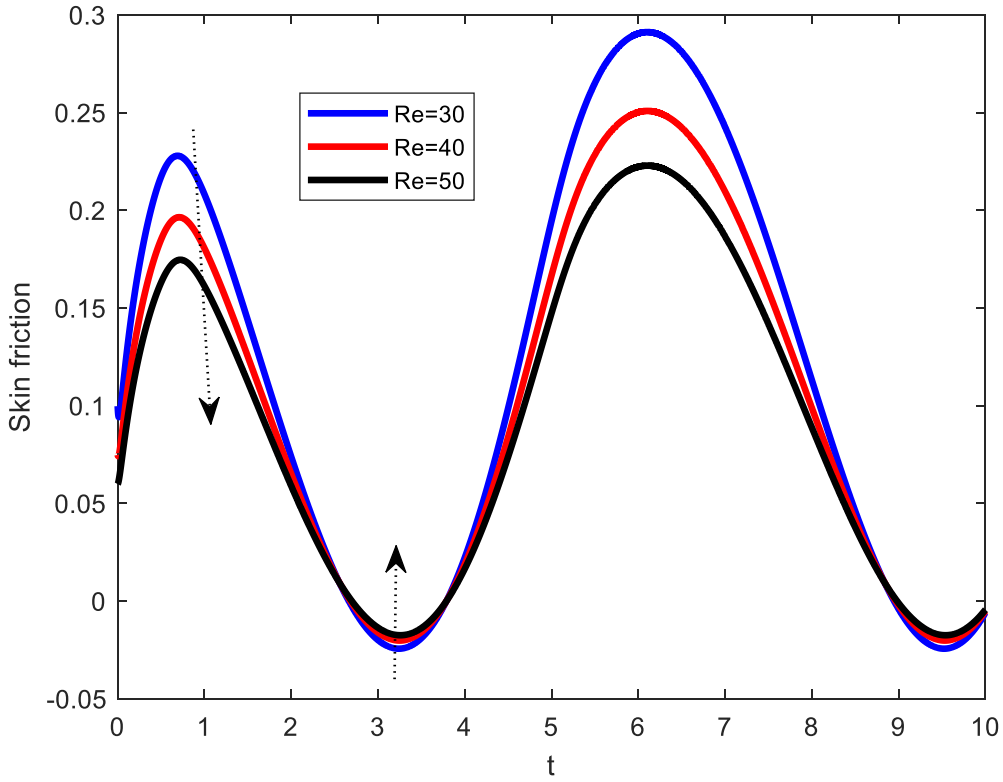

Figure 32: Effect of Reynolds number on Cf

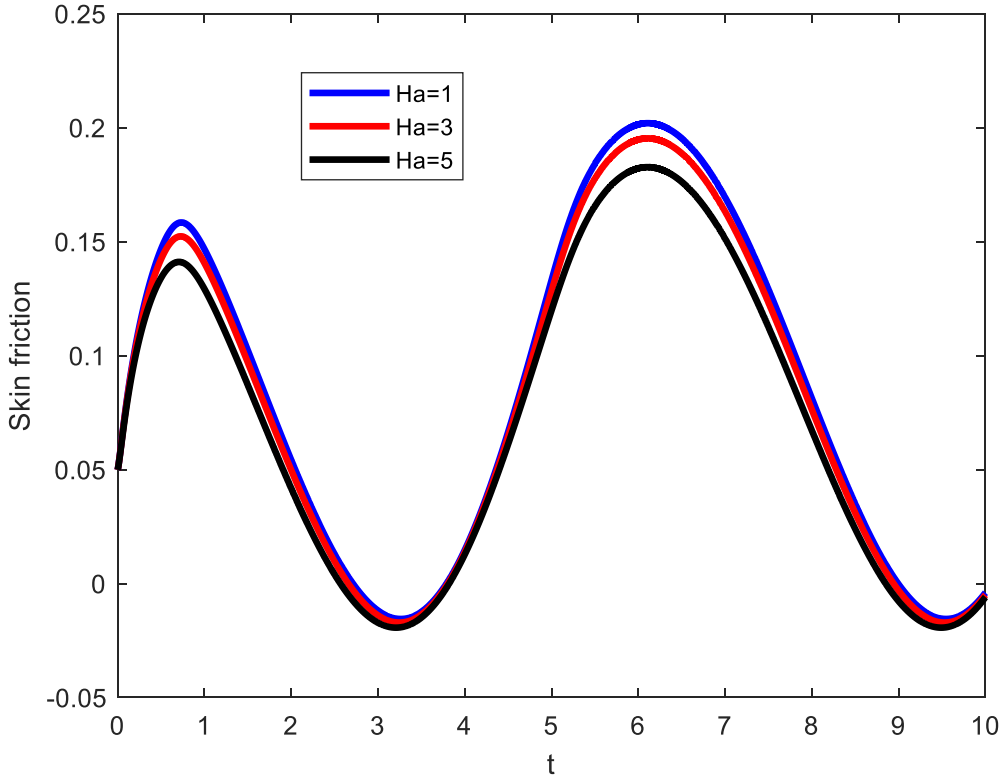

Figure 33: Effect of Hartman number on Cf

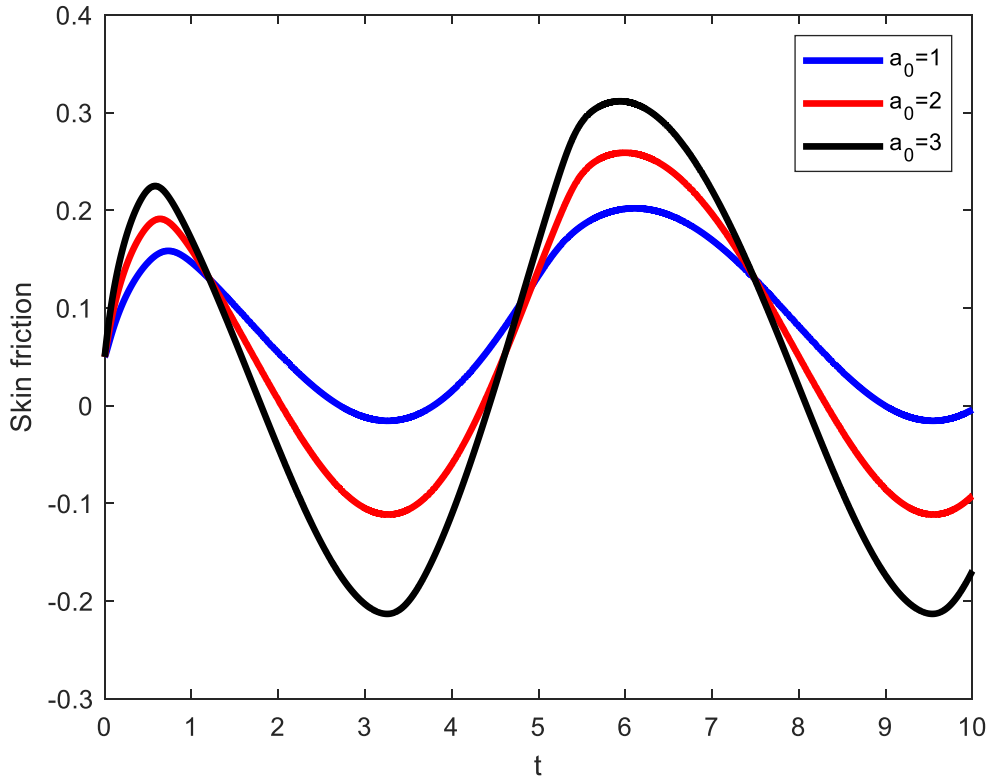

Figure 34: Effect of body acceleration on Cf

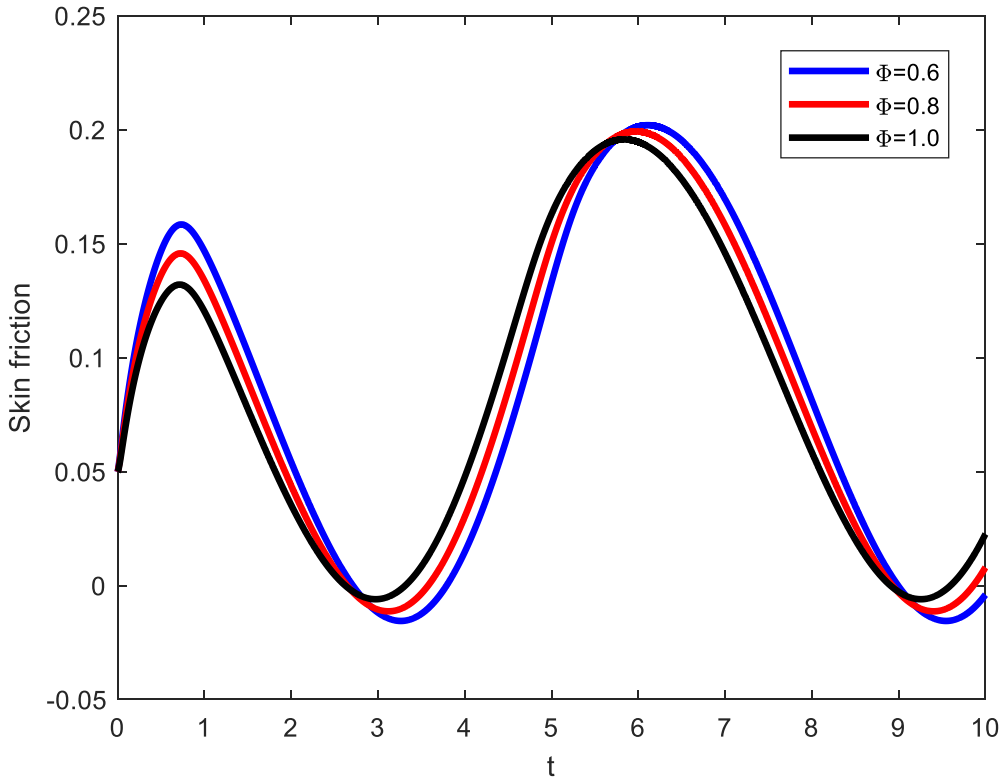

Figure 35: Effect of phase angle on Cf

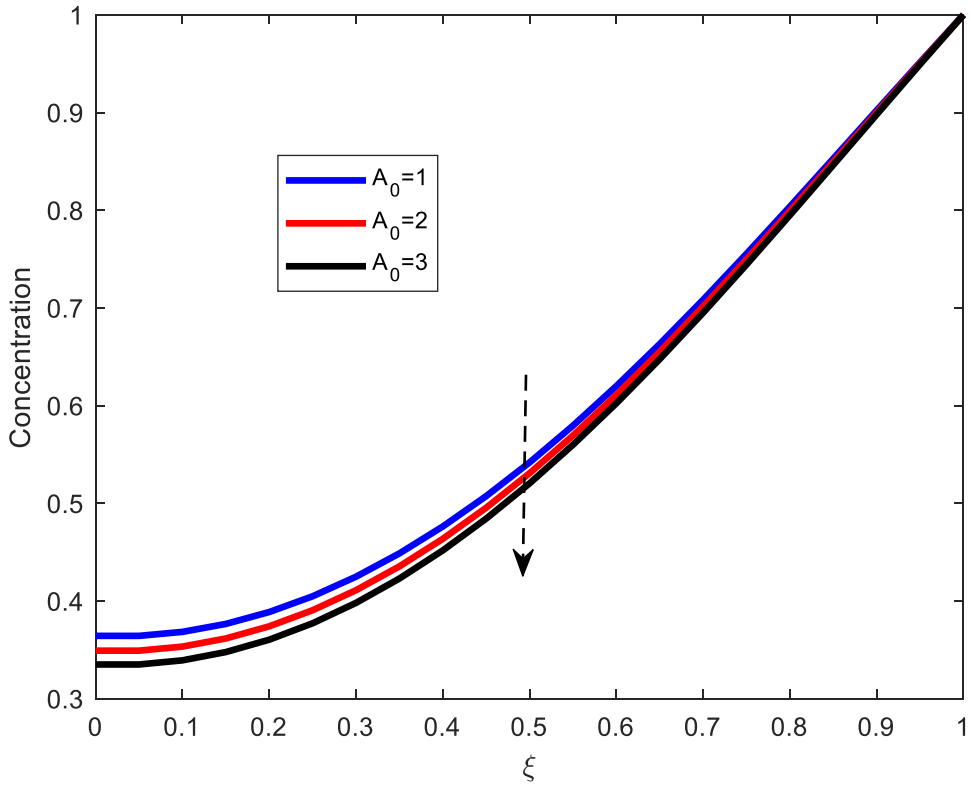

Figure 36: Effect of steady-state part of the pressure gradient on concentration

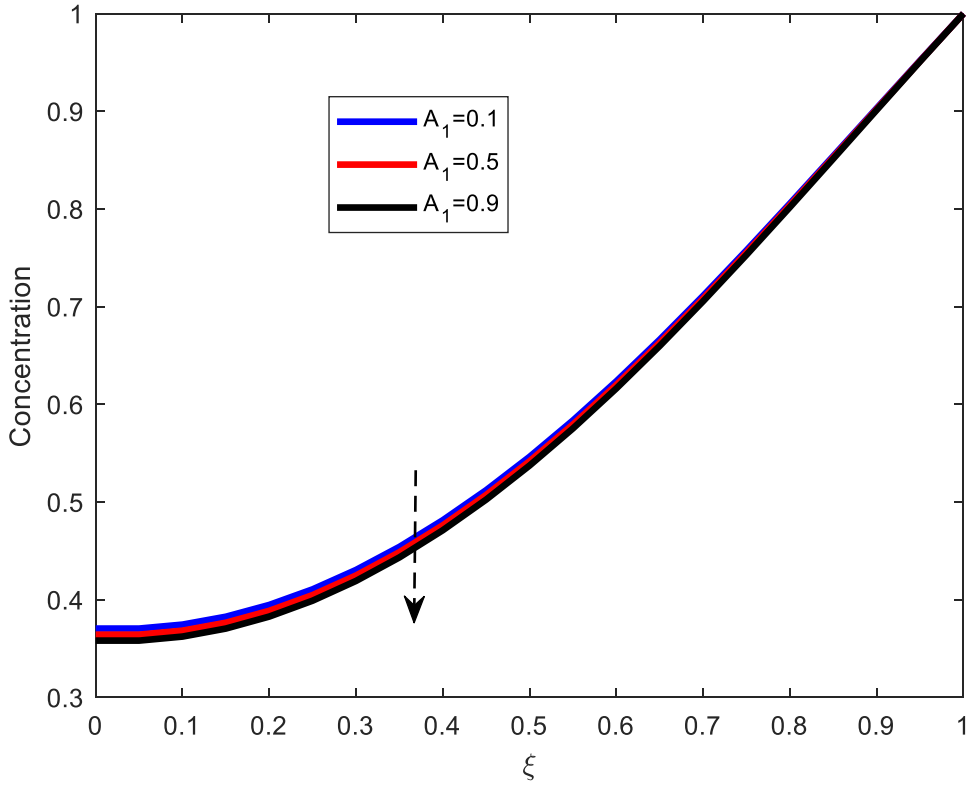

Figure 37: Effect of amplitude of pressure oscillation on concentration

Figure 36 illustrates the effect of increasing the constant steady-state part of the pressure gradient (A_0) on concentration. The graph shows that as A_0 increases, the concentration profile decreases. In Fig. 12 it was observed that increasing the steady-state of pressure gradient, increases the velocity profile of blood. Now, the increase in velocity results into the decrease in the blood's concentration profile. Figure 37 displays the effect of the amplitude of pressure oscillation responsible for enhancing the systolic and diastolic pressures on the concentration profile. From the graph, it is observed, (like A_0) that increasing A_1 reduces the concentration profile. On the other hand, concentration profile decreases with increase in the phase angle (Φ). This is as displayed in Fig. 38. The decrease of the concentration is due to the reason that, increase in Φ, increases the velocity profile of blood, which in turn, declines the concentration.

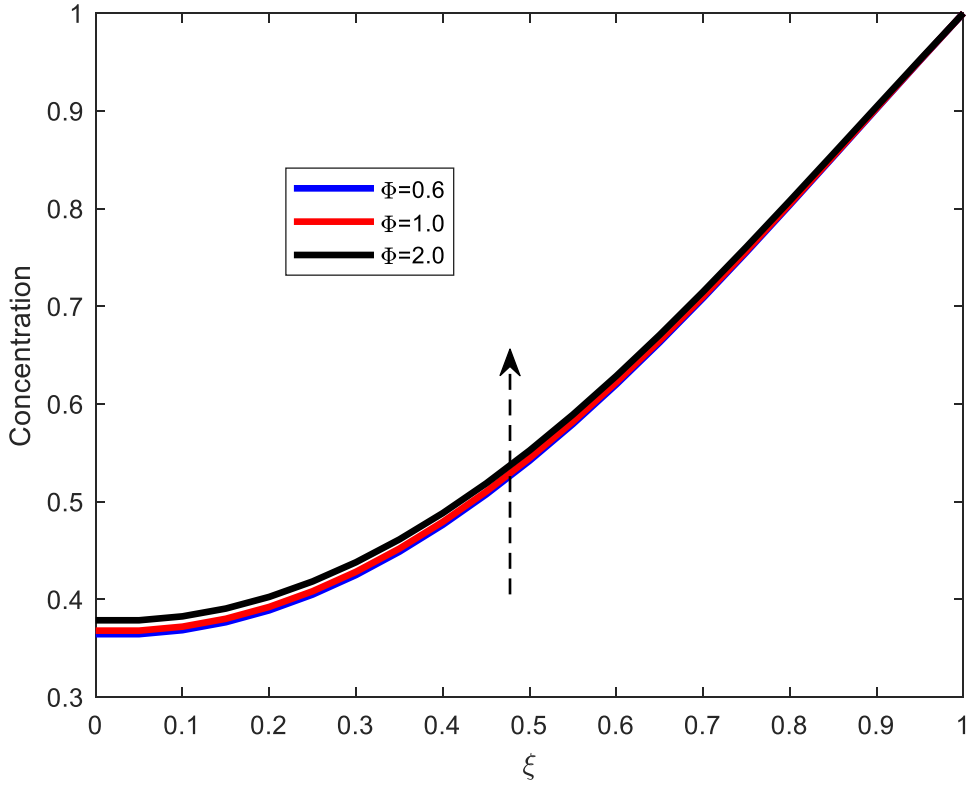

Figure 38: Effect of increasing phase angle on concentration

The combined effect of stenosis, body acceleration, magnetic fields and chemical reaction is shown in Fig. 39. From the graph it is seen that, the presence of stenosis, (in absence of body acceleration, magnetic fields and chemical reaction) highly increases the concentration profile. The presence of magnetic field has also observed to have similar effect (like stenosis) of increasing the concentration profile, however stenosis has been observed to increase more concentration than the magnetic field. (Figure 39, profiles colored with red for stenosis and magenta for magnetic fields). This therefore tells us that the presence of stenosis in arterial

wall highly affects the concentration and therefore it is important to take medication or avoid feedings that lead to stenosis easily. On the other hand, from the same Fig. 39, it is seen that, the presence of chemical reaction (in the absence of stenosis, body acceleration and magnetic fields) diminishes the concentration profiles. The same is observed for the case of body acceleration, that the presence of body acceleration in the absence of stenosis, magnetic fields and chemical reaction, decreases the concentration profile. In this regard, body acceleration is observed to have more impact of reducing concentration profile than the chemical reaction. From the same Fig. 39, it is observed the interesting result that the combined effect of stenosis, body acceleration, magnetic fields and chemical reaction generally increases the concentration profile. It is noticed that, the presence of stenosis alone, highly increases concentration than the combined effect of stenosis, body acceleration, magnetic fields and chemical reaction. In this finding therefore, the magnetic therapy taken during sports for the sake of reducing pain is also affecting the concentration by decreasing concentration profile of a stenosed person. However, the case will be different if magnetic therapy is taken to person without stenosis. In that regard, the magnetic therapy in sports will increase the concentration profile.

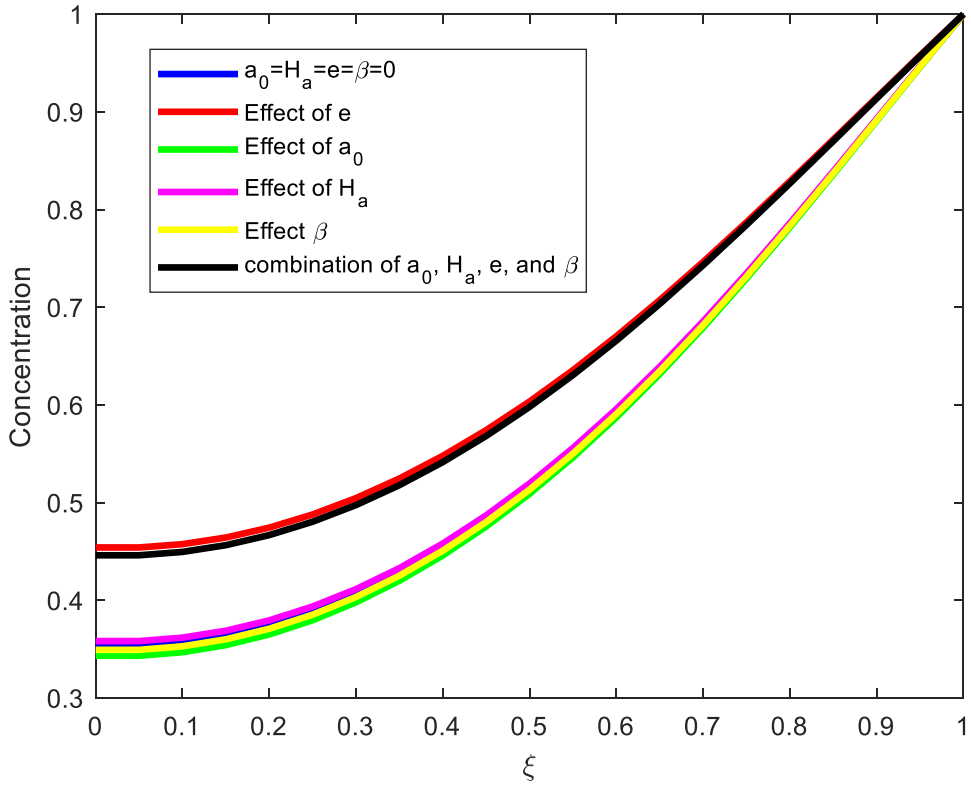

Figure 39: The combined effect of e, a_0, H_a and β on concentration

The computational analysis results of arterial blood flow through a stenosed artery for a case of a non-Newtonian is now presented. In this part, the blood was assumed to follow Herschel-Bulkley (H-B) fluid characteristics. The main parameters for H-B model are the yield stress τ_0, power law index n and the consistency index K. The effects of Hartman number, stenotic height, body acceleration and Reynolds number are displayed and discussed. The constants and values of the parameters used in simulations were chosen by following other scholars, some of the values were assumed based on reality in medical grounds and the type of flow considered (Table 4). Some of the parameter shown in Table 4 were varied to see their effect. The power

Table 4: Parameter values used

Parameter or constant	**value (unit free)**	**Source**
Yield stress τ_0	0.2	Sankar and Lee (2008)
Power law index n	0.95	Sankar and Lee (2008)
Hartman number H_a	1	Sharma and Yadav (2019)
Stenotic height e	0.1	Sankar and Ismail (2010)
Generalized Reynolds number R_{eG}	1	Assumed
Eckert number E_c	1	Tripathi and Sharma (2020)
Peclet number P_e	1	Tripathi and Sharma (2020)
Soret number S_r	0.002	Assumed
Chemical reaction parameter β	0.1	Assumed
Phase angle Φ	0.3	Sankar and Ismail (2010)
Steady state part of pressure gradient A_0	0.8	Mathur and Jain (2011)
Amplitude of the pulsatile A_1	0.5	Mathur and Jain (2011)
Pulse frequency m_1	10	Assumed
Body acceleration frequency m_2	10	Assumed

law index (also known as behavior index) n was varied in a range $0 \leq n \leq 3$. On the other hand, the yield stress τ_0 was varied from $\tau_0 = 0$ to $\tau_0 = 0.5$.

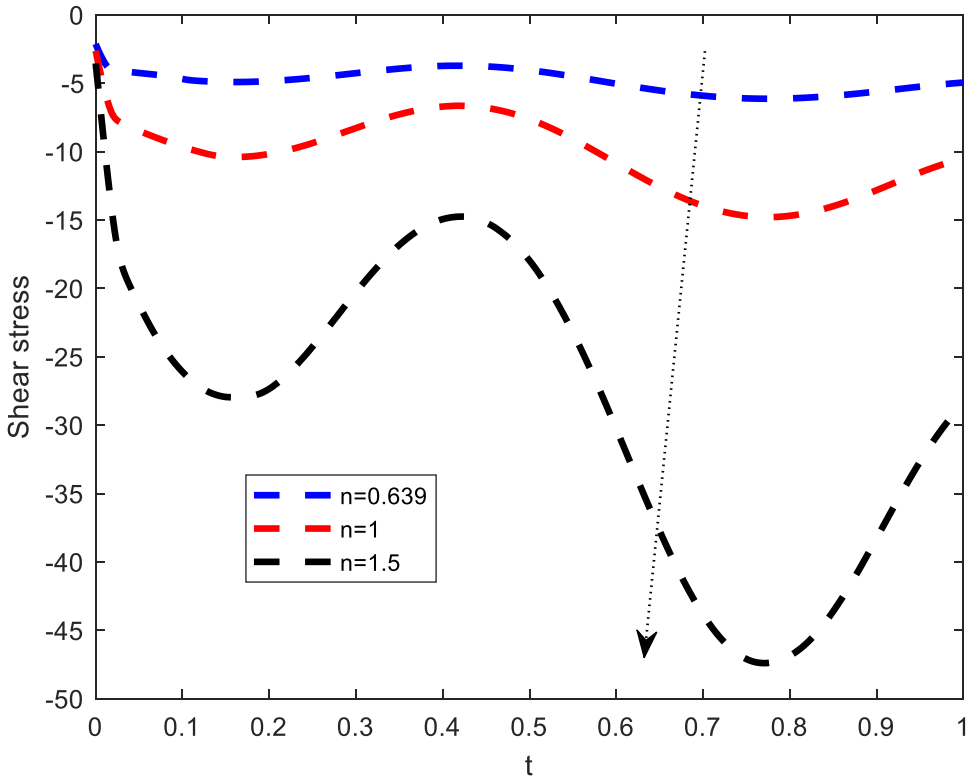

Figure 40: Effect of power law index on shear stress

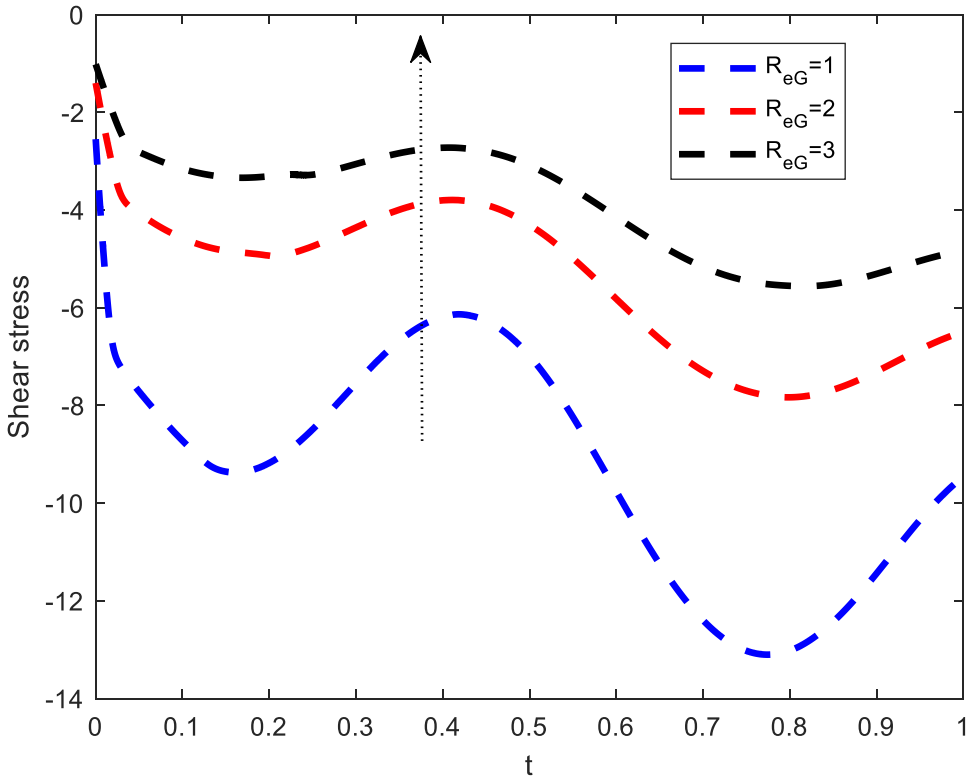

Figure 41: Effect of generalized Reynolds number on shear stress

Figures 40-45 display the results of shear stresses. From the graphs, it is revealed that, the magnitude of shear stress increases as the power law index n increases. This is shown in Fig. 40. The opposite behavior is illustrated in Fig. 41, where the magnitude of shear stress declines towards positive values as generalized Reynolds's number R_{eG} increases. In this regard, increasing the generalized Reynolds's number implies lowering the consistency index. This also implies that as the inertial forces increases, the magnitude of shear stress decreases.

Figure 42 illustrates the effect of yield stress on shear stress. It is observed that as the yield stress increases, the shear stress increases in magnitude. This therefore implies that increasing certain a amount of stress for blood to flow, increases the shear stress. On the other hand, a comparison of shear stress for different fluid behaviors of Herschel-Bulkley, Newtonian, power law and Bingham is shown in Fig. 43. From Fig. 43 it is observed that, the power law fluid when $n > 1$ has higher magnitude of shear stress compared to power law fluid for $n < 1$. The same has been observed for Herschel-Bulkley fluid where the higher the power law index the higher the magnitude of shear stress. It is interesting to note further that when power law index $n > 1$ the shear stress exhibits more difference than when $n < 1$ where the difference is small. This tells us that, shear stress deviates more when $n > 1$ than when $n < 1$. Figure 44 shows the effect of body acceleration on shear stress. It is seen that as body acceleration increases, the shear stress increases in magnitude. The opposite trend is observed in Fig. 45 where, the increase in Hartman number diminishes the magnitude of the shear stress. Hartman number is a ratio of electromagnetic forces to viscous forces. Increasing the Hartman number implies that the viscous forces become lower than the electromagnetic forces. Physically, the Hartman number enhances the Lorentz force which opposes the blood's motion.

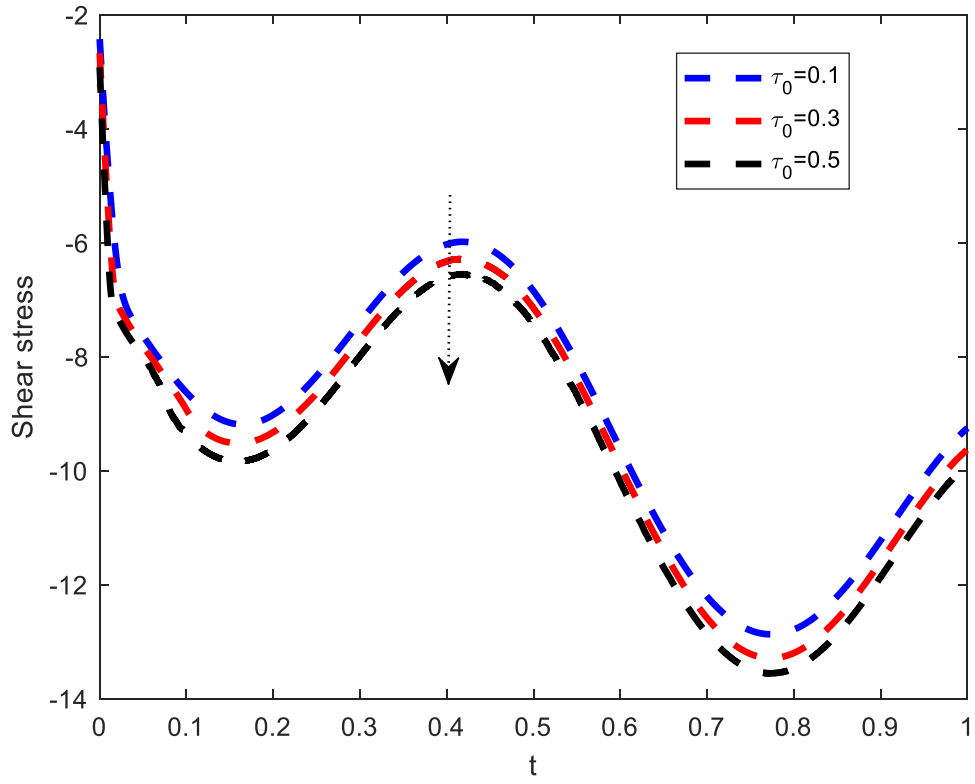

Figure 42: Effect of yield stress τ_0 on shear stress

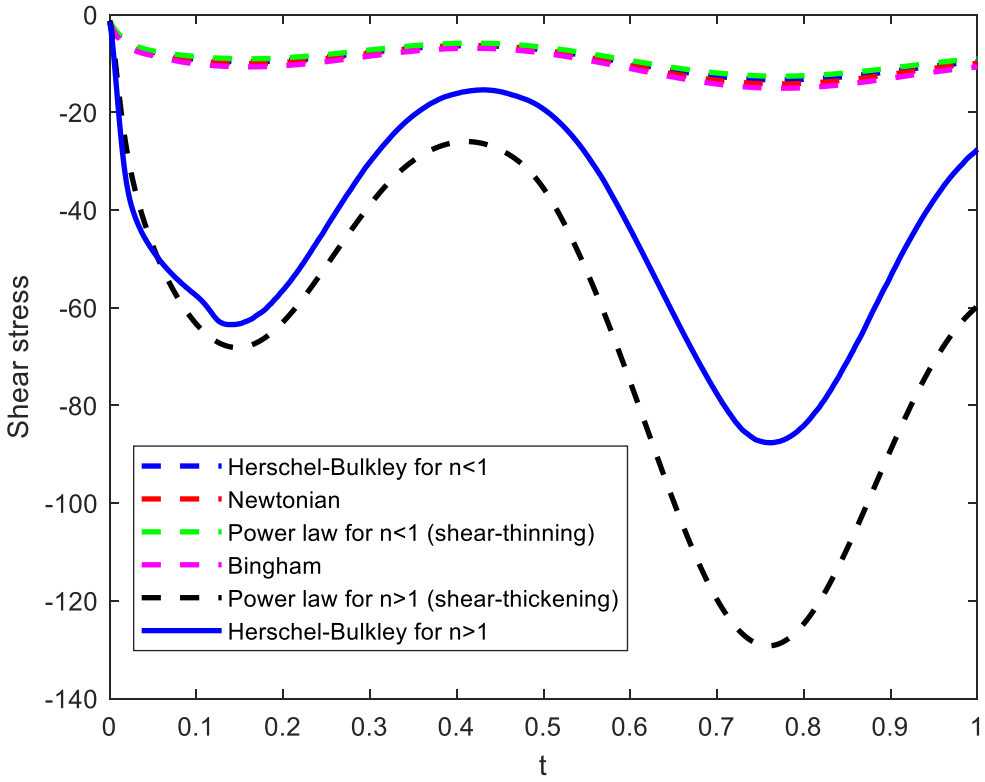

Figure 43: Variation of shear stress for different fluid models

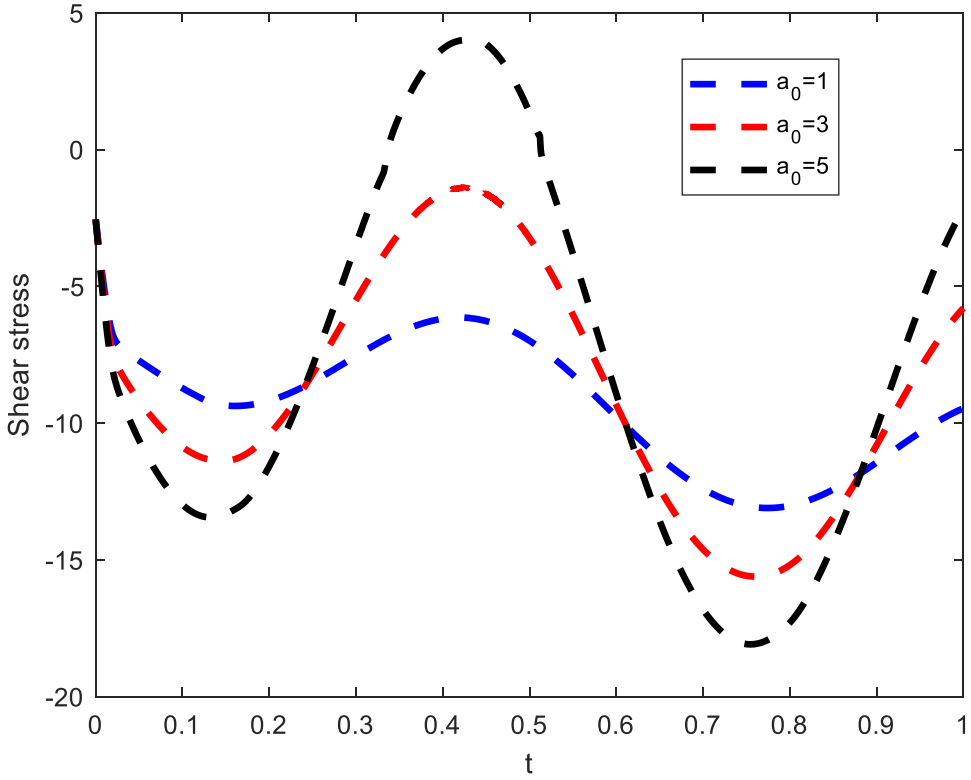

Figure 44: Effect of body acceleration a_0 on shear stress

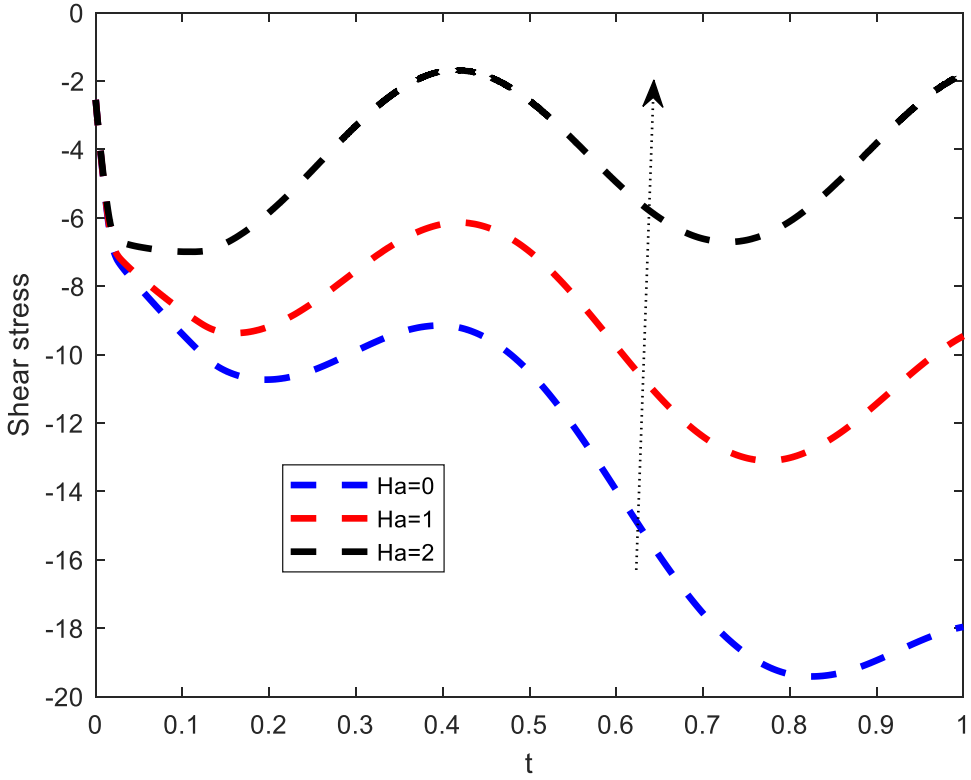

Figure 45: Effect of Hartman number on shear stress

Figures 46-49 below show the variation of axial velocity profiles. In Fig. 46, it is exhibited that, an increase in body acceleration, raises the axial velocity profile. Similar was observed for a case of Newtonian blood. This therefore physically implies that increase in body acceleration (such as body exercise) increase the heart beat and pulse rate as during exercises, muscles and different parts need more supply of oxygen which is carried by blood. This makes blood's velocity raise. Similar as in Newtonian case of blood, it is again seen that increase in Hartman number declines the blood's velocity as illustrated in Fig. 47. Presence of magnetic fields induces the Lorentz force which slows down the motion of blood. This is made possible as blood contains iron oxide whose motion can easily be affected when subjected to magnetic fields. Variation of axial velocity due to generalized Reynolds's number is displayed in Fig. 48. From the Fig. 48, it is observed that increase in the generalized Reynolds's number increases the velocity of the blood. Increasing the Reynolds's number implies that, the inertial forces increase than the viscous forces. Now as inertial forces become more dominant than the viscous forces, the velocity of blood is increased accordingly. The effect of stenosis on blood flow is illustrated in Fig. 49. It is seen that, increasing the stenotic height, diminishes the blood's velocity. Similar behavior was also revealed in a Newtonian case. When stenotic height increases, the radius of the artery is reduced. This makes more blood be on walls of the artery. As blood is viscous in nature, it therefore declines in its velocity. This was also expected as mathematically radius is inversely proportional to the resistance to flow.

Interestingly, it is observed that the effect of body acceleration, Hartman number, and stenosis on the radial velocity is the same as in axial velocity. The only interesting difference discovered is that, the increase in stenotic height diminishes axial velocity but enhances the radial velocity. The graphs for radial velocity are displayed in Fig. 50-53.

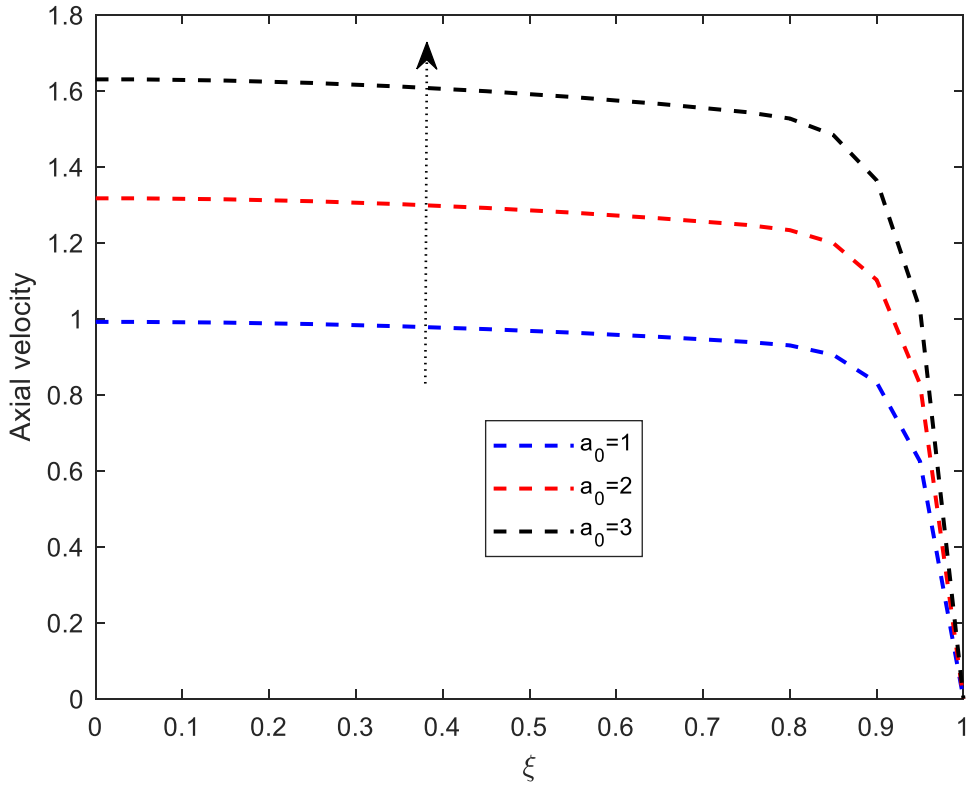

Figure 46: Effect of body acceleration a_0 on axial velocity

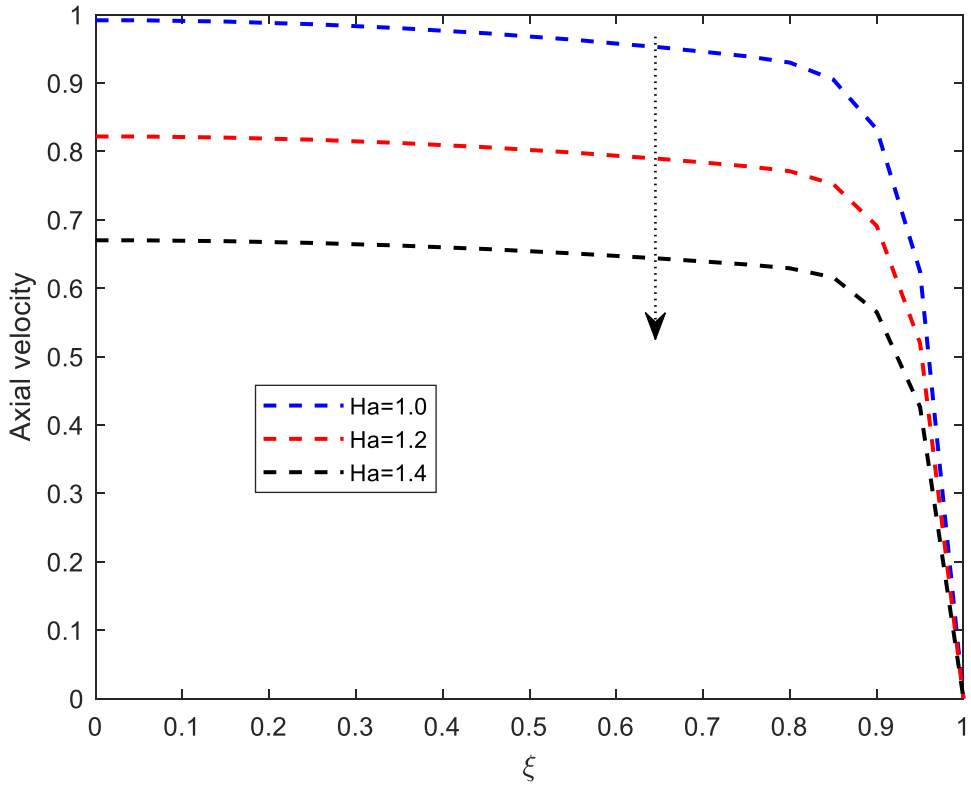

Figure 47: Effect of Hartman number on axial velocity

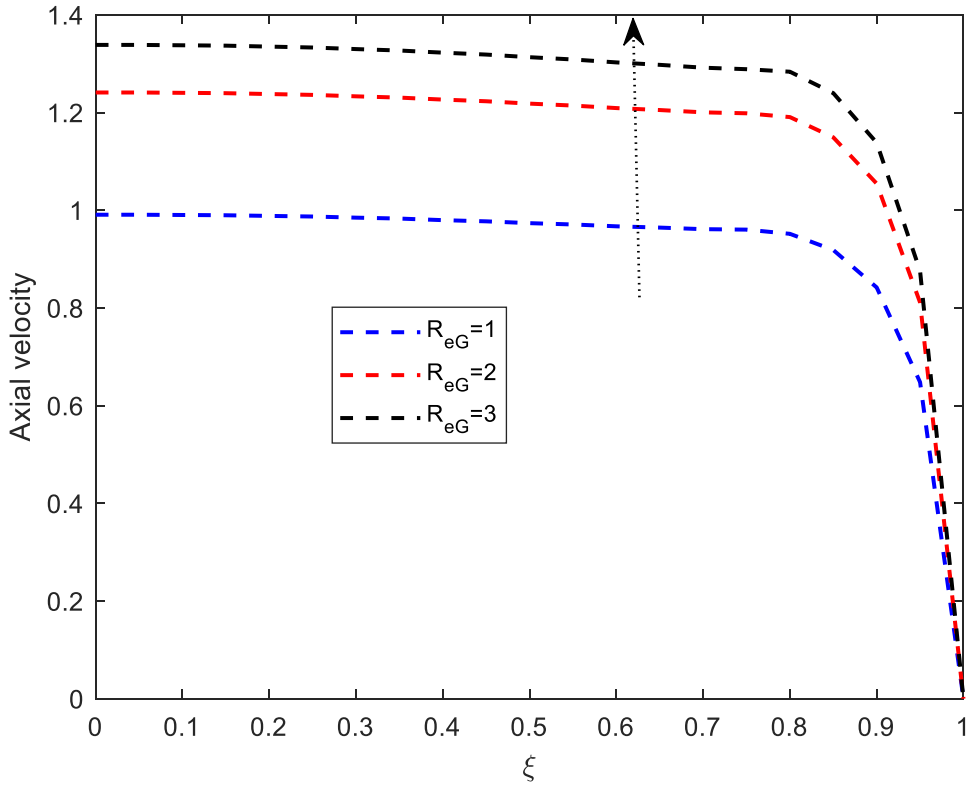

Figure 48: Effect of generalized Reynold'd number on axial velocity

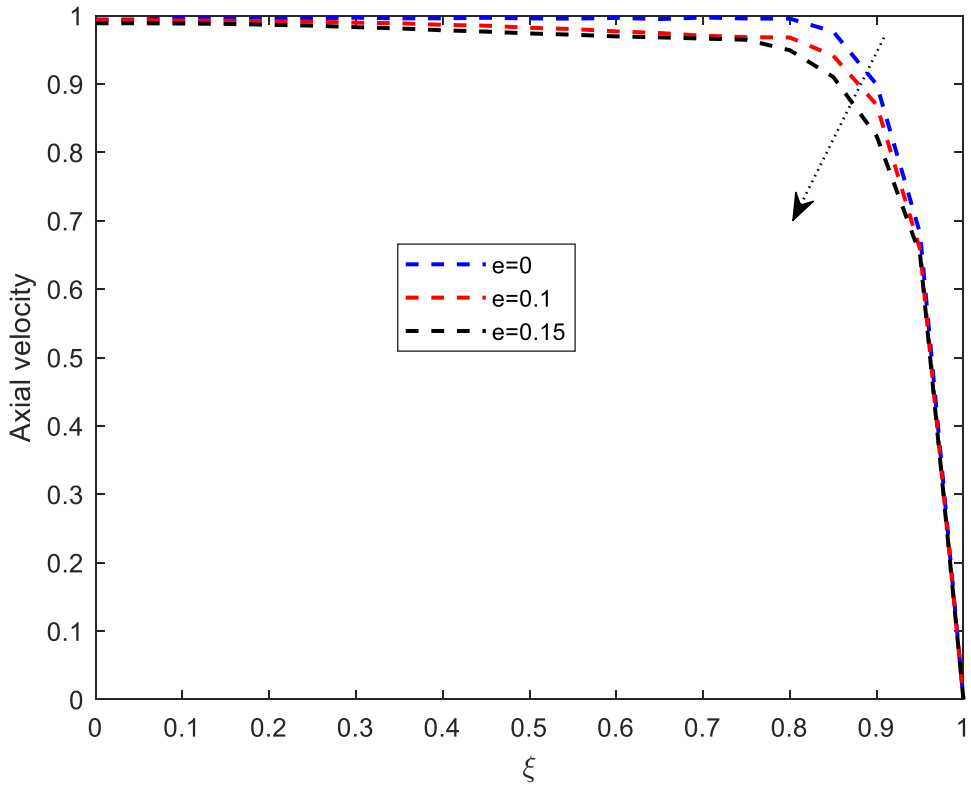

Figure 49: Effect of stenosis e on the axial velocity

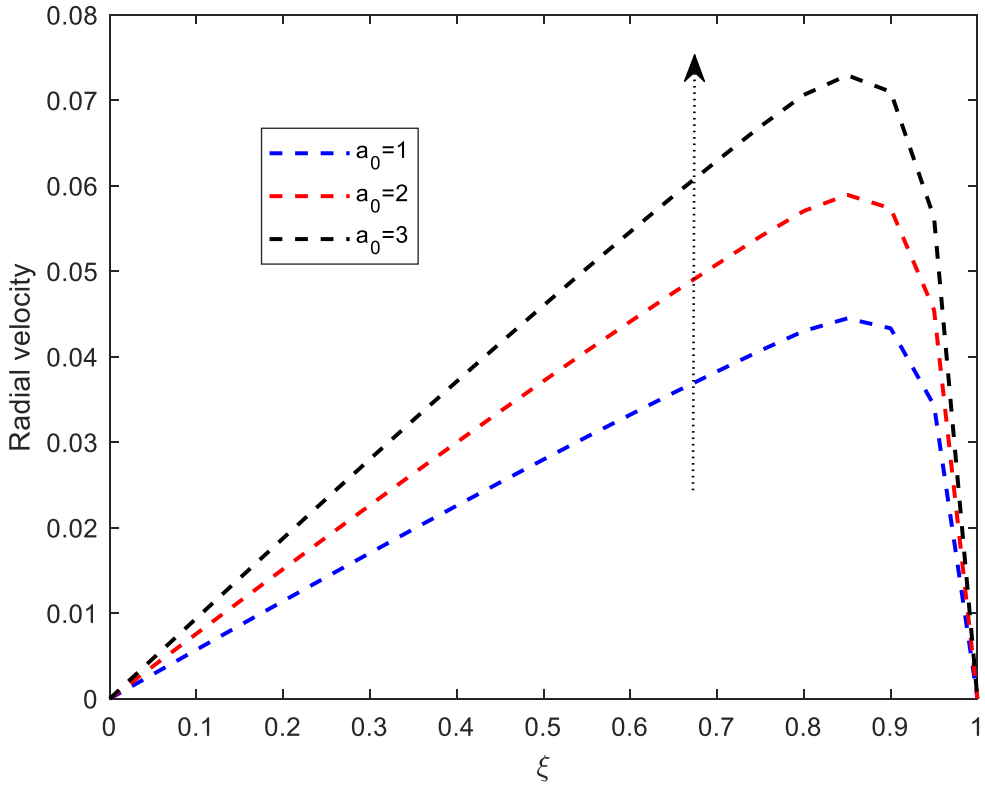

Figure 50: Effect of body acceleration on radial velocity

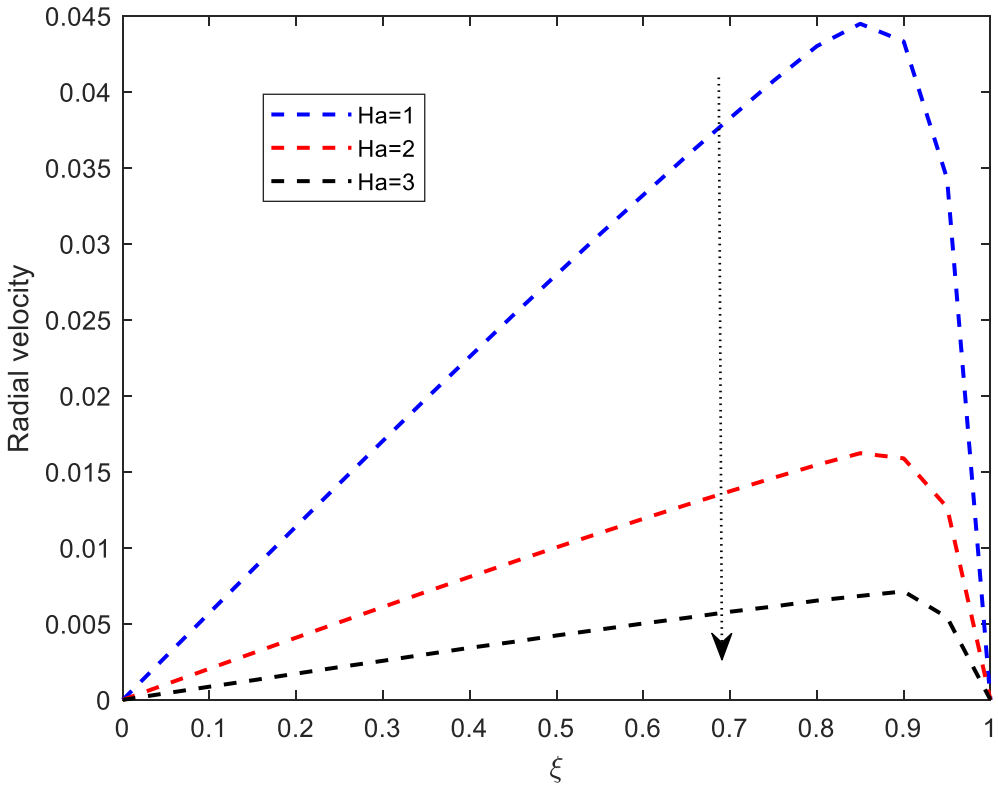

Figure 51: Effect of Hartman number radial velocity

Temperature profiles against radial distance are displayed in Fig. 54-58. One of the core functions of blood is to transfer heat. Now, the illustration of variation of temperature due to various

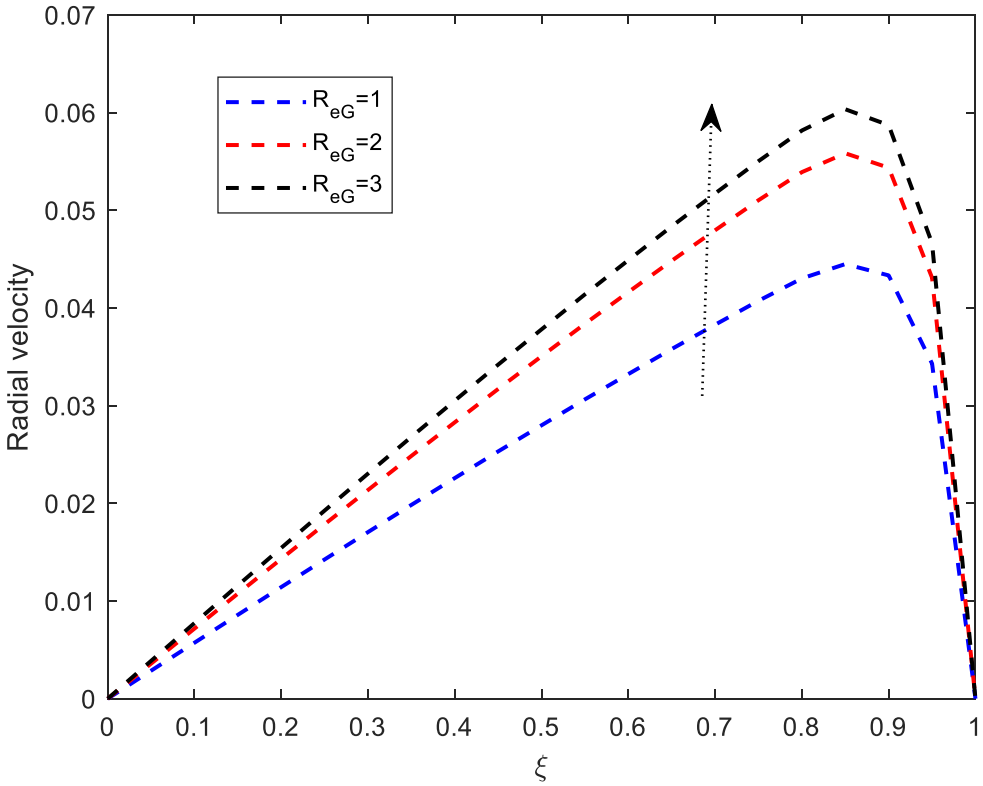

Figure 52: Effect of the generalized Reynolds's number on radial velocity

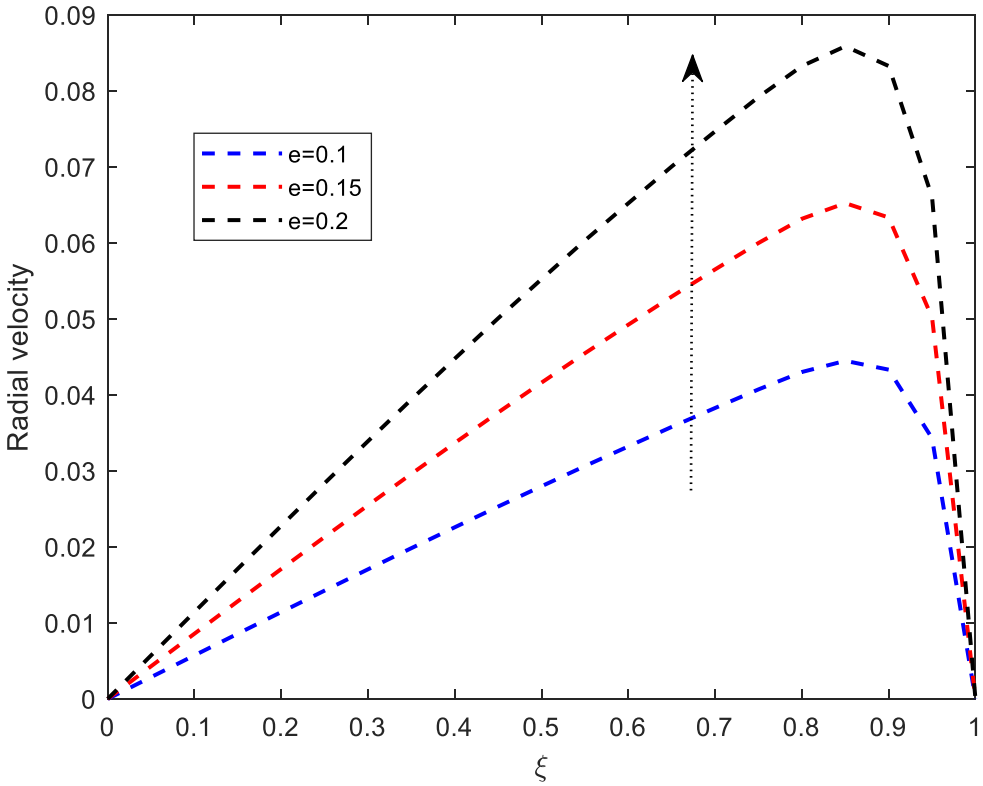

Figure 53: Effect of stenosis on radial velocity

factors is done. Figure 54 shows the effect of Peclet number on temperature profile. Peclet number is the ratio of the heat transferred by convection to the heat transferred by conduction.

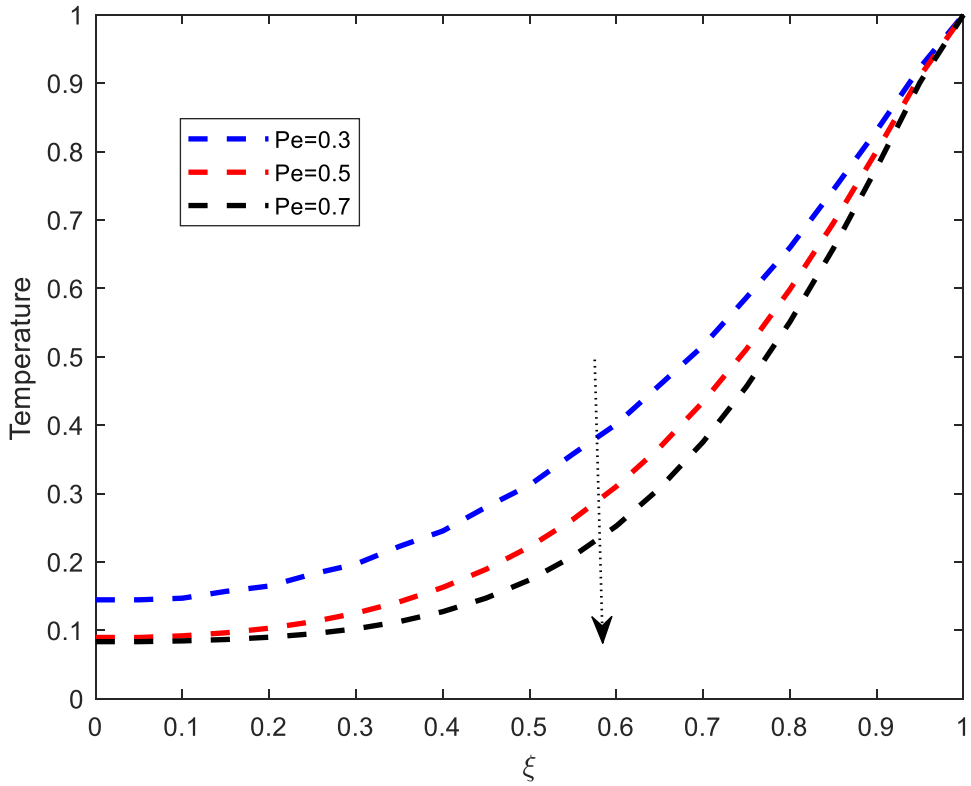

Figure 54: Effect of Peclet number on temperature profiles

It is observed that, increase in Peclet number diminishes temperature profile. This means that heat transfer by motion of blood increases than heat transfer by conduction.

In Fig. 55 it is observed, as expected that, increase in body acceleration raises temperature profile. This implies that body exercise give rise to the core body temperature. It was used to know that the core body temperature raises if someone has an abnormal condition of a body, say a disease. However, through this study it is therefore true to include body exercise as one of the factors that raises the core body temperature.

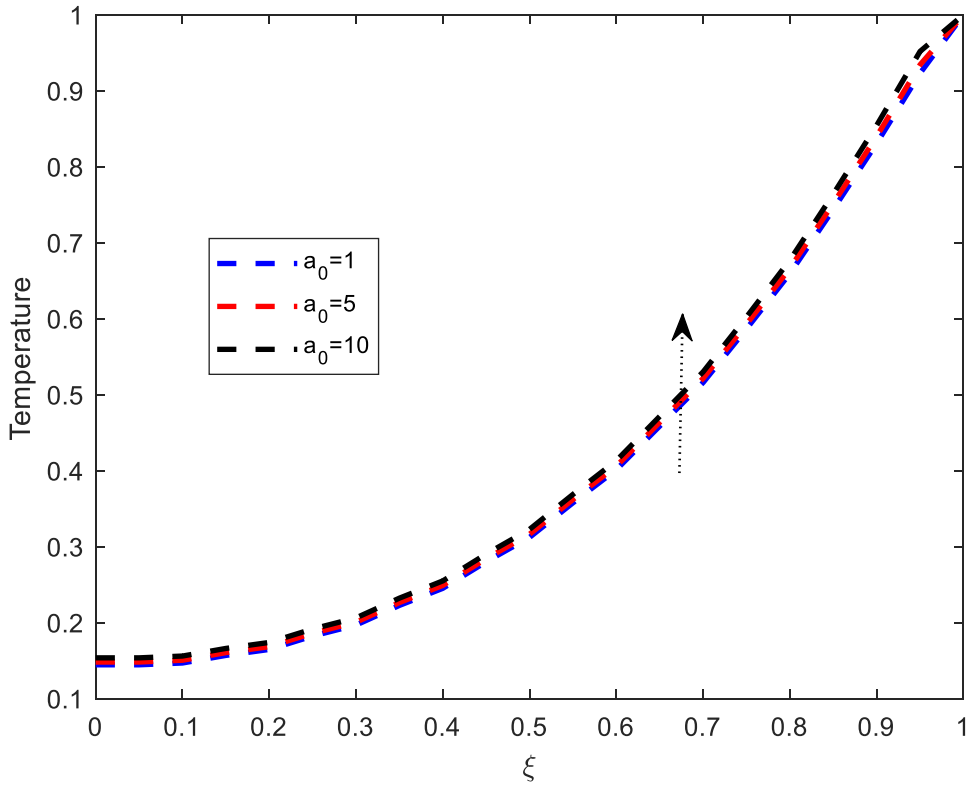

Figure 55: Effect of body acceleration on temperature profiles

Eckert number is defined as the ratio of the advective mass transfer to the heat dissipation potential. It offers a measure of the kinetic energy of the flow relative to the enthalpy difference across the thermal boundary layer. It is observed in Fig. 56 that the increase in Eckert number increases the temperature profile, physically implying that as Eckert number increases, the advective mass transfer dominates the heat dissipation potential and therefore the temperature increases. Therefore, it is noticed that the increase in the Eckert number is to enhance the temperature distribution. This is due to the fact that the energy is stored in the fluid region as a consequence of dissipation due to viscosity. It is also illustrated on Fig. 57 that the temperature diminishes with increase in Hartman number. This is because, the rate of increase of axial velocity decreases with Hartman number. Further more, as displayed in the Fig. 58, the dimensionless temperature decreases with the increase of the generalized Reynolds number R_{eG}.

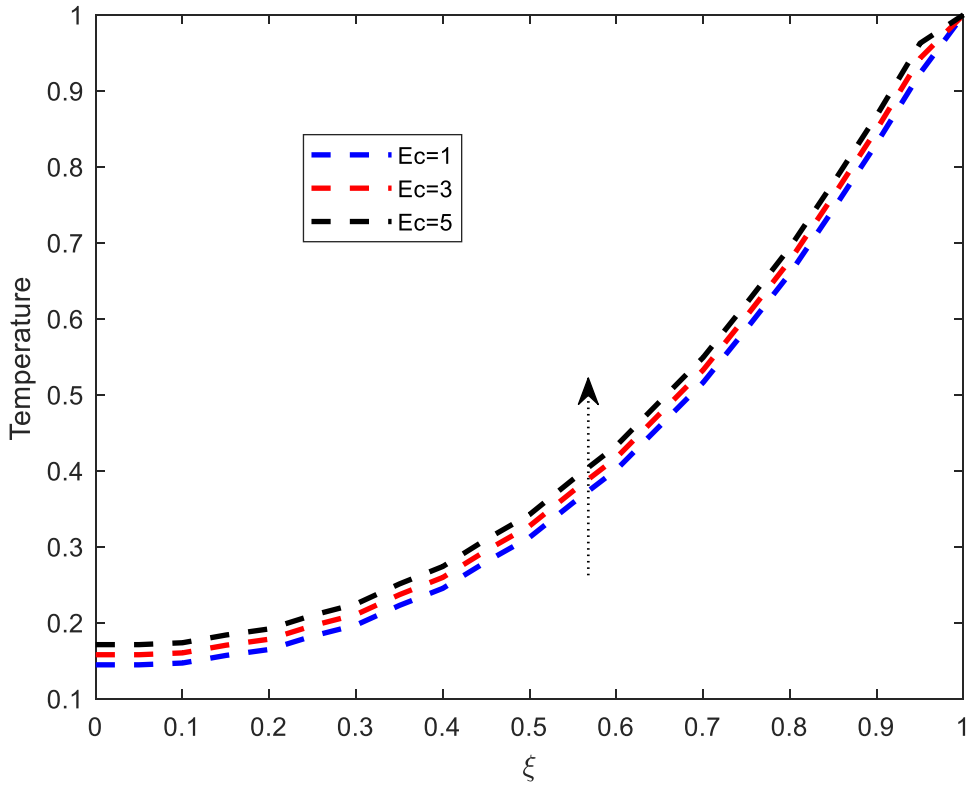

Figure 56: Effect of Eckert number on temperature profiles

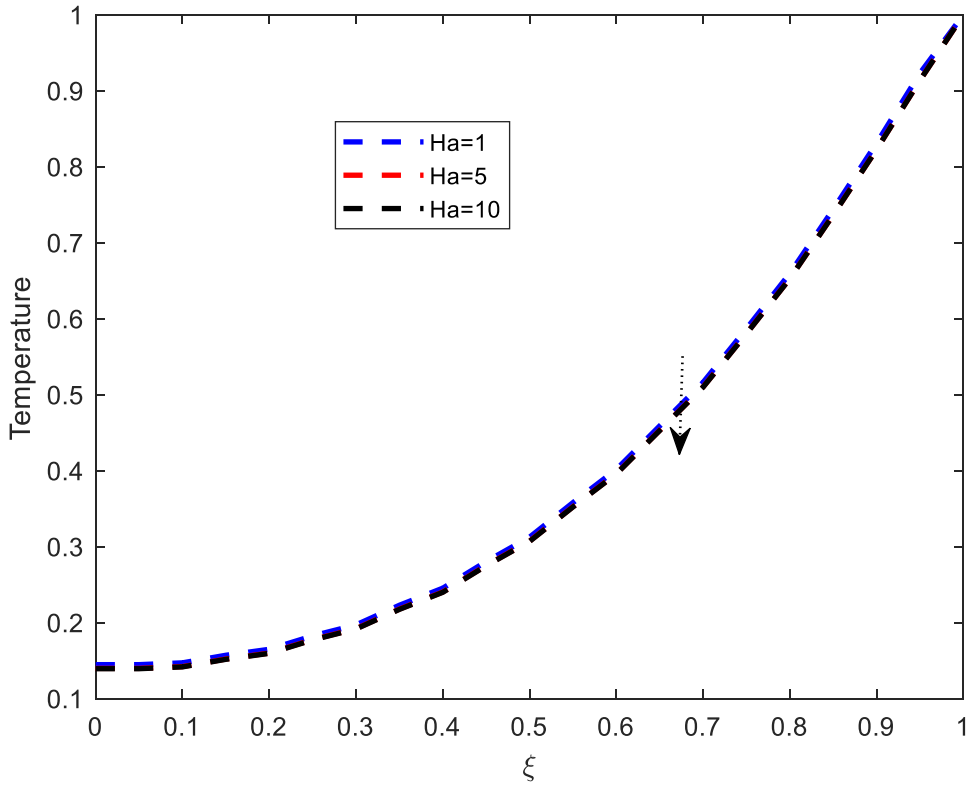

Figure 57: Effect of Hartman number on temperature profiles

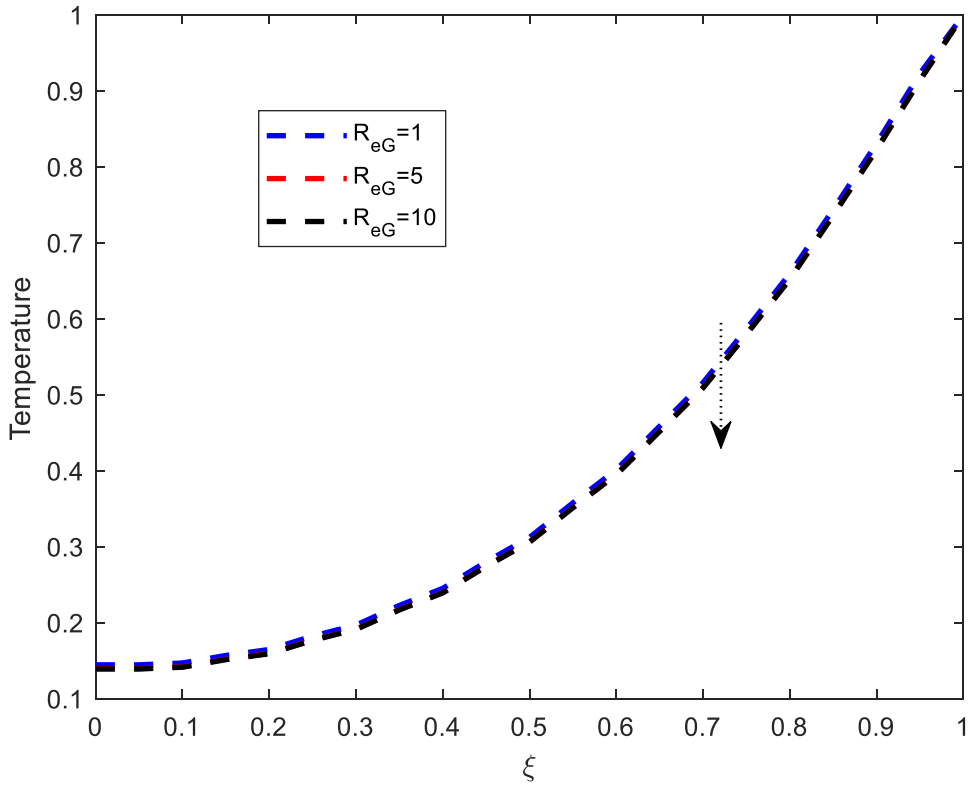

Figure 58: Effect of Generalized Reynolds number on temperature profiles

Figures 59-61 illustrate the variations of concentration profiles. From Fig. 59 it is observed that, the concentration profile decreases with increasing chemical reaction parameter, which implies that the chemical reaction parameter acts as a destructive agent of chemical species in blood. On the other hand, Fig. 60 shows the effect of increasing the Soret number on concentration profile. Soret number is the ratio of temperature difference to the concentration. From Fig. 60, it is observed two patterns, first the increase in Soret number, declines the concentration profiles however later, close to the arterial wall, the Soret number is observed to enhance the concentration profile. The Peclet number may be defined as the ratio of the species transport by fluid convective motion to the species transport by molecular diffusion that is P_e, is measure of the mass transfer by convection compared to that due to diffusion. Figure 61 exhibits the effect of increasing P_e on concentration profile. From Fig. 61, it is revealed that increasing Peclet number, reduces the concentration profile. This decrease in concentration is expected because of the loss of solute in the blood. Similar results have been reported by Raja *et al.* (2017).

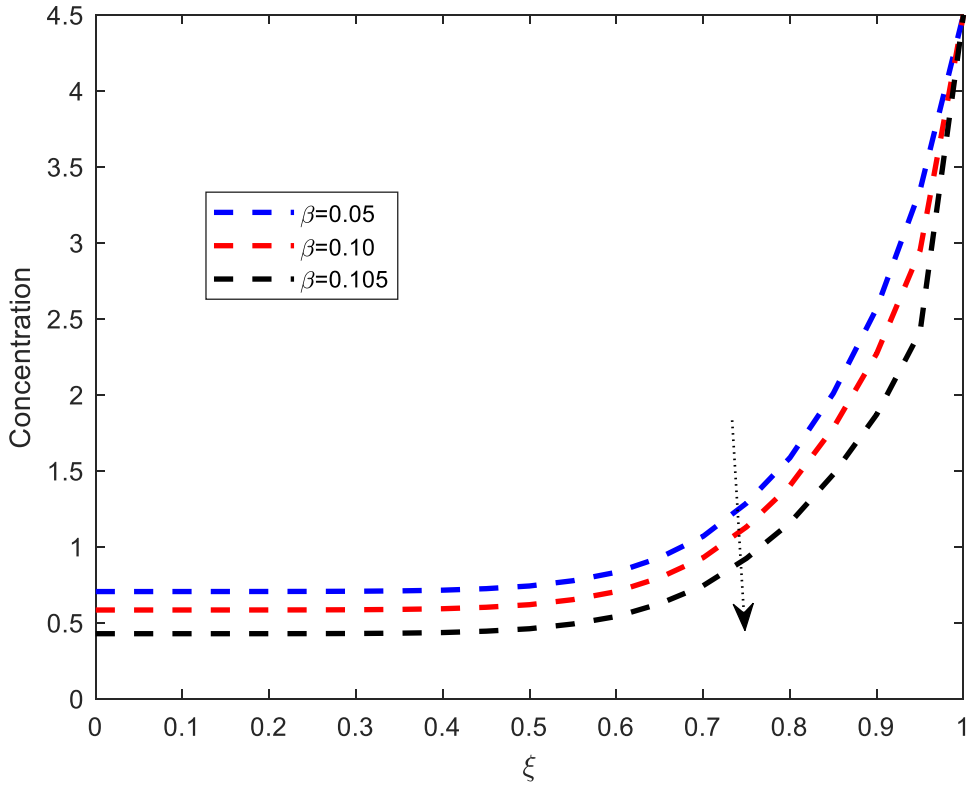

Figure 59: Effect of reaction on concentration profiles

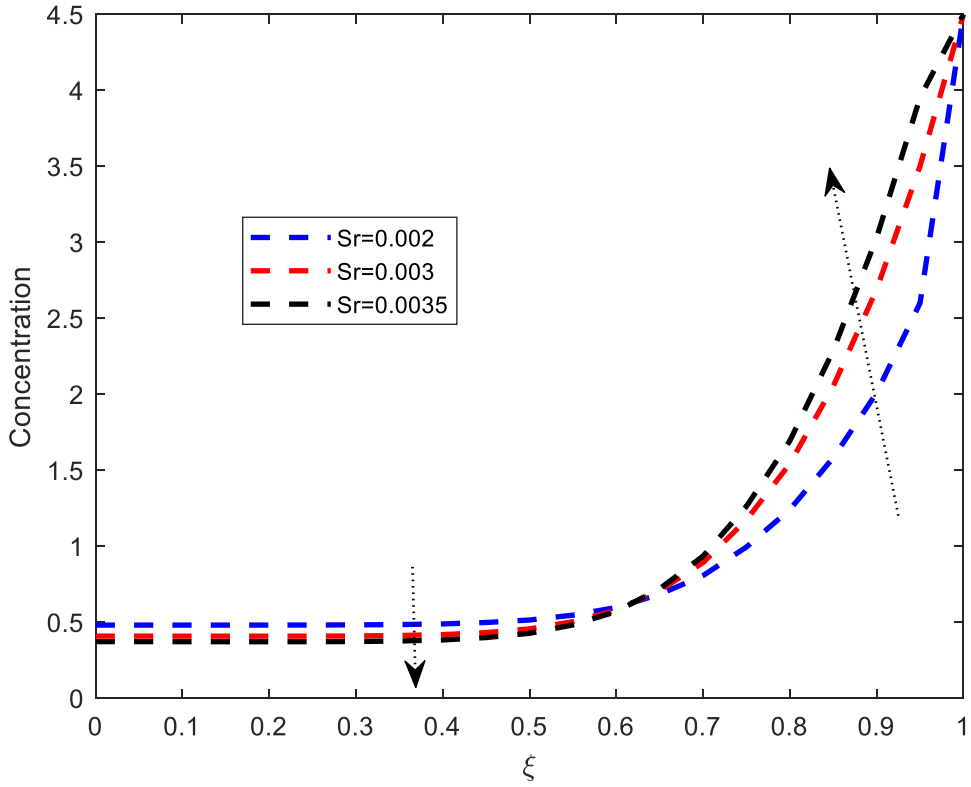

Figure 60: Effect of Soret number S_r on concentration profiles

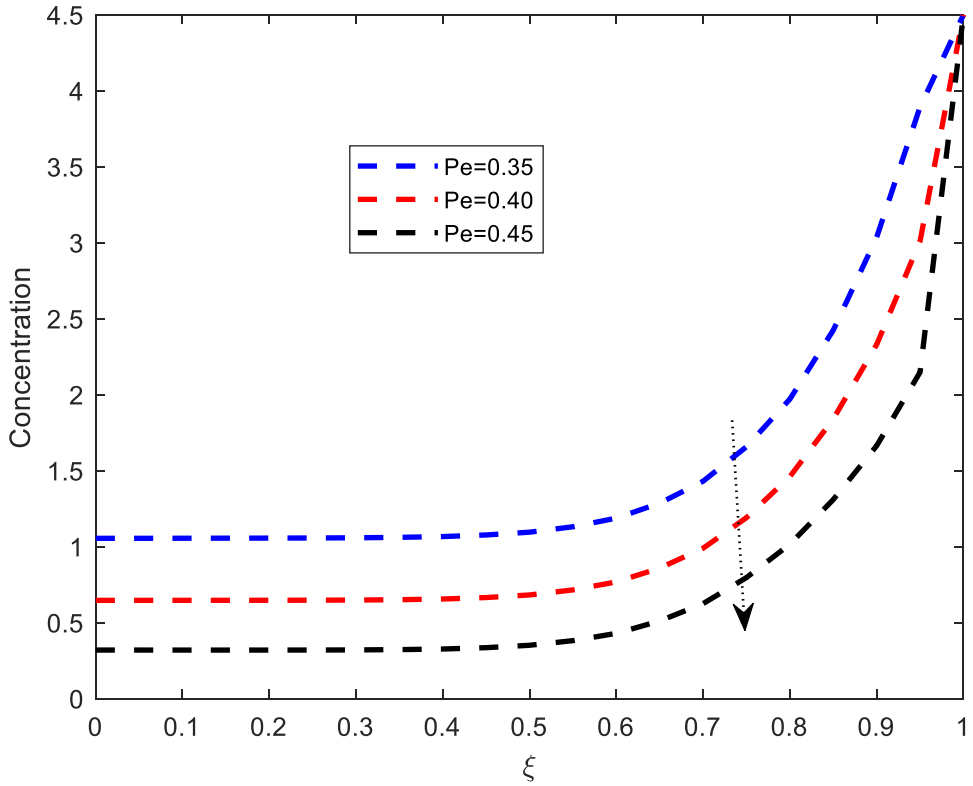

Figure 61: Effect of Peclet number P_e on concentration profiles

In order to validate the model, the profile of axial velocity for Newtonian model was compared with Changidar and De (2015). The result is as shown in Fig. 62. The result is found to be in good agreement though their study did not include magnetic fields. In that regard therefore, For the purpose of validating model, in the current study, the Hartman number was set to zero. This way of validation was also done by Changidar and De (2015) and Misra *et al.* (2018).

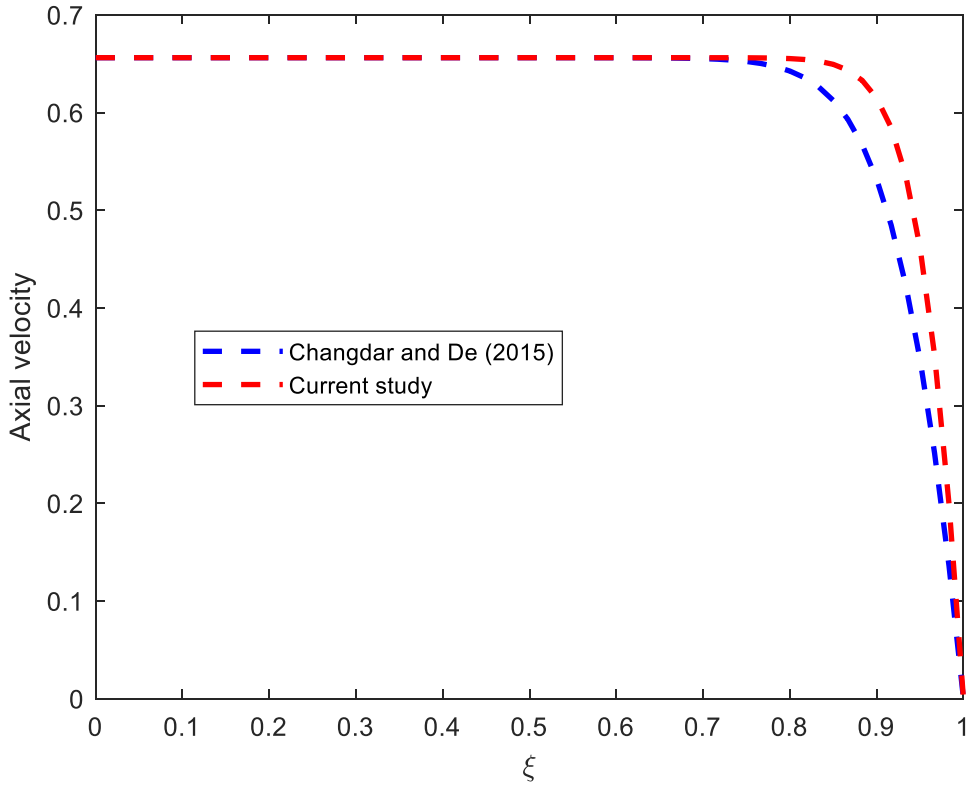

Figure 62: Validation of axial velocity

CHAPTER FIVE

CONCLUSION AND RECOMMENDATIONS

5.1 Conclusion

The current study investigates the unsteady flow of blood through a stenosed artery in the presence of body acceleration, uniform magnetic fields and chemical reaction. The study has considered the blood to behave both, as a Newtonian and a non-Newtonian fluid. The quantities of radial velocity u, axial velocity w, temperature T and concentration C have been portrayed. The study has also investigated the effects of varying the flow parameters such as Reynolds, Hartman, Peclet, Eckert, Schmidt, and Soret numbers on profiles of velocity, temperature and concentration.

The model equations for both the Newtonian and Non-Newtonian fluid were discretized using the explicit Finite Difference Method (FDM). Before discretization, the model equations were transformed from a cylindrical polar coordinated system to a rectangular Cartesian system. The constriction H(z) was transformed by introducing another variable $\xi = \frac{\eta}{H(z)}$. The discretized equations were then implemented in MATLAB package and doing simulations to analyse and study the effects of various parameters and flow variables.

The study established that the presence of stenosis, body acceleration and magnetic fields have effects on the flow of blood. Chemical reaction is observed to reduce the concentration profiles. For the case when blood is considered to be Newtonian, it is established that increasing the stenotic height, diminishes the axial velocity and increases the radial velocity. The study reveals further, that the combined effects of stenosis, magnetic fields and body acceleration reduces the velocity of the blood. In this regard therefore, since body exercise highly raises the blood's speed, magnetic therapy for a stenosed person will therefore be more advantageous, not only for reducing pain but also regulating blood rheology by reducing blood's velocity.

In the Non-Newtonian case, blood was considered to be a Herschel-Bulkley fluid. It is established that the Herschel-Bulkley fluid experience higher velocity than the power law (for both when $n < 1$ and when $n > 1$), the Bingham and the Newtonian fluids. Further more, shear stress is observed to deviate more when $n > 1$ than when $n < 1$. Considering the shear stresses for different fluids, it is suggested that it is much better to set the power law index n to be less than

one for modeling blood flow. This is because, (as observed in figure 43) that for power law index n greater than 1, the shear stress experience higher values than when the power law index is less than 1. Low shear stress will allow the blood to flow like a liquid as expected.

5.2 Recommendations

According to the findings presented in the previous chapter, the current study recommends the following:

(i) MRI scanning in hospitals should be done with care, taking into account that the blood velocity of a patient being subjected to the MRI machine decreases.

(ii) Magnetic therapy in sports is recommended, this provides multiple benefits. The current study indicates that magnetic therapy helps in regulating blood flow which has been increased by body accelerations.

(iii) Blood can be modeled as Newtonian or non-Newtonian, however, through this study it is strongly recommended that blood should be modeled as a non-Newtonian fluid. This is after studying the difference in shear stress and velocity profiles between the Newtonian and Herschel-Bulkley fluids.

(iv) It is better to set the value of power law index n to be less than 1 when modeling blood flow using the non-Newtonian models.

The following are possible extensions of research:

(i) One can extend the current research by considering that the arterial wall has multiple stenoses

(ii) One can extend the current research by considering that the constriction is a function of time t (the geometry of the time-variant stenosis) such that $\frac{\partial R}{\partial t} \neq 0$.

(iii) One can consider the viscosity of blood as a variable (varying with different physical factors such as temperature) and not a constant.

REFERENCES

Agarwal, R., & Varshney, N. (2016). Pulsatile flow of Herschel-Bulkley fluid through an inclined multiple stenoses artery with periodic body acceleration. *Pelagia Research Library, Advances in Applied Science Research,* 7(3), 102–113.

Alsemiry, R. D., Mandal, P. K., Sayed, H. M., & Amin, N. (2020). Numerical solution of blood flow and mass transport in an elastic tube with multiple stenoses. *BioMed Research International,* 1–14.

Awaludin, I. S., & Ahmad, R. R. (2013). Blood flow velocity in stenosed artery. In: AIP Conference Proceedings. *American Institute of Physics*, 1522, 261–268.

Awojoyogbe, O. B., Faromika, O., Dada, M., Boubaker, K., & Ojambati, O. (2011). Mathematical models of real geometrical factors in restricted blood vessels for the analysis of CAD (coronary artery diseases) using Legendre, Boubaker and Bessel polynomials. *Journal of Medical systems*, 35(6), 1513–1520.

Biswas, D., & Laskar, R. B. (2011). Steady flow of blood through a stenosed artery: A non-Newtonian fluid model. *Assam University Journal of Science and Technology*, 7(2),144–153.

Bunonyo, K., Israel-Cookey, C., & Amos, E. (2018). Modeling of blood flow through stenosed artery with heat in the presence of magnetic field. *Asian Research Journal of Mathematics*, 8(1), 1–14.

Casiday, R., Frey, R., & Mao, K. (2012). Blood, sweat, and buffers: PH regulation during exercise. *Washington University,* 1–12.

Changdar, S., & De, S. (2015). Numerical simulation of nonlinear pulsatile Newtonian blood flow through a multiple stenosed artery. *International scholarly research notices*, 1–10.

Chitra, M., & Bhaskaran, R. (2019). Dynamical influence of heat and mass transfer on unsteady visco-elastic fluid on blood flow through an artery: Effects of chemical reaction. *International Journal of Research in Advent Technology,* 7(1), 101–109.

Das, K., & Saha, G. (2009). Arterial MHD pulsatile flow of blood under periodic body acceleration. *Bulletin of Society of Mathematicians Banja Luka*, 16, 21–42.

Davidson, P. A. (2001). *An introduction to Magnetohydrodynamics*. Cambridge University Press.

DeSaix, P., Betts, J. G., Johnson, E., Johnson, J. E., Korol, O., Kruse, D. H., Poe, B., Wise, J. A., & Young, K. A. (2018). *Anatomy and Physiology*. OpenStax.

Gijsen, F., Allanic, E., Van de Vosse, F., & Janssen, J. (1999). The influence of the non-Newtonian properties of blood on the flow in large arteries: Unsteady flow in a 90 curved tube. *Journal of Biomechanics*, 32(7), 705–713.

Haghighi, A. R., & Aliashrafi, N. (2018). A mathematical modeling of pulsatile blood flow through a stenosed artery under effect of a magnetic field. *Journal of Mathematical Modeling*, 6(2), 149–164.

Hauke, G. (2008). *An introduction to fluid mechanics and transport phenomena.* Volume 86. Springer.

Hossain, K. E., & Haque, M. M. (2017). Influence of magnetic field on the chemically reactive blood flow through stenosed bifurcated arteries. *In: AIP Conference Proceedings*, 1851, 1–13.

Ismail, Z., Abdullah, I., Mustapha, N., & Amin, N. (2008). A power-law model of blood flow through a tapered overlapping stenosed artery. *Applied Mathematics and Computation*, 195(2), 669–680.

Jamil, D. F., Roslan, R., Abdulhameed, M., Che-Him, N., Sufahani, S., Mohamad, M., & Kamardan, M. G. (2018). Unsteady blood flow with nanoparticles through stenosed arteries in the presence of periodic body acceleration. *Journal of Physics*, 995, 1– 9.

Joshua, T. M., Anwar, K., & Abdullah, N. (2020). Numerical simulation of non – Newtonian blood flow through a tapered stenosed artery using the cross model. *In: IOP Conference Series: Materials Science and Engineering*, 864, 1–12.

Keener, J. P., & Sneyd, J. (1998). *Mathematical physiology*. Springer.

Khambhampati, T. K. (2013*). A comparative study between Newtonian and non – Newtonian models in a stenosis of a carotid artery*. Master's thesis. Texas A and M University.

Kumar, D., Satyanarayana, B., Kumar, R., Kumar, S., & Deo, N. (2021). Application of heat source and chemical reaction in MHD blood flow through permeable bifurcated arteries with inclined magnetic field in tumor treatments. *Results in Applied Mathematics*, 10(2021), 1–13.

Kumari, S., Rathee, R., & Nandal, J. (2019). Unsteady peristaltic transport of MHD fluid through an inclined stenosed artery with slip effect. *International Journal of Applied Engineering Research*, 14(8), 1881–1891.

Liu, Y., & Liu, W. (2020). Blood flow analysis in tapered stenosed arteries with the influence of heat and mass transfer. *Journal of Applied Mathematics and Computing*, 63(1), 123–141.

Maiti, S., Shaw, S., & Shit, G. (2020). Fractional order model for thermochemical flow of blood with Dufour and Soret effects under magnetic and vibration environment. *Colloids and Surfaces B: Bio interfaces*, 197, 1–18.

Majee, S., & Shit, G. (2017). Numerical investigation of MHD flow of blood and heat transfer In a stenosed arterial segment. *Journal of Magnetism and Magnetic Materials*, 424(2017), 137–147.

Mandal, P. K. (2005). An unsteady analysis of non-Newtonian blood flow through tapered arteries with a stenosis. *International Journal of Non-Linear Mechanics*, 40(1), 151–164.

Mathur, P., & Jain, S. (2011). Pulsatile flow of blood through a stenosed tube: effect of periodic body acceleration and a magnetic field. *Journal of Biorheology*, 25(1), 71–77.

Mekheimer, K. S., & El Kot, M. (2015). Suspension model for blood flow through catheterized curved artery with time-variant overlapping stenosis. *Engineering Science and Technology, an International Journal*, 18(3), 452–462.

Mekheimer, K. S., Haroun, M. H., & El Kot, M. (2012). Influence of heat and chemical reactions on blood flow through an anisotropically tapered elastic arteries with overlapping stenosis. *Applied Mathematics*, 6(2), 281–292.

Misra, J., & Adhikary, S. (2016). MHD oscillatory channel flow, heat and mass transfer in a physiological fluid in presence of chemical reaction. *Alexandria Engineering Journal*, 55(1), 287–297.

Misra, J., Adhikary, S., Mallick, B., & Sinha, A. (2018). Mathematical modeling of blood flow in arteries subject to a vibrating environment. *Journal of Mechanics in Medicine and Biology*, 18(1), 1–20.

Mustapha, N., & Amin, N. (2008). The unsteady power law blood flow through a multi-irregular stenosed artery. *MATEMATIKA: Malaysian Journal of Industrial and Applied Mathematics*, 24, 187–198.

Mwangi, K. J. (2016). *Unsteady magnetohydrodynamic fluid flow in a collapsible tube*. Master's thesis. Jomo Kenyatta University of Agriculture and Technology.

Mwapinga, A. (2012). *Computational modelling of arterial blood flow in the presence of body exercise*. Master's thesis. University of Dar es Salaam.

Nagarani, P., & Sarojamma, G. (2007). Flow of a Casson fluid through a stenosed artery subject to periodic body acceleration. *In: Proceedings of the 9th WSEAS intern. Conf. Mathematical and computational methods in science and engineering*, 2007, 237–244.

Nagarani, P., & Sarojamma, G. (2008). Effect of body acceleration on pulsatile flow of Casson fluid through a mild stenosed artery. *Korea-Australia Rheology Journal*, 20(4), 189–196

Nallapu, S., & G., R. (2015). Jeffrey fluid flow through a narrow tube in the presence of a magnetic field. *Procedia Engineering*, 127, 185–192.

Nezamidoost, S., Sadeghy, K., & Askari, V. (2013). Pulsatile flow of thixotropic fluids through a partially-constricted tube. *Nihon Reoroji Gakkaishi*, 41(2), 45–52.

Noutchie, S. C. O. (2005*). Flow of a Newtonian fluid the case of blood in large arteries.* Master's thesis. University of South Africa.

Payne, S. (2017). *Cerebral blood flow and metabolism: A quantitative approach.* World Scientific Publishing Company Limited.

Priyadharshini, S., & Ponalagusamy, R. (2019). A numerical study on unsteady flow of Herschel-Bulkley nanofluid through an inclined artery with body acceleration and magnetic field. *International Journal of Applied and Computational Mathematics*, 5(1), 1–26.

Raja, S. W., Murthy, M., & Rahim, M. A. (2017). Effect of Peclet number on the dispersion of a solute in a blood flowing in non-uniform tube. *International Journal of Computational and Applied Mathematics*, 12(2), 449–456.

Reddy, J. R., Srikanth, D., & Mandal, P. (2017). Computational hemodynamic analysis of flow through flexible permeable stenotic tapered artery. *International Journal of Applied and Computational Mathematics*, 3(1), 1261–1287.

Rodkiewicz, C., Sinha, P., & Kennedy, J. (1990). On the application of a constitutive equation for whole human blood. *Journal of Biomechanical Engineering*, 112(2), 198–206.

Saleem, N., & Munawar, S. (2016). A mathematical analysis of MHD blood flow of Eyring – Powell fluid through a constricted artery. *International Journal of Biomathematics*, 9(2), 1–12.

Sankar, D., Goh, J., & Ismail, A. M. (2010). FDM analysis for blood flow through stenosed tapered arteries. *Boundary Value Problems*, 1–6.

Sankar, D., & Ismail, A. (2010). Effect of periodic body acceleration in blood flow through stenosed arteries - A theoretical model. *Journal of Nonlinear Sciences and Numerical Simulation*, 11(4), 243–257.

Sankar, D., & Lee, U. (2008). Two-fluid Herschel-Bulkley model for blood flow in catheterized arteries. *Journal of Mechanical Science and Technology*, 22(5), 1008–1018.

Sarojamma, G., Vishali, B., & Ramana, B. (2012). Flow of blood through a stenosed catheterized artery under the influence of a body acceleration modeling blood as a Casson fluid. *International Journal of Applied Mathematics and Mechanics*, 8(11), 1–17.

Sharma, B. D., & Yadav, P. K. (2019). A mathematical model of blood flow in narrow blood vessels in presence of magnetic field. *National Academy Science Letters*, 42(3), 239–243.

Sinha, A., Misra, J., & Shit, G. (2016). Effect of heat transfer on unsteady MHD flow of blood in a permeable vessel in the presence of non-uniform heat source. *Alexandria Engineering Journal*, 55(3), 2023–2033.

Sochi, T. (2015). Further validation to the variational method to obtain flow relations for generalized Newtonian fluids. *Korea-Australia Rheology Journal*, 27(2), 113–124.

Stoppard, M. (2017). *New kind of MRI scan could bypass the need for a prostate biopsy*. URL: https://i2rod.mirror.co.uk/incoming/article11514596.ece/ALTERNATES/s810/Man-Receiving-Medical-Scan-for-Prostate-Cancer-Diagnosis.jpg

Tanwar, V. K., Varshney, N., & Agarwal, R. (2016). Effect of body acceleration on pulsatile blood flow through a catheterized artery. *Advances in Applied Science Research*, 7(2), 155 – 166.

Thomas, B., & Sumam, K. (2016). Blood flow in human arterial system – a review. *Procedia Technology*, 24, 339–346.

Tripathi, B., & Sharma, B. (2018). Effect of variable viscosity on MHD inclined arterial blood flow with chemical reaction. *International Journal of Applied Mechanics and Engineering*, 23(3), 767–785.

Tripathi, B., & Sharma, B. K. (2020). Influence of heat and mass transfer on two-phase blood flow with Joule heating and variable viscosity in the presence of variable magnetic field. *International Journal of Computational Methods*, 17(3), 767–785.

Tu, C., & Deville, M. (1996). Pulsatile flow of non-Newtonian fluids through arterial stenoses. *Journal of Biomechanics*, 29(7), 899–908.

Turkyilmazoglu, M. (2010). Response to comment on primary instability mechanisms on the Magnetohydrodynamic boundary layer flow over a rotating disk subject to a uniform radial flow. *Physics of Fluids*, 22(2), 1–2.

Uddin, S., Mohamad, M., Rahimi-Gorji, M., Roslan, R., & Alarifi, I. M. (2020). Fractional Electro-magneto transport of blood modeled with magnetic particles in cylindrical tube without singular kernel. *Microsystem Technologies*, 26(2), 405–414.

Vajravelu, K., Sreenadh, S., Devaki, P., & Prasad, K. (2011). Mathematical model for a Herschel-Bulkley fluid flow in an elastic tube. *Open Physics*, 9(5), 1357–1365.

Yaduvanshi, R. S., & Parthasarathy, H. (2010). Design, development and simulations of MHD equations with its prototype implementations. *International Journal of Advanced Computer Science and Applications*, 1(4), 27–32.

Zaman, A., Ali, N., Sajid, M., & Hayat, T. (2015). Effects of unsteadiness and non-Newtonian rheology on blood flow through a tapered time-variant stenotic artery. *AIP Advances*, 5(3), 1–12.

Zaman, A., & Khan, A. A. (2020). Time dependent non-Newtonian nano-fluid (blood) flow in w-shape stenosed channel; with curvature effects. *Mathematics and Computers in Simulation*, 181, 82–97.

APPENDICES

Appendix 1: The way Reynold's and Hartman numbers were obtained during scaling of variables

As explained before that, the current study considers blood to obey the Herschel-Bulkley constitutive model. The stress tensor presented was:

$$\tau_{ij} = \left(K\dot{\gamma}^{n-1} + \frac{\tau_0}{\dot{\gamma}} \right) \dot{\gamma}_{ij} \quad \text{for} \quad \tau \geq \tau_0$$

$$\dot{\gamma} = 0 \quad \text{for} \quad \tau < \tau_0$$

Now writing the above equation in component form, say τ_{zz} for example, taking into consideration that $\dot{\gamma} = \sqrt{2\left[\left(\frac{\partial u}{\partial r}\right)^2 + \left(\frac{u}{r}\right)^2 + \left(\frac{\partial w}{\partial z}\right)^2\right] + \left(\frac{\partial u}{\partial z} + \frac{\partial w}{\partial r}\right)^2}$ the following is obtained:

$$\tau_{zz} = K\left(2\left[\left(\frac{\partial u}{\partial r}\right)^2 + \left(\frac{u}{r}\right)^2 + \left(\frac{\partial w}{\partial z}\right)^2\right] + \left(\frac{\partial u}{\partial z} + \frac{\partial w}{\partial r}\right)^2\right)^{\frac{n-1}{2}} \frac{\partial w}{\partial z}$$

$$+\tau_0\left(2\left[\left(\frac{\partial u}{\partial r}\right)^2 + \left(\frac{u}{r}\right)^2 + \left(\frac{\partial w}{\partial z}\right)^2\right] + \left(\frac{\partial u}{\partial z} + \frac{\partial w}{\partial r}\right)^2\right)^{\frac{-1}{2}} \frac{\partial w}{\partial z}$$

The non-dimensional variables are substituted to obtain:

$$\rho w_c^2 \tau_{zz}^* = K\left(\left(\frac{w_c^2}{r_0^2}\right)^{\frac{n-1}{2}} \frac{w_c}{r_0} 2\left[\left(\frac{\partial u^*}{\partial \eta}\right)^2 + \left(\frac{u^*}{\eta}\right)^2 + \left(\frac{\partial w^*}{\partial z^*}\right)^2\right] + S\right)^{\frac{n-1}{2}} \frac{\partial w^*}{\partial z}$$

$$+\rho w_c^2 \tau_0^*\left(\left(\frac{w_c^2}{r_0^2}\right)^{\frac{-1}{2}} \frac{w_c}{r_0} 2\left[\left(\frac{\partial u^*}{\partial \eta}\right)^2 + \left(\frac{u^*}{\eta}\right)^2 + \left(\frac{\partial w^*}{\partial z^*}\right)^2\right] + S\right)^{\frac{-1}{2}} \frac{\partial w^*}{\partial z^*}$$

where

$$S = \left(\frac{\partial u^*}{\partial z^*} + \frac{\partial w^*}{\partial \eta}\right)^2$$

upon simplifying, the following is obtained:

$$\tau_{zz}^* = K\frac{w_0^{n-2}}{\rho r_0^n}\left(2\left[\left(\frac{\partial u^*}{\partial \eta}\right)^2 + \left(\frac{u^*}{\eta}\right)^2 + \left(\frac{\partial w^*}{\partial z^*}\right)^2\right] + \left(\frac{\partial u^*}{\partial z^*} + \frac{\partial w^*}{\partial \eta}\right)^2\right)^{\frac{n-1}{2}} \frac{\partial w^*}{\partial z}$$

$$+\tau_0^*\left(2\left[\left(\frac{\partial u^*}{\partial \eta}\right)^2 + \left(\frac{u^*}{\eta}\right)^2 + \left(\frac{\partial w^*}{\partial z^*}\right)^2\right] + \left(\frac{\partial u^*}{\partial z^*} + \frac{\partial w^*}{\partial \eta}\right)^2\right)^{\frac{-1}{2}} \frac{\partial w^*}{\partial z^*}$$

It is now written in non-dimensional form as follows:

$$\tau_{zz}^{*} = \left(\frac{1}{R_{eG}} \dot{\gamma}^{n-1} + \tau_0^{*} \dot{\gamma}^{-1} \right) \frac{\partial w^{*}}{\partial z^{*}}$$

where

$$R_{eG} = \frac{r_0^n \rho}{K w_c^{n-2}}$$

The **generalized Reynolds number** is therefore defined as $R_{eG} = \frac{r_0^n \rho}{K w_c^{n-2}}$.

THE HARTMAN NUMBER

From the last term of the axial momentum equation, the following is obtained:

$$-\sigma B_0^2 w$$

Now substituting the non dimensional velocity $-w_c \sigma B_0^2 w^{*}$ is obtained. Dividing by $\frac{\rho w_c^2}{r_0}$ which comes from LHS of the said equation yields:

$$-\frac{r_0 \sigma B_0^2 w^{*}}{\rho w_c}$$

Thus the term $-\frac{r_0 \sigma B_0^2}{\rho w_c}$ is defined as **Magnetic interaction parameter**, let it be M so that $M = -\frac{r_0 \sigma B_0^2}{\rho w_c}$

However, it is known that $M = \frac{Ha^2}{Re}$ where Ha is the Hartman number. Therefore the Hartman number is obtained as

$$\left(\frac{\sigma r_0^{n+1} B_0^2}{K w_c^{n-1}} \right)^{\frac{1}{2}} = B_0 \sqrt{\frac{\sigma r_0^{n+1}}{K w_c^{n-1}}}$$

Therefore, our **Hartman number** is Ha such that

$$Ha = \left(\frac{\sigma r_0^{n+1} B_0^2}{K w_c^{n-1}} \right)^{\frac{1}{2}} = B_0 \sqrt{\frac{\sigma r_0^{n+1}}{K w_c^{n-1}}}$$

APPENDIX 2: Nomenclature

S/No	Constant or variable	Symbol
1	Radial velocity	u
2	Axial velocity	w
3	Dimensional radial distance	r
4	Axial distance	z
5	Radius of the normal artery	r_0
6	Dimensional radius of the stenosed artery	h
7	Mass concentration	C
8	Density	ρ
9	Time	t
10	Dynamic viscosity	μ
11	Steady state part of pressure gradient	A_0
12	Amplitude of oscillatory	A_1
13	Heart pulse frequency	n_1
14	Body acceleration frequency	n_2
15	Protuberance	δ
16	Body acceleration amplitude	a_0
17	Electrical conductivity	σ
18	Magnetic strength	B_0
19	Diffusion coefficient	D
20	Reaction rate (first order)	β
21	Shear stress	τ_{ij}
22	Temperature	T
23	Specific heat capacity	C_p
24	Thermal conductivity	k
25	Thermal-diffusion ratio	K_T
26	Yield stress	τ_0
27	Consistency index	K
28	Flow behavior index/power law index	n
29	Shear rate	$\dot{\gamma}$
30	Non-dimensional radius of the stenosed artery	H
31	Reynolds Number	Re

32	Hartman number	Ha
33	Schmidt number	Sc
34	Generalized Reynolds number	R_{eG}
35	Peclet number	Pe
36	Eckert number	E_c
37	Soret number	S_r
38	Dimensionless radial distance	η
39	Transformed radial distance	ξ
40	Coefficient of skin friction	C_f

Appendix 3: MATLAB codes

(a) MATLAB codes for Newtonian blood

```
L=2;
r=1;
t=5;
M=40;
N=20;
maxt=5000;
dt= t/(maxt);
dxi=r/(N);
dz=L/(M);
A0=1.5; A1=0.5;  omegap=1 ; omegab=1 ; ReG=300; Re=3; e=0.1;a0=1; Ha=1; ppsi=0.6;
z0=1; K=1;n=1; tau0=0.2;  Ec=1; Pe=25; Pec=25; beTA=0.002; Sc=1;Sr=0.001 ;
for j=1:N+1
xi(j)=(j-1)*dxi;      % w(:,:,1)
end
for i=1:M+1
z(i)=(i-1)*dz;
end
for k=1:maxt+1
t(k)=(k-1)*dt;
end
for i=1:M+1
R(i)=1-e*(1+cos(((pi/2)*z(i))/(z0)));
dR(i)=(pi/2*z0)*e*sin((pi/2)*z(i)/z0);
ddR(i)=((pi/2*z0))^2*e*cos((pi/2)*z(i)/z0);
end
w=zeros(M+1,N+1,maxt+1);
u=zeros(M+1,N+1,maxt+1);
for k=1:maxt+1
for j=1:N
for i=1:M+1
w(i,j,1)=((A0+A1)/4)*(1-(R(i)*xi(j))^2);
```

```
u(i,j,1)=0;
end
end
end
% % %we now put or insert here the boundary conditions!!
for i=1:M+1
for k=1:maxt+1
w(i,N+1,k)=0;          %boundary condition on the boundary i.e at xi=1
u(i,N+1,k)=0;
end
end
for k=1:maxt
for i=2:M
for j=2:N
w(i,1,k)= w(i,2,k);
w(i,j,k+1)=w(i,j,k)+dt*(A0+A1*cos((omegap*t(k))))+dt*a0*cos((omegab*t(k))+ppsi)-
dt*((Ha)^2/(Re))*w(i,j,k)...
-dt*(xi(j)/R(i))*(dR(i))*w(i,j,k)*(w(i,j+1,k)-w(i,j-1,k))/(2*dxi)...
-dt*w(i,j,k)*(w(i+1,j,k)-w(i-1,j,k))/(2*dz)...
+dt*w(i,j,k)*xi(j)/R(i)*dR(i)*((w(i,j+1,k)-w(i,j-1,k))/(2*dxi))...
+(dt/(Re*(R(i))^2))*((w(i,j+1,k)-2*w(i,j,k)+w(i,j-1,k))/(dxi^2))...
+(dt/(Re*(R(i))^2)*(xi(j)))*((w(i,j+1,k)-w(i,j-1,k))/(2*dxi))...
+(dt/(Re)*((w(i+1,j,k)-2*w(i,j,k)+w(i-1,j,k))/(dz)^2))...
-(dt/(Re))*(xi(j)/(R(i)))*ddR(i)*((w(i,j+1,k)-w(i,j-1,k))/(2*dxi))...
+(dt/(Re))*(xi(j)/R(i))^2*((w(i,j+1,k)-2*w(i,j,k)+w(i,j-1,k))/(dxi^2))...
+(dt/(Re))*(3*xi(j)/(R(i))^2)*((dR(i))^2)*(w(i,j+1,k)-w(i,j-1,k))/(2*dxi);
u(i,j,k)=xi(j)*dR(i)*w(i,j,k);
end
end
end
L1=2;
r1=1;
t1=5;
M1=40;
```

```
N1=20;
maxt1=5000;
dt1= t1/(maxt1);
dxi1=r1/(N1);
dz1=L1/(M1);
A0=1.5; A1=0.5;  omegap=1 ; omegab=1 ; ReG=300; Re=3; e=0.1;a0=2; Ha=1; ppsi=0.6;
z0=1; K=2;n=1; tau0=0;  Ec=1; Pe=25; Pec=25; beTA=0.002; Sc=1;Sr=0.001 ;
for j=1:N1+1
xi1(j)=(j-1)*dxi1;      % w(:,:,1)
end
for i=1:M1+1
z1(i)=(i-1)*dz1;
end
for k=1:maxt1+1
t1(k)=(k-1)*dt1;
end
for i=1:M1+1
R1(i)=1-e*(1+cos(((pi/2)*z1(i))/(z0)));
dR1(i)=(pi/2*z0)*e*sin((pi/2)*z1(i)/z0);
ddR1(i)=((pi/2*z0))^2*e*cos((pi/2)*z1(i)/z0);
end
w1=zeros(M1+1,N1+1,maxt1+1);
u1=zeros(M1+1,N1+1,maxt1+1);
for k=1:maxt1+1
for j=1:N1
for i=1:M1+1
w1(i,j,1)=((A0+A1)/4)*(1-(R1(i)*xi1(j))^2);
u1(i,j,1)=0;
end
end
end
% % %we now put or insert here the boundary conditions!!
for i=1:M1+1
for k=1:maxt1+1
```

```
w1(i,N1+1,k)=0;          %boundary condition on the boundary i.e at xi=1
u1(i,N1+1,k)=0;
end
end
for k=1:maxt1
for i=2:M1
for j=2:N1
w1(i,1,k)= w1(i,2,k);
w1(i,j,k+1)=w1(i,j,k)+dt1*(A0+A1*cos((omegap*t1(k))))+dt1*a0*cos((omegab*t1(k))+ppsi)
-dt1*((Ha)^2/(Re))*w1(i,j,k)...
-dt1*(xi1(j)/R1(i))*(dR1(i))*w1(i,j,k)*(w1(i,j+1,k)-w1(i,j-1,k))/(2*dxi1)...
-dt1*w1(i,j,k)*(w1(i+1,j,k)-w1(i-1,j,k))/(2*dz1)...
+dt1*w1(i,j,k)*xi1(j)/R1(i)*dR1(i)*((w1(i,j+1,k)-w1(i,j-1,k))/(2*dxi1))...
+(dt1/(Re*(R1(i))^2))*((w1(i,j+1,k)-2*w1(i,j,k)+w1(i,j-1,k))/(dxi1^2))...
+(dt1/(Re*(R1(i))^2)*(xi1(j)))*((w1(i,j+1,k)-w1(i,j-1,k))/(2*dxi1))...
+(dt1/(Re)*((w1(i+1,j,k)-2*w1(i,j,k)+w1(i-1,j,k))/(dz1)^2))...
-(dt1/(Re))*(xi1(j)/(R1(i)))*ddR1(i)*((w1(i,j+1,k)-w1(i,j-1,k))/(2*dxi1))...
+(dt1/(Re))*(xi1(j)/R1(i))^2*((w1(i,j+1,k)-2*w1(i,j,k)+w1(i,j-1,k))/(dxi1^2))...
+(dt1/(Re))*(3*xi1(j)/(R1(i))^2)*((dR1(i))^2)*(w1(i,j+1,k)-w1(i,j-1,k))/(2*dxi1);
u1(i,j,k)=xi1(j)*dR1(i)*w1(i,j,k);
end
end
end
L2=2;
r2=1;
t2=5;
M2=40;
N2=20;
maxt2=5000;
dt2= t2/(maxt2);
dxi2=r2/(N2);
dz2=L2/(M2);
A0=1.5; A1=0.5;  omegap=1 ; omegab=1 ; ReG=300; Re=3; e=0.1;a0=3; Ha=1; ppsi=0.6;
z0=1; K=2;n=1; tau0=0;  Ec=1; Pe=25; Pec=25; beTA=0.002; Sc=1;Sr=0.001 ;
```

```
for j=1:N2+1
xi2(j)=(j-1)*dxi2;      % w(:,:,1)
end
for i=1:M2+1
z2(i)=(i-1)*dz2;
end
for k=1:maxt2+1
t2(k)=(k-1)*dt2;
end
for i=1:M2+1
R2(i)=1-e*(1+cos(((pi/2)*z2(i))/(z0)));
dR2(i)=(pi/2*z0)*e*sin((pi/2)*z2(i)/z0);
ddR2(i)=((pi/2*z0))^2*e*cos((pi/2)*z2(i)/z0);
end
w2=zeros(M2+1,N2+1,maxt2+1);
u2=zeros(M2+1,N2+1,maxt2+1);
for k=1:maxt2+1
for j=1:N2
for i=1:M2+1
w2(i,j,1)=((A0+A1)/4)*(1-(R2(i)*xi2(j))^2);
u2(i,j,1)=0;
end
end
end
% % %we now put or insert here the boundary conditions!!
for i=1:M2+1
for k=1:maxt2+1
w2(i,N2+1,k)=0;          %boundary condition on the boundary i.e at xi=1
u2(i,N2+1,k)=0;
end
end
for k=1:maxt2
for i=2:M2
for j=2:N2
```

```
w2(i,1,k)= w2(i,2,k);
w2(i,j,k+1)=w2(i,j,k)+dt2*(A0+A1*cos((omegap*t2(k))))+dt2*a0*cos((omegab*t2(k))+ppsi)
-dt2*((Ha)^2/(Re))*w2(i,j,k)...
-dt2*(xi2(j)/R2(i))*(dR2(i))*w2(i,j,k)*(w2(i,j+1,k)-w2(i,j-1,k))/(2*dxi2)...
-dt2*w2(i,j,k)*(w2(i+1,j,k)-w2(i-1,j,k))/(2*dz2)...
+dt2*w2(i,j,k)*xi2(j)/R2(i)*dR2(i)*((w2(i,j+1,k)-w2(i,j-1,k))/(2*dxi2))...
+(dt2/(Re*(R2(i))^2))*((w2(i,j+1,k)-2*w2(i,j,k)+w2(i,j-1,k))/(dxi2^2))...
+(dt2/(Re*(R2(i))^2)*(xi2(j)))*((w2(i,j+1,k)-w2(i,j-1,k))/(2*dxi2))...
+(dt2/(Re)*((w2(i+1,j,k)-2*w2(i,j,k)+w2(i-1,j,k))/(dz2)^2))...
-(dt2/(Re))*(xi2(j)/(R2(i)))*ddR2(i)*((w2(i,j+1,k)-w2(i,j-1,k))/(2*dxi2))...
+(dt2/(Re))*(xi2(j)/R2(i))^2*((w2(i,j+1,k)-2*w2(i,j,k)+w2(i,j-1,k))/(dxi2^2))...
+(dt2/(Re))*(3*xi2(j)/(R2(i))^2)*((dR2(i))^2)*(w2(i,j+1,k)-w2(i,j-1,k))/(2*dxi2);
u2(i,j,k)=xi2(j)*dR2(i)*w2(i,j,k);
end
end
end
plot(xi,w(6,:,800),'b','LineWidth',2.5)
hold on
plot(xi1,w1(6,:,800),'r','LineWidth',2.5)
hold on
plot(xi2,w2(6,:,800),'k','LineWidth',2.5)
hold off
xlabel('\xi')
ylabel('Axial velocity')\\
```

(b) Matlab codes for Non-Newtonian Blood (Herschel-Bulkley Model)

```
clear all;
L=4;
r=1;
t=1;
M=50;
N=20;
maxt=5000;
```

```
dt= t/(maxt);
dxi=r/(N);
dz=L/(M);
A0=0.8; A1=0.5;  omegap=10; omegab=10; ReG=1; Re=0.0001; e=0.1;a0=1; Ha=1;
ppsi=0.3;
z0=1; K=2;n=0.95; tau0=0.2;  Ec=1; Pe=1; beTA=0.1; Sc=1;Sr=0.001 ;
for j=1:N+1
xi(j)=(j-1)*dxi;      % w(:,:,1)
end
for i=1:M+1
z(i)=(i-1)*dz;
end
for k=1:maxt+1
t(k)=(k-1)*dt;
end
for i=1:M+1
R(i)=1-e*(1+cos(((90)*z(i))/(z0)));
dR(i)=(pi/2*z0)*e*sin((90)*z(i)/z0);
ddR(i)=((pi/2*z0))^2*e*cos((90)*z(i)/z0);
end
w=zeros(M+1,N+1,maxt+1);
u=zeros(M+1,N+1,maxt+1);
tauxixi=zeros(M+1,N+1,maxt+1);
tauxiz=zeros(M+1,N+1,maxt+1);
tauzz=zeros(M+1,N+1,maxt+1);
T=zeros(M+1,N+1,maxt+1);
C=zeros(M+1,N+1,maxt+1);
Nusselt=zeros(M+1,N+1,maxt+1);
Volu=zeros(M+1,N+1,maxt+1);
Sherwood=zeros(M+1,N+1,maxt+1);
for j=1:N+1
for i=1:M+1
w(i,j,1)=((A0+A1)/4)*(1-(R(i)*xi(j))^2);
u(i,j,1)=0;
```

```
T(i,j,1)=0.1;
C(i,j,1)=0.1;
end
end
for i=1:M+1
for k=1:maxt+1
w(i,N+1,k)=0;          %boundary condition on the boundary i.e at xi=1
u(i,N+1,k)=0;
T(i,N+1,k)=1;
C(i,N+1,k)=4.5;
end
end
for k=1:maxt+1
for i=1:M+1
tauxiz(i,1,k)=0;          %boundary condition on the boundary i.e at xi=1
end
end
for k=1:maxt+1
for i=2:M
for j=2:N
w(i,1,k)= w(i,2,k);
GAMA(i,j,k)=(2*(((1/R(i))*dR(i)*xi(j)*(((w(i,j+1,k)-w(i,j-
1,k))/(2*dxi))+w(i,j,k)))^2)+((1/R(i))*dR(i)*w(i,j,k))^2)...
+2*(((w(i+1,j,k)-w(i-1,j,k))/(2*dz))-(xi(j)/R(i))*((w(i,j+1,k)-w(i,j-1,k))/(2*dxi)))^2+     (
(xi(j)*(dR(i)*((w(i+1,j,k)-w(i-1,j,k))/(2*dz))+w(i,j,k)*ddR(i)))   +   -
((xi(j)/R(i))*(dR(i))^2)*(xi(j)*((w(i,j+1,k)-w(i,j-1,k))/(2*dxi)))-
(xi(j)/R(i))*((dR(i))^2)*w(i,j,k)+(w(i,j+1,k)-w(i,j-1,k))/(2*R(i)*dxi)  )^2;
gama(i,j,k)=nthroot(GAMA(i,j,k),2);%sqrt(GAMA(i,j,k));
tauxixi(i,j,k)=2*((1/ReG)*(gama(i,j,k)^(n-1))+tau0*(gama(i,j,k)^(-
1)))*(1/R(i))*dR(i)*(xi(j)*((w(i,j+1,k)-w(i,j-1,k))/(2*dxi))+w(i,j,k));
tauxiz(i,j,k)=2*((1/ReG)*(gama(i,j,k)^(n-1))+tau0*(gama(i,j,k)^(-
1)))*(xi(j)*dR(i)*(w(i+1,j,k)-w(i-1,j,k))/(2*dz))...
+2*((1/ReG)*(gama(i,j,k)^(n-1))+tau0*(gama(i,j,k)^(-1)))*w(i,j,k)*xi(j)*ddR(i)...
```

```
-2*((1/ReG)*(gama(i,j,k)^(n-1))+tau0*(gama(i,j,k)^(-
1)))*(xi(j)/R(i))*(dR(i))^2*((xi(j)*((w(i,j+1,k)-w(i,j-1,k))/(2*dxi))+w(i,j,k)))...
+2*((1/ReG)*(gama(i,j,k)^(n-1))+tau0*(gama(i,j,k)^(-1)))*(w(i,j+1,k)-w(i,j-
1,k))/(2*R(i)*dxi);
tauzz(i,j,k)= 2*((1/ReG)*(gama(i,j,k)^(n-1))+tau0*(gama(i,j,k)^(-1)))*(w(i+1,j,k)-w(i-
1,j,k))/(2*dz)-...
2*((1/ReG)*(gama(i,j,k)^(n-1))+tau0*(gama(i,j,k)^(-1)))*(xi(j)/R(i))*dR(i)*(w(i,j+1,k)-w(i,j-
1,k))/(2*dxi);
w(i,j,k+1)=w(i,j,k)+dt*(A0+A1*cos((omegap*t(k))))+dt*a0*cos((omegab*t(k))+ppsi)-
dt*((Ha)^2/(ReG))*w(i,j,k)...
-dt*(xi(j)/R(i))*(dR(i))*w(i,j,k)*(w(i,j+1,k)-w(i,j-1,k))/(2*dxi)...
-dt*w(i,j,k)*(w(i+1,j,k)-w(i-1,j,k))/(2*dz)...
+dt*w(i,j,k)*xi(j)/R(i)*dR(i)*((w(i,j+1,k)-w(i,j-1,k))/(2*dxi))...
+(dt*((tauxiz(i,j,k))))/(R(i)*xi(j))...
+(dt)/(R(i))*(tauxiz(i,j+1,k)-tauxiz(i,j-1,k))/(2*dxi)...
+dt*(tauzz(i+1,j,k)-tauzz(i-1,j,k))/(2*dz)...
-dt*(xi(j)/R(i))*(dR(i))*(tauzz(i,j+1,k)-tauzz(i,j-1,k))/(2*dxi);%...
u(i,j,k)=xi(j)*dR(i)*w(i,j,k);
T(i,1,k)= T(i,2,k);
T(i,j,k+1)=T(i,j,k)-dt*(xi(j)/R(i))*(dR(i))*w(i,j,k)*(T(i,j+1,k)-T(i,j-1,k))/(2*dxi)...
-dt*w(i,j,k)*(T(i+1,j,k)-T(i-1,j,k))/(2*dz)...
+dt*(xi(j)/R(i))*(dR(i))*w(i,j,k)*(T(i,j+1,k)-T(i,j-1,k))/(2*dxi)...
+(dt/(Pe))*((T(i,j+1,k)-2*T(i,j,k)+T(i,j-1,k))/(R(i)^2*dxi^2))...
+(dt/(Pe))*((T(i,j+1,k)-T(i,j-1,k))/(2*xi(j)*R(i)^2*dxi))...
+(dt/(Pe))*((T(i+1,j,k)-2*T(i,j,k)+T(i-1,j,k))/(dz)^2)...
+(dt*Ec)*(1/R(i))*tauxixi(i,j,k)*dR(i)*(xi(j)*((w(i,j+1,k)-w(i,j-1,k))/(2*dxi))+w(i,j,k))...
+(dt*Ec)*(1/R(i))*tauxiz(i,j,k)*((w(i,j+1,k)-w(i,j-1,k))/(2*dxi))...
+(dt*Ec)*tauxiz(i,j,k)*xi(j)*(dR(i)*((w(i+1,j,k)-w(i-1,j,k))/(2*dz))+w(i,j,k)*ddR(i)) -
(dt*Ec)*tauxiz(i,j,k)*(xi(j)/R(i))*dR(i)* (dR(i)*xi(j)*((w(i,j+1,k)-w(i,j-
1,k))/(2*dxi))+w(i,j,k))...
+(dt*Ec)*tauzz(i,j,k)*((w(i+1,j,k)-w(i-1,j,k))/(2*dz))-
(dt*Ec)*tauzz(i,j,k)*((xi(j)/R(i))*dR(i)*((w(i,j+1,k)-w(i,j-1,k))/(2*dxi)))...
+(dt/(Pe))*(3*xi(j)/(R(i))^2)*((dR(i))^2)*(T(i,j+1,k)-T(i,j-1,k))/(2*dxi)...
```

```
-((2*xi(j)*dt)/(Pe*R(i)))*dR(i)*((T(i+1,j+1,k)-T(i-1,j+1,k)-T(i+1,j-1,k)+T(i-1,j-
1,k))/(4*dxi*dz))...
-(dt/(Pe))*(xi(j)/(R(i)))*ddR(i)*((T(i,j+1,k)-T(i,j-1,k))/(2*dxi))...
+(2*dt/(Pe))*((xi(j)/R(i))*dR(i))^2*(T(i,j+1,k)-2*T(i,j,k)+T(i,j-1,k)/((dxi)^2));
C(i,1,k)= C(i,2,k);
C(i,j,k+1)=C(i,j,k)-dt*(xi(j)/R(i))*(dR(i))*w(i,j,k)*(C(i,j+1,k)-C(i,j-1,k))/(2*dxi)...
-dt*w(i,j,k)*((C(i+1,j,k)-C(i-1,j,k))/(2*dz))+dt*(xi(j)/R(i))*(dR(i))*w(i,j,k)*(C(i,j+1,k)-C(i,j-
1,k))/(2*dxi)...
+(dt/(Pe))*(C(i,j+1,k)-2*C(i,j,k)+C(i,j-1,k)/((dxi)^2*R(i)^2))...
+(dt/(Pe))*((C(i,j+1,k)-C(i,j-1,k))/(2*xi(j)*dxi*(R(i))^2)+((C(i+1,j,k)-2*C(i,j,k)+C(i-
1,j,k))/((dz)^2)))...
+(dt/(Pe))*(3*xi(j)/(R(i))^2)*((dR(i))^2)*(C(i,j+1,k)-C(i,j-1,k))/(2*dxi)...
-((2*xi(j)*dt)/(Pe*R(i)))*dR(i)*((C(i+1,j+1,k)-C(i-1,j+1,k)-C(i+1,j-1,k)+C(i-1,j-
1,k))/(4*dxi*dz))...
-(dt/(Pe))*(xi(j)/(R(i)))*ddR(i)*((C(i,j+1,k)-C(i,j-1,k))/(2*dxi))...
+(2*dt/(Pe))*((xi(j)/R(i))*dR(i))^2*(C(i,j+1,k)-2*C(i,j,k)+C(i,j-1,k)/((dxi)^2))-
(dt/Re)*beTA*C(i,j,k)...
+Sr*(((T(i,j+1,k)-2*T(i,j,k)+T(i,j-1,k))/(R(i)^2*dxi^2)))...
+Sr*((T(i,j+1,k)-T(i,j-1,k))/(2*xi(j)*R(i)^2*dxi))...
+Sr*((T(i+1,j,k)-2*T(i,j,k)+T(i-1,j,k))/(dz)^2)...
+(dt*Sr)*(3*xi(j)/(R(i))^2)*((dR(i))^2)*(T(i,j+1,k)-T(i,j-1,k))/(2*dxi)...
-((2*xi(j)*dt*Sr)/(R(i)))*dR(i)*((T(i+1,j+1,k)-T(i-1,j+1,k)-T(i+1,j-1,k)+T(i-1,j-
1,k))/(4*dxi*dz))...
-(dt*Sr)*(xi(j)/(R(i)))*ddR(i)*((T(i,j+1,k)-T(i,j-1,k))/(2*dxi))...
+(2*dt*Sr)*((xi(j)/R(i))*dR(i))^2*(T(i,j+1,k)-2*T(i,j,k)+T(i,j-1,k)/((dxi)^2));
end
end
end
plot(t,squeeze(tauxiz(4,20,:)),'b--','LineWidth',2.0)
xlabel('t')
ylabel('Shear stress')
```

RESEARCH OUTPUTS

Mwapinga, A., Mureithi, E., Makungu, J., & Masanja, V. (2020). Non-Newtonian heat and mass transfer on MHD blood flow through a stenosed artery in the presence of body exercise and chemical reaction. *Communications in Mathematical Biology and Neuroscience*, 1–27.

Mwapinga, A., Mureithi, E., Makungu, J., & Masanja, V. (2020). MHD arterial blood flow and mass transfer under the presence of stenosis, body acceleration and chemical reaction: A case of magnetic therapy. *Journal of Mathematics and Informatics*, 18, 85–103.

Output 1

Journal of Mathematics and Informatics
Vol. 18, 2020, 85-103
ISSN: 2349-0632 (P), 2349-0640 (online)
Published 17 February 2020
www.researchmathsci.org
DOI: http://dx.doi.org/10.22457/jmi.v18xxxxx

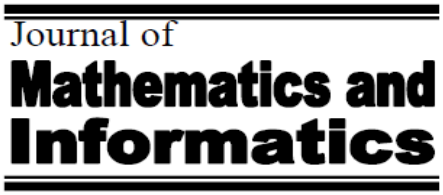

MHD Arterial Blood Flow and Mass Transfer under the Presence of Stenosis, Body Acceleration and Chemical Reaction: A Case of Magnetic Therapy

***Annord Mwapinga*[1], *Eunice Mureithi*[2], *James Makungu*[2] and *Verdiana Masanja*[1]**

[1]School of Computational and Communication Science and Engineering
The Nelson Mandela African Institution of Science and Technology
P.O.Box 447, Arusha, Tanzania
Email: mwapingaa@nm-aist.ac.tz; verdiana.masanja@nm-aist.ac.tz
[2]Department of Mathematics, University of Dar es Salaam
P.O. Box 35091 Dar es Salaam
Email: ewambui02@gmail.com; makungu_j@yahoo.com
Corresponding author. Email: mwapingaa@nm-aist.ac.tz

Received 20 January 2020; accepted 11 February 2020

Abstract. A mathematical model has been developed and used to study pulsatile blood flow and mass transfer through a stenosed artery in the presence of body acceleration and magnetic fields. An explicit Finite Difference Method (FDM) has been used to discretize the formulated mathematical model. The discretized model equations were solved in MATLAB software to produce simulations. The effect of Hartman number, Reynolds number, Schmidt number, stenotic height, body acceleration and chemical reactions have been investigated. It has been observed that, the velocity, concentration and skin friction, decrease with increasing stenotic height. Velocity on the other hand increases, as body acceleration increases. It has further been observed that as the Hartman number increases, both the radial and axial velocities diminish. Increase of the Reynolds number results in the increase of the velocity profiles. The higher the chemical reaction parameter is, the lower are the concentration profiles.

Keywords: Pulsatile flow, stenosis, body acceleration, magnetic fields, chemical reaction, magnetic therapy

AMS Mathematics Subject Classification (2010): 78A30

1. Introduction

The use of magnetic fields in health-related interventions is manifested in various situations, this includes in treatment of ailments. In sports such as football and athletics,magnets are used to perform magnetic therapy so as to maintain health and treat illnesses.Magnetic therapy is an alternative medical practice that uses magnets to alleviate pain and other health concerns. It is therefore possible that the magnetic therapy

in sports can be applied to a person with stenosis because all people are susceptible to have stenosis or plaques in the body.

Biologically blood has a number of functions that are central for the survival of human being, this includes *inta alia*, supplying oxygen to cells and tissues, providing essential nutrients to cells (such as amino acids, fatty acids, and glucose), removing waste materials, such as carbon dioxide, urea, and lactic acid, transporting hormones from one part of the body to another. In this regard therefore, blood can be described as the transporting agent in the human body. Blood consists of red blood cells which are negatively charged. It is therefore possible that the flow of blood can get affected by the magnetic fields.

Stenosis is one of the causes of the anomalies of blood flow in arteries. The abnormal growth of deposits such as fats along the arterial wall causes reduction of the diameter of the artery and thus disturbs the normal flow of blood. In day to day activities, human being may also be subjected to external body acceleration. This includes, travelling in vehicles, airplanes, sports and other activities such as using the lathe machine or jack hammer.In this regard therefore, magnetic therapy in sports implies that, there is existence of magnetic fields and body acceleration.

Mathematical modelling of blood flow in a stenosed artery under the presence of magnetic fields has been worked on by several researchers. Kumari *et al,* (2019) [1], Haghighi and Aliashrafi (2018) [3], Sharma *et al* (2019) [4], Rajashekhar *et al* (2017) [7], Mwanthi *et al* (2017) [8], Shit *et al* (2014) [6], studied Magnetohydrodynamics through a stenosed artery. Their studies revealed that the application of the magnetic field causes a decrease in axial speed of blood.

Karthikeyan and Jeevitha (2019) [2], analyzed the heat and mass transfer effects on the two-phase model of the unsteady pulsatile blood flow when it flows through a stenosed artery with permeable wall under the effect of chemical reaction. The study showed that as the chemical reaction parameter increases, the concentration profiles decrease.Further, plots of the volumetric flow rate and the velocity exhibitsinusoidal behavior with time. A similar study with similar results was done by Hossain and Haque (2017) [13] for bifurcated artery. These studies neglected the presence of body acceleration despite the fact that the situation is very common in sports.

Tanwar *et al* (2016) [5] investigated the effect of body acceleration on pulsatile blood flow through a catheterized artery. The blood was assumed to be a Newtonian fluid and the perturbation method was used to solve the problem. In their study, it was observed that the velocity of blood increases with the increase in body acceleration and the velocity decreases with the increase in phase angle.

Furthermore, a mathematical model for the blood flow through an overlapping stenosed artery under the effect of magnetic field was also studied by Parmar *et al.* (2013) [9]. The flow was assumed to be laminar, incompressible and fully developed. The blood was also assumed to follow Herschel-Bulkley fluids. The effects of magnetic fields and stenosis was discussed. Their findings found that magnetic fields and stenosis affect the normal flow of blood.

Sharma and Gaur (2017) [14] reported that, blood is maintained in a delicate balance by a variety of chemical reactions, some that aid its coagulation and others its dissolution. Biologically blood reacts and is soluble at the arterial wall as arteries may be basically considered as a living tissues that need supply of metabolites including oxygen and removal of waste products. In this regard therefore, chemical reaction in blood flow exists, and it is therefore important know how are macromolecules transported or affected by the presence of chemical reaction. Modelling the combined effect of stenosis, body acceleration and chemical reactions for magnetic therapy (to the best of our knowledge) is missing in all literature despite of its manifestation in different situation like magnetic therapy in sports. The current study therefore aims at determining the combined effect of stenosis, body acceleration and chemical reaction in in magnetic therapies.

2. Mathematical formulation

We consider chemically reacting blood flowing through a stenosed artery in the presence of body acceleration and magnetic fields. The flow of blood is assumed to be two dimensional, unsteady, laminar, axisymmetric flow, fully developed and incompressible. We also assumethat the flow is under the influence of a constant electrical conductivity. Blood is assumed to be a Newtonian fluid. We further consider that $r = 0$ is the axis of the axisymmetric flow where $\frac{\partial(.)}{\partial\theta} = 0$ and (u, w) are components of the velocityin $r,\ z$ directions respectively. Figure 1 shows the schematic diagram of the flow.

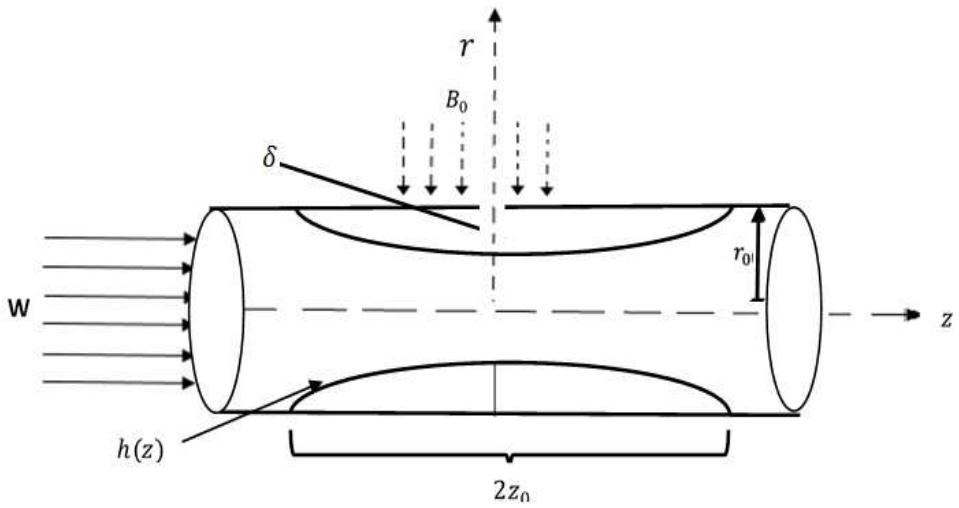

Figure 1: Schematic flow diagram

In cylindrical polar coordinate, under the mentioned assumptions, equations of continuity, motion and mass concentration reduce to:

$$\frac{\partial u}{\partial r} + \frac{u}{r} + \frac{\partial w}{\partial z} = 0 \tag{1}$$

$$\rho\left(\frac{\partial u}{\partial t}+u\frac{\partial u}{\partial r}+w\frac{\partial u}{\partial z}\right)=-\frac{\partial P}{\partial r}+\mu\left(\frac{\partial^2 u}{\partial r^2}+\frac{1}{r}\frac{\partial u}{\partial r}-\frac{u}{r^2}+\frac{\partial^2 u}{\partial z^2}\right) \quad (2)$$

$$\rho\left(\frac{\partial w}{\partial t}+u\frac{\partial w}{\partial r}+w\frac{\partial w}{\partial z}\right)=-\frac{\partial P}{\partial z}+\mu\left(\frac{\partial^2 w}{\partial r^2}+\frac{1}{r}\frac{\partial w}{\partial r}+\frac{\partial^2 w}{\partial z^2}\right)+G(t)-\sigma B_0^2 w \quad (3)$$

$$\rho\left(\frac{\partial C}{\partial t}+u\frac{\partial C}{\partial r}+w\frac{\partial C}{\partial z}\right)=D\left(\frac{\partial^2 C}{\partial r^2}+\frac{1}{r}\frac{\partial C}{\partial r}+\frac{\partial^2 C}{\partial z^2}\right)-\beta C \quad (4)$$

where $r, z$are the radial and axial directions whose corresponding velocities are respectively u and w. ρ is the density of the blood and μ is the blood's viscosity.P is the pressure,σ is the electrical conductivity, B_0 is the applied magnetic field intensity, $G(t)$ is the body acceleration, t is time, C is the mass concentration, while D and β are the diffusion coeffient and chemical reaction parameters, respectively.

In the radial direction we assume that the pressure gradient is small due to the fact that the lumen radius of an artery is small in comparison to the pressure wave. Under such assumption therefore, the radial pressure gradient $\frac{\partial p}{\partial r}\approx 0$. Following Mustapha and Amin (2008), the pressure gradient for a human being in the axial direction can be written as

$$-\frac{\partial P}{\partial z}=A_0+A_1\cos(n_1 t) \quad (5)$$

where A_0 is the steady state part of pressure gradient, A_1 is the amplitude of the pulsatile blood flow, that gives rise to systolic and diastolic pressure, $n_1=2\pi f_1$, with f_1 being the pulse frequency. On other hand, according to Nagarani *et al* (2007), body acceleration may be given as

$$G(t)=\rho a_0\cos(n_2 t+\phi) \quad (6)$$

where ρa_0 is the amplitude of body acceleration, $n_2=2\pi f_2$ with f_2 being body acceleration frequency, and ϕ is the phase angle.

The governing equations $1-4$ can now be written as follows;

$$\frac{\partial u}{\partial r}+\frac{u}{r}+\frac{\partial w}{\partial z}=0 \quad (7)$$

$$\rho\left(\frac{\partial u}{\partial t}+u\frac{\partial u}{\partial r}+w\frac{\partial u}{\partial z}\right)=+\mu\left(\frac{\partial^2 u}{\partial r^2}+\frac{1}{r}\frac{\partial u}{\partial r}-\frac{u}{r^2}+\frac{\partial^2 u}{\partial z^2}\right) \quad (8)$$

$$\rho\left(\frac{\partial w}{\partial t}+u\frac{\partial w}{\partial r}+w\frac{\partial w}{\partial z}\right)=A_0+A_1\cos(n_1 t)+\rho a_0\cos(n_2 t+\phi)+\mu\left(\frac{\partial^2 w}{\partial r^2}+\frac{1}{r}\frac{\partial w}{\partial r}+\frac{\partial^2 w}{\partial z^2}\right)-\sigma B_0^2 w \quad (9)$$

$$\rho\left(\frac{\partial C}{\partial t}+u\frac{\partial C}{\partial r}+w\frac{\partial C}{\partial z}\right)=D\left(\frac{\partial^2 C}{\partial r^2}+\frac{1}{r}\frac{\partial C}{\partial r}+\frac{\partial^2 C}{\partial z^2}\right)-\beta C \quad (10)$$

Following Das and Saha (2009), the geometry of stenosis (See Figure 1) can mathematically be expressed as follows;

$$h(z) = \begin{cases} r_0 - \delta\left(1 + \cos\dfrac{\pi z}{2z_0}\right), & -z_0 \le z \le z_0 \\ r_0 \text{otherwise} \end{cases} \quad (11)$$

where $h(z)$ represents the radius of the stenosed artery, r_0 is the radius of the normal artery, $2z_0$ is the length of the stenosis and δ is the protuberance of the stenosis.

Boundary and initial conditions

It is assumed that there is no slip condition on the arterial wall, that is

$$u(r,z,t) = 0, \qquad w(r,z,t) = 0 \quad \text{at } r = h(z) \quad (12)$$

and at the center of the artery (at the line of symmetry) it is assumed that there is no shear rate and no radial flow, such that

$$\frac{\partial w(r,z,t)}{\partial r} = 0, \qquad u(r,z,t) = 0 \quad \text{at } r = 0 \quad (13)$$

For mass concentration, symmetric conditions are and concentration is considered uniform at the wall, Khan and Mohidul 2017.

$$\frac{\partial C(r,z,t)}{\partial r} = 0 \quad \text{at } r = 0 \quad \text{and } C(r,z,t) = 0 \quad \text{at} \quad r = h(z) \quad (14)$$

Since blood can flow even in the absence of magnetic field and body acceleration, it is therefore assumed that initially, there is non-zero velocity and concentration when $t = 0$

$$u(r,z,0) = u_0, \qquad w(r,z,0) = w_0 \ , C(r,z,0) = C_0 \quad (15)$$

Non- dimensionalisation of variables

In this part we introduce the following non-dimensional variables. The variables w_c and r_0 used are fluid characteristic velocity and distance. For this case, blood flowing in an artery, w_c is the average blood velocity, and r_0 is the radius of the normal artery.

$$\eta = \frac{r}{r_0}, \qquad z^* = \frac{z}{r_0}, \qquad u^* = \frac{u}{w_c}, w^* = \frac{w}{w_c}, \quad \tau = \frac{t w_c}{r_0}, a_0^* = \frac{a_0 r_0^3}{v^2}, A_0^* = \frac{A_0 r_0^3}{\rho v^2}$$

$$A_1^* = \frac{A_1 r_0^3}{\rho v^2}, \qquad e = \frac{\delta}{r_0}, \qquad C^* = \frac{C}{C_0}, \qquad D^* = \frac{D}{v}, \qquad \beta^* = \frac{\beta r_0^2}{v}, M = B_0 r_0 \sqrt{\frac{\sigma}{\mu}}$$

Substituting these non-dimensional variables into equations 7-11 we get

Continuity equation

$$\frac{\partial u^*}{\partial \eta} + \frac{u^*}{\eta} + \frac{\partial w^*}{\partial z^*} = 0 \quad (16)$$

Equation of motion in the radial direction:

$$\frac{\partial u^*}{\partial \tau} + u^* \frac{\partial u^*}{\partial \eta} w^* \frac{\partial u^*}{\partial z^*} = \frac{1}{R_e}\left(\frac{\partial^2 u^*}{\partial \eta^2} + \frac{1}{\eta}\frac{\partial u^*}{\partial \eta} - \frac{u^*}{\eta^2} + \frac{\partial^2 u^*}{\partial z^{*2}}\right) \quad (17)$$

Equation of motion in the axial direction

$$\frac{\partial w^*}{\partial \tau} + u^* \frac{\partial w^*}{\partial \eta} + w^* \frac{\partial w^*}{\partial z^*} = A_0^* + A_1^* \cos(m_1 \tau) + a_0^* \cos(m_2 \tau + \phi)$$
$$+ \frac{1}{R_e}\left(\frac{\partial^2 w^*}{\partial \eta^2} + \frac{1}{\eta}\frac{\partial w^*}{\partial \eta} + \frac{\partial^2 w^*}{\partial z^{*2}}\right) - \frac{M^2}{R_e} w^* \tag{18}$$

Mass concentration equation

$$\frac{\partial C^*}{\partial \tau} + u^* \frac{\partial C^*}{\partial \eta} + w^* \frac{\partial C^*}{\partial z^*} = D^*\left(\frac{\partial^2 C^*}{\partial \eta^2} + \frac{1}{\eta}\frac{\partial C^*}{\partial \eta} + \frac{\partial^2 C^*}{\partial z^{*2}}\right) - \beta C^* \tag{19}$$

where$R_e = \frac{w_c r_0}{\nu}$, $D^* = \frac{D}{\nu} = \frac{1}{Sc}$, Sc are, respectively, the Reynolds number, and Schmidt number, and $M = B_0 r_0 \sqrt{\frac{\sigma}{\mu}}$ is the Hartmann number. The mass concentration equation becomes

$$\frac{\partial C^*}{\partial \tau} + u^* \frac{\partial C^*}{\partial \eta} + w^* \frac{\partial C^*}{\partial z^*} = \frac{1}{Sc}\left(\frac{\partial^2 C^*}{\partial \eta^2} + \frac{1}{\eta}\frac{\partial C^*}{\partial \eta} + \frac{\partial^2 C^*}{\partial z^{*2}}\right) - \beta C^* \tag{20}$$

The geometry of stenosis (Equation 5) in dimensionless form becomes

$$H(z^*) = \begin{cases} 1 - e\left(1 + \cos\left(\frac{\pi z^*}{2}\right)\right) & \text{for} -1 \le z^* \le 1 \\ 1 & \text{otherwise} \end{cases} \tag{21}$$

The boundary and initial conditions $12 - 15$ in dimensionless form become:

$$\begin{cases} u^*(\eta, z^*, \tau) = 0, \quad w^*(\eta, z^*, \tau) = 0 \quad \text{at} \eta = H(z^*) \\ \dfrac{\partial w(\eta, z^*, \tau)}{\partial \eta} = 0, \quad u^*(\eta, z^*, \tau) = 0 \quad \text{at} \eta = 0 \end{cases} \tag{22}$$

$$C^*(\eta, z^*, \tau) = 0, \quad \text{at} \eta = H(z^*), \quad \frac{\partial C^*(\eta, z^*, \tau)}{\partial \eta} = 0, \quad \text{at} \eta = 0 \tag{23}$$

$$u^*(\eta, z^*, 0) = u_0^*, \quad w^*(\eta, z^*, 0) = w_0^*,, \quad C^*(\eta, z^*, 0) = 1, \tag{24}$$

In this work, the initial condition for velocity was obtained from the steady state of the equation of motion as

$$w(\eta) = \left(\frac{A_0 + A_1}{4}\right)(1 - \eta^2) = w_0 \tag{25}$$

3. Solutions

3.1. Radial coordinate transformation

In this section we are going to transform the equations from cylindrical to rectangular domain. Assuming that the artery is cylindrical with stenosis, we transform the constriction by introducing another variable ξ such that

$$\xi = \frac{\eta}{H(z)} \tag{26}$$

This suitable radial coordinate transformation helps to map the constricted domain intoa rectangular one. That is, this has the effect of immobilizing the arterial wall in thetransformed coordinate ξ. Using the above transformation, re-arranging and dropping the asterisks, theequations of continuity, motion, and mass concentration transfer become:

$$\frac{\partial u}{H\partial\xi} + \frac{u}{H\xi} + \frac{\partial w}{\partial z} - \frac{\xi}{H}\frac{dH}{dz}\frac{\partial w}{\partial \xi} = 0 \tag{27}$$

$$\frac{\partial u}{\partial \tau} = -\frac{u}{H}\frac{\partial u}{\partial \xi} - w\left[\frac{\partial u}{\partial z} - \frac{\xi}{H}\frac{dH}{dz}\frac{\partial u}{\partial \xi}\right] + \frac{1}{R_e}\frac{1}{H^2}\left(\frac{\partial^2 u}{\partial \xi^2} + \frac{1}{\xi}\frac{\partial u}{\partial \xi} - \frac{u}{\xi^2}\right) + \frac{1}{R_e}\left[\frac{\partial^2 u}{\partial z^2} - \frac{2\xi}{H}\frac{dH}{dz}\frac{\partial^2 u}{\partial \xi \partial z}\right.$$
$$\left. - \frac{\xi}{H}\frac{d^2H}{dz^2}\frac{\partial u}{\partial \xi} + \frac{\xi^2}{H^2}\left(\frac{dH}{dz}\right)^2\frac{\partial^2 u}{\partial \xi^2} + \frac{3\xi}{H^2}\left(\frac{dH}{dz}\right)^2\frac{\partial u}{\partial \xi}\right] \tag{28}$$

$$\frac{\partial w}{\partial \tau} = -\frac{u}{H}\frac{\partial w}{\partial \xi} - w\left[\frac{\partial w}{\partial z} - \frac{\xi}{H}\frac{dH}{dz}\frac{\partial w}{\partial \xi}\right] + A_0 + A_1\cos(m_1\tau) + \cos(m_2\tau + \phi)$$
$$+ \frac{1}{R_e}\frac{1}{H^2}\left(\frac{\partial^2 w}{\partial \xi^2} + \frac{1}{\xi}\frac{\partial w}{\partial \xi}\right) + \frac{1}{R_e}\left[\frac{\partial^2 w}{\partial z^2} - \frac{2\xi}{H}\frac{dH}{dz}\frac{\partial^2 w}{\partial \xi \partial z} - \frac{\xi}{H}\frac{d^2H}{dz^2}\frac{\partial w}{\partial \xi} + \frac{\xi^2}{H^2}\left(\frac{dH}{dz}\right)^2\frac{\partial^2 w}{\partial \xi^2}\right.$$
$$\left. + \frac{3\xi}{H^2}\left(\frac{dH}{dz}\right)^2\frac{\partial w}{\partial \xi}\right] - \frac{1}{R_e}M^2 w \tag{29}$$

$$\frac{\partial C}{\partial \tau} = -\frac{u}{H}\frac{\partial C}{\partial \xi} - w\left[\frac{\partial C}{\partial z} - \frac{\xi}{H}\frac{dH}{dz}\frac{\partial C}{\partial \xi}\right] + \frac{1}{Sc}\left(\frac{\partial^2 C}{\partial \xi^2} + \frac{1}{\xi}\frac{\partial C}{\partial \xi}\right) + \frac{1}{Sc}\left[\frac{\partial^2 C}{\partial z^2} - \frac{2\xi}{H}\frac{dH}{dz}\frac{\partial^2 C}{\partial \xi \partial z} - \frac{\xi}{H}\frac{d^2H}{dz^2}\frac{\partial C}{\partial \xi}\right.$$
$$\left. + \frac{\xi^2}{R^2}\left(\frac{dH}{dz}\right)^2\frac{\partial^2 C}{\partial \xi^2} + \frac{3\xi}{H^2}\left(\frac{dH}{dz}\right)^2\frac{\partial C}{\partial \xi}\right] - \beta C \tag{30}$$

Similarly, the boundary conditions 22-24 under the given radial coordinate transformation, become:

$$\begin{cases} u(\xi, z, \tau) = 0, \quad w(\xi, z, \tau) = 0 \quad \text{at} \quad \xi = 1 \\ \dfrac{\partial w(\xi, z, \tau)}{\partial \xi} = 0, u(\xi, z, \tau) = 0 \quad \text{at} \quad \xi = 0 \end{cases} \tag{31}$$

$$C(\xi, z, \tau) = 0, \quad \text{at} \quad \xi = 1, \quad \frac{\partial C(\xi, z, \tau)}{\partial \xi} = 0, \quad \text{at} \quad \xi = 0 \tag{32}$$

$$u(\xi, z, 0) = u_0, \quad w(\xi, z, 0) = w_0, \quad C(\xi, z, 0) = c_0, \tag{33}$$

Initial velocity w_0 becomes

$$w_0 = \left(\frac{A_0 + A_1}{4}\right)(1 - (H\xi)^2) \tag{34}$$

3.2. Radial velocity

To obtain the radial momentum, we use the continuity equation, we therefore multiply equation 27 by ξH and integratethe resulting equation with respect to ξ. This gives

$$u(\xi,z,\tau)=\xi\frac{dH}{dz}w-\frac{2}{H}\frac{dH}{dz}\int_0^{\xi}w\xi d\xi-\frac{H}{\xi}\int_0^{\xi}\xi\frac{\partial w}{\partial z}d\xi \tag{35}$$

Now, applying the boundary condition 31, we obtain

$$\int_0^1\frac{2}{H}\frac{dH}{dz}w\xi d\xi=-\int_0^1\xi\frac{\partial w}{\partial z}d\xi \tag{36}$$

Comparing integrals and the integrands of equation 36, we have;

$$\frac{\partial w}{\partial z}=-\frac{2}{H}\frac{dH}{dz}w \tag{37}$$

Substituting equation 37 into 35 we obtain

$$u(\xi,z,\tau)=\xi\frac{dH}{dz}w \tag{38}$$

Equation 38 is the radial velocity component which has to be calculated. However, equation 38 will now be substituted into equations 29 and 30 and obtain:

$$\frac{\partial w}{\partial\tau}=\left(-\frac{\xi}{H}\frac{dH}{dz}w\right)\frac{\partial w}{\partial\xi}-w\left[\frac{\partial w}{\partial z}-\frac{\xi}{H}\frac{dH}{dz}\frac{\partial w}{\partial\xi}\right]+A_0+A_1\cos(m_1\tau)+\cos(m_2\tau+\phi)$$
$$+\frac{1}{R_e}\frac{1}{H^2}\left(\frac{\partial^2 w}{\partial\xi^2}+\frac{1}{\xi}\frac{\partial w}{\partial\xi}\right)+\frac{1}{R_e}\left[\frac{\partial^2 w}{\partial z^2}-\frac{2\xi}{H}\frac{dH}{dz}\frac{\partial^2 w}{\partial\xi\partial z}-\frac{\xi}{H}\frac{d^2H}{dz^2}\frac{\partial w}{\partial\xi}+\frac{\xi^2}{H^2}\left(\frac{dH}{dz}\right)^2\frac{\partial^2 w}{\partial\xi^2}+\frac{3\xi}{H^2}\left(\frac{dH}{dz}\right)^2\frac{\partial w}{\partial\xi}\right]$$
$$-\frac{1}{R_e}M^2w \tag{39}$$

$$\frac{\partial C}{\partial\tau}=\left(-\frac{\xi}{H}\frac{dH}{dz}w\right)\frac{\partial C}{\partial\xi}-w\left[\frac{\partial C}{\partial z}-\frac{\xi}{H}\frac{dH}{dz}\frac{\partial C}{\partial\xi}\right]+\frac{1}{Sc}\left(\frac{\partial^2 C}{\partial\xi^2}+\frac{1}{\xi}\frac{\partial C}{\partial\xi}\right)+\frac{1}{Sc}\left[\frac{\partial^2 C}{\partial z^2}-\frac{2\xi}{H}\frac{dH}{dz}\frac{\partial^2 C}{\partial\xi\partial z}-\frac{\xi}{H}\frac{d^2H}{dz^2}\frac{\partial C}{\partial\xi}\right.$$
$$\left.+\frac{\xi^2}{H^2}\left(\frac{dH}{dz}\right)^2\frac{\partial^2 C}{\partial\xi^2}+\frac{3\xi}{H^2}\left(\frac{dH}{dz}\right)^2\frac{\partial C}{\partial\xi}\right]-\beta C \tag{40}$$

3.3. Finite difference schemes

Equations (39) and (40) are solved numerically using the FDM.The finite difference discretization is based on central differences for space and forward difference for time.

$$\left.\begin{aligned}&\frac{\partial w}{\partial\xi}=\frac{w_{i,j+1}^k-w_{i,j-1}^k}{2(\Delta\xi)},\quad\frac{\partial w}{\partial z}=\frac{w_{i+1,j}^k-w_{i-1,j}^k}{2(\Delta z)},\frac{\partial C}{\partial z}=\frac{C_{i+1,j}^k-C_{i-1,j}^k}{2(\Delta z)}\frac{\partial C}{\partial\xi}=\frac{C_{i,j+1}^k-C_{i,j-1}^k}{2(\Delta\xi)}\\&\frac{\partial^2 w}{\partial\xi^2}=\frac{w_{i,j+1}^k-2w_{i,j}^k+w_{i,j-1}^k}{(\Delta\xi)^2},\frac{\partial^2 w}{\partial z^2}=\frac{w_{i+1,j}^k-2w_{i,j}^k+w_{i-1,j}^k}{(\Delta z)^2},\frac{\partial^2 C}{\partial z^2}=\frac{C_{i+1,j}^k-2C_{i,j}^k+C_{i-1,j}^k}{(\Delta z)^2}\\&\frac{\partial^2 C}{\partial\xi^2}=\frac{C_{i,j+1}^k-2C_{i,j}^k+C_{i,j-1}^k}{(\Delta\xi)^2},\text{ and for time we have }\frac{\partial w}{\partial\tau}=\frac{w_{i,j}^{k+1}-w_{i,j}^k}{\Delta\tau},\frac{\partial C}{\partial\tau}=\frac{C_{i,j}^{k+1}-C_{i,j}^k}{\Delta\tau}\end{aligned}\right\} \tag{41}$$

We now substitute the finite difference approximationsfrom equation 42 to equations 39 and 40 and we make $w_{i,j}^{k+1}$ and $C_{i,j}^{k+1}$ the subject, and obtain:

$$w_{i,j}^{k+1} = w_{i,j}^{k} + \Delta\tau\left\{\left(-\frac{\xi_j}{H_i}\left(\frac{dH}{dz}\right)_i w_{i,j}^{k}\right)\left(\frac{w_{i,j+1}^{k} - w_{i,j-1}^{k}}{2(\Delta\xi)}\right) - w_{i,j}^{k}\left[\frac{w_{i+1,j}^{k} - w_{i-1,j}^{k}}{2(\Delta z)} - \left(\frac{\xi_j}{H_i}\left(\frac{dH}{dz}\right)_i\right)\frac{w_{i,j+1}^{k} - w_{i,j-1}^{k}}{2(\Delta\xi)}\right]\right.$$
$$+\frac{1}{R_e}\left(\frac{w_{i+1,j}^{k} - 2w_{i,j}^{k} + w_{i-1,j}^{k}}{(\Delta z)^2}\right) - \frac{1}{R_e}\frac{2\xi_j}{H_i}\left(\frac{dH}{dz}\right)_i\left(\frac{w_{i+1,j+1}^{k} + w_{i-1,j-1}^{k} - w_{i-1,j+1}^{k} - w_{i+1,j-1}^{k}}{4(\Delta\xi)(\Delta z)}\right)$$
$$-\frac{1}{R_e}\frac{\xi_j}{H_i}\left(\frac{d^2H}{dz^2}\right)_i\frac{w_{i,j+1}^{k} - w_{i,j-1}^{k}}{2(\Delta\xi)} + \frac{1}{R_e}\frac{\xi_j^2}{H_i^2}\left(\frac{dH}{dz}\right)^2_i\left(\frac{w_{i,j+1}^{k} - 2w_{i,j}^{k} + w_{i,j-1}^{k}}{(\Delta\xi)^2}\right)$$
$$\left.+\frac{1}{R_e}\frac{3\xi_j}{H_i^2}\left(\frac{dH}{dz}\right)^2_i\left(\frac{w_{i,j+1}^{k} - w_{i,j-1}^{k}}{2(\Delta\xi)}\right) - \frac{1}{R_e}M^2 w_{i,j}^{k}\right\} \quad (42)$$

$$C_{i,j}^{k+1} = C_{i,j}^{k} + \Delta\tau\left\{\left(\xi_j\left(\frac{dH}{dz}\right)_i w_{i,j}^{k}\right)\frac{C_{i,j+1}^{k} - C_{i,j-1}^{k}}{2(\Delta\xi)} - w_{i,j}^{k}\left[\frac{C_{i,j+1}^{k} - C_{i,j-1}^{k}}{2(\Delta z)} - \left(\frac{\xi_j}{H_i}\left(\frac{dH}{dz}\right)_i\right)\frac{C_{i,j+1}^{k} - C_{i,j-1}^{k}}{2(\Delta\xi)}\right]\right.$$
$$+\frac{1}{Sc}\left[\frac{C_{i,j+1}^{k} - 2C_{i,j}^{k} + C_{i,j-1}^{k}}{(\Delta\xi)^2} + \frac{1}{\xi_i}\left(\frac{C_{i,j+1}^{k} - C_{i,j-1}^{k}}{2(\Delta\xi)}\right)\right] + \frac{1}{Sc}\left[\frac{C_{i+1,j}^{k} - 2C_{i,j}^{k} + C_{i-1,j}^{k}}{(\Delta z)^2}\right.$$
$$-\frac{2\xi_j}{H_i}\left(\frac{dH}{dz}\right)_i\left(\frac{C_{i+1,j+1}^{k} + C_{i-1,j-1}^{k} - C_{i-1,j+1}^{k} - C_{i+1,j-1}^{k}}{4(\Delta\xi)(\Delta z)}\right) - \frac{\xi_j}{H_i}\left(\frac{d^2H}{dz^2}\right)_i\left(\frac{C_{i,j+1}^{k} - C_{i,j-1}^{k}}{2(\Delta\xi)}\right)$$
$$\left.+\frac{\xi_j}{H_i}\left(\frac{d^2H}{dz^2}\right)_i\frac{C_{i,j+1}^{k} - C_{i,j-1}^{k}}{2(\Delta\xi)}\right\} - \Delta\tau\beta C_{i,j}^{k} + \frac{\xi_j^2}{H_i^2}\left(\frac{dH}{dz}\right)^2_i\left(\frac{C_{i,j+1}^{k} - 2C_{i,j}^{k} + C_{i,j-1}^{k}}{(\Delta\xi)^2}\right)$$
$$\left.+\frac{3\xi_j}{H_i^2}\left(\frac{dH}{dz}\right)^2_i\left(\frac{C_{i,j+1}^{k} - w_{i,j-1}^{k}}{2(\Delta\xi)}\right)\right] - \beta C_{i,j}^{k}\right\} \quad (43)$$

where we define

$z_i = (i-1)\Delta z, \quad i = 1, 2, \ldots, M+1;\ \xi_j = (j-1)\Delta\xi, \quad j = 1, 2, \ldots, N+1$

$\tau_k = (i-1)\Delta\tau, \quad k = 1, 2, \ldots$ Here Δz and $\Delta\xi$ represent the spatial increments, respectively, in the axial and radial directions while $\Delta\tau$ represents a small increment in time. We also discretize the boundary conditions as follows:

The Neumann boundary condition at $\xi = 0$ we have

$$\frac{\partial w}{\partial\xi} = \frac{w_{i,j+1}^{k} - w_{i,j-1}^{k}}{2(\Delta\xi)} = 0 \quad (44)$$

This gives

$w_{i,j+1}^{k} - w_{i,j-1}^{k} = 0$ this implies that $w_{i,j+1}^{k} = w_{i,j-1}^{k}$ now at $\xi = 0$ means that $j = 1$, thus this means $w_{i,2}^{k} = w_{i,0}^{k}$. However, $w_{i,0}^{k}$ is outside the domain of interest. It is therefore the ghost point. To get rid of this ghost point we further approximate the derivative for the interval $\Delta\xi$ as follows

$$\left.\frac{\partial w}{\partial \xi}\right|_{j=1} \cong \frac{w_{i,j+1}^{k} - w_{i,j}^{k}}{\Delta \xi} = 0 \tag{45}$$

This gives $w_{i,2}^{k} = w_{i,1}^{k}$, we therefore have

$$u_{i,1}^{k} = u_{i,N+1}^{k} = w_{i,N+1}^{k} = 0 \ , \quad w_{i,j}^{1} = w_0, \ C_{i,j}^{1} = c_0 \ , w_{i,2}^{k} = w_{i,1}^{k} \ , C_{i,2}^{k} = C_{i,1}^{k} \tag{46}$$

The axial initial velocity is therefore discretized as $w_0 = \left(\frac{A_0 + A_1}{4}\right)(1 - (H\xi_i)^2)$

4. Results and discussion

4.1. Numerical simulation

In this section we implemented the numerical model (equations 42, 43, and 46) and performed computer simulations using MATLAB codes. To maintain stability, we ensured that $0 < \frac{\Delta\tau}{(\Delta\xi)^2} \leq 0.5$. Forconvenience, constants were wisely chosen as follows; $A_0 = 1, A_1 = 0.5, m_1 = 1 m_2 = 1, \phi = 0.6, e = 0.1, B_0 = 1, a_0 = 1, S_c = 3, Re = 3, z = 0.2$

$\tau = 0.1990, \Delta\tau = 0.001$. Some of these parameters were varied to observe their effects as illustrated in Fig. 1 to Fig. 23.

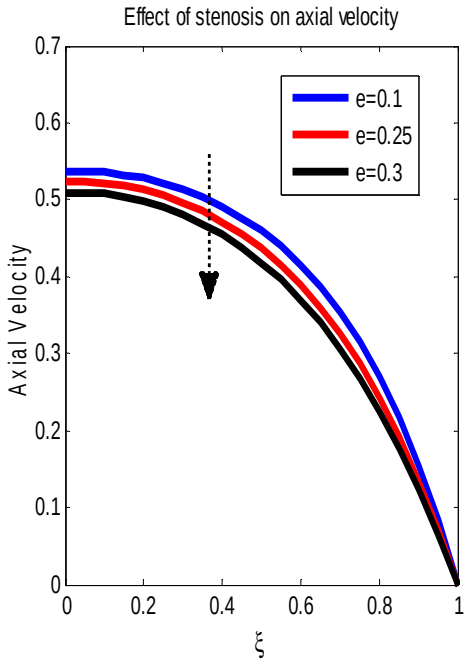

Figure 2:

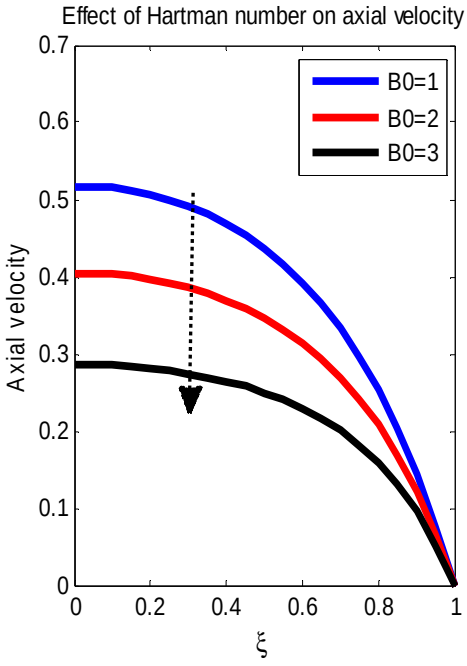

Figure 3:

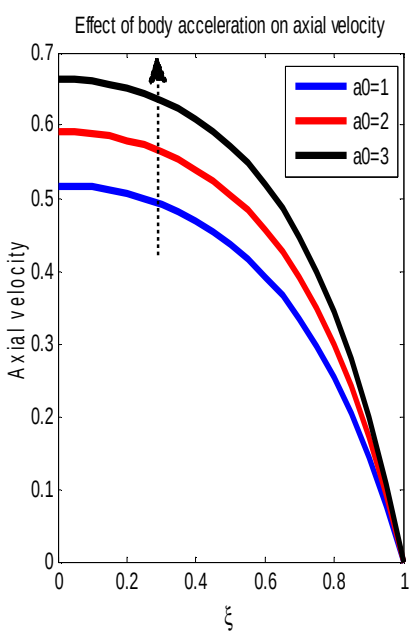

Figure 4:

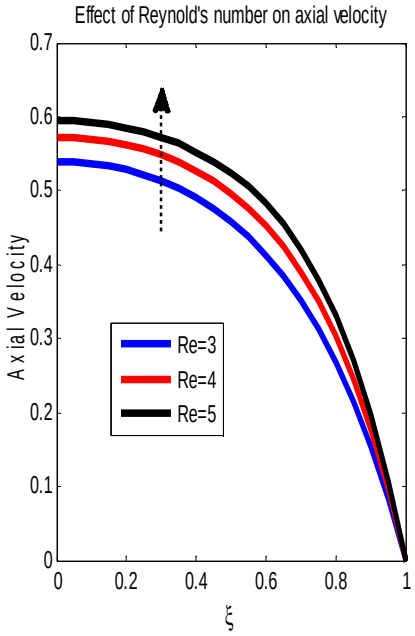

Figure 5:

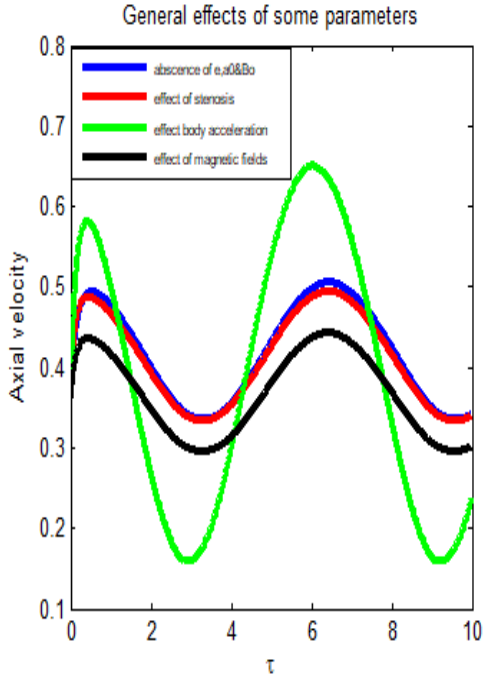

Figure 6:

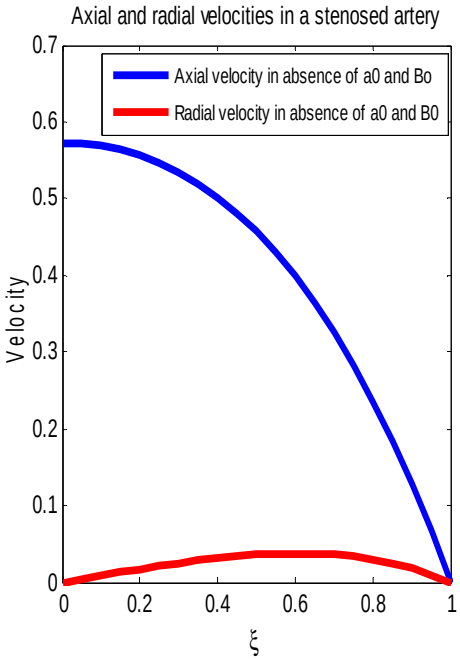

Figure 7:

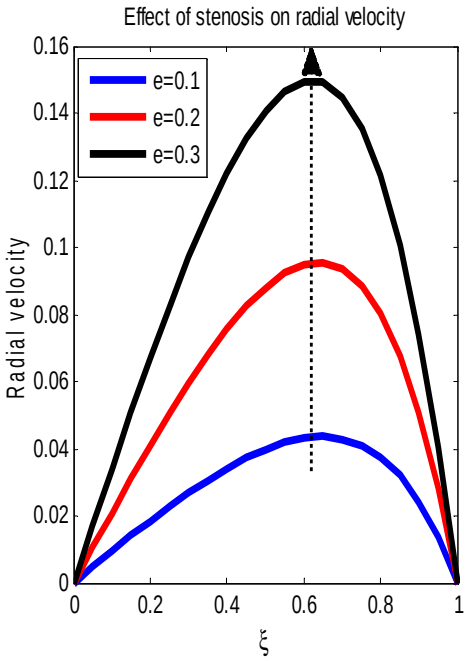

Figure 8:

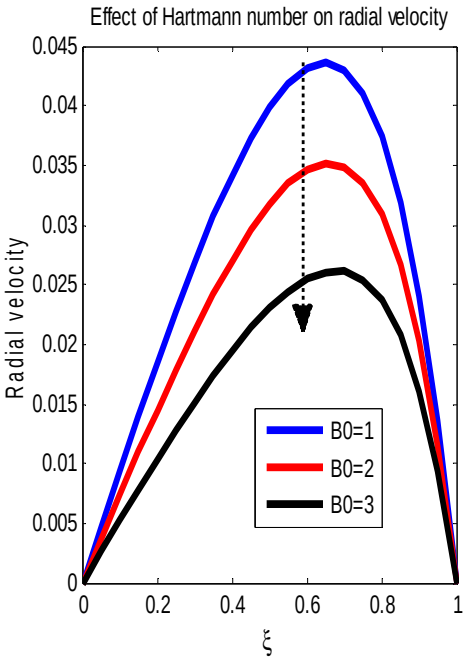

Figure 9:

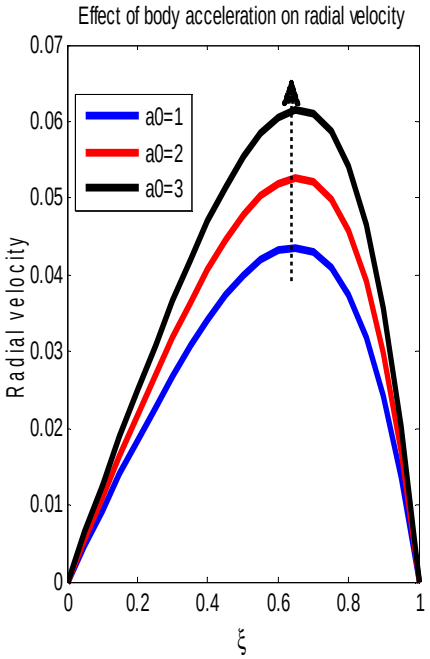

Figure 10:

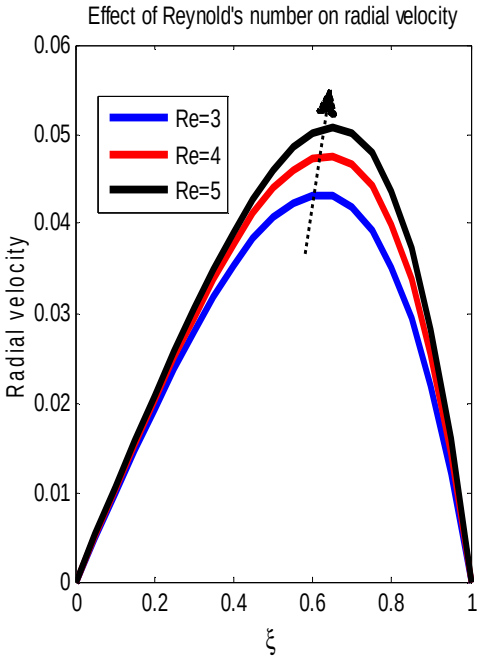

Figure 11:

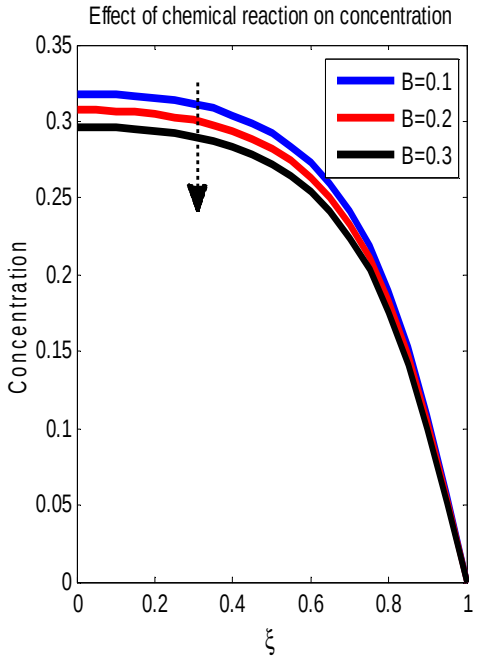

Figure 12:

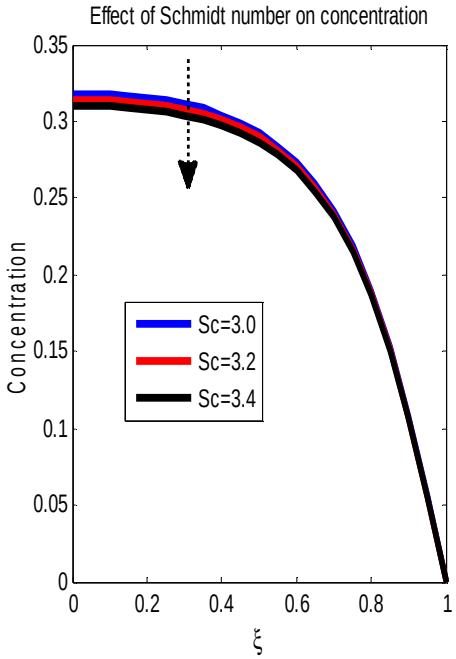

Figure 13:

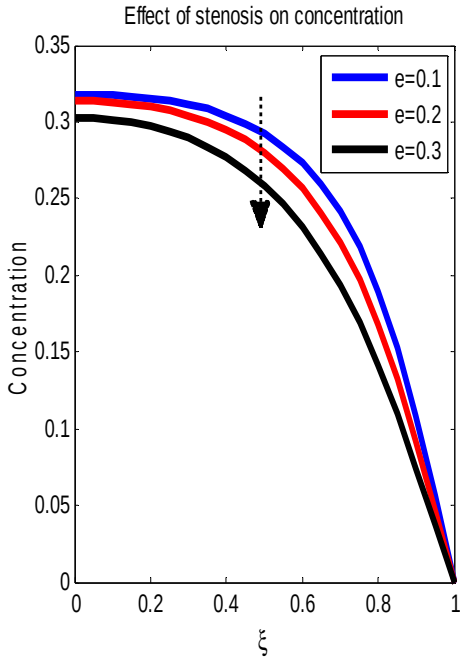

Figure 14:

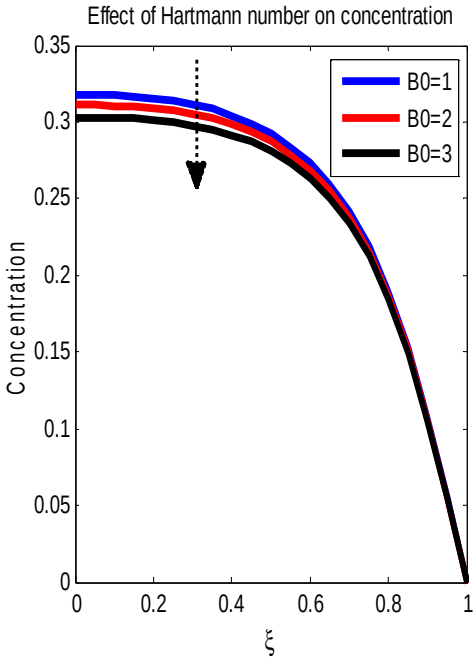

Figure 15:

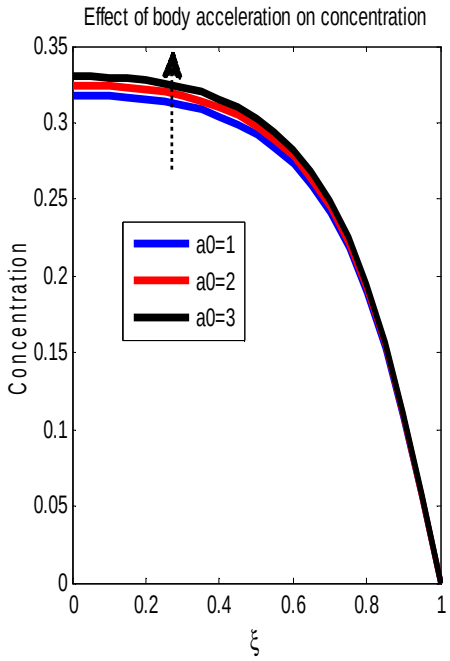

Figure 16:

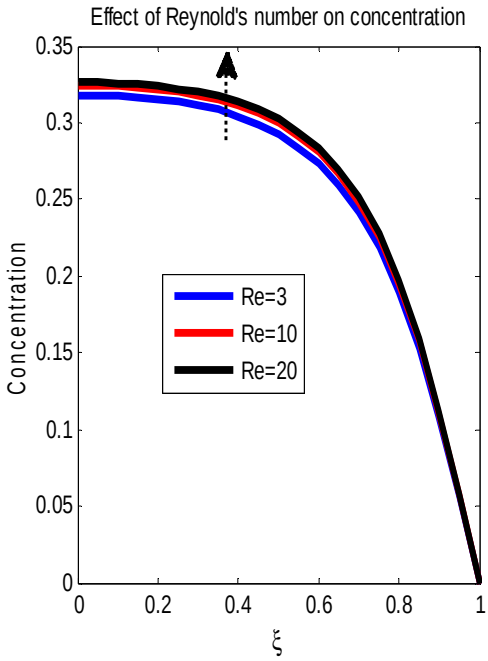

Figure 17:

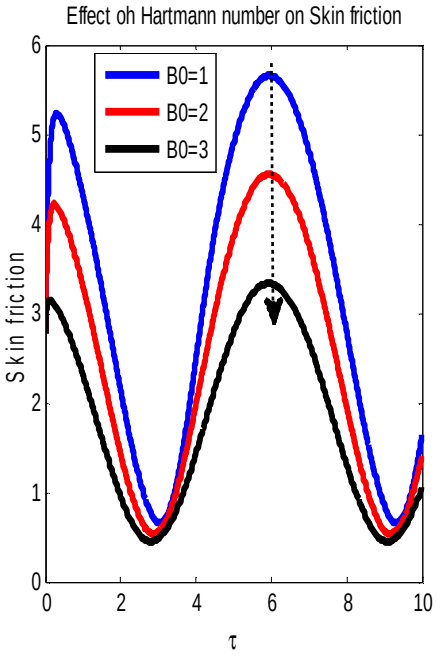

Figure 18:

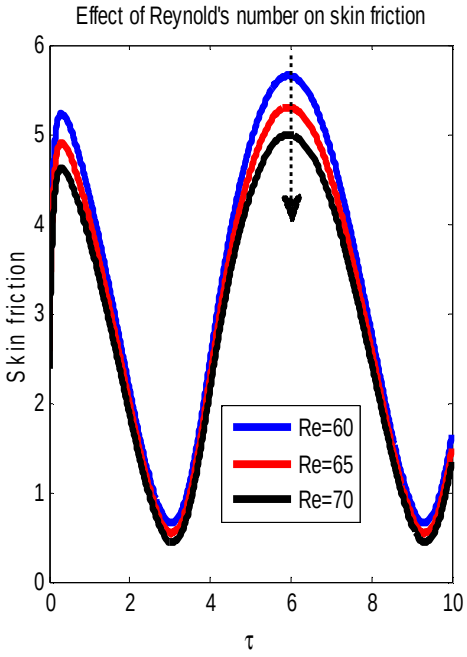

Figure 19:

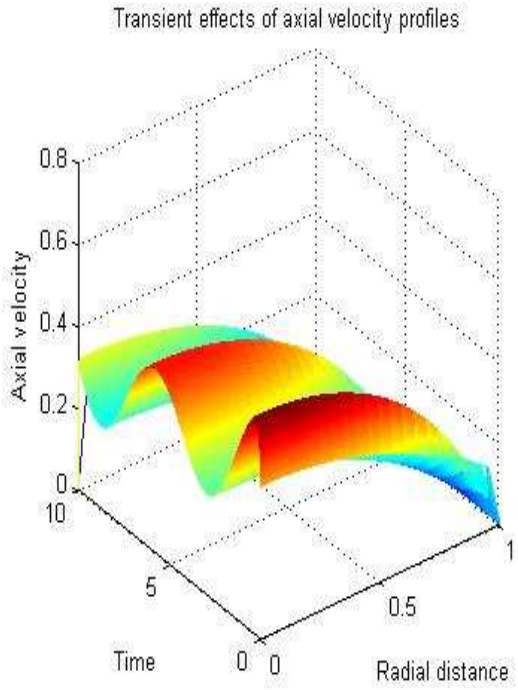

Figure 20:

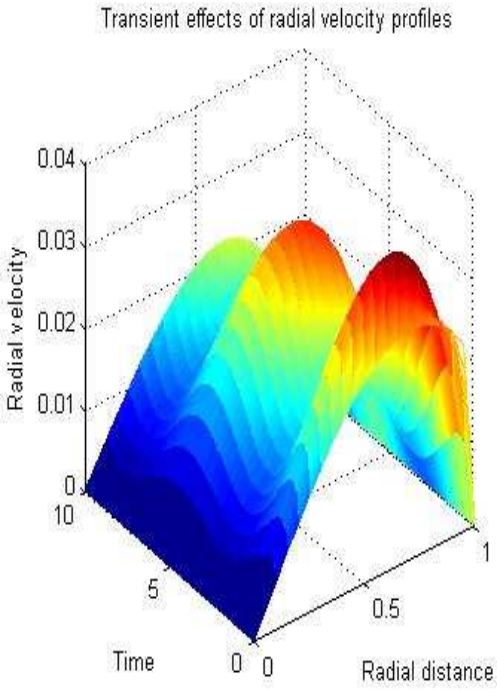

Figure 21:

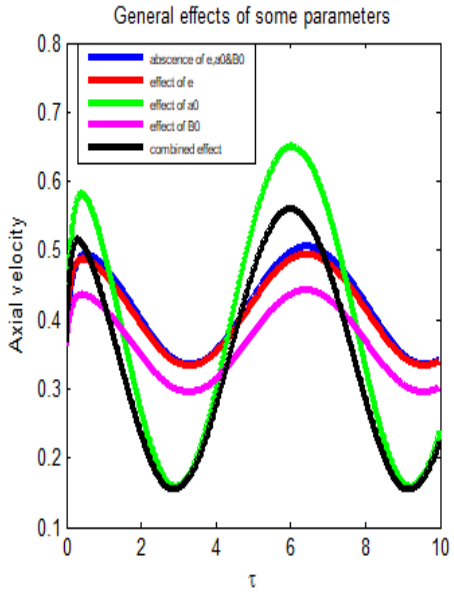

Figure 22:

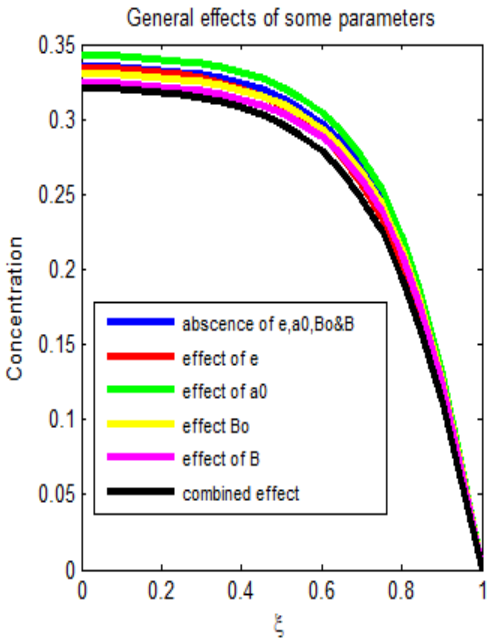

Figure 23:

4.2. Discussion of the simulations

The effect of Hartmann number on axial velocity profiles is illustrated by figure 3. From the graph we observe that as the Hartmann number increases, the velocity decreases due to the fact that as the magnetic fields is applied to the body, the Lorentz force tend to oppose the flow of blood. The Lorentz force is able to oppose the motion of the blood flow because blood consists of red blood cells which contains ions. Similar results were obtained by Kumari *et al,* (2019) [1] and Sharma *et al* (2019) [4] who considered the navier slip.

Figure 4 shows the effect of increasing body acceleration on axial velocity. From the graph it is observed that for the fixed values of Hartmann number and height of stenosis, axial velocity increases as body acceleration increases. The increase in velocity is due to the reason that body acceleration increases the heart beats and the pulse rate. When the body is subjected to body acceleration, the heart speeds up to pumping blood so that more blood can reach the muscles.

This study also investigated the effect of Reynolds number on axial velocity. From the graph we see that, as Reynolds numbers increase, the axial velocity increases. The increase in Reynold's number implies more increase of inertial forces than the viscous forces. Thus, as the inertial force increases, the velocity increases.

Figure 7 shows both, the axial velocity and the radial velocity. From the graph we see that the axial velocity is higher than the radial velocity. This is due to the fact that the pressure gradient is more dominant in the axial direction than in radial direction. On the other hand, we also observe that, the axial velocity is maximum along the axis of symmetry and it is zero on the boundary. The axial velocity is decreasing as we move towards the boundary because of the no slip condition at the boundary. The radial velocity is zero along the line of symmetry because there is no radial flow along that axis. Also, it is zero at the boundary, to satisfy the no slip condition. It is very interesting to note that it has been revealed that increase in the severity of stenosis, decreases the axial velocity but increase the radial velocity. The radial velocity increases as compensation to the axial velocity which decreases. However, this may medically endanger a person by harming the arterial wall for prolonged situation.

The effect of Hartman number, body acceleration and Reynolds number on radial velocity are shown in figures 9, 10 and 11 respectively. The effect of increasing these parameters on the radial velocity is observed to be the same as it is manifested on the axial velocity.

The effect of increasing the chemical reaction parameter on concentration profile is illustrated in figure 12. From the graph, we clearly observe that, as the chemical reaction parameter increases, the concentration decreases. The decrease of the concentration is due to the fact that the presence of chemical reaction acts as the consumption or destructive agent of chemical species. This leads to the reduction of the concentration.

Figure 13 shows the effect of increasing the Schmidt number on concentration profiles. From the graph it is observed that, as the Schmidt number increases the concentration profile increases. This can physically be explained that, the increase in Schmidt number implies that the molecular diffusion decreases that is, an increase in the Schmidt number, increases the concentration boundary layer thickness, which in turn

increases the concentration profiles. Figure 14 shows the effect of increasing the stenotic height on concentration profile. From the graph, we have observed that, as the stenotic height slightly increases, the concentration profiles decreases. The decrease of the concentration profile is due to the reason that the size of artery gets decreased as the stenotic height increases, thus the concentration decreases too. Similar effect is observed in figure 15 where the increase in Reynolds number reduces the concentration. Figure 18 shows the effect of increasing the Hartmann number on the skin friction. From the graph, we have observed that, as the Hartman number increases, the skin friction profiles decreases. The skin friction again varies periodically with time. This physically mean that the shear stress decreases due to the presence of magnetic field. Reduction of the shear stress in turn leads to the decrease in the skin friction coefficient. On the other hand, increasing the Reynolds number implies that the inertial force increases than the viscous force. As viscous force is smaller, skin friction gets reduced. This means that, with increase of the Reynolds number, the inertial force is more dominant than the viscous force. This lowers the skin friction. This has been shown in figure 19.

The combined effect of stenosis, body acceleration, magnetic field and chemical reaction has further been shown in figures 22 and 23. From the graphs we clearly see that the combined effect highly reduces the velocity of the blood. However, body exercise seems to have more effect than magnetic fields and stenosis. In this regard therefore, since body exercise highly raises the blood's speed, magnetic therapy for a stenosed person will therefore be of more advantageous, not only for reducing pain but also regulating blood rheology by reducing blood's velocity. Figure 23 shows the same for concentration, from the figure we see that the combined effect of stenosis, body acceleration, magnetic field and chemical reaction for the given values of parameters, generally reduce the concentration. Thus, the magnetic therapy taken during sports for the sake of reducing pain, causes reduction of transportation of some information and macromolecules in arterial blood flow. From this study we can therefore say that magnetic therapy in sports should be done with care because if a person has stenosed artery and such therapy is applied, concentration is generally affected. Medically this implies that the transfer of atherogenic molecules such as oxygen and even low-density lipoproteins from the blood to the wall get reduced. However, increasing body exercise increases the concentration.

5. Conclusion

Formulation of a mathematical model and computer simulations of two-dimensional blood flow through a stenosed artery in the presence of body acceleration, magnetic fields and chemical reaction has been done. Similar with previous studies, it is observed that the presence of magnetic fields affects the flow of blood. In this study it has been shown that the presence of magnetic fields in the presence of stenosis and body acceleration again affects the flow of blood. The current study gives more insights in medical use of magnetic fields in treating various diseases related to blood rheology like hypertension. It has also been observed that body exercise increases the blood's velocity. Furthermore, the presence of chemical reaction has been shown to reduce the mass concentration. In

this regard we suggest that for patients with heart diseases, exposing them to physical exercises should be done with care as prolonged exposure to body accelerations may cause some serious health problems such as high pulse rate or even sudden death. Therapies that involve vibrations should also be handled with care by taking into account that blood's velocity will be increased. In conclusion therefore, magnetic therapy in sports is very important, it may offer multiple benefits such as reducing pain and regulating blood flow which has been increased by body accelerations.

REFERENCES

1. S.Kumari, R.Rathee and J.Nandal, Unsteady peristaltic transport of MHD Fluid through an inclined stenosed artery with slip effect, *International Journal of Applied Engineering Research,* 14(8) (2019) 1881-1891.
2. D.Karthikeyan and G.Jeevitha, Heat and mass transfer on MHD two phase blood flow through a stenosed artery with permeable, Wall *International Journal of Innovative Technology and Exploring Engineering,* 8 (2019) 1224-1232.
3. A.R.Haghighi and N.Aliashrafi, A mathematical modeling of pulsatile blood flow through a stenosed artery under effect of a magnetic field, *Journal of Mathematical Modeling,* 6(2)(2018)149-164.
4. M.Sharma, R.Gaur and B.Sharma, Radiation effect on MHD blood flow through a tapered porous stenosed artery with thermal and mass diffusion, *International Journal of Applied Mechanics and Engineering,* 24(2) (2019) 411-423.
5. V.K.Tanwar, N.Varshney and R.Agarwal, Effect of body acceleration on pulsatile blood flow through a catheterized artery, *Advances in Applied Science Research,* 7(2) (2016) 155-166.
6. G.Shit, M.Roy and A.Sinha, Mathematical modelling of blood flow through a tapered overlapping stenosed artery with variable viscosity, *Applied Bionics and Biomechanics,* 11 (2014) 185-195.
7. C.Rajashekhar, G.Manjunatha and K.Basavarajappa, Analytical solution of FHD flow of blood through two layered model in the presence of magnetic field, *Journal of Mechanical Engineering Research and Developments,* 40(2) (2017) 365-370.
8. V.Mwanthi, E.Mwenda and K.K.Gachoka, Velocity profiles of unsteady blood flow through an inclined circular tube with magnetic field, *Journal of Advances in Mathematics and Computer Science,* 24(6) (2017) 1-10.
9. L.Parmar, S.B.Kulshreshtha and D. P. Singh, The role of magnetic field intensity in blood flow through overlapping stenosed artery: A Herschel-Bulkley fluid model, *Advances in Applied Science Research,* 4(6) *(*2013) 318-328.
10. N.Mustapha and NAmin, The unsteady power law blood flow through a multi-irregular stenosed artery *Malaysian Journal of Industrial and Applied Mathematics,* 24(2) (2008) 187–198.
11. P.Nagarani and G.Sarojamma, Flow of a Casson fluid through a stenosed artery subject to periodic body acceleration, *Proceedings of the 9th WSEAS intern.Conf. Mathematical and computational methods in science and engineering,* (2007) 237-244.
12. K.Das and G.Saha, Arterial MHD pulsatile flow of blood under periodic body acceleration, *Bulletin of Society of Mathematicians Banja Luka,* 16 (2009) 21-42.

13. K.E.Hossain and M.M.Haque, Influence of magnetic field on chemically reactive blood flow through stenosed bifurcated arteries, *AIP Publishing*, 1851 (2017) 1-13.
14. M.Sharma and R.Gaur, Effect of variable viscosity on chemically reacting magneto-blood flow with heat and mass transfer, *Global Journal of Pure and Applied Mathematics*, 13(3) (2017) 26-35.

Output 2

Available online at http://scik.org
Commun. Math. Biol. Neurosci. 2020, 2020:64
https://doi.org/10.28919/cmbn/4906
ISSN: 2052-2541

NON-NEWTONIAN HEAT AND MASS TRANSFER ON MHD BLOOD FLOW THROUGH A STENOSED ARTERY IN THE PRESENCE OF BODY EXERCISE AND CHEMICAL REACTION

ANNORD MWAPINGA[1,*], EUNICE MUREITHI[2], JAMES MAKUNGU[2], VERDIANA MASANJA[1]

[1]Department of Applied Mathematics and Computational Sciences, The Nelson Mandela African Institution of Science and Technology, P.O.Box 447, Arusha, Tanzania

[2]Department of Mathematics, University of Dar es salaam, P.O. Box 35091 Dar es Salaam, Tanzania

Abstract. A mathematical model of non-Newtonian blood flow, heat and mass transfer through a stenosed artery is studied. The non-Newtonian model is chosen to suit the Herschel-Bulkley fluid characteristics, taking into account the presence of body acceleration, magnetic fields and chemical reaction. The study assumed that, the flow is unsteady, laminar, two-dimensional and axisymmetric. The governing flow equations of motion were solved numerically using explicit finite difference schemes. The study found that velocity profile diminishes with increase in Hartman number and increases with body acceleration. The temperature profile is raised by the increase of body acceleration and the Eckert number, while it diminishes with the increase of the Peclet number. It was found also that the concentration profile increases with the increase of the Soret number and decreases with the increase of the chemical reaction. It was further observed that the shear stress deviates more when $n > 1$ than when $n < 1$. Shear stress for power law fluid when $n > 1$ exhibited higher magnitude value than Newtonian, Bingham and Herschel-Bulkley fluids.

Keywords: herschel-bulkley fluid; non-newtonian; magnetic field; chemical reaction.

2010 AMS Subject Classification: 76A05.

*Corresponding author
E-mail address: mwapingaa@nm-aist.ac.tz
Received August 3, 2020

1. INTRODUCTION

The cardiovascular system involves blood, the heart and the blood vessel. Blood is important because it is a transporting agent in the human body. It is very unfortunate that the human blood vessels such as arteries and capillaries may contain plaques which disturb the normal flow of blood and hence leading to cardiovascular diseases such as heart attack and stroke. The abnormal flow of blood has drawn attention to many researchers due to its implications in medicine and fluid mechanics.

Blood is categorically classified as a non-Newtonian fluid, thus studies which involve modelling blood flow should not disregard the non-Newtonian character of blood. In day to day activities, human body is exposed to situation which disturb the normal flow of blood. This include (among others), physical exercises, travelling using vehicles and applying magnetic therapy to a patient.

A number of investigators have carried out theoretical studies on blood flow. Misra et al [15] modeled blood flow in arteries subject to the vibrating environment. In their study, the fluid (blood) was treated as a couple stress fluid. However, their study did not take into consideration the presence of stenoses despite the fact that human arteries are often subjected to fat or solid deposits that lead to constricted arterial wall.

A recent study of non-Newtonian blood flow in a stenosed artery that was conducted by Liu and Liu [14] involved the flow of blood in a tapered artery and took into consideration heat and mass transfer. The study established that as the maximum depth of the stenosis increases, the blood's axial velocity increases. Another study on blood flow in a stenosed artery was done by Jamil et al [12] that took into consideration the effects periodic body acceleration and nanoparticles. It was proved that velocity decreases as yield stress increases and the velocity could be controlled by nanoparticles. Numerical solution of blood flow and mass transport in an elastic tube with multiple stenoses was also investigated by Alsemiry et al [3], where blood was treated a Newtonian fluid. The result of their study was that the double stenoses and pulsatile inlet conditions increase the number of recirculation regions and effect higher mass transfer rate at the throat. Changdar and De [6] conducted a similar study like Alsemiry et al [3] but considered the presence of body acceleration. As it was expected, the result revealed that the

presence of body acceleration enhances the axial velocity.

Computational modelling of arterial blood flow for non - Newtonian fluid was investigated (inta alia) by Sharma and Yadav [18], Jamalabadi et al [1], Dixit et al [7] and Prasad and Yasa [16]. These studies did not include the aspect of vibration or body acceleration and the heat transfer in the body which is very important to take into consideration. On the other hand, Bunonyo et al [5], Eldesoky [8] and Sinha et al [19] studied MHD blood flow along the arterial wall. However, all these studies, the aspect of body acceleration and mass transfer were not investigated. As expected, all these studies showed among other things, that magnetic fields affect the blood's velocity.

Arteries as living tissues, require supply of metabolites, including oxygen, and removal of waste products, Akbar et al [2]. Zaman et al [23], pointed out that, it is generally accepted that the rheological behavior of blood is assumed as Newtonian for values of shear rate greater than $100s^{-1}$ and a such situation occurs in larger arteries. But in smaller arteries the blood does not obey the Newtonian postulate and therefore cannot be modeled as a Newtonian fluid. Several more scholars conclude that it is very crucial that blood is model as a non – Newtonian fluid. These include Rodkiewicz et al [17], Tu and Deveille [21], and Gijsen et al [9].

There are several theoretical studies which have attempted to model blood flow in arteries by considering blood to obey the Herschel-Bulkley fluid characteristics. These include studies by Srivastava[20] and Kumar and Gupta et al [13]. All these studies assumed unidirectional blood flow. The Herschel-Bulkley fluid is of general type and can be reduced to Newtonian, Bingham plastic and Power-law fluid models, by selecting appropriate flow parameters, Biswas and Laskar [4]. According to Vajravelu et al,[22], the Herschel-Bulkley constitutive equation contains one more parameter than the Casson equation does, and thus more information about the blood properties can be obtained when the Herschel-Bulkley equation is used than when the Casson one is used.

Based on the reviewed literature, the unsteady, MHD flow of blood through a stenosed artery in the presence of body acceleration, chemical reaction, with mass and heat transfer taking place, and treating blood as Herschel-Bulkley fluid, has not been considered. Such flows have manifested themselves in several situations like magnetic therapy in sports and in MRI testing. The

current study therefore intends to fill that gap where, computational analysis of unsteady non – Newtonian MHD blood flow involving heat and mass transfer in the presence of body acceleration and chemical reaction is investigated.

2. FORMULATION OF THE PROBLEM

In the current study we consider that the flow is unsteady, laminar, two-dimensional, pulsatile, incompressible, axisymmetric in the sense that there is no variation of the velocity with the angle θ in the cylindrical polar coordinate system (r,θ,z), with the z-axis coinciding with the axis of symmetry of the flow. In that regard therefore, $u_\theta = 0$ and $\frac{\partial \mathbf{u}}{\partial \theta} = 0$. The blood is considered to be a non - Newtonian fluid satisfying the Herschel-Bulkley model. Furthermore, body acceleration $(F(t))$, and the strength of magnetic field (B_0) act in the axial direction of the artery. Every cell in the body can produce heat which needs to be spread around the body, and this is done by the blood, which heats some organs and cools others by conduction and other processes. Thus, the study takes into account for the chemical reaction such as exothermic reaction K for mass transfer.

We define the geometry of stenosis as shown in equation (2.1)

$$R(z) = \begin{cases} r_0 - \delta\left(1 + \cos\frac{\pi z}{2z_0}\right) & -2z_0 \le z \le 2z_0 \\ r_0 & \text{otherwise} \end{cases} \tag{2.1}$$

Under the mentioned assumptions, the governing blood flow equations, continuity, momentum, energy and concentration equations in the cylindrical polar coordinate system are as written in equations (2.2) to (2.6).

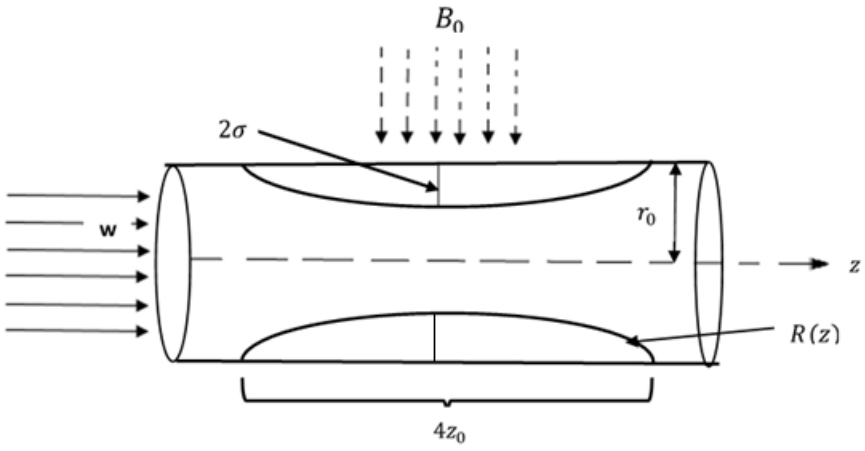

FIGURE 1. Schematic flow diagram

$$\frac{\partial u}{\partial r}+\frac{u}{r}+\frac{\partial w}{\partial z}=0 \tag{2.2}$$

$$\rho\left(\frac{\partial u}{\partial t}+u\frac{\partial u}{\partial r}+w\frac{\partial u}{\partial z}\right)=-\frac{\partial P}{\partial r}+\frac{1}{r}\frac{\partial(r\tau_{rr})}{\partial r}+\frac{\partial(\tau_{rz})}{\partial z} \tag{2.3}$$

$$\rho\left(\frac{\partial w}{\partial t}+u\frac{\partial w}{\partial r}+w\frac{\partial w}{\partial z}\right)=-\frac{\partial P}{\partial z}+\frac{1}{r}\frac{\partial(r\tau_{rz})}{\partial r}+\frac{\partial(\tau_{zz})}{\partial z}+F(t)-\sigma B_0^2 w \tag{2.4}$$

(2.5)

$$\rho c_p\left(\frac{\partial T}{\partial t}+u\frac{\partial T}{\partial r}+w\frac{\partial T}{\partial z}\right)=k\left(\frac{\partial^2 T}{\partial r^2}+\frac{1}{r}\frac{\partial T}{\partial r}+\frac{\partial^2 T}{\partial z^2}\right)+\tau_{rr}\frac{\partial u}{\partial r}+\tau_{rz}\frac{\partial w}{\partial r}+\tau_{rz}\frac{\partial u}{\partial z}+\tau_{zz}\frac{\partial w}{\partial z}$$

$$\left(\frac{\partial C}{\partial t}+u\frac{\partial C}{\partial r}+w\frac{\partial C}{\partial z}\right)=D_f\left(\frac{\partial^2 C}{\partial r^2}+\frac{1}{r}\frac{\partial C}{\partial r}+\frac{\partial^2 C}{\partial z^2}\right)+\frac{D_f K_T}{T_0}\left(\frac{\partial^2 T}{\partial r^2}+\frac{1}{r}\frac{\partial T}{\partial r}+\frac{\partial^2 T}{\partial z^2}\right)$$

$$-\beta(C-C_0) \tag{2.6}$$

In the above equations, u, w, T and C are respectively radial velocity, axial velocity, temperature and concentration of the fluid. $c_p, k, K_T, D_f,$ andβ are, respectively the specific heat capacity, thermal conductivity, the thermal-diffusion ratio, diffusion coefficient, and chemical reaction parameter. Furthermore, $\tau_{rr},$ andτ_{zz} represent the normal stress components. τ_{rz} is the

shear stress component. The current study considers that blood obeys the Herschel-Bulkley constitutive model. The stress tensor components are as given in equation (2.7)

$$\tau_{ij} = \left(K\dot{\gamma}^{n-1} + \frac{\tau_0}{\dot{\gamma}}\right)\dot{\gamma}_{ij} \quad \text{for} \quad \tau \geq \tau_0 \qquad \dot{\gamma} = 0 \quad \text{for} \quad \tau < \tau_0 \tag{2.7}$$

where,K is the consistency index, n is the flow behavior index and τ_0 is the yield stress at zero shear rate. From equation (2.7) there are special cases that can arise as we can be able to see different types of behaviors of fluids. This is as shown in table 1.

Type of fluid model	K	n	τ_0
Herschel-Bulkley	>0	0<n<∞	>0
Newtonian	>0	1	0
Power law for $n < 1$ (shear-thinning)	>0	0<n<1	0
Bingham	>0	1	>0
Power law for $n > 1$ (shear-thickening)	>0	1<n<∞	0

TABLE 1. Different types of behaviors of fluids

In equation (2.7), $\dot{\gamma}$ is the second invariant of the rate of strain which is as given in equation (2.8).

$$\dot{\gamma} = \sqrt{2\left[\left(\frac{\partial u}{\partial r}\right)^2 + \left(\frac{u}{r}\right)^2 + \left(\frac{\partial w}{\partial z}\right)^2\right] + \left(\frac{\partial u}{\partial z} + \frac{\partial w}{\partial r}\right)^2} \tag{2.8}$$

Again, from equation (2.7) we can write the stresses

$$\tau_{rr} = 2\left(K\dot{\gamma}^{n-1} + \tau_0\dot{\gamma}^{-1}\right)\left(\frac{\partial u}{\partial r}\right) \tag{2.9}$$

$$\tau_{zz} = 2\left(K\dot{\gamma}^{n-1} + \tau_0\dot{\gamma}^{-1}\right)\left(\frac{\partial w}{\partial z}\right) \tag{2.10}$$

$$\tau_{rz} = 2\left(K\dot{\gamma}^{n-1} + \tau_0\dot{\gamma}^{-1}\right)\left(\frac{\partial u}{\partial z} + \frac{\partial w}{\partial r}\right) \tag{2.11}$$

The pulsatile pressure gradient which is responsible for driving the blood's flow in the axial direction is given as $-\frac{\partial P}{\partial z} = A_0 + A_1\cos(\omega t), \quad t > 0$ where, we define A_0 and A_1 as the steady component of pressure gradient and amplitude of its pulsatile component respectively. $\omega = 2\pi f_p, f_p$ being the pulse frequency. We further define the body acceleration which acts in our system as $F(t) = \rho a_0 \cos(\omega_b t + \psi)$ where, ρa_0 is the amplitude of body acceleration, ψ is the phase angle and $\omega_b = 2\pi f_b$, with f_b the body acceleration frequency.

2.1. Boundary and initial conditions. In this study we assume that initially as shown in equation (2.12) that;

$$w(r,z,0) = w_0, \quad T(r,z,0) = T_0, \quad C(r,z,0) = C_0, \tag{2.12}$$

The boundary conditions for the developed model are as shown in equations (2.13) to (2.16).

$$w(r,z,t) = 0, \quad u(r,z,t) = 0 \quad \text{on} \quad r = R(z) \tag{2.13}$$

$$\frac{\partial w(r,z,t)}{\partial r} = 0, \quad u(r,z,t) = 0 \quad \text{on} \quad r = 0 \tag{2.14}$$

$$\frac{\partial T(r,z,t)}{\partial r} = 0, \quad \text{on} \quad r = 0 \quad \text{and} \quad T(r,z,t) = T_w \quad \text{on} \quad r = R(z) \tag{2.15}$$

$$\frac{\partial C(r,z,t)}{\partial r} = 0, \quad \text{on} \quad r = 0 \quad \text{and} \quad C(r,z,t) = C_w \quad \text{on} \quad r = R(z) \tag{2.16}$$

Where, T_w, C_w stands for arterial wall temperature and concentration on the arterial wall, respectively.

3. Non - Dimensionalisation of the Model Variables

We now introduce the non-dimensional variables. We use w_c as the average fluid's velocity which is therefore our characteristic velocity. We define r_0 as the radius of normal artery. Our dimensionless variables are shown in equations (3.1) to (3.3).

$$\eta = \frac{r}{r_0}, w^* = \frac{w}{w_c}, u^* = \frac{u}{w_c}, \quad t^* = \frac{t w_c}{r_0}, z^* = \frac{z}{r_0}, P^* = \frac{P}{\rho w_c^2}, \quad \tau_{ij}^* = \frac{\tau_{ij}}{\rho w_c^2}, \tag{3.1}$$

$$A_0^* = \frac{A_0 r_0}{\rho w_c^2}, A_1^* = \frac{A_1 r_0}{\rho w_c^2}, \omega^* = \frac{r_0 \omega}{w_c}, \omega_b^* = \frac{r_0 \omega}{w_c}, \quad a_0^* = \frac{r_0 a_0}{w_c^2}, \quad R^*(z^*) = \frac{R(z)}{r_0} \tag{3.2}$$

$$T^* = \frac{T - T_0}{T_w - T_0}, \quad C^* = \frac{C - C_0}{C_w - C_0}, \quad \beta^* = \frac{\beta r_0^2}{\nu}, \quad e = \frac{\delta}{r_0}. \tag{3.3}$$

We now substitute equations (3.1)to (3.3) into equations (2.2)to (2.16) so that after dropping all the asterisks, we to get equations (3.4)to (3.16).

$$\frac{\partial u}{\partial \eta} + \frac{u}{\eta} + \frac{\partial w}{\partial z} = 0 \tag{3.4}$$

$$\frac{\partial u}{\partial t} + u\frac{\partial u}{\partial \eta} + w\frac{\partial u}{\partial z} = \frac{\partial P}{\partial \eta} + \left(\frac{\partial \tau_{rr}}{\partial \eta} + \frac{1}{\eta}\tau_{rr} + \frac{\partial \tau_{rz}}{\partial z} \right) \tag{3.5}$$

$$\begin{aligned} \frac{\partial w}{\partial t} + u\frac{\partial w}{\partial \eta} + w\frac{\partial w}{\partial z} &= (A_0 + A_1 \cos(\omega t)) + \left(\frac{\partial \tau_{rz}}{\partial \eta} + \frac{1}{\eta}\tau_{rz} + \frac{\partial \tau_{zz}}{\partial z} \right) \\ &\quad + a_0 \cos(\omega_b t + \psi) - \frac{H_a^2}{R_{eG}} w \end{aligned} \tag{3.6}$$

$$\begin{aligned} \frac{\partial T}{\partial t} + u\frac{\partial T}{\partial \eta} + w\frac{\partial T}{\partial z} &= \frac{1}{P_e}\left(\frac{\partial^2 T}{\partial \eta^2} + \frac{\partial T}{\eta \partial \eta} + \frac{\partial^2 T}{\partial z^2} \right) \\ &\quad + E_c \left[\tau_{rr}\frac{\partial u}{\partial \eta} + \tau_{rz}\frac{\partial w}{\partial \eta} + \tau_{rz}\frac{\partial u}{\partial z} + \tau_{zz}\frac{\partial w}{\partial z} \right] \end{aligned} \tag{3.7}$$

$$\begin{aligned} \frac{\partial C}{\partial t} + u\frac{\partial C}{\partial \eta} + w\frac{\partial C}{\partial z} &= \frac{1}{P_e}\left(\frac{\partial^2 C}{\partial \eta^2} + \frac{1}{\eta}\frac{\partial C}{\partial \eta} + \frac{\partial^2 C}{\partial z^2} \right) \\ &\quad + S_r \left(\frac{\partial^2 T}{\partial \eta^2} + \frac{1}{\eta}\frac{\partial T}{\partial \eta} + \frac{\partial^2 T}{\partial z^2} \right) - \frac{\beta C}{Re} \end{aligned} \tag{3.8}$$

Where, $R_{eG} = \dfrac{r_0^n \rho}{K w_c^{n-2}}$, $\quad Ha = B_0 \sqrt{\dfrac{\sigma r_0^{n+1}}{K w_c^{n-1}}}$, $\quad P_e = \dfrac{\rho w_c r_0 c_p}{k}$, $\quad E_c = \dfrac{w_c^2}{c_p(T_w - T_0)}$ and $S_r = \dfrac{D_f K_T (T_w - T_0)}{\nu T_m (C_w - C_0)}$ are the, generalized Reynold, Hartman, Peclet, Eckert, and Soret numbers respectively.

$$\begin{aligned} \tau_{ij} &= \left(\frac{1}{R_{eG}} \dot{\gamma}^{n-1} + \tau_0 \dot{\gamma}^{-1} \right) \dot{\gamma}_{ij} \\ \dot{\gamma} &= 0 \quad \text{for} \quad \tau < \tau_0 \end{aligned} \tag{3.9}$$

with second invariant of the rate of strain given in equation (3.10)

$$\dot{\gamma} = \sqrt{2\left[\left(\frac{\partial u}{\partial \eta}\right)^2 + \left(\frac{u}{\eta}\right)^2 + \left(\frac{\partial w}{\partial z}\right)^2\right] + \left(\frac{\partial u}{\partial z} + \frac{\partial w}{\partial \eta}\right)^2} \tag{3.10}$$

and

$$\tau_{rr} = 2\left(R_{eG}\dot{\gamma}^{n-1} + \tau_0\dot{\gamma}^{-1}\right)\left(\frac{\partial u}{\partial \eta}\right) \tag{3.11}$$

$$\tau_{zz} = 2\left(R_{eG}\dot{\gamma}^{n-1} + \tau_0\dot{\gamma}^{-1}\right)\left(\frac{\partial w}{\partial z}\right) \tag{3.12}$$

$$\tau_{rz} = 2\left(R_{eG}\dot{\gamma}^{n-1} + \tau_0\dot{\gamma}^{-1}\right)\left(\frac{\partial u}{\partial z} + \frac{\partial w}{\partial \eta}\right) \tag{3.13}$$

subject to the dimensionless initial and boundary conditions

$$w(\eta,z,0) = w_0, \quad T(\eta,z,0) = T_0, \quad C(\eta,z,0) = C_0 \tag{3.14}$$

$$w(\eta,z,t) = u(\eta,z,t) = 0, T(\eta,z,t) = T_w, C(\eta,z,t) = C_w \quad \text{on} \quad \eta = R(z) \tag{3.15}$$

$$\frac{\partial w(\eta,z,t)}{\partial \eta} = \quad \frac{\partial T(\eta,z,t)}{\partial \eta} = \quad \frac{\partial C(\eta,z,t)}{\partial \eta} = \quad u(\eta,z,t) = 0, \quad \text{on} \quad \eta = 0 \tag{3.16}$$

4. Solution of the Problem

To obtain the numerical solution, we first of all, transform our cylindrical domain into the rectangular domain by using the following radial transformation. We introduce new variable ξ such that $\xi = \dfrac{\eta}{R(z)}$. Making use of this transformation, equations (3.4) to (3.16) becomes equations (4.1) to (4.12).

$$\frac{1}{R}\frac{\partial u}{\partial \xi} + \frac{u}{R\xi} + \frac{\partial w}{\partial z} - \frac{\xi}{R}\frac{dR}{dz}\frac{\partial w}{\partial \xi} = 0 \tag{4.1}$$

$$\frac{\partial u}{\partial t} = -\frac{\partial P}{R\partial \xi} - \frac{u\partial u}{R\partial \xi} - w\left(\frac{\partial u}{\partial z} - \frac{\xi}{R}\frac{dR}{dz}\frac{\partial u}{\partial \xi}\right) + \frac{1}{R}\frac{\partial \tau_{\xi\xi}}{\partial \xi} + \frac{\tau_{\xi\xi}}{R\xi} + \frac{\partial \tau_{\xi z}}{\partial z} - \frac{\xi}{R}\frac{dR}{dz}\frac{\partial \tau_{\xi z}}{\partial \xi} \tag{4.2}$$

$$\frac{\partial w}{\partial t} = (A_0 + A_1\cos(\omega t)) - \frac{u\partial w}{R\partial \xi} - w\left(\frac{\partial w}{\partial z} - \frac{\xi}{R}\frac{dR}{dz}\frac{\partial w}{\partial \xi}\right) + \frac{1}{R}\frac{\partial \tau_{\xi z}}{\partial \xi} + \frac{\tau_{\xi z}}{R\xi} + \frac{\partial \tau_{zz}}{\partial z}$$
$$- \frac{\xi}{R}\frac{dR}{dz}\frac{\partial \tau_{zz}}{\partial \xi} + a_0\cos(\omega_b t + \psi) - \frac{H_a^2}{R_{eG}}w \tag{4.3}$$

$$\frac{\partial T}{\partial t} = -\frac{u\partial T}{R\partial\xi} - w\left(\frac{\partial T}{\partial z} - \frac{\xi}{R}\frac{dR}{dz}\frac{\partial T}{\partial\xi}\right) + \frac{1}{P_e}\left(\frac{\partial^2 T}{R^2\partial\xi^2} + \frac{1}{R^2\xi}\frac{\partial T}{\partial\xi} + \frac{\partial^2 T}{\partial z^2}\right)$$

$$+\frac{1}{P_e}\left[\frac{3\xi}{R^2}\left(\frac{dR}{dz}\right)^2\frac{\partial T}{\partial\xi} - \frac{2\xi}{R}\frac{dR}{dz}\frac{\partial^2 T}{\partial\xi\partial z} - \frac{\xi}{R}\frac{d^2R}{dz^2}\frac{\partial T}{\partial\xi} + 2\left(\frac{\xi}{R}\frac{dR}{dz}\right)^2\frac{\partial^2 T}{\partial\xi^2}\right] \tag{4.4}$$

$$+E_c\left(\frac{\tau_{\xi\xi}}{R}\frac{\partial u}{\partial\xi} + \frac{\tau_{\xi z}}{R}\frac{\partial w}{\partial\xi}\right) + E_c\tau_{\xi z}\left(\frac{\partial u}{\partial z} - \frac{\xi}{R}\frac{dR}{dz}\frac{\partial u}{\partial\xi}\right) + E_c\tau_{zz}\left(\frac{\partial w}{\partial z} - \frac{\xi}{R}\frac{dR}{dz}\frac{\partial w}{\partial\xi}\right)$$

$$\frac{\partial C}{\partial t} = -\frac{u\partial C}{R\partial\xi} - w\left(\frac{\partial C}{\partial z} - \frac{\xi}{R}\frac{dR}{dz}\frac{\partial C}{\partial\xi}\right) + \frac{1}{P_e}\left(\frac{\partial^2 C}{R^2\partial\xi^2} + \frac{1}{R^2\xi}\frac{\partial C}{\partial\xi} + \frac{\partial^2 C}{\partial z^2}\right)$$

$$+\frac{1}{P_e}\left[\frac{3\xi}{R^2}\left(\frac{dR}{dz}\right)^2\frac{\partial C}{\partial\xi} - \frac{2\xi}{R}\frac{dR}{dz}\frac{\partial^2 C}{\partial\xi\partial z} - \frac{\xi}{R}\frac{d^2R}{dz^2}\frac{\partial C}{\partial\xi} + 2\left(\frac{\xi}{R}\frac{dR}{dz}\right)^2\frac{\partial^2 C}{\partial\xi^2}\right] - \frac{\beta C}{Re}$$

$$+S_r\left[\frac{3\xi}{R^2}\left(\frac{dR}{dz}\right)^2\frac{\partial T}{\partial\xi} - \frac{2\xi}{R}\frac{dR}{dz}\frac{\partial^2 T}{\partial\xi\partial z} - \frac{\xi}{R}\frac{d^2R}{dz^2}\frac{\partial T}{\partial\xi} + 2\left(\frac{\xi}{R}\frac{dR}{dz}\right)^2\frac{\partial^2 T}{\partial\xi^2}\right] \tag{4.5}$$

With,

$$\dot{\gamma} = \sqrt{2\left[\left(\frac{\partial u}{R\partial\xi}\right)^2 + \left(\frac{u}{R\xi}\right)^2 + \left(\frac{\partial w}{\partial z} - \frac{\xi}{R}\frac{dR}{dz}\frac{\partial w}{\partial\xi}\right)^2\right] + \left(\frac{\partial u}{\partial z} - \frac{\xi}{R}\frac{dR}{dz}\frac{\partial u}{\partial\xi} + \frac{\partial w}{R\partial\xi}\right)^2} \tag{4.6}$$

and

$$\tau_{\xi\xi} = 2\left(R_{eG}\dot{\gamma}^{n-1} + \tau_0\dot{\gamma}^{-1}\right)\left(\frac{\partial u}{R\partial\xi}\right) \tag{4.7}$$

$$\tau_{zz} = 2\left(R_{eG}\dot{\gamma}^{n-1} + \tau_0\dot{\gamma}^{-1}\right)\left(\frac{\partial w}{\partial z} - \frac{\xi}{R}\frac{dR}{dz}\frac{\partial w}{\partial\xi}\right) \tag{4.8}$$

$$\tau_{\xi z} = 2\left(R_{eG}\dot{\gamma}^{n-1} + \tau_0\dot{\gamma}^{-1}\right)\left(\frac{\partial u}{\partial z} - \frac{\xi}{R}\frac{dR}{dz}\frac{\partial u}{\partial\xi} + \frac{\partial w}{\partial\eta}\right) \tag{4.9}$$

subect to conditions in equations (4.10)to (4.12).

$$w(\xi,z,0) = w_0, \quad T(\xi,z,0) = T_0, \quad C(\xi,z,0) = C_0 \tag{4.10}$$

$$w(\xi,z,t) = u(\xi,z,t) = 0, \quad T(\xi,z,t) = T_w, C(\xi,z,t) = C_w \quad \text{on} \quad \xi = 1 \tag{4.11}$$

$$\frac{\partial w(\xi,z,t)}{\partial\xi} = \quad \frac{\partial T(\xi,z,t)}{\partial\xi} = \quad \frac{\partial C(\xi,z,t)}{\partial\xi} = \quad u(\xi,z,t) = 0, \quad \text{on} \quad \xi = 0 \tag{4.12}$$

We use the initial velocity w_0, which is obtained as the solution at steady state in the absence of body acceleration and magnetic fields. Applying the radial transformation, the initial velocity is as given in equation (4.13).

$$w_0 = \left(\frac{A_0 + A_1}{4}\right)(1 - (H\xi)^2) \tag{4.13}$$

4.1. The Radial Momentum. We are now going to obtain the radial velocity. We use the continuity equation (4.1) to get the radial velocity $u(\xi,z,t)$. We multiply equation (4.1) by ξR and then integrate it with respect to ξ to obtain equation (4.14).

$$\int \xi \frac{\partial u}{\partial \xi} d\xi + \int u d\xi + \int \xi R \frac{\partial w}{\partial z} d\xi + \int \xi^2 \frac{dR}{dz} \frac{\partial w}{\partial \xi} d\xi \tag{4.14}$$

Re-arranging equation (4.14) we get equation (4.15).

$$\int \xi \frac{\partial u}{\partial \xi} d\xi + \int u d\xi = \int \xi^2 \frac{dR}{dz} \frac{\partial w}{\partial \xi} d\xi - \int \xi R \frac{\partial w}{\partial z} d\xi \tag{4.15}$$

Applying integration by parts and simplifying the equation (4.15) we have equation (4.16).

$$u = \frac{dR}{dz} \xi w - \frac{2}{\xi} \frac{dR}{dz} \int w \xi d\xi - \frac{R}{\xi} \int \xi \frac{\partial w}{\partial z} d\xi \tag{4.16}$$

Making use of the boundary conditions in equations (4.11) and (4.12) and re-arranging we have (4.17)

$$\frac{2}{\xi} \frac{dR}{dz} \int_0^1 w \xi d\xi = -\frac{R}{\xi} \int_0^1 \xi \frac{\partial w}{\partial z} d\xi \tag{4.17}$$

multiplying by ξ and dividing by R we get (4.18)

$$\frac{2}{R} \frac{dR}{dz} \int_0^1 w \xi d\xi = -\int_0^1 \xi \frac{\partial w}{\partial z} d\xi \tag{4.18}$$

making comparison of the integrals and the integrands of equation (4.18), we easily get equation (4.19)

$$\frac{\partial w}{\partial z} = -\frac{2}{R} \frac{dR}{dz} w \tag{4.19}$$

We now substitute equation (4.19) into equation (4.16). Such substitution gives equation (4.20)

$$u = \frac{dR}{dz} \xi w - \frac{2}{\xi} \frac{dR}{dz} \int w \xi d\xi - \frac{R}{\xi} \int \xi \left(-\frac{2}{R} \frac{dR}{dz} w \right) d\xi \tag{4.20}$$

which simplifies to equation (4.21)

$$u = \left(\xi \frac{dR}{dz} w\right) \tag{4.21}$$

Equation (4.21) above, is the radial velocity component which needs to be calculated as well. However, we substitute this radial velocity into our axial momentum, energy and concentration equations. Also, using the product rule we find the derivatives, $\frac{\partial u}{\partial \xi} = \frac{dR}{dz}\left(\xi \frac{\partial w}{\partial \xi} + w\right)$ and $\frac{\partial u}{\partial z} = \xi\left(\frac{dR}{dz}\frac{\partial w}{\partial z} + w\frac{d^2R}{dz^2}\right)$. This process therefore eliminates u,as we write radial velocity u in terms of axial velocity w. We now have equations (4.22)to (4.28);

$$\begin{aligned}\frac{\partial w}{\partial t} &= (A_0 + A_1\cos(\omega t)) - \left(\xi\frac{dR}{dz}w\right)\frac{\partial w}{R\partial\xi} - w\left(\frac{\partial w}{\partial z} - \frac{\xi}{R}\frac{dR}{dz}\frac{\partial w}{\partial \xi}\right) + \frac{1}{R}\frac{\partial \tau_{\xi z}}{\partial \xi} + \frac{\tau_{\xi z}}{R\xi} + \frac{\partial \tau_{zz}}{\partial z} \\ &\quad - \frac{\xi}{R}\frac{dR}{dz}\frac{\partial \tau_{zz}}{\partial \xi} + a_0\cos(\omega_b t + \psi) - \frac{H_a^2}{R_{eG}}w\end{aligned} \tag{4.22}$$

$$\begin{aligned}\frac{\partial T}{\partial t} &= -\left(\frac{\xi}{R}\frac{dR}{dz}w\right)\frac{\partial T}{\partial \xi} - w\left(\frac{\partial T}{\partial z} - \frac{\xi}{R}\frac{dR}{dz}\frac{\partial T}{\partial \xi}\right) + \frac{1}{P_e}\left(\frac{\partial^2 T}{R^2\partial\xi^2} + \frac{1}{R^2\xi}\frac{\partial T}{\partial \xi} + \frac{\partial^2 T}{\partial z^2}\right) \\ &\quad + \frac{1}{P_e}\left[\frac{3\xi}{R^2}\left(\frac{dR}{dz}\right)^2\frac{\partial T}{\partial \xi} - \frac{2\xi}{R}\frac{dR}{dz}\frac{\partial^2 T}{\partial\xi\partial z} - \frac{\xi}{R}\frac{d^2R}{dz^2}\frac{\partial T}{\partial\xi} + 2\left(\frac{\xi}{R}\frac{dR}{dz}\right)^2\frac{\partial^2 T}{\partial\xi^2}\right]\end{aligned}$$

$$\begin{aligned}&+ E_c\left[\frac{\tau_{\xi\xi}}{R}\frac{dR}{dz}\left(\xi\frac{\partial w}{\partial\xi} + w\right) + \frac{\tau_{\xi z}}{R}\frac{\partial w}{\partial\xi}\right] + E_c\tau_{\xi z}\left[\xi\left(\frac{dR}{dz}\frac{\partial w}{\partial z} + w\frac{d^2R}{dz^2}\right)\right] \\ &- E_c\tau_{\xi z}\left[\frac{\xi}{R}\left(\frac{dR}{dz}\right)^2\left(\xi\frac{\partial w}{\partial\xi} + w\right)\right] + E_c\tau_{\xi z}\left(\frac{\partial w}{\partial z} - \frac{\xi}{R}\frac{dR}{dz}\frac{\partial w}{\partial\xi}\right)\end{aligned} \tag{4.23}$$

$$\begin{aligned}\frac{\partial C}{\partial t} &= -\left(\frac{\xi}{R}\frac{dR}{dz}w\right)\frac{\partial C}{\partial\xi} - w\left(\frac{\partial C}{\partial z} - \frac{\xi}{R}\frac{dR}{dz}\frac{\partial C}{\partial\xi}\right) + \frac{1}{P_e}\left(\frac{\partial^2 C}{R^2\partial\xi^2} + \frac{1}{R^2\xi}\frac{\partial C}{\partial\xi} + \frac{\partial^2 C}{\partial z^2}\right) \\ &\quad + \frac{1}{P_e}\left[\frac{3\xi}{R^2}\left(\frac{dR}{dz}\right)^2\frac{\partial C}{\partial\xi} - \frac{2\xi}{R}\frac{dR}{dz}\frac{\partial^2 C}{\partial\xi\partial z} - \frac{\xi}{R}\frac{d^2R}{dz^2}\frac{\partial C}{\partial\xi} + 2\left(\frac{\xi}{R}\frac{dR}{dz}\right)^2\frac{\partial^2 C}{\partial\xi^2}\right] \\ &\quad + S_r\left[\frac{3\xi}{R^2}\left(\frac{dR}{dz}\right)^2\frac{\partial T}{\partial\xi} - \frac{2\xi}{R}\frac{dR}{dz}\frac{\partial^2 T}{\partial\xi\partial z} - \frac{\xi}{R}\frac{d^2R}{dz^2}\frac{\partial T}{\partial\xi} + 2\left(\frac{\xi}{R}\frac{dR}{dz}\right)^2\frac{\partial^2 T}{\partial\xi^2}\right]\end{aligned}$$

$$+ S_r\left(\frac{\partial^2 T}{R^2\partial\xi^2} + \frac{1}{R^2\xi}\frac{\partial T}{\partial\xi} + \frac{\partial^2 T}{\partial z^2}\right) - \frac{\beta C}{Re} \tag{4.24}$$

With,

$$\dot{\gamma}=\sqrt{\begin{array}{l}2\left[\left(\frac{dR}{Rdz}\left(\xi\frac{\partial w}{\partial\xi}+w\right)\right)^2+\left(\frac{dR}{Rdz}w\right)^2+\left(\frac{\partial w}{dz}-\frac{\xi}{R}\frac{dR}{dz}\frac{\partial w}{\partial\xi}\right)^2\right]\\ \quad+\left(\xi\left(\frac{dR}{dz}\frac{\partial w}{\partial z}+w\frac{d^2R}{dz^2}\right)-\frac{\xi}{R}\frac{dR}{dz}\frac{dR}{dz}\left(\xi\frac{\partial w}{\partial\xi}+w\right)+\frac{\partial w}{R\partial\xi}\right)^2\end{array}} \tag{4.25}$$

and

$$\tau_{\xi\xi}=2\left(R_{eG}\dot{\gamma}^{n-1}+\tau_0\dot{\gamma}^{-1}\right)\left(\frac{dR}{dz}\left(\xi\frac{\partial w}{\partial\xi}+w\right)\right) \tag{4.26}$$

$$\tau_{zz}=2\left(R_{eG}\dot{\gamma}^{n-1}+\tau_0\dot{\gamma}^{-1}\right)\left(\frac{\partial w}{\partial z}-\frac{\xi}{R}\frac{dR}{dz}\frac{\partial w}{\partial\xi}\right) \tag{4.27}$$

$$\tau_{\xi z}=2\left(R_{eG}\dot{\gamma}^{n-1}+\tau_0\dot{\gamma}^{-1}\right)\left[\xi\left(\frac{dR}{dz}\frac{\partial w}{\partial z}+w\frac{d^2R}{dz^2}\right)-\frac{\xi}{R}\left(\frac{dR}{dz}\right)^2\left(\xi\frac{\partial w}{\partial\xi}+w\right)+\frac{\partial w}{R\partial\xi}\right] \tag{4.28}$$

4.2. Numerical Procedure. In this sub-section, we move from continuous model equations to discrete model equations through discretization. The finite difference schemes for discretization of our model equations are based on the forward difference approximations for time derivatives and central for all spatial derivatives, using the explicit finite difference method. This method was also used by [10] and [11]. The approximate derivatives are as given in equations (4.29) and (4.30).

$$\frac{\partial w}{\partial\xi}=\frac{w^k_{i,j+1}-w^k_{i,j-1}}{2\Delta\xi},\frac{\partial^2 w}{\partial\xi^2}=\frac{w^k_{i,j+1}-2w^k_{i,j}+w^k_{i,j-1}}{(\Delta\xi)^2},\frac{\partial w}{\partial t}=\frac{w^{k+1}_{i,j}-w^k_{i,j}}{\Delta t} \tag{4.29}$$

The approximate derivatives for temperature and concentration are obtained in a similar way as in equation (4.29)

Similarly, the approximations of derivatives of $\tau_{\xi z}$, and τ_{zz} are as given in equation (4.30)

(4.30)

$$\frac{\partial\tau_{\xi z}}{\partial\xi}=\frac{\left(\tau_{\xi z}\right)^k_{i,j+1}-\left(\tau_{\xi z}\right)^k_{i,j-1}}{2\Delta\xi},\frac{\partial\tau_{zz}}{\partial\xi}=\frac{(\tau_{zz})^k_{i,j+1}-(\tau_{zz})^k_{i,j-1}}{2\Delta\xi},\frac{\partial\tau_{zz}}{\partial z}=\frac{(\tau_{zz})^k_{i+1,j}-(\tau_{zz})^k_{i-1,j}}{2\Delta z}$$

We here now define $\xi_j=(j-1)\Delta\xi; j=1,2,3...N+1$ where, $\xi_{N+1}=1, z_i=(j-1)\Delta z; i=1,2,3...M+1$ and $t_k=(k-1)\Delta t; k=1,2,3...$

We now substitute finite difference schemes into equations $(4.22)-(4.28)$ and we make subject $w, T,$ and C. We also include the discretization of radial velocity from equation

(4.21). We therefore have equations (4.31)-(4.40).

$$u_{i,j}^{k+1} = \xi_j \left(\frac{dR}{dz}\right)_i w_{i,j}^k \tag{4.31}$$

$$\begin{aligned} w_{i,j}^{k+1} &= w_{i,j}^k + \Delta t \left(A_0 + A_1\cos(\omega t_k) + a_0\cos(\omega_b t_k + \psi) - \frac{H_a^2}{R_{eG}} w_{i,j}^k\right) \\ &\quad - \Delta t \left(\frac{\xi_j}{R_i}\left(\frac{dR}{dz}\right)_i w_{i,j}^k\right)\left(\frac{w_{i,j+1}^k - w_{i,j-1}^k}{2\Delta\xi}\right) - \Delta t w_{i,j}^k \left(\frac{w_{i+1,j}^k - w_{i-1,j}^k}{2\Delta z}\right) \\ &\quad + \Delta t w_{i,j}^k \frac{\xi_j}{R_i}\left(\frac{dR}{dz}\right)_i \left(\frac{w_{i,j+1}^k - w_{i,j-1}^k}{2\Delta\xi}\right) - \frac{\xi_j}{R_i}\left(\frac{dR}{dz}\right)_i \left(\frac{(\tau_{zz})_{i,j+1}^k - (\tau_{zz})_{i,j-1}^k}{2\Delta\xi}\right) \\ &\quad + \Delta t \left[\frac{1}{R_i}\left(\frac{(\tau_{\xi z})_{i,j+1}^k - (\tau_{\xi z})_{i,j-1}^k}{2\Delta\xi}\right) + \frac{(\tau_{\xi z})_{i,j}^k}{R_i\xi_j} + \left(\frac{(\tau_{zz})_{i+1,j}^k - (\tau_{zz})_{i-1,j}^k}{2\Delta z}\right)\right] \end{aligned} \tag{4.32}$$

$$\begin{aligned} T_{i,j}^{k+1} &= T_{i,j}^k - \Delta t \left[\frac{\xi_j}{R_i}\left(\frac{dR}{dz}\right)_i (w_{i,j}^k)\left(\frac{T_{i,j+1}^k - T_{i,j-1}^k}{2\Delta\xi}\right)\right] - \Delta t w_{i,j}^k \left(\frac{T_{i+1,j}^k - T_{i-1,j}^k}{2\Delta z}\right) \\ &\quad + \Delta t \left[w_{i,j}^k \frac{\xi_j}{R_i}\left(\frac{dR}{dz}\right)_i \left(\frac{T_{i,j+1}^k - T_{i,j-1}^k}{2\Delta\xi}\right)\right] + \frac{\Delta t}{P_e}\left(\frac{T_{i,j+1}^k - 2T_{i,j}^k + T_{i,j-1}^k}{R_i^2(\Delta\xi)^2}\right) \\ &\quad + \frac{\Delta t}{P_e}\left[\frac{T_{i,j+1}^k - T_{i,j-1}^k}{2\xi_j R_i^2 \Delta\xi} + \frac{T_{i+1,j}^k - 2T_{i,j}^k + T_{i-1,j}^k}{(\Delta z)^2}\right] + \frac{\Delta t}{P_e}\left[\frac{3\xi_j}{R_i^2}\left(\frac{dR}{dz}\right)_i^2 \left(\frac{T_{i,j+1}^k - T_{i,j-1}^k}{2\Delta\xi}\right)\right] \\ &\quad - \frac{2\xi_j(\Delta t)}{P_e R_i}\left(\frac{dR}{dz}\right)_i \left(\frac{T_{i+1,j+1}^k - T_{i-1,j+1}^k - T_{i+1,j-1}^k + T_{i-1,j-1}^k}{4\Delta\xi\Delta z}\right) \\ &\quad - \frac{\Delta t}{P_e}\left[\frac{\xi_j}{R_i}\left(\frac{d^2R}{dz^2}\right)_i \left(\frac{T_{i,j+1}^k - T_{i,j-1}^k}{2\Delta\xi}\right)\right] + \frac{2\Delta t}{P_e}\left(\frac{\xi_j}{R_i}\frac{dR}{dz}\right)_i^2 \left(\frac{T_{i,j+1}^k - 2T_{i,j}^k + T_{i,j-1}^k}{(\Delta\xi)^2}\right) \\ &\quad + \Delta t E_c \left[\frac{(\tau_{\xi\xi})_{i,j}^k}{R_i}\left(\frac{dR}{dz}\right)_i \left(\xi_j\left(\frac{w_{i,j+1}^k - w_{i,j-1}^k}{2\Delta\xi}\right) + w_{i,j}^k\right) + \frac{(\tau_{\xi z})_{i,j}^k}{R_i}\left(\frac{w_{i,j+1}^k - w_{i,j-1}^k}{2\Delta\xi}\right)\right] \\ &\quad + \Delta t E_c (\tau_{\xi z})_{i,j}^k \left[\xi_j\left(\left(\frac{dR}{dz}\right)_i \left(\frac{w_{i+1,j}^k - w_{i-1,j}^k}{2\Delta z}\right) + w_{i,j}^k \left(\frac{d^2R}{dz^2}\right)_i\right)\right] \\ &\quad - \Delta t E_c (\tau_{\xi z})_{i,j}^k \left[\frac{\xi_j}{R_i}\left(\frac{dR}{dz}\right)_i^2 \left(\xi_j\left(\frac{w_{i,j+1}^k - w_{i,j-1}^k}{2\Delta\xi}\right) + w_{i,j}^k\right)\right] + \Delta t E_c (\tau_{\xi z})_{i,j}^k \left(\frac{w_{i+1,j}^k - w_{i-1,j}^k}{2\Delta z}\right) \\ &\quad - \Delta t E_c (\tau_{\xi z})_{i,j}^k \frac{\xi_j}{R_i}\left(\frac{dR}{dz}\right)_i \left(\frac{w_{i,j+1}^k - w_{i,j-1}^k}{2\Delta\xi}\right) \end{aligned} \tag{4.33}$$

$$
\begin{aligned}
C_{i,j}^{k+1} &= C_{i,j}^{k} - \Delta t \left[\frac{\xi_j}{R_i} \left(\frac{dR}{dz} \right)_i \left(w_{i,j}^{k} \right) \left(\frac{C_{i,j+1}^{k} - C_{i,j-1}^{k}}{2\Delta\xi} \right) \right] \\
&\quad - \Delta t \left[w_{i,j}^{k} \left(\frac{C_{i+1,j}^{k} - C_{i-1,j}^{k}}{2\Delta z} - \frac{\xi_j}{R_i} \left(\frac{dR}{dz} \right)_i \left(\frac{C_{i,j+1}^{k} - C_{i,j-1}^{k}}{2\Delta\xi} \right) \right) \right] \\
&\quad + \frac{\Delta t}{P_e} \left[\frac{C_{i,j+1}^{k} - 2C_{i,j}^{k} + C_{i,j-1}^{k}}{R_i^2 (\Delta\xi)^2} + \frac{C_{i,j+1}^{k} - C_{i,j-1}^{k}}{2\xi_j R_i^2 \Delta\xi} + \frac{C_{i+1,j}^{k} - 2C_{i,j}^{k} + C_{i-1,j}^{k}}{(\Delta z)^2} \right]
\end{aligned}
\tag{4.34}
$$

$$
\begin{aligned}
&+ \frac{\Delta t}{S_c R_e} \left[\frac{3\xi_j}{R_i^2} \left(\frac{dR}{dz} \right)_i^2 \left(\frac{C_{i,j+1}^{k} - C_{i,j-1}^{k}}{2\Delta\xi} \right) \right] \\
&- \frac{2\xi_j(\Delta t)}{P_e R_i} \left(\frac{dR}{dz} \right)_i \left(\frac{C_{i+1,j+1}^{k} - C_{i-1,j+1}^{k} - C_{i+1,j-1}^{k} + C_{i-1,j-1}^{k}}{4\Delta\xi\Delta z} \right) \\
&- \frac{\Delta t}{P_e} \left[\frac{\xi_j}{R_i} \left(\frac{d^2R}{dz^2} \right)_i \left(\frac{C_{i,j+1}^{k} - C_{i,j-1}^{k}}{2\Delta\xi} \right) \right] + \frac{2\Delta t}{P_e} \left(\frac{\xi_j}{R_i} \frac{dR}{dz} \right)_i^2 \left(\frac{C_{i,j+1}^{k} - 2C_{i,j}^{k} + C_{i,j-1}^{k}}{(\Delta\xi)^2} \right) \\
&+ S_r \Delta t \frac{3\xi_j}{R_i^2} \left(\frac{dR}{dz} \right)_i^2 \left(\frac{T_{i,j+1}^{k} - T_{i,j-1}^{k}}{2\Delta\xi} \right) - \frac{2\xi_j \Delta t}{R_i} \left(\frac{dR}{dz} \right)_i \left(\frac{T_{i+1,j+1}^{k} - T_{i-1,j+1}^{k} - T_{i+1,j-1}^{k} + T_{i-1,j-1}^{k}}{4\Delta\xi\Delta z} \right) \\
&- S_r \Delta t \left[\frac{\xi_j}{R_i} \left(\frac{d^2R}{dz^2} \right)_i \left(\frac{T_{i,j+1}^{k} - T_{i,j-1}^{k}}{2\Delta\xi} \right) \right] + 2\Delta t S_r \left(\frac{\xi_j}{R_i} \right)^2 \left(\frac{dR}{dz} \right)_i^2 \left(\frac{T_{i,j+1}^{k} - 2T_{i,j}^{k} + T_{i,j-1}^{k}}{(\Delta\xi)^2} \right)
\end{aligned}
\tag{4.34}
$$

With,

$$
\dot{\gamma}^2 = 2 \left[\left(\left(\frac{dR}{dz} \right)_i \left(\xi_j \left(\frac{w_{i,j+1}^{k} - w_{i,j-1}^{k}}{2\Delta\xi} + w_{i,j}^{k} \right) \right) \right)^2 + \left(\left(\frac{1}{R_i} \right) \left(\frac{dR}{dz} \right)_i w_{i,j}^{k} \right)^2 \right] \tag{4.35}
$$

$$
+ 2 \left(\frac{w_{i+1,j}^{k} - w_{i-1,j}^{k}}{2\Delta z} - \frac{\xi_j}{R_i} \left(\frac{dR}{dz} \right)_i \left(\frac{w_{i,j+1}^{k} - w_{i,j-1}^{k}}{2\Delta\xi} \right) \right)^2 \tag{4.36}
$$

$$
+ \left\{ \begin{array}{l} \left[\xi_j \left(\frac{dR}{dz} \right)_i \left(\frac{w_{i+1,j}^{k} - w_{i-1,j}^{k}}{2\Delta z} \right) + w_{i,j}^{k} \left(\frac{d^2R}{dz^2} \right)_i \right] \\ \quad - \left[\frac{\xi_j}{R} \left(\frac{dR}{dz} \right)_i^2 \left(\xi_j \frac{w_{i,j+1}^{k} - w_{i,j-1}^{k}}{2\Delta\xi} + w_{i,j}^{k} \right) + \frac{1}{R_i} \frac{w_{i,j+1}^{k} - w_{i,j-1}^{k}}{2\Delta\xi} \right] \end{array} \right\}^2 \tag{4.37}
$$

and

$$
\left(\tau_{\xi\xi} \right)_{i,j}^{k} = 2 \left(R_{eG} \dot{\gamma}^{n-1} + \tau_0 \dot{\gamma}^{-1} \right) \left(\left(\frac{dR}{dz} \right)_i \left(\xi_j \frac{w_{i,j+1}^{k} - w_{i,j-1}^{k}}{2\Delta\xi} + w_{i,j}^{k} \right) \right) \tag{4.38}
$$

(4.39)

$$\left(\tau_{\xi z}\right)_{i,j}^{k} = 2\left(R_{eG}\dot{\gamma}^{n-1} + \tau_0\dot{\gamma}^{-1}\right)\left[\begin{array}{l}\xi_j\left(\left(\frac{dR}{dz}\right)_i\left(\frac{w_{i+1,j}^k - w_{i-1,j}^k}{2\Delta z}\right)\right) + w_{i,j}^k\left(\frac{d^2R}{dz^2}\right)_i - \\ \frac{\xi_j}{R_i}\left(\frac{dR}{dz}\right)_i^2\left(\xi_j\frac{w_{i,j+1}^k - w_{i,j-1}^k}{2\Delta\xi} + w_{i,j}^k\right) + \frac{w_{i,j+1}^k - w_{i,j-1}^k}{2R_i\Delta\xi}\end{array}\right]$$

(4.40)

$$\left(\tau_{zz}\right)_{i,j}^{k} = 2\left(R_{eG}\dot{\gamma}^{n-1} + \tau_0\dot{\gamma}^{-1}\right)\left[\frac{w_{i+1,j}^k - w_{i-1,j}^k}{2\Delta z} - \frac{\xi_j}{R_i}\left(\frac{dR}{dz}\right)_i\left(\frac{w_{i,j+1}^k - w_{i,j-1}^k}{2\Delta\xi}\right)\right]$$

The conditions in equations (4.10) to (4.12) are discretized as shown in equations (4.41) and (4.42)

$$w_{i,j}^1 = w_0, \quad T_{i,j}^1 = T_0, \quad C_{i,j}^1 = C_0; \quad w_{i,2}^k = w_{i,1}^k, \quad T_{i,2}^k = T_{i,1}^k, \quad C_{i,2}^k = C_{i,1}^k \tag{4.41}$$

$$w_{i,N+1}^k = 0, \quad u_{i,N+1}^k = 0, \quad T_{i,N+1}^k = T_w, \quad C_{i,N+1}^k = C_w, \quad \left(\tau_{\xi z}\right)_{i,1}^k = 0. \tag{4.42}$$

5. Simulation and Discussion

In this section, we display and discuss the numerical simulation of the discretized equations (4.31) to (4.40). The simulation was done using MATLAB software using the following parameter values. $A_1 = 0.8$, $A_0 = 0.5$, $\omega_p = 10$, $\omega_b = 10$, $a_0 = 1$, $Ha = 1$, $\psi = 0.3$, $R_{eG} = 1$, $e = 0.1$, $z_0 = 1$, $\Delta t = 0.0002$, $\Delta z = 0.08$, $\Delta\xi = 0.05$, $\tau_0 = 0.2$, $E_c = 1$, $P_e = 1$, $\beta = 0.1$, $S_r = 0.002$ and $n = 0.95$. The parameters were varied to determine their effect.

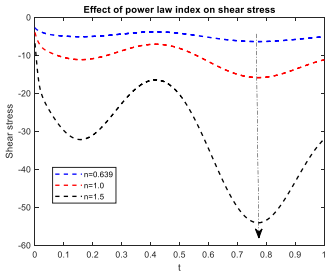

FIGURE 2

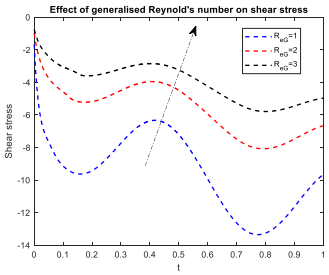

FIGURE 3

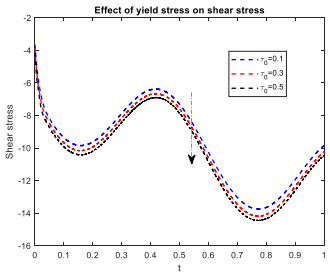

FIGURE 4

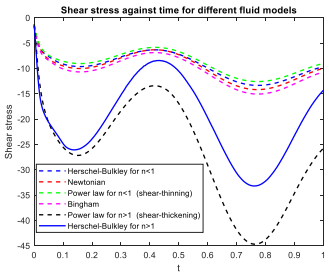

FIGURE 5

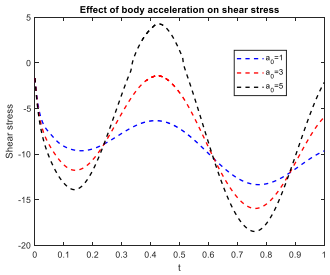

FIGURE 6

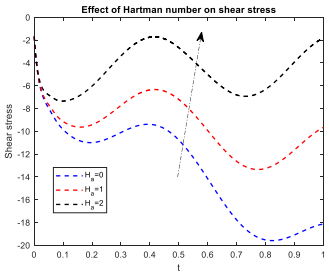

FIGURE 7

Figures 2-7 give the results for shear stresses. From the graphs, it is seen that, the magnitude of shear stress increases as the power law index increases. This is shown in figure 2. Opposite behavior is shown in figure 3, where the magnitude of shear stress declines towards positive values as generalized Reynold's number increases. This implies that as the inertial forces increases, the magnitude of shear stress decreases. Figure 4 illustrates the effect of yield stress on shear stress. It is observed that as the yield stress increases, the shear stress increases in magnitude. This therefore implies that increasing certain the amount of stress required for blood to flow, increases the shear stress. Comparison of shear stress for different fluid behaviors for Herschel-Bulkley, Newtonian, power law and Bingham is illustrated in figure 5. From figure 5 we observe that the power law fluid when $n > 1$ has higher magnitude of shear stress compared to power law fluid for $n < 1$. The same has been observed for Herschel-Bulkley fluid where the higher the power law index the higher the magnitude of shear stress. It is interesting to note further that when power law index $n > 1$ the shear stress exhibits more difference than when $n < 1$ where the difference is small. This tells us that, it deviates more when $n > 1$ than when $n < 1$. Figure 6 shows the effect of body acceleration on shear stress. It is seen that as body acceleration increases, the shear stress increases in magnitude. The opposite trend is observed in figure 7 where, the increase in Hartman number diminishes the magnitude of the shear stress. Hartman number is a ratio of electromagnetic forces to viscous forces. Increasing the Hartman number implies that the viscous forces become lower than the electromagnetic forces. Physically, the Hartman number enhances the Lorentz force which opposes the blood's motion.

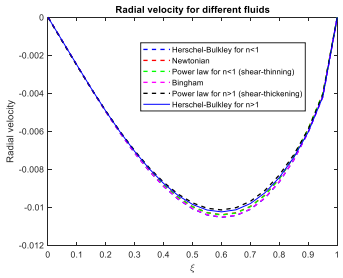

FIGURE 8

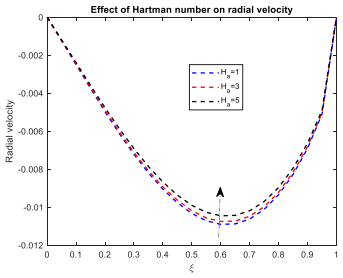

FIGURE 9

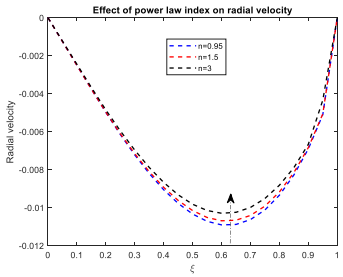

FIGURE 10

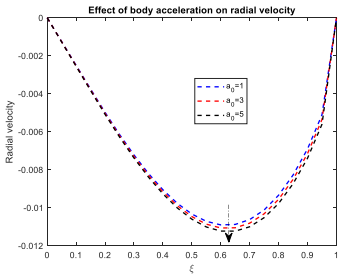

FIGURE 11

The results of radial velocity are presented in figures 8-11. From these figures, it is noted that the radial velocities are negative in sign. The radial velocity is shown to be zero on the axis of symmetry as it was assumed that no radial flow takes place along the axis of the symmetry. The velocity is also zero on the arterial wall ($\xi = 1$) to satisfy the no slip condition. In figure 8 we observe that when the power law index n is greater than 1, the radial velocity exhibits smaller magnitude values than when $n < 1$. From the same figure 8, we observe that radial velocity for Herschel-Bulkley fluid when $n < 1$ has higher values in magnitude as compared to power law, Bingham, Newtonian and Herschel-Bulkley for $n > 1$. It is also observed that radial velocity diminishes in magnitude as Hartman number and power law index increase as shown in figures 9 and 10 respectively. This finding is in good agreement with [10]. On the other hand, it is further shown that increase in body acceleration increases the magnitude of radial velocity.

Like in radial velocity, it is also illustrated in axial velocity that body acceleration enhances axial velocity while the Hartman number diminishes the axial velocity due to the Lorentz force which tend to oppose fluid's motion. Furthermore, the axial velocity is shown to increase with increase in steady state part of pressure gradient and the amplitude of pressure oscillation responsible for enhancing the systolic and diastolic pressures. This is as illustrated in figures 12-15 below.

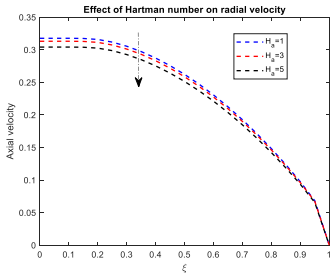

FIGURE 12

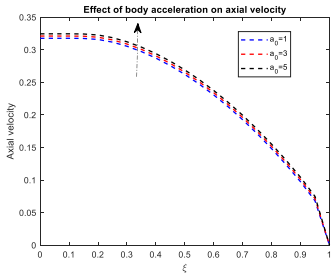

FIGURE 13

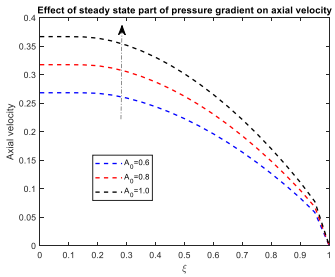

FIGURE 14

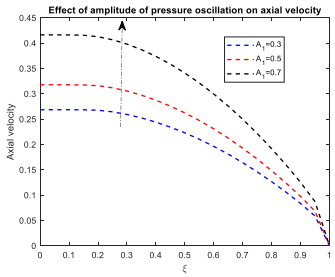

FIGURE 15

Temperature profiles against radial distance are displayed in figures 16-19 below. Figure 16 shows the effect of Peclet number on temperature profile. Peclet number is the ratio of the heat transferred by convection to the heat transferred by conduction. It is observed that, increase in Peclet number diminishes temperature profile. This means that heat transfer by motion of blood increases than heat transfer by conduction. In figure 17 we observe as expected that, increase in body acceleration raises temperature profile. This implies that body exercise give rise to the core body temperature. Eckert number is defined as the ratio of the advective mass transfer to the heat dissipation potential. It offers a measure of the kinetic energy of the flow relative to the enthalpy difference across the thermal boundary layer. It is observed in figure 18 that the increase in Eckert number increases the temperature profile, physically implying that as Eckert number increases, the advective mass transfer dominates the heat dissipation potential and therefore the temperature increases. Figure 19 reveals that as the Hartman number increases, the temperature profile decreases.

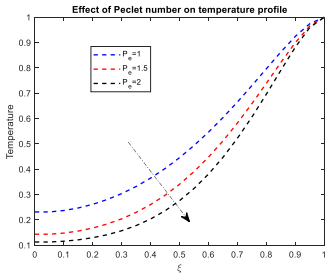

FIGURE 16

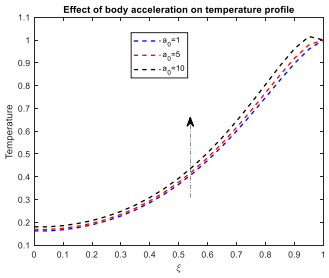

FIGURE 17

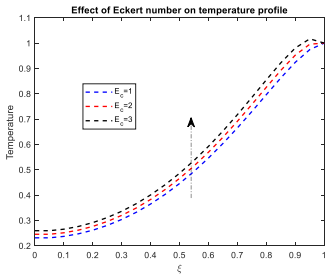

FIGURE 18

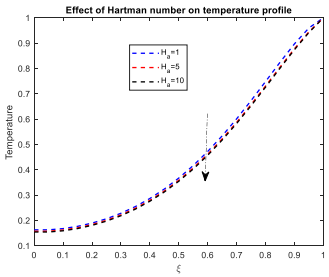

FIGURE 19

The effect of chemical reaction on concentration is observed in figure 20. From the figure, we observe that, the concentration profile decreases with increasing chemical reaction parameter, which implies that the chemical reaction parameter acts as a destructive agent. On the other hand, figure 21 shows the effect of increasing the Soret number on concentration profile. Soret number is the ratio of temperature difference to the concentration. As expected, the concentration profile increases with increasing the Soret number.

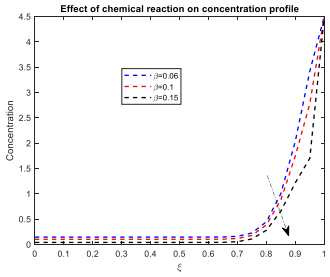

FIGURE 20

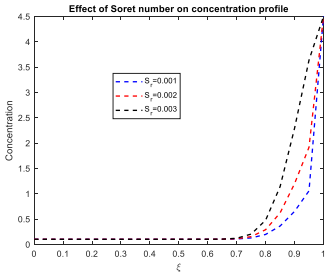

FIGURE 21

6. CONCLUSION

The current study presents numerical results of an unsteady heat and mass transfer blood flow through a stenosed artery in the presence of magnetic field, body acceleration and chemical reaction. Blood is considered to be non-Newtonian of Herschel-Bulkley type. It is established that the presence of magnetic field diminishes the blood's velocity; the body acceleration and Eckert numbers enhance temperature profile; while the concentration profile is reduced by increased chemical reaction. The study strongly suggests that for people with stenosed arteries, physical exercises in hot environment should be done with care. Further, the study has found out that the Herschel-Bulkley fluid experience higher velocity than the power law (for both when $n < 1$ and when $n > 1$), Bingham and Newtonian fluids. For non-Newtonian models, Herschel-Bulkley when $n < 1$ is also observed to be suitable to blood flow than the Bingham and the power law. Further more, shear stress is observed to deviate more when $n > 1$ than when $n < 1$. Considering the difference in shear stress and velocity profiles between the Newtonian and Herschel-Bulkley fluids, it is suggested that it is better to model blood flow using Herschel-Bulkley constitutive model than Newtonian.

CONFLICT OF INTERESTS

The author(s) declare that there is no conflict of interests.

REFERENCES

[1] M. Y. Abdollahzadeh Jamalabadi, M. Daqiqshirazi, H. Nasiri, M. R. Safaei, and T. K. Nguyen, Modeling and analysis of biomagnetic blood carreau fluid flow through a stenosis artery with magnetic heat transfer: A transient study, PLoS One, 13 (2018), e0192138.

[2] N. S. Akbar, S. Nadeem, and M. Ali, Influence of heat and chemical reactions on hyperbolic tangent fluid model for blood flow through a tapered artery with a stenosis, Heat Transfer Res. 43 (2012), 69-94.

[3] R. D. Alsemiry, P. K. Mandal, H. M. Sayed, N. Amin, et al., Numerical solution of blood flow and mass transport in an elastic tube with multiple stenoses, BioMed Res. Int. 2020 (2020), 7609562.

[4] D. Biswas and R. B. Laskar, Steady flow of blood through a stenosed artery: A non-newtonian fluid model, Assam Univ. J. Sci. Technol. 7 (2011), 144–153.

[5] K. Bunonyo, C. Israel-Cookey, and E. Amos, Mhd oscillatory flow of jeffrey fluid in an indented artery with heat source, Asian Res. J. Math. 7 (2017), Article no. ARJOM.37604.

[6] S. Changdar and S. De, Numerical simulation of nonlinear pulsatile newtonian blood flow through a multiple stenosed artery, Int. Sch. Res. Not. 2015 (2015), 628605.

[7] A. Dixit, A. Gupta, and N. Garg, Observations of blood flow in an inclined improved generalized multiple stenosed artery influenced by a magnetic field, Available at SSRN: https://dx.doi.org/10.2139/ssrn.3154042. (2018).

[8] I. Eldesoky, Unsteady MHD Pulsatile Blood Flow through Porous Medium in a Stenotic Channel with Slip at the Permeable Walls Subjected to Time Dependent Velocity (Injection/Suction), The International Conference on Mathematics and Engineering Physics. 7 (2014) 1–25.

[9] F. J. H. Gijsen, E. Allanic, F. N. van de Vosse, J. D. Janssen, The influence of the non-Newtonian properties of blood on the flow in large arteries: unsteady flow in a 90° curved tube, J. Biomech. 32 (1999), 705–713.

[10] M. A. Ikbal, S. Chakravarty, K. K. Wong, J. Mazumdar, and P. K. Mandal, Unsteady response of non-newtonian blood flow through a stenosed artery in magnetic field, J. Comput. Appl. Math. 230 (2009), 243–259.

[11] Z. Ismail, I. Abdullah, N. Mustapha, and N. Amin, A power-law model of blood flow through a tapered overlapping stenosed artery, Appl. Math. Comput. 195 (2008), 669–680.

[12] D. F. Jamil, R. Roslan, M. Abdulhameed, N. Che-Him, S. Sufahani, M. Mohamad, and M. G. Kamardan, Unsteady blood flow with nanoparticles through stenosed arteries in the presence of periodic body acceleration, J. Phys. 995 (2018), 012032.

[13] S. Kumar, N. Garg, and A. Gupta, Herschel bulkley model for blood flow through an artieral segment with stenosis, Int. J. Sci. Tech. Manage. 4 (2015), 93–100.

[14] Y. Liu and W. Liu, Blood flow analysis in tapered stenosed arteries with the influence of heat and mass transfer, J. Appl. Math. Comput. 63 (2020), 523–541.

[15] J. Misra, S. Adhikary, B. Mallick, and A. Sinha, Mathematical modeling of blood flow in arteries subject to a vibrating environment, J. Mech. Med. Biol. 18 (2018), 1850001.

[16] K. Prasad Maruthi and Y. P. Reddy, Mathematical modelling on an electrically conducting fluid flow in an inclined permeable tube with multiple stenoses, Int. J. Innov. Technol. Explor. Eng. 9 (2019), 2278–3075.

[17] C. Rodkiewicz, P. Sinha, and J. Kennedy, On the application of a constitutive equation for whole human blood., J. Biomech. Eng. 112 (1990), 198–206.

[18] B. D. Sharma and P. K. Yadav, A mathematical model of blood flow in narrow blood vessels in presence of magnetic field, Nat. Acad. Sci. Lett. 42 (2019), 239–243.

[19] A. Sinha, J. Misra, and G. Shit, Effect of heat transfer on unsteady mhd flow of blood in a permeable vessel in the presence of non-uniform heat source, Alex. Eng. J. 55 (2016), 2023–2033.

[20] N. Srivastava, Herschel-bulkley magnetized blood flow model for an inclined tapered artery for an accelerated body, J. Sci. Technol. 10 (2018), 53–59.

[21] C. Tu and M. Deville, Pulsatile flow of non-newtonian fluids through arterial stenoses, J. Biomech. 29 (1996), 899–908.

[22] K. Vajravelu, S. Sreenadh, P. Devaki, and K. Prasad, Mathematical model for a herschel-bulkley fluid flow in an elastic tube, Open Phys. 9 (2011), 1357–1365.

[23] A. Zaman, N. Ali, M. Sajid, and T. Hayat, Effects of unsteadiness and non-newtonian rheology on blood flow through a tapered time-variant stenotic artery, AIP adv. 5 (2015), 037129.

OUTPUT 3: POSTER

COMPUTATIONAL ANALYSIS OF MHD BLOOD FLOW THROUGH A STENOSED ARTERY IN THE PRESENCE OF BODY ACCELERATION AND CHEMICAL REACTION

Introduction

In day-to-day activities, the human body is subjected to different situations that disturb the normal flow of blood.

The presence of stenosis in arteries has attracted many mathematicians to model blood flow. The current study is motivated by the need to continue investigating the blood flow in stenosed arteries. In particular, the study focus is to model blood flow through a stenosed artery subject to different situations that disturb the normal flow of blood. Magnetic fields and chemical reactions are considered in the current work. Both, Newtonian and non-Newtonian blood are studied and simulations put in place. For the non-Newtonian blood, the Herschel-Bulkley constitutive model

Stenosed artery

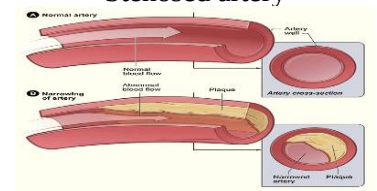

Model Equations

Non-Newtonian Blood (The Herschel-Bulkley constitutive model)

$$\frac{\partial u}{\partial r}+\frac{u}{r}+\frac{\partial w}{\partial z}=0$$

$$\rho\left(\frac{\partial u}{\partial t}+u\frac{\partial u}{\partial r}+w\frac{\partial u}{\partial z}\right)=-\frac{\partial P}{\partial r}+\frac{1}{r}\frac{\partial}{\partial r}(r\tau_{rz})+\frac{\partial}{\partial z}(r\tau_{zz})$$

$$\rho\left(\frac{\partial w}{\partial t}+u\frac{\partial w}{\partial r}+w\frac{\partial w}{\partial z}\right)=-\frac{\partial P}{\partial z}+\frac{1}{r}\frac{\partial}{\partial r}(r\tau_{rr})+\frac{\partial}{\partial z}(r\tau_{rz})+F(t)-\sigma B_0^2 w$$

$$\rho c_p\left(\frac{\partial T}{\partial t}+u\frac{\partial T}{\partial r}+w\frac{\partial T}{\partial z}\right)=k\left(\frac{\partial^2 T}{\partial r^2}+\frac{1}{r}\frac{\partial T}{\partial r}+\frac{\partial^2 T}{\partial z^2}\right)+\tau_{rr}\frac{\partial u}{\partial r}+\tau_{rz}\frac{\partial w}{\partial r}+\tau_{rz}\frac{\partial u}{\partial z}+\tau_{zz}\frac{\partial w}{\partial z}$$

$$\frac{\partial C}{\partial t}+u\frac{\partial C}{\partial r}+w\frac{\partial C}{\partial z}=D_f\left(\frac{\partial^2 C}{\partial r^2}+\frac{1}{r}\frac{\partial C}{\partial r}+\frac{\partial^2 C}{\partial z^2}\right)-\frac{D_f K_T}{T_0}\left(\frac{\partial^2 T}{\partial r^2}+\frac{1}{r}\frac{\partial T}{\partial r}+\frac{\partial^2 T}{\partial z^2}\right)-B(C-C_0)$$

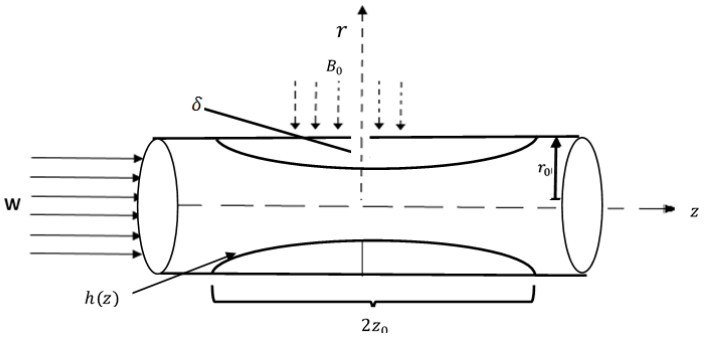

Simulations

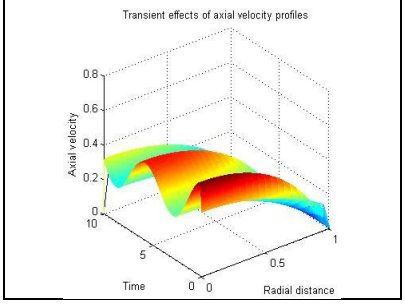

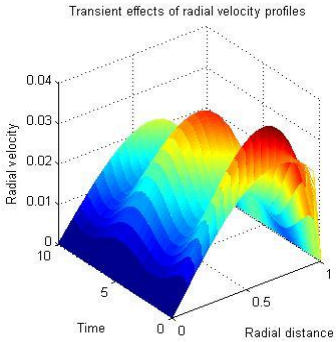

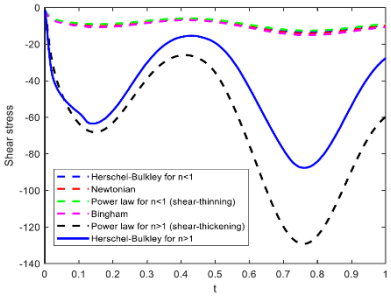

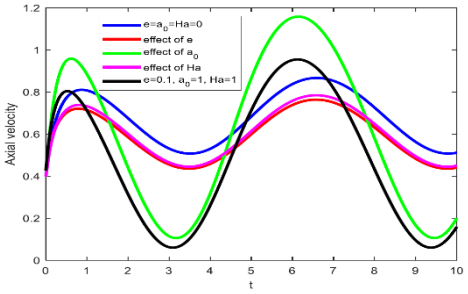

Results

It is found that body acceleration increases the blood's velocity, magnetic fields diminish blood's velocity, chemical reaction reduces the mass concentration. The temperature profile rises by the increase of body acceleration and the Eckert number, while it diminished with the increase of the Peclet number. It was further observed that the shear stress deviated more when the power law index, $n >$ 1than when $n < 1$.

Conclusion

Magnetic therapy in sports is very important, it may offer multiple benefits such as reducing pain and regulating blood flow which has been increased by body accelerations.

Recommendations

MRI scanning in hospitals should be done with care, taking into account that the blood velocity of a patient being subjected to the MRI machine decreases. It is better to set the value of power law index n to be greater than 1 when modeling blood flow using the non-Newtonian models. The current work can be extended by considering multiple stenoses in arteries. One can also can also extend the current work by considering the elasticity of the arterial wall.